University of Alberta

Hydrology of Forested Hillslopes on the Boreal Plain, Alberta, Canada

by

Todd Ernest Redding

A thesis submitted to the Faculty of Graduate Studies and Research
in partial fulfillment of the requirements for the degree of

Doctor of Philosophy
in
Ecology

Department of Biological Sciences

Fall 2009
Edmonton, Alberta

Examining Committee

Kevin Devito, Biological Sciences

Carl Mendoza, Earth and Atmospheric Sciences

Uldis Silins, Renewable Resources

Erin Bayne, Biological Sciences

James Buttle, Trent University

Abstract

Understanding the controls on water movement on forested uplands is critical in predicting the potential effects of disturbance on the sustainability of water resources. I examined the controls on vertical and lateral water movement on forested uplands on a range of landforms (coarse textured outwash, fine textured moraine) and time periods (individual events, during snowmelt, through the growing season, annually, and long-term) at the Utikuma Region Study Area (URSA) on the sub-humid Boreal Plains of Alberta, Canada. To quantify vertical and lateral water movement, hydrometric and tracer measurements were made under natural and experimental conditions at plot and hillslope scales.

Vertical flow and unsaturated zone storage dominated hydrologic response to snowmelt and rainfall at the plot and hillslope scales. Plot-scale snowmelt infiltration was greater than near-surface runoff, and when runoff occurred it was limited to south-facing outwash hillslopes underlain by concrete frost. Rainfall simulation studies showed that even under the extreme conditions tested, vertical flow and storage dominated the hydrologic response. Soils at field capacity and precipitation inputs of 15-20 mm or greater at high intensities were required to generate lateral flow via the transmissivity feedback mechanism. The threshold soil moisture and precipitation conditions are such that lateral flow will occur infrequently under natural conditions. Seasonal vertical water movement under natural conditions was greater on outwash than moraine uplands. The maximum downward vertical movement occurred in response to snowmelt, with little subsequent movement over the growing season. Recharge following snowmelt was similar for outwash and moraine sites and was followed by declining water tables through the growing season. Tracer estimates of long-term root zone drainage were low, while estimates of recharge for the moraine were high, raising questions about the appropriateness of this method for these sites.

These results emphasize the dominance of vertical relative to lateral water flow on Boreal Plain uplands. Detailed understanding of the controls on water movement can be used to predict the potential effects of disturbance on hydrology and water resources.

Acknowledgements

I wish to thank my supervisor Dr. Kevin Devito for his support, guidance, enthusiasm and patience in helping me develop and complete this research. Kevin's continued support and encouragement following my departure to BC for work and family reasons made the completion of this thesis possible. Input from my advisory committee members, Dr. Carl Mendoza and Dr. Uldis Silins, greatly improved the quality of my research.

Funding for this research was provided by a variety of sources, including: Natural Sciences and Engineering Research Council (NSERC) Collaborative Research and Development (CRD) grant for the Hydrology Ecology and Disturbance Project; Sustainable Forest Management Network research grant to Kevin Devito; Circumpolar/Boreal Alberta Research Grants; Syncrude Canada Ltd. equipment grant (thanks to Clara Qualizza). In addition, a number of granting agencies generously supported me through scholarships: NSERC Industrial Postgraduate Scholarship (sponsored by Syncrude Canada Ltd.); NSERC Canada Graduate Scholarship; Alberta Ingenuity Fund PhD Studentship; Walter H. Johns graduate fellowship. I would also like to thank my employer FORREX for support while I have been completing this degree.

I am indebted to a number of fellow students, technicians and volunteers who assisted with field and laboratory data collection, including: Brian Smerdon, Stephen Kaufman, JR van Haarlem, Scott Brown, Jason Leech, Jeremy Hrynkiw, Joe Riddell, Joanne Livingstone, Greg Piorkowski, Catherine Brown, Zabrinna Gibbons, Gunther Tondelier, Brendan Brabendar, Wayne Bell, Kirsten Hannam, Peter Crown and John Robertson. Thanks to Carolyn Forsyth at the Artis Inn.

Graduate school would have been much less interesting and fun without the collaborations and friendships developed with a number of fellow students, especially Brian, Steve and Jason. I would like to thank my parents Barb and Ernie Redding for their life-long love, support and encouragement. Successful completion of this thesis would not have been possible without the love and support of my amazing wife, Dr. Kirsten Hannam and our sons Matthias and Gabriel, who have endured an absent husband and father working on his thesis for too long.

Table of Contents

List of Tables

List of Figures

List of Acronyms and Abbreviations

DOY	Day of year
FF	Forest floor horizon
K_s	Saturated hydraulic conductivity
LA	Loam-aspen study site
Nf	North-facing slope aspect
RC	Runoff coefficient
RE	Root exclusion study plot
RU	Root uptake study plot
SA	Sand-aspen study site
Sf	South-facing slope aspect
SP	Sand-pine study site
SWE	Snow water equivalent
TDR	Time domain reflectometry
UZ	Unsaturated zone
VWC	Volumetric water content
WT	Water table

Chapter 1
Introduction

1.1 Western Boreal Forest

The boreal forest covers approximately one-third of Canada's land base (Canadian Forest Service 2006). The western boreal forest is a mosaic of coniferous and deciduous upland forests, wetlands, lakes, and ponds. The Boreal Plains ecozone of the western boreal forest extends across portions of British Columbia, Alberta, Saskatchewan, and Manitoba (Natural Resources Canada 2007). Forestry and oil and gas development is rapidly intensifying in the Boreal Plains, which is potentially leading to impacts on water resources (Alberta Environmental Protection 1998) and associated environmental values. Thus, it is necessary to increase our understanding of, and ability to predict, potential impacts of resource development on the hydrology and water resources of this region.

There are large gaps in our understanding of the hydrology of forested uplands, wetlands, and ponds in the western Boreal Plains region of Canada (Buttle et al. 2005, Devito et al. 2005a). Interpreting and predicting the potential impacts of anthropogenic disturbance in the region is difficult due to the large temporal variability in climate and spatial variability in surficial geology (Devito et al. 2005a). Annual precipitation in the region is approximately equal to or slightly less than potential evapotranspiration (Devito et al. 2005a). In addition, the seasonal maximums of both precipitation and evapotranspiration occur during the summer growing season, resulting in a low probability of protracted periods of moisture surplus. The geology of the Boreal Plains is heterogeneous, and is comprised of glacial sediments that range from 20 to 240 m in thickness over shale bedrock (Vogwill 1978). Topographic relief is subdued. The primary glacial landforms in the region include outwash, moraine, and lowland plains. This combination of climate and heterogeneous geology results in complex hydrological cycling that differs greatly from other boreal forest regions, such as the Boreal Shield (Buttle et al. 2005).

Hydrological research on the Boreal Plains includes studies on the effects of climate and geology on water cycling at the Utikuma Region Study Area (URSA). The URSA is located near Utikuma Lake in north-central Alberta (lat. 56^{o}N, long. 115^{o}30' W)), where the landscape is a mosaic of forested uplands, wetlands, and ponds. The study area encompasses the three major glacial landforms representative of the Boral Plains (Figure 1.1): a sandy outwash zone, a hummocky moraine zone, and a lacustrine plain. Uplands on outwash deposits are forested with jack pine or aspen and have sandy Brunisolic soils with high permeability to depth. On the moraine, the upland forest cover is dominated by aspen on fine-textured Luvisolic soils, which have increasing clay content with depth (Redding and Devito 2008). Soils on the moraine have the most heterogeneous texture and a wide variation in permeability, which typically decreases with depth. Uplands on the lacustrine plain are dominated by aspen forests and feature fine-textured Luvisolic soils with low permeability. To date, hydrological research has investigated hydrological dynamics on the lacustrine plain (Ferone and Devito 2004), fine-textured moraine (Ferone and Devito 2004, Redding and Devito 2008), coarse-textured outwash (Smerdon et al. 2005, 2008), and transitional zone between outwash-moraine (Riddell 2008). These studies have shown that water movement is dominantly vertical and that the timing of precipitation relative to plant demand is a key control over the hydrology of uplands and wetlands on the Boreal Plains.

1.2 Hydrology of Forested Uplands on the Boreal Plains

Understanding when hillslopes become hydrologically connected with surface waters is critical to predicting the long-term sustainability of regional water resources and water quality in the Boreal Plains region of northern Alberta (Devito et al. 2005a). On the Boreal Plains, natural variability in streamflow is high, with generally low annual streamflow interspersed with infrequent years of larger response. The combination of a subhumid climate, with precipitation that is slightly less than potential evapotranspiration, and the complex geology of deep glacial sediments results in large available soil storage capacity relative to

moisture surpluses or deficits; thus, water cycling is complex, non-linear, and threshold dependent (Devito et al. 2005a, Schoeneberger and Wysocki 2005). This threshold-type response indicates that the combination of precipitation depth and timing, in relation to available storage capacity, strongly controls runoff in this region (Devito et al., 2005b, Redding and Devito 2008). It is important to understand this threshold behaviour in order to predict the effects of future climate change and landscape disturbance on water cycling and hillslope runoff. Understanding the potential hydrologic coupling of hillslopes with receiving surface waters is critically important in predicting the potential sustainability (e.g., maintaining water levels and biological functioning) and biogeochemistry of wetlands and ponds, and in understanding the potential effects of forest harvesting on water resources.

On forested hillslopes on the Boreal Plains, vertical flowpaths and unsaturated zone storage, rather than lateral flow, tend to dominate the hillslope water balance under both natural (Devito et al. 2005b) and experimental (Chapter 3, Redding and Devito 2008) conditions. A study of runoff generation in a partially harvested Boreal Plains headwater catchment showed that surface water runoff is generally minor, with hillslope contributions to catchment runoff limited to only one out of five years (Devito et al. 2005b). When hillslope runoff happened in response to a large rainfall event concomitant with high antecedent soil moisture storage, and it was speculated to have occurred through rapid vertical preferential flow to a clay-rich layer, and then lateral flow was generated via the transmissivity feedback mechanism (Devito et al. 2005b). Vertical preferential flow through cracks and fissures has also been noted in similar soils on the Canadian Prairies (Hendry 1982, Hayashi et al. 1998). Given the low frequency of observed hillslope runoff on the Boreal Plains, manipulative experiments are required to understand under what conditions hillslopes contribute flow to receiving wetlands and surface waters, and to determine which flowpaths are followed.

To understand the linkages between climate and wetland and pond water levels in the URSA, it is necessary to determine the threshold soil moisture and

precipitation conditions required for surface or subsurface runoff from forested uplands (Torres 2002). There are likely a number of storage thresholds that have to be overcome before runoff occurs: those of the forest floor, the unsaturated upper mineral soil (rooting zone) and a deeper unsaturated zone, and the precipitation intensity and soil moisture conditions required for vertical connections with shallow groundwater or preferential subsurface flow in unsaturated soils. These types of hydrological thresholds and pathways have been extensively studied in steep, humid temperate forest ecosystems with surface runoff-dominated hydrology (McDonnell 2003, Weiler et al. 2005). However, the deep soils of the Boreal Plains region have a large moisture storage capacity and no confining layers to direct shallow subsurface runoff. Therefore, it is difficult to model runoff in the Boreal Plains region using traditional topographically based methods (Grayson and Western 2001). In areas of hummocky topography, such as those on the Boreal Plains, complex multi-scale hydrological interactions occur between groundwater and surface water (Winter 2001). In the Boreal Plains environment, it is also necessary to consider the role of snowmelt in runoff generation and recharge of soil moisture and groundwater (Devito et al. 2005b).

Snowmelt is one of the largest annual inputs of water in the Boreal Plains region of northern Alberta. Snowmelt occurs at a time of year when evapotranspiration is very low, so moisture surpluses are possible. This is in contrast to the growing season where, in this subhumid climate, precipitation (rain) is less than evapotranspiration (Devito et al. 2005b). Snowmelt infiltration has been found to be a major source of annual groundwater recharge on the Boreal Plains (Smerdon et al. 2008). Climate change has the potential to affect the amount of snow accumulated and the timing and rate of melt in this region (Barnett et al. 2005). It is critical, therefore, to understand the controls on snowmelt runoff, infiltration, and recharge from hillslopes in this region to understand and model the effects of climate change on hydrological processes and landscape-scale runoff.

1.3 Thesis Objectives and Format

The research questions addressed in this thesis are:

1. What are the dominant hillslope flowpaths (vertical and lateral) for outwash and moraine landforms for spring snowmelt and growing season rainfall?
2. What are the thresholds for and mechanisms of lateral flow generation on forested moraine hillslopes?
3. When and how much recharge can be expected from forested hillslopes across a range of vegetation and landforms?

A combination of hydrometric monitoring, tracer studies, and manipulative experiments were used to quantify the magnitude and direction of water movement on forested Boreal Plain uplands. Research was carried out on both moraine and outwash landscapes using a combination of plot and hillslope-scale studies.

This thesis follows the paper format style, and has been organized into six chapters. Chapter 2 examines the controls on near-surface snowmelt infiltration and runoff for aspen and jack pine forested hillslopes on moraine and outwash landforms. Chapter 3 presents a rainfall simulation experiment that quantifies the soil moisture and precipitation thresholds required to generate lateral subsurface flow for fine-textured soils on an aspen forested moraine hillslope (Redding and Devito 2008). Chapter 4 examines the mechanisms and flowpaths of vertical and lateral flow generation from the rainfall simulation experiment by using detailed soil moisture, pore pressure, and tracer data to develop a conceptual model of when and how lateral flow generation occurs for hillslopes with Luvisolic soils. Chapter 5 reports on the use of tracers and hydrometric measurements to quantify vertical water movement and groundwater recharge at seasonal, annual, and long-term time scales for sites on the outwash and moraine. Finally, Chapter 6 presents a summary of the previous four chapters and a discussion of the implications of these results for Boreal Plains hydrology and potential effects of forest management. The chapter also provides suggestions for future research.

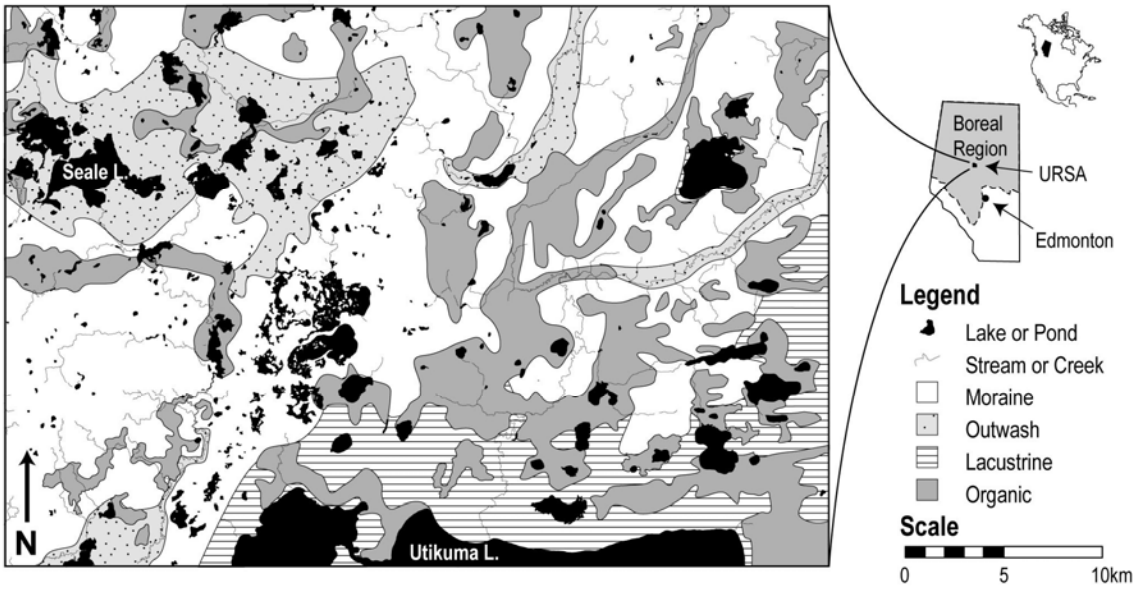

Figure 1.1. Location and surficial geology of the Utikuma Region Study Area (URSA). Map compiled by W. Bell and B. Smerdon (University of Alberta).

1.4 References

Alberta Environmental Protection. 1998. The boreal forest natural region of Alberta. Natural Resources Services, Recreation and Protection, Special Report.

Barnett, T.P., Adam, J.C. and Lettenmaier, D.P. 2005. Potential impacts of a warming climate on water availability in snow-dominated regions. Nature 438: 303-309

Buttle, J.M., Creed, I.F., and Moore, R.D. 2005. Advances in Canadian forest hydrology, 1999-2003. Hydrological Processes 19: 169-200. DOI:10.1002/hyp.5773.

Canadian Forest Service. 2006. The state of Canada's forests 2004-2005: The boreal forest. Canadian Forest Service, Ottawa, Ontario.

Devito, K., Creed, I., Gan, T., Mendoza, C., Petrone, R., Silins, U., and Smerdon, B. 2005a. A framework for broad-scale classification of hydrologic response units on the Boreal Plain: Is topography the last thing to consider? Hydrological Processes 19: 1705-1714.

Devito, K.J., Creed, I.F., and Fraser, C.J.D. 2005b. Controls on runoff from a partially harvested aspen-forested headwater catchment, Boreal Plain, Canada. Hydrological Processes 19: 3-25.

Ferone, J.M. and Devito, K.J. 2004. Shallow groundwater-surface water interactions in pond-peatland complexes along a Boreal Plains topographic gradient. Journal of Hydrology 292: 75-92.

Grayson, R. and Western, A. 2001. Terrain and the distribution of soil moisture. Hydrological Processes 15: 2689-2690.

Hayashi, M., van der Kamp, G., and Rudolph, D.L. 1998. Water and solute transfer between a prairie wetland and adjacent uplands, 1. Water balance. Journal of Hydrology 207: 42-55.

Hendry, M.J. 1982. Hydraulic conductivity of a glacial till in Alberta. Ground Water 20: 162-169.

McDonnell, J.J. 2003. Where does the water go when it rains? Moving beyond the variable source area concept of rainfall-runoff response. Hydrological Processes 17: 1869-1875.

Natural Resources Canada. 2007. Forested ecozones of Canada. http://ecosys.cfl.scf.rncan.gc.ca/classification/classif04-eng.asp [accessed March 10, 2009]

Redding, T.E. and. Devito, K.J. 2008. Lateral and vertical flow thresholds for aspen forested hillslopes on the Western Boreal Plain, Alberta, Canada, Hydrological Processes 23: 4287-4300.

Riddell, J.T.F. 2008. Assessment of surface water-groundwater interaction at perched boreal wetlands, north-central Alberta. M.Sc. Thesis, University of Alberta, Edmonton, Alberta, 106 pp.

Schoeneberger, P.J. and Wysocki, D.A. 2005. Hydrology of soils and deep regolith: A nexus between soil geography, ecosystems and land management. Geoderma 126: 117-128.

Smerdon, B.D., Mendoza, C.A. and Devito, K.J. 2005, Interactions of groundwater and shallow lakes on outwash sediments in the sub-humid Boreal Plains of Canada. Journal of Hydrology 314: 246-262.

Smerdon, B.D., Mendoza, C.A. and Devito, K.J. 2008, Influence of sub-humid climate and water table depth on groundwater recharge in shallow outwash aquifers. Water Resources Research. 44: doi:10.1029/2007WR005950.

Torres, R. 2002. A threshold condition for soil-water transport. Hydrological Processes 16: 2703-2706.

Vogwill, R. 1978. Hydrogeology of the Lesser Slave Lake area, Alberta. Edmonton, AB. Alberta Research Council. 30 pp.

Weiler, M., McDonnell, J., Tromp van Meerveld, I. and Uchida, T. 2005. Subsurface Stormflow. In: Vol. 3 of 5, Encyclopedia of Hydrologic Sciences, Anderson, M.G., McDonnell, J.J. (eds). John Wiley and Sons: New York; 1719-1732.

Winter, T.C. 2001. The concept of hydrologic landscapes. Journal of the American Water Resources Association 37: 335-349.

Chapter 2

Snowmelt Infiltration and Runoff from Forested Boreal Plain Hillslopes

2.1 Introduction

In the Boreal Plains ecozone, snowmelt produces a large input of water during a relatively short period at a time of year when evapotranspiration is very low and moisture surpluses are possible. This is in contrast to the growing season where, in the subhumid climate of this region, precipitation (rain) is less than potential evapotranspiration (Devito et al. 2005b). Infiltration of snowmelt and early spring rain is a major source of annual groundwater recharge on some landforms in the Boreal Plains (Smerdon 2006). Climate change has the potential to decrease the amount of snow accumulated and accelerate the timing and rate of melt in this region (Barnett et al. 2005). In the western boreal forest, regional groundwater recharge and streamflow volumes are low; therefore, it is important to understand the controls on snowmelt runoff and infiltration from hillslopes on the Boreal Plain to understand and model the potential effects of climate change on hydrological processes and landscape-scale runoff. Rapid changes in land use on the Boreal Plains have the potential to alter snow accumulation and melt dynamics by removing forest cover, which will result in decreased interception of snow and increase melt rates. To accurately predict the effects of resource development, it is critical to understand the controls on snowmelt infiltration and runoff.

In the boreal forest, infiltration often dominates over surface runoff at the hillslope scale during the snowmelt period (Mace 1968, Kachanoski and De Jong 1982, Elliott et al. 1998, Kalef 2002, Whitson et al. 2004) due to the high infiltration capacity of most forest soils, even under frozen conditions (Pierce et al. 1958). A large available soil moisture storage capacity prior to snowmelt plays an important role in reducing snowmelt runoff in soils that have high infiltration rates (Kalef 2002, Devito et al. 2005b). It has been suggested that under certain conditions, near surface runoff (over the mineral soil surface, but through the forest floor layers) may occur due to the presence of concrete frost that impedes

infiltration (e.g., Stein et al. 1994). Given the large heterogeneity in texture of the deep, dry soils on the Boreal Plains (Whitson et al. 2004, Devito et al. 2005b) and the potentially high infiltration rates during frozen conditions (Kalef 2002), there is considerable uncertainty about the importance and magnitude of snowmelt runoff contributions from upland forested hillslopes to wetlands.

Surface runoff occurs when the snowmelt rate is greater than the surface infiltration rate. The dominant controls on snowmelt runoff have been shown to be amount of snow (snow water equivalent [SWE]), fall soil moisture content, and snowmelt rate (Zhao and Gray 1999). Fall soil moisture content is a control on infiltration because wetter soils have a greater potential to develop frost, which may impede infiltration rates, and they have less available soil moisture storage during snowmelt (Zhao and Gray 1999). Soil frost may also develop due to meteorological conditions during winter and snowmelt periods that involve periodic melting and refreezing events (Mace 1968, Proulx and Stein 1997). Slope aspect can have a large influence on snowmelt rate and therefore runoff potential. Greater snowmelt rates typically occur on south-facing than north-facing slopes (Hart and Lomas 1979, Harms and Chanasyk 1999, Woo 2005) due to greater incoming solar radiation (Bonan 2002). However, greater snowmelt runoff may occur on north-facing (hereafter Nf) slopes due to the presence of frozen soils (Carey and Woo 1999) or to decreased available storage due to reduced evaporation and transpiration (Cline et al. 1977, Hart and Lomas 1979). These trends may be enhanced or moderated by soil texture, which is a control over water storage and transmission properties, and by forest canopy vegetation (deciduous and coniferous), which influences snow interception and radiation transmission based.

On the western Boreal Plains, high spatial variability in soil texture is related to the spatial distribution of glacial landforms. Vegetation tends to co-vary with landforms. Aspen grows on uplands with soils that have greater water holding capacity, while on coarse-textured soils with less water holding capacity, jackpine is the dominant forest canopy species. The variation in forest vegetation communities may result in high spatial variability in snow accumulation and melt

rates, and potentially in runoff. Therefore, understanding where and when upland snowmelt runoff contributes to downslope wetlands or surface waters is critical to understanding the potential impacts of resource development or climate change. The objective of this research was to examine the controls on snowmelt runoff generation on forested hillslopes on the western Boreal Plains. Near-surface snowmelt runoff, infiltration, and snowmelt season water balances were measured on two landforms and within two vegetation types (outwash-jack pine, outwash-aspen and moraine-aspen) to assess the relative importance of aspect (north, south), soil texture (sand, loam), and fall soil moisture content (fall irrigation, non-irrigated) on snowmelt runoff. Specifically, it was hypothesized that near-surface runoff would be greater from north-facing slopes on loam soils that had been irrigated in fall 2003.

2.2 Study Sites

The snowmelt runoff experiments were carried out at the Utikuma Region Study Area (URSA), near Utikuma Lake (lat. 56^{o} N, long. 115^{o}30' W) in north-central Alberta (Devito et al. 2005a). The site is located within the Boreal Plains ecozone (EcoRegions Working Group 1989), and has a mean annual temperature of 1.2^{o}C and mean monthly temperatures over the snowmelt period of -12.1, -5.5, and 3.4ºC in February, March, and April, respectively (Marshall et al. 1999). The mean annual precipitation is 481 mm with 137 mm falling as snow, and annual potential evapotranspiration is 518 mm (Marshall et al. 1999). Mean month-end depth of snow on the ground at Slave Lake (100 km south of URSA) is 0.25, 0.16, and 0.01 m for February, March, and April, respectively (Environment Canada 2004). The long-term (1987–2001) mean annual runoff for Red Earth Creek (619 km^{2}, 70 km north of URSA) is 67 mm yr^{-1}, and ranges between 4 and 246 mm yr^{-1} (median: 58 mm yr^{-1}), which corresponds to runoff coefficients between 1 and 53% (median: 14%) (Environment Canada 2006).

Three sites with a range of surfical geology, soils, and forest cover were selected for this study: sand-jack pine (SP), sand-aspen (SA), and loam-aspen (LA). In the study region, glacial till deposits range from 20 to 240 m in thickness

over Upper Cretaceous Smoky Group shale bedrock (Vogwill 1978). The SP site is located in an area of glacial outwash (Fenton et al. 2003) with soils developed from sand and classified as Dystric Brunisols (Soil Classification Working Group 1998). The SA site is also located in an area of glacial outwash (Fenton et al. 2003); however, there are bands of finer-textured materials through the soil profile, which are classified as Eutric Brunisols (Soil Classification Working Group 1998). The LA site is located on a disintegration moraine (Fenton et al. 2003) featuring heterogeneous soils with a dominant loam texture near the surface and which are classified as Gray Luvisolic (Soil Classification Working Group 1998). The overstory at the SP site is comprised of jack pine (*Pinus banksiana*), while the overstory at the SA and LA sites is dominated by trembling aspen (*Populus tremuloides*). There is very little shrubby understory vegetation at the SP site, but the ground is covered by a layer of feathermoss on north-facing slopes and by lichens on south-facing slopes. The SA site has a shrubby understory comprised largely of rose (*Rosa acicularis*), whereas the LA site has a thick understory of rose and high-bush cranberry (*Viburnum edule*).

2.3 Methods

At each of the three sites (SP, SA, and LA), four runoff frames, each with an area of 1 m^2, were constructed at plots on a south-facing (hereafter Sf) and on a north-facing (Nf) slope. In total, eight runoff frames were constructed per site; 24 were established for the full study. Aluminum flashing was used around all sides of each frame and was inserted 0.05 m into the mineral soil (e.g., Harms and Chanasyk 1998) below the forest floor (FF) horizons. At the down slope end of the plot, a section of trough was inserted 0.06 m into the soil to collect flow from the top 0.05 m of mineral soil and the overlying forest floor. Water collected in the troughs was routed to a bucket in a pit down slope from the frame to allow for measurement of runoff volumes. Within each frame, vegetation was clipped to a height of 0.05 m above the ground surface to eliminate differences in understory interception between plots. Given that the runoff collection trough extended under approximately 6% of the frame area and may have collected only vertical

infiltration, the detection limit for runoff collection was set at a runoff coefficient (RC) of 6%.

To manipulate the fall soil moisture content and assess the potential for surface runoff under unfrozen conditions, half of the runoff frames were randomly selected to receive irrigation treatments (e.g., Kane and Stein 1984). On the irrigated frames, 40 mm of water was applied at an intensity of 80 mm hr^{-1} on October 21, 2003 (DOY 294), and included a Br^- tracer for a related experiment. The water was applied using a hand-held watering can. The plots that did not receive 40 mm of water were irrigated with the equivalent of 4 mm of precipitation to apply a Br^- tracer for a related experiment. The plots irrigated with 4 mm are hereafter referred to as non-irrigated.

To measure the amount of snowmelt water available for runoff or infiltration at each study plot, a snowmelt lysimeter was installed at each plot. The lysimeters were located adjacent to runoff frames with similar aspect, slope, and canopy cover. The lysimeters were constructed of whitish, opaque plastic pans that had an area of 0.47 m^2 (0.52 x 0.9 m) and a depth of 0.11 m. The pans were installed so that all water would drain to one corner, where a hole was cut, and outflow was routed into a collection bucket buried down slope. Water volumes in the bucket were measured at the same time as runoff frame outflow.

During each site visit, snow depth was measured with a ruler at five locations within each frame and lysimeter. Snow depths were converted to snow water equivalent (SWE) using density values obtained approximately weekly from snow tube measurements adjacent to the frames at each study plot. Periodic snow surveys were also made across the study hillslopes at different topographic positions (crest, mid-slope, toe-slope, and adjacent wetland) to quantify the spatial variability in snow accumulation.

The presence of near-surface soil frost was measured periodically within each frame and at the same locations as the snow surveys. Frost was measured in the runoff frames using a metal pin (0.002 m diameter) once the snow depth was less than 0.3 m to minimize potential disturbance to the snow surface. The pin was inserted into the soil at five locations per plot. If the pin met resistance and

was not able to penetrate into the mineral soil, the measurement was considered to be concrete frost. At the hillslope scale, frost measurements were made along transects across various slope positions using a pointed metal rod 0.008 m diameter, and a subsample of probing locations was inspected for ice content (e.g., Young et al. 1997).

The method of Proulx and Stein (1997) was used to examine the long-term potential for concrete frost development during the winter and spring based on meteorological conditions. The method examines the potential of weather conditions to melt some amount of snow and deliver it to the ground surface (Proulx and Stein 1997). These weather conditions consist of mean daily temperature greater than 0 C to melt snow followed by a period where the maximum daily temperature is below 0 C to freeze liquid water at the soil sufrace. For this analysis, daily air temperature data (maximum, minimum, and mean) from Red Earth Creek was used for the period 1995–2006 (Environment Canada 2006).

The soils at all plots were described in the field, and samples were collected for laboratory analysis of bulk density and particle size. Soil bulk density was sampled using 0.06 m diameter and 0.05 m long cores. Mineral soil samples were dried at 105^{o}C for 24 hrs; forest floor (FF) samples were dried at 70^{o}C for 48 hours. Porosity was calculated using the measured bulk density data and particle density values of 1.54 Mg m^{-3} for FF and 2.65 Mg m^{-3} for mineral soil (Redding et al. 2005). Particle size was analyzed in 63 soil samples per plot using the hydrometer method with carbonate pre-treatment (Kalra and Maynard 1991).

Infiltration rates were measured at the slope crest above all plots in both frozen and unfrozen conditions. Four metal rings of 0.15 m diameter were inserted 0.05 m into the mineral soil, and the forest floor was left intact within the rings. Since rings were installed on relatively flat ground to ensure accuracy of measurement, statistical tests for aspect effects were not possible; therefore, results are presented by site. During fall 2003, four of the eight infiltration rings at each plot were measured prior to soil freezing. During spring 2004, all eight rings

were measured at each site. Spring measurements were made once the snow had melted from the rings but while the soils were still frozen. All spring measurements were made using water that had been allowed to cool outdoors overnight during subfreezing temperatures so that water temperatures were between 1–2^{o}C at the time of infiltration measurement. Infiltration was measured and calculated based on the method of Reynolds and Elrick (2002).

Within each frame, soil temperature was measured in the forest floor (0.02 m above the mineral soil surface) and at 0.1, 0.3, and 0.5 m depth in the mineral soil using thermocouples (PR-T-25, Omega Engineering). Measurements were made using a handheld meter (HH-25-TC, Omega Engineering) with an accuracy of +/- 0.6^{o}C. At a central location within each plot, soil temperature was measured at depths of 0.5, 1.0, 1.5, and 2.0 m using thermocouples.

At the three south-facing plots, a data logger (CR10X, Campbell Scientific Inc., Logan Utah) was installed at a central location between the frames to monitor continuous temperature and moisture conditions. Air temperature was measured at 1 m in the air, and soil temperature was measured at 0.1 and 0.3 m into the mineral soil using thermocouples (105T, Campbell Scientific Inc., Logan Utah). Soil moisture was monitored in each Sf frame using TDR probes (CS616, Campbell Scientific Inc., Logan Utah). The probes were installed at an angle to monitor moisture content over the top 0-0.15 m of the mineral soil. Due to technical problems, a continuous record was not available for all Sf plots during the melt period.

Soil moisture storage in the top 1 m was also monitored manually using the Profile Probe (PR-1, Delta-T Designs, UK). The Profile Probe (similar to TDR) does not sense ice due to its low dielectric content; therefore, measurements were not made during the period of frozen soils. The Profile Probe access tubes were installed and initial measurements were made in fall 2003 prior to soil freezing. Measurements were also made following soil thaw in June 2004. The use of factory calibrations for the profile probe could lead to water contents greater than the porosity of the soil, therefore, a site-specific calibration was developed for the soils at SP, SA and LA sites using the formula:

$$VWC = (0.00004 \times V^{1.4364}) \quad \text{[Equation 1]}$$

where VWC is the volumetric water content ($m^3\ m^{-3}$) and V is the voltage reading from the profile probe. The relationship has $r^2 = 0.62$, and constrains the VWC estimates to realistic values at higher V, which has been shown to be a problem with the factory calibration equation (Evett et al. 2006).

To test the effects of aspect and irrigation on snowmelt runoff, a randomized complete block ANOVA was used to compare RCs between aspect (Sf and Nf) and fall irrigation (irrigated and non-irrigated). In this design, site was used as the block, and the ANOVA tested the effects of aspect, fall irrigation and the interaction between the two treatments. To test for differences between time to steady state infiltration among the fall, spring irrigated, and spring not-irrigated trials, a one-way ANOVA was used followed by a Tukey multiple comparison test (Zar 1984). All analyses were assessed for significance at the $P = 0.05$ level, and analysis was completed using PopTools (CSIRO, Canberra, Australia).

2.4 Results

2.4.1 Site and Soil Characteristics

The vegetation cover and soil texture characteristics of the study plots are presented in Table 2.1. The sand-jack pine (SP) site had an overstory of jack pine with a coniferous canopy that persisted through the winter period (Table 2.1). Winter canopy cover was greatest at the SP-Nf plot relative to all other plots (Table 2.1). At the SA and LA sites, canopy cover increased greatly during the leafed-out growing season.

Slope gradients ranged from 14 to 23% across all study plots. The SA site had the steepest slopes; the SP site had the gentlest slopes (Table 2.1).

The sand + clay proportion of soils in the LA site was much higher than in the sand-rich SA and SP sites, and showed greater variability between frames and with depth, especially in the LA-Sf plot (Table 2.2). Forest floor thickness and composition also varied between sites and plots. The SP-Sf plot had the thinnest

forest floor, which was comprised of lichens and needles. It was less than 50% of the thickness of the feathermoss/needle FF on the SP-Nf plot (Table 2.2). The SA and LA sites both had an aspen/litter FF, but it was slightly thicker on the LA site (Table 2.2). Steady state infiltration rates, measured in fall 2003, were slightly higher on the SP and SA sites than the LA site, which also had a greater spatial variability (Table 2.1).

No surface runoff was measured during the initial 40 mm irrigation. The probability of daily rainfall of 40 mm in October is < 1%. In addition, there was no statistically significant difference in soil moisture at 0–0.05 m depth in the mineral soil between irrigated and non-irrigated frames ($P = 0.66$) 8 days after the irrigation applications and immediately prior to soil freezing.

There were site differences in the initial soil moisture conditions. There was a statistically significant negative relationship between initial soil moisture content and sand content ($P < 0.001$). Initial soil moisture content was greatest in the LA frames (range 0.06–0.26 $m^3\ m^{-3}$) (Table 2.2). Initial moisture content at the sand-rich SP and SA sites were similar and generally less than 0.10 $m^3\ m^{-3}$ (Table 2.2).

2.4.2 Snow Accumulation

During the winter, prior to the start of intensive field measurements (November 1, 2003 to March 14, 2004, day of year [DOY] 74), total precipitation recorded by Belfort gauges near the SP and LA sites was 85 and 62 mm, respectively (Table 2.3). At the closest Environment Canada stations at Red Earth Creek and Slave Lake, the total precipitation over the same period was 60 and 62 mm, respectively (Table 2.3). At the start of the intensive measurements, average SWE on the study sites ranged from 9 mm on the SA-Sf plot to 37 mm on the SA-Nf plot (Table 2.3). At the start of the intensive measurements there was less snow on the Sf than on the Nf plots at the SP and SA sites; however, there were no differences in snow accumulation between aspects at the LA site. By the start of the intense measurement period, the lysimeters at the SP-Sf and SA-Sf plots

had collected significant meltwater (26 and 36 mm, respectively), which resulted from melt that occurred between February 4 and March 3, 2004.

During the period of March 15 to April 19, 2004 (DOY 75–110), measured precipitation was 70 mm at the LA site and 86 mm the SP site (Table 2.3, Figure 2.1), compared to 25 mm and 42 mm at Red Earth Creek and Slave Lake, respectively. More than 50% of the annual snowfall came in the last 6 weeks of winter. Small but almost daily snowfalls occurred during the first 2 weeks of the intensive measurement period, and a large snowfall event occurred in mid-April (Figure 2.1). There was considerable variability in measured precipitation among sites—the approximately 30 mm event recorded on DOY 88 near the SP site deposited only about 8 mm at the LA site (Figure 2.1).

Maximum snow accumulation occurred on most plots by DOY90, with the exception of the SP-Nf and SA-Sf plots, where only slight increases in SWE were observed from DOY81 to 90 (Figure 2.1). Accumulation was much more pronounced at the LA site between DOY82 and 90. The peak accumulation at SA-Sf most likely occurred during the large snowfall in mid-April and was missed by the field measurements. The equivalent meltwater depth collected in the lysimeters was greater than the calculated melt based on changes in SWE measurements prior to DOY 89. Peak accumulation amounts varied considerably with aspect and among sites, and in general were less than 60 mm at the SP and SA sites, and greater than 70 mm at the LA site (Figure 2.2).

2.4.3 Snowmelt

High variability in snow depth and total melt occurred among sites and aspects. Prior to the start of intensive measurements at the three sites, there was significant melt at the SP and SA Sf plots (Table 2.3). During the period from DOY 82 to 90, melt occurred at some sites when the air temperature rose above 0ºC during several days, which reduced SWE accumulation, especially at the SA-Sf plot (Figure 2.1). Intense and complete snowmelt occurred after the DOY88 snowstorm, when average air temperature rose well above 0ºC for more than 10 days (Figure 2.1, Table 2.4). Snow disappeared earlier on Sf plots than Nf plots at

all sites, and on the sand outwash sites (SP and SA), which was a reflection of low SWE at the start of the study (Tables 2.3 and 2.4, Figure 2.1). During the main melt period, the timing and rate of snowmelt differed among sites and aspects (Table 2.4). The Sf plots had shorter melt periods than Nf plots and almost double the average and maximum melt rates of Nf plots (Table 2.4). The maximum daily snowmelt rate ranged from 9.8 to 23.7 mm d^{-1} (Table 2.4). The maximum hourly snowmelt rate measured was 2.5 mm hr^{-1} over a 2-hr period at the SA-Sf plot on DOY 90. The SP-Sf and -Nf plots and the LA-Sf plot had maximum melt rates on DOY 95, which had a daily maximum temperature of near 20^{o}C and was preceded by five days with mean temperatures greater than 0^{o}C (Figure 2.2).

2.4.4 Snowmelt Runoff

Prior to March 13 (DOY 73), runoff was restricted to a few south-facing SP and SA frames, where significant snowmelt had been measured (Figure 2.2). Significant runoff (runoff coefficient greater than 6%) was observed only during DOY 90-97, when air temperatures increased and the greatest snowmelt rates occurred. Runoff was largely restricted to SP-Sf and SA-Sf frames, with greatest amounts at SA-Sf frames. Despite high snowmelt rates in LA-Sf plots, runoff was measured only during one day from one frame (Figure 2.2). Few of the Nf frames had RCs greater than 6%, and thus can not be confidently interpreted as having runoff.

Cumulative runoff to DOY 110 varied from 1 to 60 mm, corresponding to RCs of 1-65% (Table 2.5). Significant runoff occurred consistently in all SA-Sf frames, and most SP-Sf frames. There was some variability at other sites. Analysis of the entire data set indicates that while there was greater runoff from Sf than Nf plots, the differences, while not statistically significant at the P=0.05 level (P = 0.08, F=3.99, df=1), indicate a strong relationship given the low statistical power of the tests (Figure 2.3).

There was no clear relationship between runoff and either fall surface soil water content or soil sand content (Figure 2.5). Nor was there a statistically significant difference (P = 0.59, F = 0.32, df = 1) in RCs between irrigated and

non-irrigated frames (Figure 2.3). The highest RCs corresponded to frames with low fall soil moisture content (Figure 2.4). This was a function of greater runoff being generated from the SP and SA sites, which have sandy soils with low water holding capacity. The sandiest soils generated a wide range of runoff, from the highest to the lowest recorded (Figure 2.3), and there was no discernable pattern except for aspect (Figure 2.5). The LA site, which featured soils that can hold more water, did not generate significant lateral flow (Figure 2.3). There was a positive relationship between runoff and the extent of concrete frost within the frames (Figure 2.4). As the extent of concrete frost, at the date of maximum melt rate, increased, so did runoff once the area of concrete frost in the plot reached 80% (Figure 2.4). The extent of concrete frost was not related to fall moisture content at these study sites.

2.4.5 Soil Temperature

Soil temperatures at all three sites followed the same pattern as air temperature; they were generally below freezing until approximately DOY 90 (Figure 2.6), and rose to 0–1^{o}C until the end of the monitoring period (DOY 110). There was no statistical difference between Nf and Sf plots. Continuous soil moisture measurements made using TDR probes in the Sf plots (data not shown) indicated that surface soils (0-0.15 m in mineral soil) began to thaw or snowmelt infiltration was occurring between DOY 95 and 100 on those plots. Depth of soil freezing (data not shown) was greater than 2.0 m for both aspects at the SP site. At the SA site, soils froze to between 1.0 and 1.5 m depth, while at the Sf and Nf plots on the LA site, soils froze to between 1.0 and 1.5 m and 1.5 and 2.0 m, respectively.

2.4.6 Concrete Frost Occurrence

Concrete frost development was not directly related to soil temperature regimes or fall irrigation treatment. The spatial extent of concrete frost within runoff frames at the time of maximum melt rate was associated with the extent of surface runoff during the intense melt period (Table 2.6, Figure 2.4). At all three

sites, the area of frames occupied by concrete frost was greatest for Sf frames; little to no concrete frost was noted in Nf frames at any of the sites (Table 2.6). Concrete frost covered 100% of all runoff frames in SA-Sf plots at the start of the intensive snowmelt period when consistent and high runoff rates were observed. While concrete frost persisted to DOY 111–112 in some frames, runoff did not occur due to the lack of snow. For upland locations, concrete frost formed at the FF mineral soil interface and ranged from one to four centimetres thick (data not shown).

A transect survey on DOY 102 indicated that the proportion of concrete frost occurrence in the runoff frames was similar to that at the midslope position for each study hillslope (plot) (data not shown), which suggests that construction of the runoff frames did not influence the formation of concrete frost.

The requisite meteorological conditions to necessary generate concrete frost formation occurred at least once in 10 of the 12 years of climate records examined. The mean number of warming and cooling events per year was 1, with a range of 0–3 events per year. The requisite meteorological conditions were recorded three times in 1995, twice in 2005, once in 1996, 1997, 2000-2004 and 2006, but not in 1998 and 1999.

2.4.7 Frozen Soil Infiltration

Infiltration rates measured in the frozen soils were orders of magnitude greater than the maximum measured snowmelt rate of 2.5 mm hr^{-1} (Figure 2.7). At the time of the infiltration measurements in April 2004, the soils were frozen, but there was no concrete frost. The time required to reach steady state infiltration increased significantly ($P = 0.02$, $F = 9.02$, $df = 2$) from unfrozen state (fall 2003; range = 1–5 minutes; median = 2 minutes) to frozen soil conditions in spring (range = 1–32 minutes; median = 9 minutes) (Figure 2.7). The time required to reach steady state flow under frozen conditions at sites not previously measured in fall 2003 ranged from 1 to 33 minutes, with a median of 5 minutes (Figure 2.7). This was not statistically significantly different ($P > 0.05$) from either the fall measurements or spring remeasurements. The infiltration measurements were

carried out after all snow had melted, so direct comparison between these measurements and the runoff measurements is not possible. The infiltration measurements demonstrate that even under frozen, but not concrete frost, conditions, these soils can transmit water at rates that exceed the maximum measured melt rates.

2.4.8 Snowmelt Infiltration and Frame Water Balances

Infiltration was greater than runoff for all frames except one (SA-Sf-4) (Table 2.5). The drainage coefficients (the proportion of the total snowmelt + rainfall inputs to DOY 165 that were residual after runoff and changes in soil moisture storage) were lowest at the SA-Sf site due to large amounts of lateral snowmelt runoff. In addition, the LA-Sf site (and the LA-Nf site, to a certain extent) had low drainage coefficients due to storage in the upper metre of the silt-clay-rich soil. Based on proportion of total snowmelt, Nf plots had greater infiltration than Sf plots; however, based on water depth equivalent, Sf plots on the SP and LA sites had greater infiltration due to greater snowmelt inputs (Table 2.5). At the SA site, due to the large amounts of runoff from the Sf plot, both the relative proportion and total depth of infiltration was greater at the Nf plot.

Increases in soil moisture storage from fall 2003 to spring 2004 were greater at the LA site than at the other sites (Table 2.5). Changes in soil moisture storage reported in Table 2.5 included some spring rainfall. The very small changes in storage at the SP and SA sites (Table 2.5) are reasonable given the low water-holding capacities of the coarse-textured soils on those sites. The soil moisture content data collected using the profile probes indicate either considerable (minimum 75 mm) vertical drainage below 1 m or lateral flow in the B or C horizons (Table 2.5).

2.5 Discussion

2.5.1 Controls on Snowmelt Runoff from Forested Hillslopes

The dominance of snowmelt infiltration over runoff on hillslopes in the boreal forest is well documented (Price and Hendrie 1983, Kachanoski and de

Jong 1984, Kane and Stein 1984, Kalef 2002, Whitson et al. 2004, Devito et al. 2005b). On the Boreal Plains, Whitson et al. (2004) measured RCs of less than 1% on a clearcut harvested hillslope with an easterly aspect that was located approximately 200 km southeast of this study site and which had soils similar to those at the LA site. The RCs in this study are similar to those of Kane and Stein (1984) who found RCs from snow plots in central Alaska ranged from 0 to 54% for a south-facing aspen-birch forested hillslope with silt loam soils. Similarly, Dunne and Black (1971) recorded hillslope scale surface RCs of 32–47% on agricultural soils in the northeastern U.S.

Although runoff amounts were low in this study, this research, along with that of others (Kachanoski and de Jong 1984, Kane and Stein 1984), clearly illustrates that runoff can occur in the boreal forest. There are some landform-vegetation combinations that show potential for snowmelt runoff; however, the controls in the western Boreal Plains (at least for 2003-04) were not necessarily what was expected. The presence of concrete frost played a critical role in the generation of near-surface runoff from the study plots by providing a nearly impermeable surface over which runoff could occur (Bayard et al. 2005). The largest amounts of concrete frost, highest melt rates, and corresponding RCs were measured on the Sf slopes at the sand-rich SP and SA sites.

The influence of fall soil moisture content on snowmelt runoff was minimal in this study. Previous research indicated that if the relative saturation of the surface soils is greater than 0.3, concrete frost development and spring snowmelt runoff will be enhanced (Granger et al. 1984, Pomeroy et al. 1997). Kane and Stein (1984) found no clear relationship between fall irrigation amounts and spring runoff. They found that spring surface runoff increased with increasing total snow accumulation and increasing melt rate. In general, the initial soil moisture conditions in the western boreal forest are often below the threshold observed in agricultural settings on the Canadian Prairies (Granger et al. 1984, Pomeroy et al. 1997) due to moisture uptake by forest vegetation and soil drainage during drier fall periods (Devito et al. 2005a). Further, concrete frost was observed only in sandier soils with relative saturation that was half that of the

threshold value hypothesized for runoff generation on prairie soils (Zhao and Gray 1999). In this study, the development of concrete frost on the silt-clay-rich moraine soils with high fall soil moisture content was less extensive than on the drier soils at the SP and SA sites. This indicates that soil frost development occurred during the winter rather than as a result of fall moisture content, and runoff is controlled by snowmelt processes.

In this study, runoff was not positively correlated with fine grain size fraction as expected. The low water holding capacity of the coarse-textured soils was expected to hinder the development of concrete frost, and hence runoff. The results presented herein on the influence of soil texture may apply only to regions or years with dry fall conditions leading to low fall soil moisture content.

The interaction of aspect with vegetation cover controls inputs of solar radiation, and proved to be the strongest influence on the generation of near-surface runoff in this study. Due to greater incoming solar radiation and lower canopy cover, which results in reduced interception and shading of the snowpack surface, snow volumes and melt rates on south-facing slopes are often greater than on north-facing slopes, and results in greater snowmelt runoff (Harms and Chanasyk 1998, Carey and Woo 1999, Bonan 2002, Murray and Buttle 2003, Woo 2005). The maximum melt rate measured in this study was 2.5 mm hr^{-1}, much less than the measured infiltration rates. However, because runoff was collected from the frames, melt rate must have been greater than infiltration rate where concrete frost occurred. In this study, higher melt rates may have been required to generate surface runoff. However, infiltration rates exceeded snowmelt rates in the LA plots, indicating that both concrete frost development and high rates of snowmelt may be required to generate surface runoff. These results contradict those of Harms and Chanasyk (1998), who measured greater surface runoff from north-facing than south-facing slopes associated with reclaimed mine soils in central Alberta; however, there was very high spatial variability among runoff frames within that site. Carey and Woo (1999) found that south-facing slopes did not contribute any runoff; even when soils were frozen, because they were sufficiently permeable to allow infiltration of all

snowmelt. Significant runoff occurred only from north-facing slopes with permafrost (Carey and Woo 1999). These studies indicate that concrete frost development and high melt rates on south-facing slopes may be driving surface runoff processes in the present study. Vegetation density as related to soil texture may control the occurrence of concrete frost on these sites.

The Sf plots at the SP and SA sites had the lowest canopy cover, which has been shown to correspond to increased development of concrete frost (Pierce et al. 1958). Similar to this study, in which runoff was generated on south-facing slopes with low canopy cover, Kachanoski and de Jong (1982) measured surface runoff from clearcut harvested slopes but not from adjacent forested areas, possibly due to reduced shading and increased energy inputs on the clearcut sites. It has also been hypothesized that concrete frost development in forest soils is limited by the presence of the forest floor layer (Hardy et al. 2001). In this study, sites with thinner forest floor layers (SP-Sf and SA) had a greater spatial extent of concrete frost than those with thicker forest floor layers (SP-Nf, LA).

The mechanism of concrete frost formation on the SP and SA sites appears to be as follows: warm temperatures for one or two days cause melting of snow, which infiltrates into the frozen upper soil and refreezes as the temperatures get colder. Typically, this occurs either during mid-winter or at the beginning of the melt period (Mace 1968, Stadler et al. 1996, Proulx and Stein 1997, Bayard et al. 2005). However, the probability of occurrence increases with increased radiation inputs at sites with southern exposures and low density canopy cover.

The characteristics of concrete frost development make it difficult to apply snowmelt infiltration/runoff equations that rely on fall moisture content (e.g., Granger et al. 1984) due to the multiple melt and freeze events that alter soil moisture content during winter (Harms and Chanasyk 1998). The analysis of daily climate data indicated that in the study area, the meteorological conditions necessary for concrete frost development are common and occurred in 10 out of 12 years. Most climate change scenarios predict reduced snow depths and warmer winter temperatures (Barnett et al. 2005), which may result in greater potential for concrete frost formation during mid-winter and early melt periods (Hardy et al.

2001). Whether the effects of climate change will result in increased hillslope runoff reaching streams is difficult to predict given the poor hydrologic connectivity between uplands and surface water bodies on the Boreal Plains.

The fact that runoff was greater on sandy soils than loamy soils in the study area is initially counterintuitive; however, in light of the effect slope aspect has on runoff, it is perhaps not surprising. The following conceptual model explains why greater runoff occurred on south-facing slopes with sandy soils. South-facing sandy slopes have the lowest water holding capacity and greatest solar radiation inputs; therefore, they cannot support dense vegetation cover (Grier and Running 1977). These drought conditions result in a more open canopy, which allows greater incoming radiation to melt the snow earlier and faster, and possibly allows for concrete frost development. Concrete frost combined with the higher melt rates increases the potential for surface runoff from south-facing slopes.

This conceptual model that combines aspect and soil texture to explain the observed runoff data accounts for the lower runoff from the LA-Sf plot, even though it had wet soils and the greatest amount of snowmelt. The low runoff was due to the limited extent of concrete frost (less than 80% frame area, Figure 2.4), which allowed infiltration at the time of maximum melt rate. These differences are related to higher canopy cover on the LA-Sf plot than on the SP and SA-Sf plots, and may also be due to site topography. The late April snowmelt did not result in any runoff, likely due to the amount of concrete frost being below the 80% threshold.

2.5.2 Snowmelt Lysimeter Water Balance

The snowmelt lysimeter data were crucial to determining runoff coefficients and net infiltration at the soil surface. The lysimeter outflows corresponded relatively closely to the measurements of accumulated precipitation at the SP and LA sites, which were located near existing winter precipitation measurement stations (Table 2.3). The lysimeter outflows were less than the accumulated precipitation, except at the LA-Sf plot, which may indicate there was

some leakage of water into the LA-Sf collection system. At the other plots, the reduced outflows relative to accumulated precipitation are likely a reflection of spatial variability in accumulation due to canopy interception (especially for the SP-Nf plot) and sublimation from the ground surface. Arain et al. (2003) measured winter evaporation rates (above canopy eddy covariance measurements) of 0.1–0.25 mm d^{-1} in a boreal black spruce stand. Pomeroy et al. (1998) found sublimation of canopy-intercepted snow was approximately 13% of annual snowfall in a mixed aspen (70%) and spruce (30%) stand in Saskatchewan. Ground surface sublimation was not measured in this study, and values for the Boreal Plains are not reported in the scientific literature. However, Molotch et al. (2007) found that approximately 37% of winter sublimation was from the ground surface snowpack in subalpine conifer forests. These estimates of sublimation losses indicate that the lysimeter outflow values are reasonable when compared to the total measured precipitation from the SP and LA Belfort gauge records. A greater understanding of sublimation processes under different stand types and canopy conditions is necessary to improve our understanding of winter water balances for the Boreal Plains.

At all plots, the total outflow from the lysimeters was greater than the maximum measured SWE. Thus, without the lysimeters, the RCs would have been overestimated due to the thin snowpack and intermittent periods of melting and accumulation during the late winter and early spring. During the study period, there were three melt periods and two accumulation periods. If manual snow surveys for estimating SWE are not frequent enough (e.g., daily), the data do not capture the snowmelt dynamics. For locations with deeper snowpacks, regular snow surveys (e.g., weekly or bi-weekly) may be adequate for capturing the melt dynamics; however, lysimeter data is valuable for developing and testing snowmelt models (Winkler 2001). The use of simple snowmelt lysimeters can improve estimates of water balance components that are critical to understanding and modelling hydrological processes in this landscape.

2.5.3 Hillslope and Landscape Scale Implications

At the hillslope scale, the connectivity of areas underlain by concrete frost will determine whether runoff water reaches receiving surface waters (Woo 2005). Given the patchy spatial distribution of concrete frost in uplands, it appears that only peatlands or ephemeral draws have consistent concrete frost formation (data not shown), and therefore regularly act as an impervious surface over which runoff may occur. This agrees with hydrometric (Kalef 2002, Devito et al. 2005b) and isotopic studies (McEachern et al. 2006) of runoff on the Boreal Plains, which have shown that streamflow originates mainly from wetland areas and only infrequently from uplands. The patchy distribution of concrete frost on hillslopes results in only periodic high runoff responses; in most years, vertical flow will dominate (Price and Hendrie 1983).

Streamflow records for Red Earth Creek (Figure 2.8) show that the watershed is not snowmelt-dominated in terms of annual peak flows, unlike many montane catchments (e.g., Moore and Scott 2005). The distribution of annual peak flows indicates that over the period of record, approximately half occur before DOY 175 (June 24). Given that snow at the URSA typically melted by early May, only two of the measured annual peak flows can likely be directly attributed to snowmelt (Figure 2.8). The later in the year that a peak flow occurs, the larger it is (Figure 2.8), which indicates that rain events and antecedent storage drive peak flow generation in this landscape. Therefore, snowmelt on the hillslopes will only infrequently influence regional runoff responses during the snowmelt period (Devito et al. 2005a, McEachern et al. 2006). The primary role of snowmelt in the generation of runoff at the watershed scale is to satisfy storage and "prime" the system for hydrological response to spring or summer rain events (Devito et al. 2005b). In 1997, there was a large streamflow peak in the early spring, and an even larger (largest daily flows on record) later in the growing season. It is also important to note that rain-on-snow events are uncommon in this region, so they are not expected to be a major driver of runoff at the hillslope or watershed scale like they are in other regions (e.g., Harr 1981, Marks et al. 2001).

However, the occurrence of rain-on-snow events may increase as the climate warms (Barnett et al. 2005).

Removal of the forest canopy by forest harvesting or oil and gas development can lead to increased snowmelt runoff from hillslopes and watersheds. When the forest canopy is removed, snow accumulation increases due to decreased interception, and melt rates increase due to greater incoming solar radiation. Similarly, the potential for concrete frost formation increases with increased solar radiation. In addition, increased surface runoff can occur where soils have been compacted by machinery (e.g., on skid trails, roads) due to the generation of concrete frost and the presence of highly compacted non-conductive materials. During the study period, surface runoff in response to snowmelt was observed only on road surfaces and in ditches at the SA and LA sites (T. Redding, personal observation). Surface runoff on roads can impact water quality of downstream surface water bodies.

2.6 Summary and Conclusions

The results of this research indicate that during the snowmelt period on the Boreal Plains, infiltration dominates over near-surface runoff over a range of hillslopes with varying soil types and vegetation covers. Slope aspect plays a crucial role in runoff generation through its relationship with concrete frost development. Runoff frames on south-facing hillslopes generated more runoff than frames on north-facing slopes due to more extensive concrete frost development near the soil surface. Concrete frost development is a result of low canopy cover reducing snowfall interception and increasing solar radiation to the ground surface, which results in greater thaw and refreeze cycles. Runoff at the hillslope scale is controlled by the connectivity of concrete frost. Where much of the hillslope is connected to receiving surface waters or wetlands, snowmelt runoff at the watershed scale may be enhanced. In this study, over the portions of the hillslope that lacked concrete frost, infiltration rates under frozen soil conditions were greater than the maximum melt rates, indicating a dominance of vertical flow and little opportunity for runoff generation. Future research needs to

examine the potential for snowmelt-driven subsurface flow from similar hillslopes, as this has been noted in previous studies on the Boreal Plains (Kachanoski and de Jong 1982) and other areas that have similar soil properties as the LA site (Newman et al. 2004). Climate change may have a large effect on near-surface runoff from hillslopes, as predicted increases in temperatures and decreases in snowpack thickness will result in conditions that are amenable to concrete frost formation and more rapid melt rates or rain-on-snow events. Resource development that reduces forest canopy cover may also result in greater potential for near-surface runoff due to increased snow accumulation, faster melt, and increased concrete frost development, and to an increase in compacted road surfaces.

Table 2.1. Site characteristics of snowmelt plots.

Site[1]	Plot[2]	Canopy species	Slope orientation (º)	Slope gradient (%)	Canopy cover (%)[3]	Unfrozen infiltration rate K_s (mm hr^{-1})[4]
SP	Sf	Jack Pine	200	16	5	787
	Nf	Jack Pine	35	14	35	(226)
SA	Sf	Aspen	206	23	5 (30)	824
	Nf	Aspen	70	20	5 (30)	(411)
LA	Sf	Aspen	160	18	10 (60)	644
	Nf	Aspen	350	20	15 (60)	(656)

[1]site labels are SP - sand-pine, SA – sand-aspen, LA – loam-aspen
[2]Sf – south-facing, Nf – north-facing
[3]canopy cover in leafless and full-leaf (in parentheses) conditions
[4]K_s is saturated hydraulic conductivity, data presented are means of Nf and Sf plots (n = 4) with standard deviation in parentheses

Table 2.2. Forest floor (FF) and upper mineral soil properties (0.05 m) in runoff frames. Texture data (S: Sand % and C: Clay %) and initial volumetric water content (VWC) were measured in the upper 0.05 m of the mineral soil. Initial moisture content was measured 8 days after the initial irrigation of plots, immediately prior to soil freezing in November 2003. Relative saturation was calculated by dividing the VWC by the soil porosity.

Site	Plot	Frame	Irrig. Depth (mm)	FF Thickness (m)	FF Composition	S (%)	C (%)	Initial VWC (m^3 m^{-3})	Rel. Sat.
SP	Sf	3	40	0.05	lichen/needles	92	6	0.05	0.09
		4	40	0.05	lichen/needles	93	5	0.09	0.16
		1		0.03	lichen/needles	93	5	0.06	0.11
		2		0.05	lichen/needles	92	6	0.08	0.14
	Nf	3	40	0.09	moss/needles	93	4	0.07	0.12
		4	40	0.09	moss/needles	93	3	0.05	0.08
		1		0.09	moss/needles	93	5	0.07	0.12
		2		0.12	moss/needles	95	4	0.03	0.05
SA	Sf	1	40	0.06	aspen litter	88	7	0.06	0.11
		3	40	0.06	aspen litter	86	6	0.06	0.11
		2		0.06	aspen litter	88	6	0.05	0.09
		4		0.07	aspen litter	86	8	0.08	0.15
	Nf	1	40	0.07	aspen litter	87	6	0.09	0.17
		2	40	0.06	aspen litter	88	7	0.09	0.17
		3		0.06	aspen litter	88	5	0.14	0.26
		4		0.06	aspen litter	88	5	0.06	0.12
LA	Sf	1	40	0.10	aspen litter	39	22	0.17	0.31
		4	40	0.08	aspen litter	80	6	0.07	0.13
		2		0.10	aspen litter	41	19	0.16	0.30
		3		0.08	aspen litter	62	13	0.06	0.11
	Nf	3	40	0.13	aspen litter	60	17	0.13	0.22
		4	40	0.13	aspen litter	30	23	0.12	0.20
		1		0.13	aspen litter	36	20	0.22	0.37
		2		0.12	aspen litter	54	16	0.26	0.43

Table 2.3. Precipitation (P), lysimeter outflow (Lys), and snow accumulation (SWE) measurements from the beginning of the experiment until the end of the snowmelt period (November 1, 2003 to April 19, 2004).

Site	Plot	Sept. 1, 2003 to Oct. 31, 2003	November 1, 2003 to March 14, 2004			March 15 to April 19, 2004		Total: November 1, 2003 to April 19, 2004	
			P (mm)	Lys (mm)	SWE[1] (mm)	P (mm)	Lys (mm)	P (mm)	Lys (mm)
SP	Sf	42	85	26	26	86	86	171	112
	Nf	42	85	8	36	86	60	171	68
SA	Sf			36	9		57		93
	Nf			4	37		83		87
LA	Sf	32	62	3	33	70	131	132	134
	Nf	32	62	0	32	70	92	132	92
Red Earth Creek		56	60			25		85	
Slave Lake		40	62			42		104	

[1]average plot SWE measured on March 13 or 14, 2004 (DOY 73/74)

Table 2.4. Snowmelt characteristics by plot. Melt depths and rates were calculated using lysimeter outflows. SWE (mm) and depth (m) values are from the lysimeters.

Site	Plot	Primary Melt Period						
		Start (DOY)	End (DOY)	Start SWE (mm) and Depth (m)	Length (days)	Mean melt rate (mm d^{-1})	Max melt rate (mm d^{-1})	DOY of Max melt rate
SP	Sf	89	98	49 (0.26)	9	9.5	23.7	95
	Nf	89	101	23 (0.15)	12	5.7	9.8	95
SA[2]	Sf	82	90	19 (0.10)	8	5.1	13.0	90
	Nf	80	96	24 (0.20)	16	4.1	12.0	90
LA	Sf	86	98	106 (0.37)	12	12.5	21.8	95
	Nf	90	105	74 (0.40)	15	5.9	14.5	102

[1] cumulative melt to DOY 110, after which there was no further snowmelt

[2] The primary melt event occurred at the SA-Sf plot when staff were not on-site to make frequent measurements

Table 2.5. Frame water balances from fall 2003 (DOY 305) to the end of snowmelt (DOY 110, 2004) and soil thaw (DOY 165, 2004). RC is runoff coefficient, ΔS is change in soil moisture storage and total inputs include snowmelt, rain and spring 2004 irrigation amounts.

Site	Plot	Frame	Fall 2003 Irrigation Depth (mm)	Snowmelt Inputs to DOY 110 (mm)	Snowmelt Runoff to DOY 110 (mm)	Snowmelt RC to DOY 110 (%)	Spring 2004 Irrigation Depth (mm)	Total inputs to DOY 165 (mm)	ΔS to DOY 165 (mm)	Drainage below 1 m to DOY 165 (mm)	Drainage Coefficient to DOY 165 (%)
SP	Sf	3	40	112	14	13	0	153	-3	142	93
		4	40	112	8	7	20	173	-1	166	96
		1	4	112	45	40	2	155	0	110	71
		2	4	112	14	13	0	153	2	137	90
	Nf	3	40	68	5	7	0	105	-5	105	100
		4	40	68	4	6	20	125	-4	125	100
		1	4	68	3	4	2	107	-2	106	99
		2	4	68	2	3	2	107 0	0	105	98
SA	Sf	1	40	93	33	35	0	128	-1	96	75
		3	40	93	38	41	20	148	-1	111	75
		2	4	93	33	35	0	128	14	81	63
		4	4	93	60	65	2	130	1	69	53
	Nf	1	40	87	4	5	0	116	0	112	97
		2	40	87	5	6	20	136	-3	134	99
		3	4	87	2	2	0	116	0	114	98
		4	4	87	22	25	2	118 0	-2	98	83
LA	Sf	1	40	134	12	9	0	205	13	180	88
		4	40	134	5	4	20	225	16	204	91
		2	4	134	9	7	0	205	39	157	77
		3	4	134	9	7	2	207	23	175	85
	Nf	3	40	92	5	5	20	160	64	91	57
		4	40	92	7	8	0	140	49	84	60
		1	4	92	3	3	2	142	20	119	84
		2	4	92	1	1	0	140	46	93	66

Table 2.6. Occurrence of concrete frost in runoff frames. Values are the percentage of locations tested (n = 5 per frame) that were underlain by concrete frost as determined by probing with a metal pin. Empty cells indicate that no measurements were made at that frame on that date

Site	Plot	Frame	Irrig Depth (mm)	April 1							April 22	May 6
				DOY								
				91	94	95	96	97	100	111	112	126
SP	Sf	3	40	60	80	80		100	80	60		0
		4	40	60	80	80		60	80	40		0
		1	4	60	80	80		60	80	20		0
		2	4	60	80	80		100	80	40		0
	Nf	3	40	0	0	0		0	40	20		0
		4	40	0	0	0		0	60	20		0
		1	4	0	0	0		0	0	0		0
		2	4	0	0	0		0	0	0		0
SA	Sf	1	40	100	100	100	100	80	80	60		0
		3	40	100	100	100	100	80	80	60		0
		2	4	100	100	100	100	80	80	60		0
		4	4	100	100	100	100	80	80	60		0
	Nf	1	40	0	0	20	20	20	20	0		0
		2	40	0	0	0	0	20	20	0		0
		3	4	0	0	0	0	20	20	0		0
		4	4	0	0	0	0	20	20	0		0
LA	Sf	1	40		0		40	60	20		50	0
		4	40		0		20	0	0		50	0
		2	4		0		40	40	20		50	0
		3	4		0		20	0	0		50	0
	Nf	3	40		0		0	0	0		40	0
		4	40		0		0	0	0		40	0
		1	4		0		0	0	0		40	0
		2	4		0		0	0	0		40	0

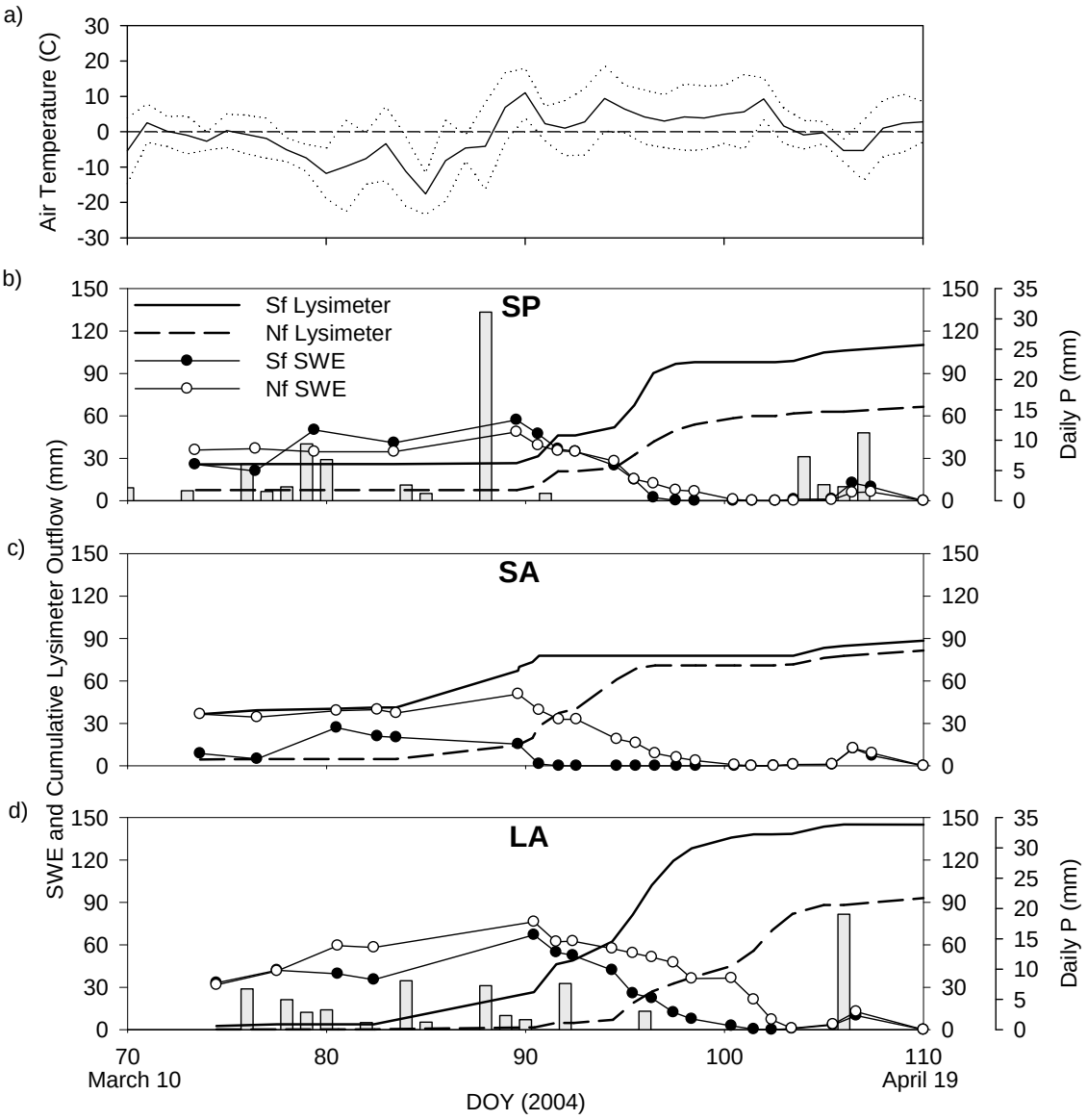

Figure 2.1. Time series of daily air temperature (a) and snow water equivalent (SWE), cumulative snowmelt outflow for lysimeters and daily precipitation at the SP (b), SA (c) and LA (d) sites. Precipitation plotted for the SP and LA sites was measured with Belfort gauges.

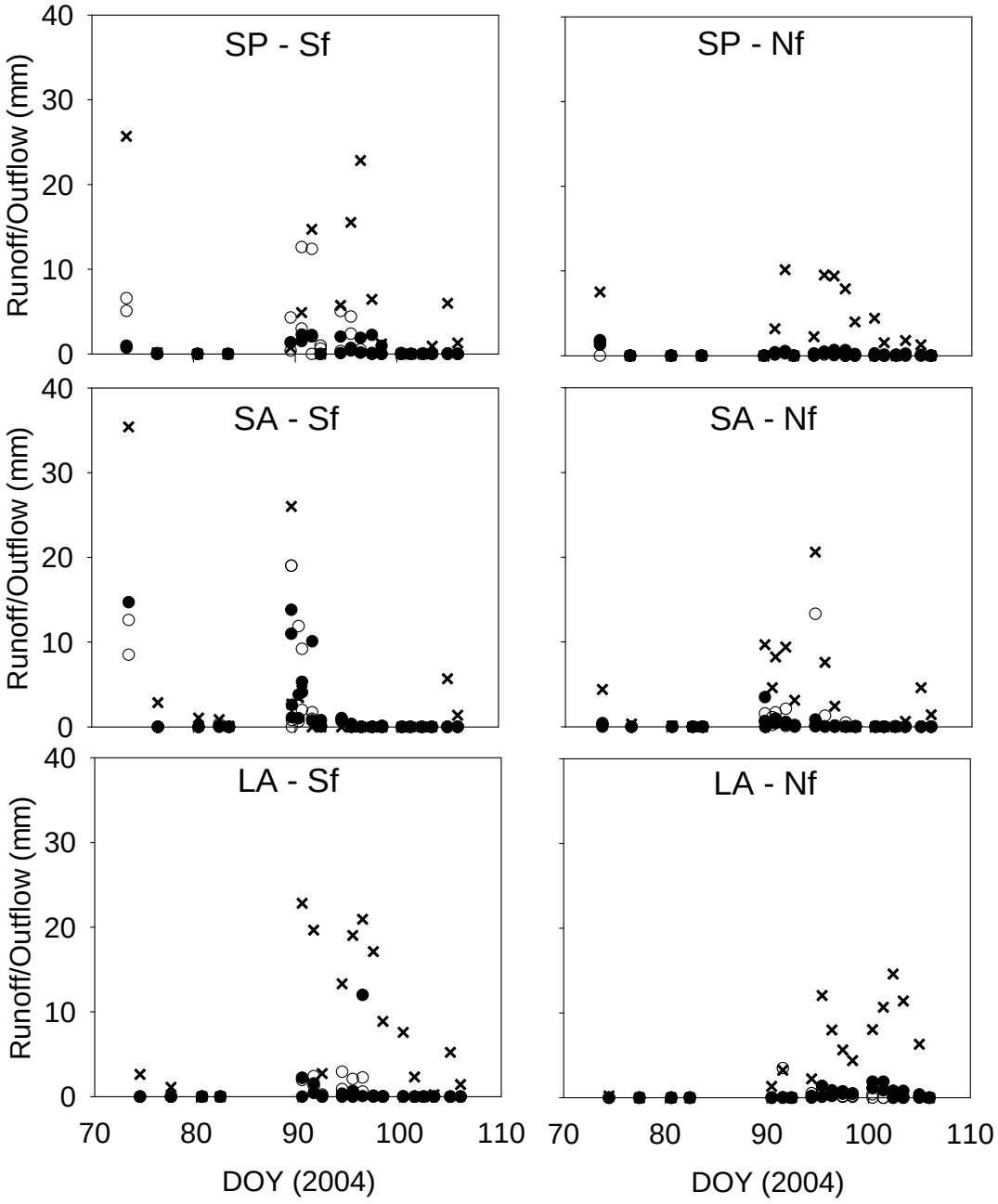

Figure 2.2. Time series of outflow from lysimeters (crosses) and runoff frames (circles) by site and plot. Frames that were irrigated in fall 2003 are indicated by filled circles; non-irrigated frames are indicated by open circles. Instances where frame runoff was greater than lysimeters outflow corresponds to times when the lysimeters were snow limited relative to the frames, due to spatial variability in snow accumulation and melt (Figure 2.5).

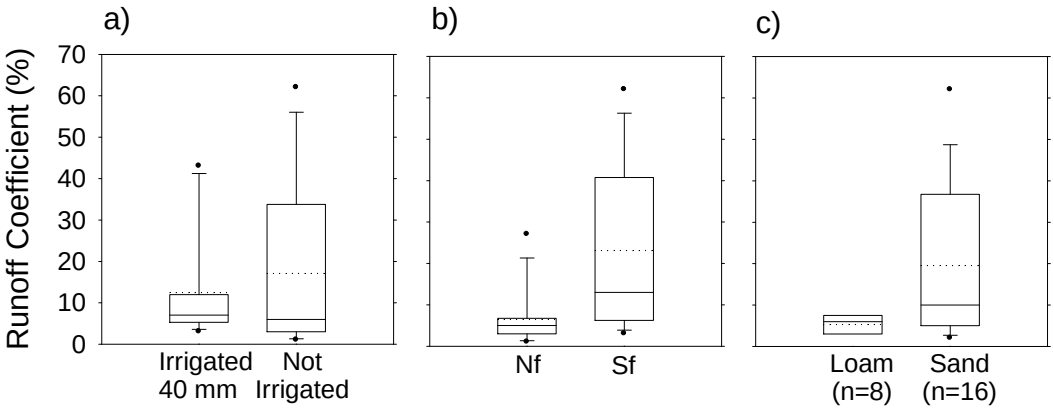

Figure 2.3. Boxplots of snowmelt runoff coefficients by site for irrigated vs. non-irrigated frames (a), aspect (b), and soil texture (c). Irrigated frames had 40 mm equivalent precipitation added in late October of 2003. The boxplot components are: centre of box is median, upper and lower ends of box are the 25 and 75th percentiles, the ends of the whiskers are the 10 and 90th percentiles, dots are outlying points and the dotted line is the mean.

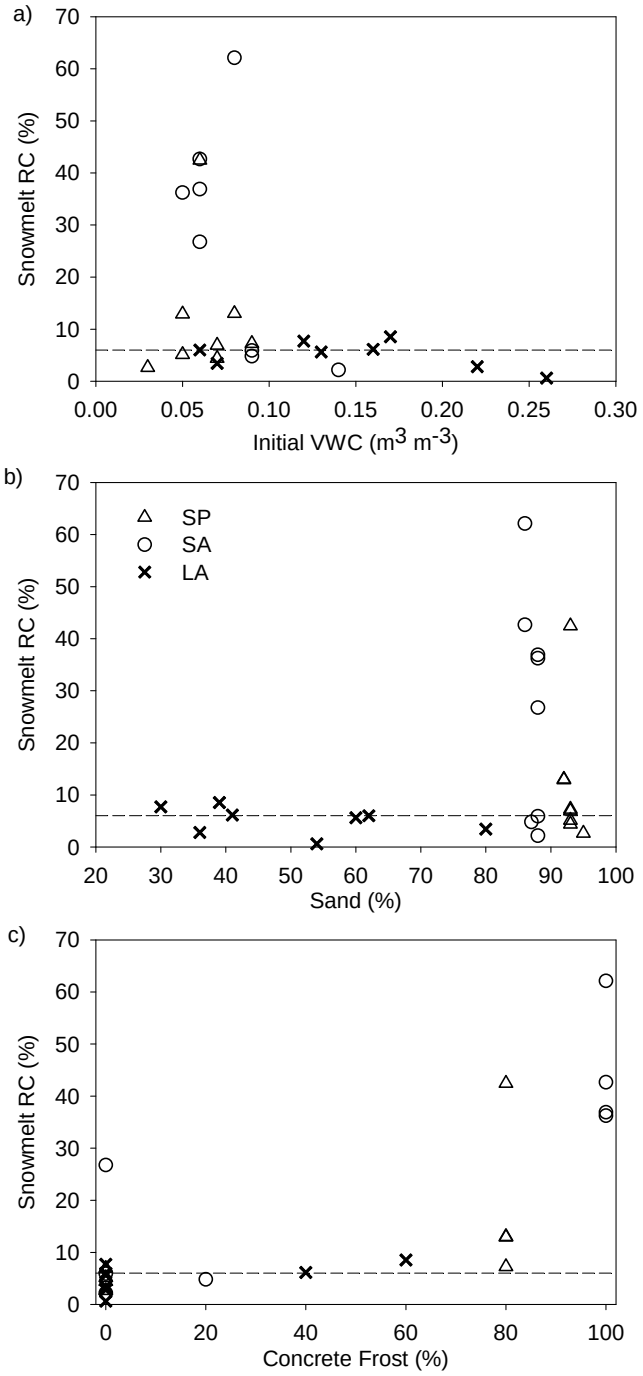

Figure 2.4. Relationship of snowmelt runoff coefficient (RC) to initial (fall) volumetric water content (a), sand content (b), and concrete frost occurrence (c) by site. Concrete frost occurrence is the proportion of sampled locations per frame as measured on (or closest date to) the date of maximum snowmelt.

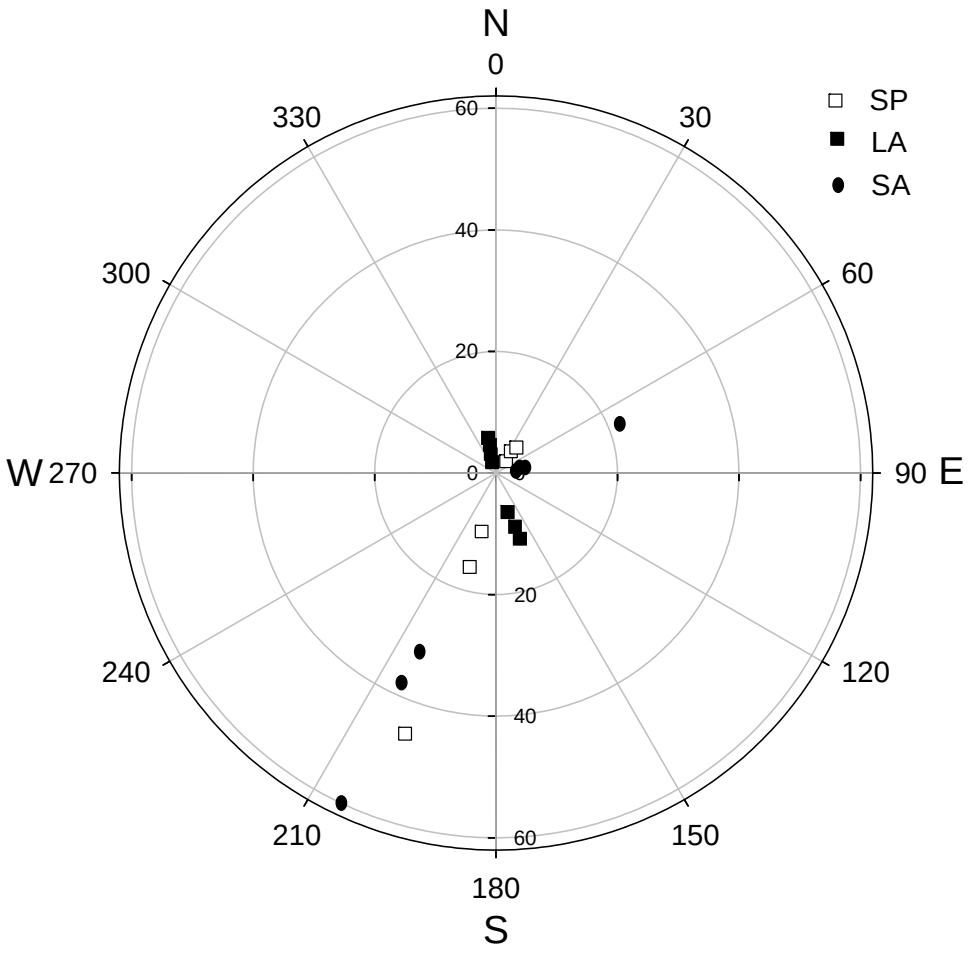

Figure 2.5. Influence of aspect (degrees from north) on runoff (mm, distance outwards from plot origin) for all plots.

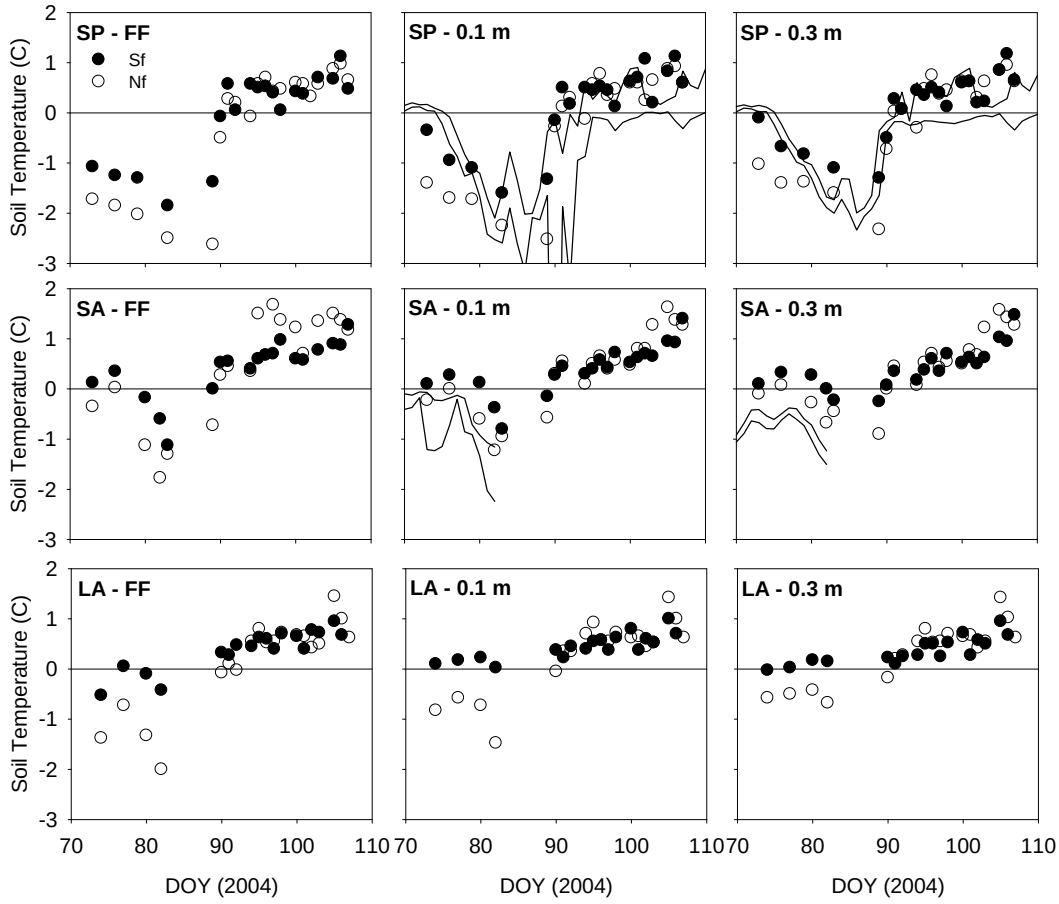

Figure 2.6. Time series of soil temperature for Sf and Nf plots at the SP, SA, and LA study sites. Point measurements were made in the forest floor (FF) (0.02 m above mineral soil surface), and at 0.1 and 0.3 m below the forest floor mineral soil interface. Continuous soil temperature measurements (daily maximum and minimum) made at the SP-Sf and SA-Sf plots are also plotted. Missing data at the SA-Sf plot are due to instrument failure. No continuous soil temperature data are available for the LA site due to instrument failure.

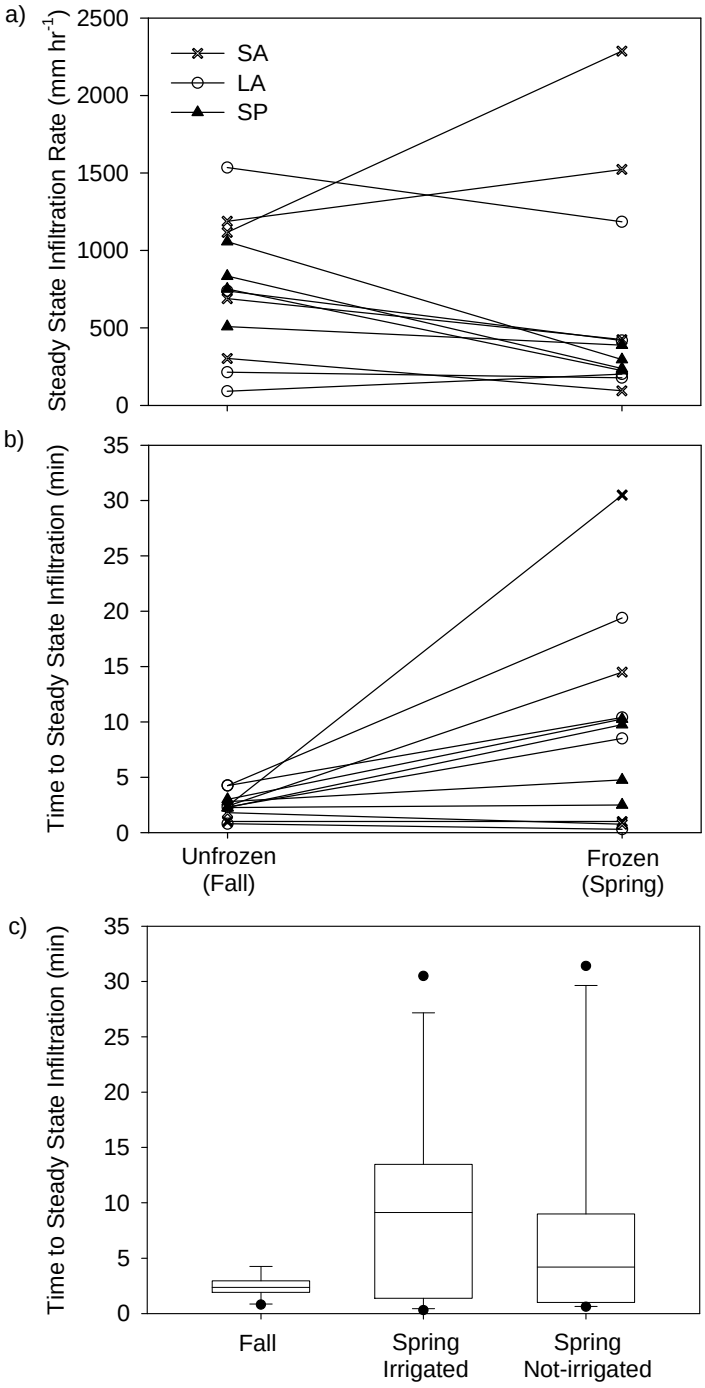

Figure 2.7. Frozen soil infiltration rates (a), infiltration time to steady state (b), and boxplots comparing infiltration rates between fall (measured October 5–7, 2003), spring previously irrigated (measured April 9–22, 2004), and spring not-irrigated (measured April 9–22, 2004) (c). For the boxplots $n = 12$. The lines between the points in panels a) & b) indicate the change in infiltration rate or time to steady state between fall and spring measurements for the same locations.

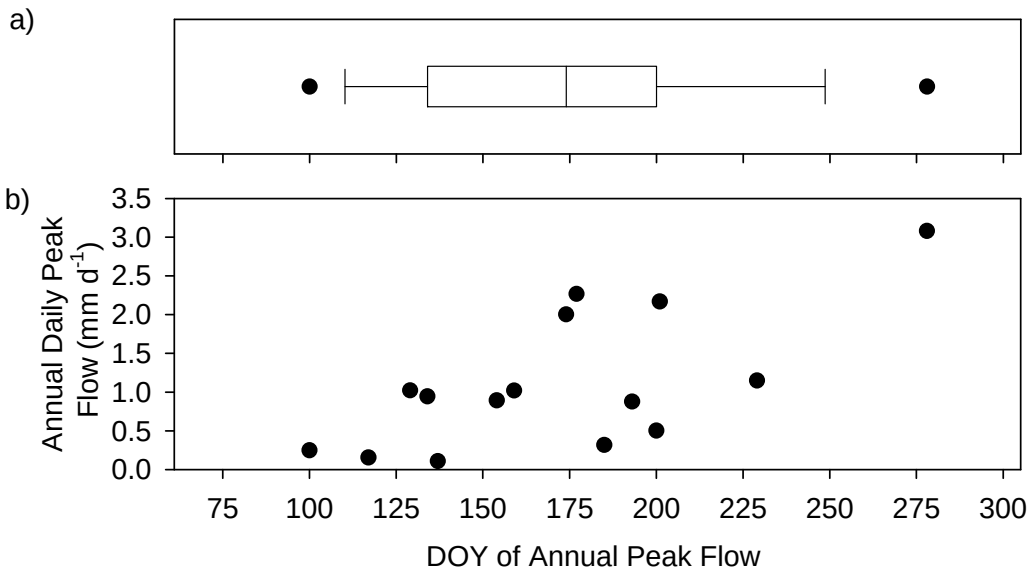

Figure 2.8. Annual daily peak streamflow for Red Earth Creek, Red Earth, Alberta, 1987-2001: temporal distribution of peak flow date (a), and the relationship between peak flow date and peak flow magnitude (b).

2.7 References

Arain, M.A., Black, T.A., Barr, A.G., Griffis, T.J., Morgenstern, K. and Nesic, Z. 2003. Year-round observations of the energy and water vapour fluxes above a boreal black spruce forest. Hydrological Processes 17: 3581-3600.

Barnett, T.P., Adam, J.C. and Lettenmaier, D.P. 2005. Potential impacts of a warming climate on water availability in snow-dominated regions. Nature 438: 303-309

Bayard, D., Stahli, M, Parriaux, A, and Fluhler, H. 2005. The influence of seasonally frozen soil on the snowmelt runoff at two alpine sites in southern Switzerland. Journal of Hydrology 309: 66-84.

Bonan, G.B. 2002. Ecological Climatology. Cambridge University Press. Cambridge, UK. 678 pp.

Carey, S.K. and Woo, M.K. 1999. Hydrology of two slopes in subarctic Yukon, Canada. Hydrological Processes 13: 2549-2562.

Cline, R.G., Haupt, H.F. and Campbell, G.S. 1977. Potential water yield response following clearcut harvesting on north and south slopes in northern Idaho. USDA Forest Service Research Paper INT-191.

Devito, K., Creed, I., Gan, T., Mendoza, C., Petrone, R., Silins, U. and Smerdon, B. 2005a. A framework for broad-scale classification of hydrologic response units on the Boreal Plain: is topography the last thing you should consider? Hydrological Processes 19: 1705-1714.

Devito, K.J., Creed, I.F. and Fraser, C.J.D. 2005b. Controls on runoff from a partially harvested aspen-forested headwater catchment, Boreal Plain, Canada. Hydrological Processes 19: 3-25.

Dunne, T. and Black, R.D. 1971. Runoff processes during snowmelt. Water Resources Research 7: 1160-1172.

Ecoregions Working Group. 1989. Ecoclimatic regions of Canada. Ecological Land Classification Series No. 23.

Elliot, J.A., Toth, B.M., Granger, R.J. and Pomeroy, J.W. 1998. Soil moisture storage in mature and replanted sub-humid boreal forest stands. Canadian Journal of Soil Science 78: 17-27.

Environment Canada. 2004. Canadian Climate Normals 1971-2000: Slave Lake, Alberta. http://climate.weatheroffice.ec.gc.ca/climate_normals/index_e.html (accessed March 22, 2009)

Environment Canada. 2006. Canadian Climate Data Online: Red Earth, Alberta. http://climate.weatheroffice.ec.gc.ca/climateData/canada_e.html (accessed March 22, 2009).

Evett, S.R., Tolk, J.A. and Howell, T.A. 2006. Sensors for soil profile moisture measurement: Accuracy, axial response, calibration, precision and temperature dependence. Vadose Zone Journal 5: 894-907.

Fenton, M.M, Paulen, R.C., and Pawlowicz, J.G. 2003. Surficial geology of Lubicon Lake area, Alberta (NTS 84B/SW). Alberta Geological Survey.

Granger, R.J., Gray, D.M. and Dyck, G.E. 1984. Snowmelt infiltration to frozen prairie soils. Canadian Journal of Earth Sciences 21: 669-677.

Grier, C.G. and Running, S.W. 1977. Leaf area of mature northwestern coniferous forests: relation to site water balance. Ecology 58: 893-899.

Hardy, J.P., Groffman, P.M., Fitzhugh, R.D., Henry, K.S., Welman, A.T., Demers, J.D., Fahey, T.J., Driscoll, C.T., Tierney, G.L. and Nolan, S. 2001. Snow depth manipulation and its influence on soil frost and water dynamics in a northern hardwood forest. Biogeochemistry 56: 151-174.

Harms, T.E. and Chanasyk, D.S. 1998. Variability of snowmelt runoff and soil moisture recharge. Nordic Hydrology 29: 179-198.

Harr, R.D. 1981. Some characteristics and consequences of snowmelt during rainfall in western Oregon. Journal of Hydrology 53: 277-304.

Hart, G.E., and Lomas, D.A. 1979. Effects of clearcutting on soil water depletion in an Engelmann spruce stand. Water Resources Research 15: 1598-1602.

Kachanoski, R.G. and DeJong, E. 1982. Comparison of the soil water cycle in clear-cut and forested sites. Journal of Environmental Quality 11: 545-549.

Kalef, N. 2002. Interlinking hydrological behaviour and inorganic nitrogen cycling a forested boreal wetland. M.Sc. Thesis, University of Alberta, Edmonton, Alberta.

Kalra, Y.P. and Maynard, D.G. 1991. Methods Manual for Forest Soil and Plant Analysis. Edmonton, AB. Forestry Canada, Northern Forestry Centre. Information Report NOR-X-319.

Kane, D.L. and Stein, J. 1984. Plot measurements of snowmelt runoff for varying soil conditions. Geophysica 20: 123-135.

Mace Jr., A.C. 1968. Effects of soil freezing on water yields. USDA Forest Service Research Note RM-121.

Marks, D., Link, T., Winstral, A. and Garen, D. 2001. Simulating snowmelt processes during rain-on-snow over a semi-arid mountain basin. Annals of Glaciology 32: 195-202.

Marshall, I.B., Schut, P., and Ballard, M. (compilers). 1999. A National Ecological Framework for Canada: Attribute Data. Environmental Quality Branch, Agriculture and Agri-Food Canada, Ottawa/Hull. http://sis.agr.gc.ca/cansis/nsdb/ecostrat/data_files.html (accessed March 22, 2009)

McEachern, P., Prepas, E.E. and Chanasyk, D.S. 2006. Landscape control of water chemistry in northern boreal streams of Alberta. Journal of Hydrology 323: 303-324.

Molotch, N.P., Blanken, P.D., Williams, M.W., Turnipseed, A.W., Monson, R.K., and Margulis, S.A. 2007. Estimating sublimation of intercepted and sub-canopy snow using eddy covariance systems. Hydrological Processes 21: 1567-1575.

Moore, R.D. and Scott, D.F. 2005. Camp Creek revisited: Streamflow changes following salvage harvesting in a medium-sized, snowmelt dominated catchment. Canadian Water Resources Journal 30: 331-344.

Murray, C.D. and Buttle, J.M. 2003. Impacts of clearcut harvesting on snow accumulation and melt in a northern hardwood forest. Journal of Hydrology 271: 197-212.

Newman, B.D., Wilcox, B.P. and Graham, R.C. 2004. Snowmelt driven macropore flow and soil saturation in a semarid forest. Hydrological Processes 18: 1035-1042.

Pierce, R.S., Lull, H.W. and Storey, H.C. 1958. Influence of land use and forest condition on soil freezing and snow depth. Forest Science 4: 247-263.

Pomeroy, J.W., Granger, R.J., Pietroniro, A., Elliott, J.E., Toth, B. and Hedstrom, N. 1997. Hydrological pathways in the Prince Albert Model Forest. The Prince Albert Model Forest Association. 154 pp.

Pomeroy, J.W., Parviainen, J., Hedstrom, N. and Gray, D.M. 1998. Coupled modeling of forest snow interception and sublimation. Hydrological Processes 12: 2317-2337.

Price, A.G. and Hendrie, L.K. 1983. Water motion in a deciduous forest during snowmelt. Journal of Hydrology 64: 339-356.

Proulx, S, and Stein, J. 1997. Classification of meteorological conditions to assess the potential for concrete frost formation in boreal forest floors. Canadian Journal of Forest Research 27: 953-958.

Redding, T.E., Hannam, K.D., Quideau, S.A. and Devito, K.J. 2005. Particle density of aspen, spruce and pine forest floors in Alberta, Canada. Soil Science Society of America Journal 69: 1503-1506.

Reynolds, W.D. and Elrick, D.E. 2002. Sing-ring and double-or concentric-ring infiltrometers. In: Dane, J.H. and Topp, G.C. Methods of Soil Analysis: Part 4, Physical Methods. Madison, WI. Soil Science Society of America. P.821-826.

Smerdon, B.C. 2006. The influence of climate on water cycling and lake-groundwater interaction in an outwash landscape on the Boreal Plains of Canada. PhD Thesis, University of Alberta, Edmonton, AB.

Soil Classification Working Group. 1998. The Canadian System of Soil Classification (Third Edition). Ottawa, ON. Agriculture and Agri-Food Canada.

Stadler, D., Wunderli, H., Auckenthaler, A., Fluhler, H. and Brundle, M. 1996. Measurement of frost-induced snowmelt runoff in a forest soil. Hydrological Processes 10: 1293-1304.

Stein, J., Proulx, S. and Levesque, D. 1994. Forest floor frost dynamics during spring snowmelt in a boreal forested basin. Water Resources Research 30: 995-1007.

Vogwill, R. 1978. Hydrogeology of the Lesser Slave Lake area, Alberta. Edmonton, AB. Alberta Research Council. 30 pp.

Whitson, I.R. and Chanasyk, D.S. and Prepas, E.E. 2004. Patterns of water movement on a logged Gray Luvisolic hillslope during the snowmelt period. Canadian Journal of Soil Science 84: 71-82.

Winkler, R.D. 2001. The effects of forest structure on snow accumulation and melt in south-central British Columbia. PhD Thesis. University of British Columbia, Vancouver, BC.

Woo, M.K. 2005. Snowmelt runoff generation (Ch. 114). In: Anderson, M.G. (ed.). Encyclopedia of Hydrological Sciences. John Wiley and Sons Ltd. Chichester, UK. 1741-1749.

Young, K.L., Woo, M.K. and Edlund, S.A. 1997. Influence of local topography, soils and vegetation on microclimate and hydrology at a high Arctic site, Ellesemere Island, Canada. Artic and Alpine Research 29: 270-284.

Zar, J.H. 1984. Biostatistical Analysis. 2nd ed. Prentice-Hall, Inc., Englewood Cliffs, N.J.

Zhao, L. and Gray, D.M. 1999. Estimating snowmelt infiltration into frozen soils. Hydrological Processes 13: 1827-1842.

Chapter 3

Lateral Flow Thresholds for Aspen Forested Hillslopes

A version of this chapter has been published:
Redding, T.E. and Devito, K.J. 2008. Lateral flow thresholds for aspen forested hillslopes on the Western Boreal Plain, Alberta, Canada. Hydrological Processes 22: 4287-4300.

3.1 Introduction

Understanding when hillslopes "turn on" and connect with surface waters is critical to predicting the long-term sustainability of regional water resources and water quality for the Boreal Plains region of northern Alberta (Devito et al. 2005a). On the Boreal Plains, natural variability in streamflow is high, with generally low annual streamflow interspersed with years of large response (Table 3.1). The combination of a subhumid climate with annual precipitation that is slightly less than potential evapotranspiration and the complex geology of deep glacial sediments results in large available soil storage capacity relative to moisture surpluses or deficits; thus, water cycling is complex, non-linear, and threshold dependent (Devito et al. 2005a, Schoeneberger and Wysocki 2005). This threshold-type response indicates that precipitation depth and timing, in relation to available storage capacity, are strong controls on runoff in this landscape (Devito et al. 2005b). Understanding this threshold behaviour is important for predicting the effects of future climate change and landscape disturbance on water cycling and hillslope runoff.

Given the climate and complex surficial geology of the Boreal Plains, it is expected that unsaturated zone storage and vertical flow dominates the hillslope water balance rather than lateral flow (Devito et al. 2005b). A study of runoff generation in a partially harvested Boreal Plains headwater catchment showed that surface water runoff is generally low; hillslope contributions to catchment runoff were noted in only one out of five years (Devito et al. 2005b). When hillslope runoff occurred in response to a large rainfall event with high antecedent soil moisture storage, the authors hypothesized that flow occurred through rapid vertical preferential flow to a clay-rich layer, and then lateral flow was generated

via the transmissivity feedback mechanism. Vertical preferential flow through cracks and fissures has also been noted in similar soils on the Canadian Prairies (Hendry 1982, Hayashi et al. 1998). The combination of vertical flow to a confining layer followed by lateral flow along the confining layer is common for hillslopes in humid and steep environments (Peters et al. 1995, Buttle and McDonald 2002, Tromp van Meerveld and McDonnell 2006); however, lateral flow is typically observed in regions that feature a shallow confining layer and large precipitation surplus relative to available soil moisture storage.

The low probability of large rain events and consequently infrequent nature of hillslope runoff inhibits monitoring studies on the Boreal Plains; thus, manipulative experiments are required to understand when hillslopes contribute flow and when the system becomes wet enough to generate lateral flow. This chapter reports the results of rainfall simulation experiments that were designed to elucidate the vertical and lateral flow thresholds for forested hillslopes on the Boreal Plains of Alberta. It was hypothesized that vertical flowpaths (soil storage and drainage below root zone) dominate hydrologic response regardless of precipitation inputs or antecedent moisture content. The potential for lateral flow to occur may increase once soils are near saturation; however, the relative contribution of upland runoff to regional flow is not known. The use of rainfall simulations allowed the manipulation of the system under study, to assess hydrologic thresholds (Kirchner 2006) and infer potential effects of forest harvest on runoff generation and recharge from forested upland hillslopes. The experimental design included the use of two contrasting antecedent soil moisture conditions to simulate the effects of forest harvesting on soil moisture content. The specific questions addressed were:

1. What are the precipitation and antecedent soil moisture thresholds required to generate vertical drainage and lateral flow in Luvisolic soils in the Boreal Plains region of Alberta?
2. What is the relative magnitude of vertical versus lateral flow?
3. What are the potential effects of forest harvesting on vertical and lateral flow on the hillslopes in the region?

Understanding the potential hydrologic coupling of hillslopes with receiving surface waters is critically important for predicting the sustainability (maintaining water levels and biological functioning) and biogeochemistry of wetlands and ponds, and for understanding the potential effects of forest harvesting on water resources.

3.2 Study Site

The rainfall simulation experiments were conducted at the Utikuma Region Study Area (URSA) near Utikuma Lake (lat: 56°04'45.05" N, long: 115°28'58.74" W), in north-central Alberta (Figure 3.1) (Devito et al. 2005a). The site is located within the Boreal Plains ecozone. Mean annual precipitation and potential evapotranspiration are 481 and 518 mm, respectively (Marshall et al. 1999). The climate at the study site is classified as subhumid in the Canadian Ecoregion system (Ecoregions Working Group 1989), and as Dfb (cold, without dry season, warm summer) using the Koppen-Geiger system (Peel et al. 2007). The long-term (1987–2001) mean annual runoff for Red Earth Creek (619 km^2, 70 km north of URSA) is 67 mm yr^{-1}, and ranges between 4 and 246 mm yr^{-1} (median: 58 mm yr^{-1}), corresponding to runoff coefficients of 1–53 % (median: 14%) (Table 3.1) (Environment Canada 2006a).

The rainfall simulation plots were established on a hillslope with Gray Luvisolic soils (Soil Classification Working Group, 1998) that had developed from disintegration of moraine deposits. These soils are typically silt-rich but spatially heterogeneous with zones of high clay or sand content (Figures 3.1 and 3.2) (Fenton et al. 2003). In the study region, glacial till deposits range from 20 to 240 m in thickness and overlay Upper Cretaceous Smoky Group shale bedrock (Vogwill, 1978). Typical hillslope-wetland-pond toposequences on hummocky moraine sites feature deep water tables in the uplands, which slope from wetland to upland (Figure 3.1). Spatial variability in water table depth is high in finer-textured sediments. The top of the hillslope under study is approximately 5 m higher than the adjacent pond. In the area of the study plots, the water table is more than 4 m below the ground surface (Figure 3.1). The top of the study

hillslope features a large peatland with a water table elevation that is higher than that of the adjacent uplands and downslope pond. Additionally, the small depression with well 511w (Figure 3.1) periodically has perched standing water or groundwater, while the adjacent wells (513w, 514w) are dry.

The overstory canopy of the study hillslope is predominantly trembling aspen (*Populus tremuloides*), with minor amounts of black cottonwood (*Populus balsamifera*) in depressions and draws. The understory vegetation at the study site includes prickly rose (*Rosa acicularis*) and high-bush cranberry (*Viburnum edule*) in the shrub layer, and twinflower (*Linnaea borealis*) in the herb layer. The forest floor surface is dominated by aspen litter with small amounts of mosses and lichens.

3.3 Methods

Two runoff plots were established at a mid-slope position on a hillslope with a westerly aspect. The plots were placed 3 m apart under an aspen canopy (Figure 3.1). One plot was used as a root exclusion plot (RE); the other was used as a root uptake (RU) plot. The RE plot was installed in mid-July 2004 (day of year [DOY] 204), 55 days prior to the initiation of the irrigation treatment applications. Roots were excluded by trenching around an area of undisturbed soil. The soil columns were then wrapped in heavy polyethylene to a depth of 0.75 m on the sides and upslope end, and the trenches were backfilled. To collect any water running down the inside of the plastic barrier, a perforated PVC pipe was installed to act as a drain. The pipe was routed to a plastic container to collect any water flow, but none was observed. During the growing season, the downslope face of the RE soil columns were also wrapped in plastic and periodically checked for accumulation of lateral flow water (none was observed). Trenching treatments prevented water uptake by tree roots but allowed understory transpiration and soil surface evaporation to occur. The RU plot was installed 3 m downslope from the RE plot, and allowed water uptake by tree roots to occur throughout the entire growing season. The RU plot was established by trenching as described above, 1 day prior to the initiation of irrigation (September 16, 2004,

DOY 260). The RE plot was 1.55 x 1.9 m (2.95 m^2), with a surface slope of 0.15; the RU plot was 1.7 x 2.0 m (3.4 m^2) with a surface slope of 0.09. Prior to the first irrigation treatment, understory vegetation in both plots was clipped to a height of approximately 0.05 m above the forest floor surface. Visual inspection of the overstory canopy indicated it was similar in both plots.

The soils of both plots were described in the field (Figure 3.2), and samples were collected for laboratory analysis of texture, bulk density, porosity, and background concentrations of Cl^- and Br^-. Soil bulk density was sampled using 0.06-m diameter and 0.05-m long cores. Samples of mineral soil were dried at 105^{o}C for 24 hours; forest floor (FF) soil samples were dried at 70^{o}C for 48 hours. Porosity was calculated using the measured bulk density data and particle density values of 1.54 Mg m^{-3} for forest floor and 2.65 Mg m^{-3} for mineral soil (Redding et al. 2005). Particle size analysis was conducted on 63 soil samples per plot using the hydrometer method with carbonate pre-treatment (Kalra and Maynard 1991). Field saturated hydraulic conductivity (K_s) was measured near the irrigation plots and across the upland in which the plots were located using a Guelph Permeameter (Reynolds and Elrick 2002) and single-ring infiltrometer (Reynolds et al. 2002) at a range of depths from the mineral soil surface to 0.75 m.

To measure lateral flow from the downslope face of each plot, metal troughs were inserted 0.05 m into the face of the soil column at the FF-Ae (FF trough), Ae-Bt (A trough), and Bt-BC or Bt-C (B trough) horizon interfaces, and at the base of the excavated downslope face to collect lateral flow from the BC and/or C (C trough) horizon (Figure 3.2). Lateral flow intercepted by troughs was routed through plastic gutters and collected in buckets (high flow) or bags (lower flow) for determination of runoff volume (Peters et al. 1995). Samples of runoff water were collected for analysis of water chemistry. Samples were collected at 5-minute intervals during high flow and at 10–60- minute intervals during low flow conditions.

Within each plot, soil moisture content was measured with time domain reflectometry (TDR) probes (CS616, Campbell Scientific Inc., Logan Utah)

connected to a data logger (CR10X, Campbell Scientific Inc., Logan Utah). The TDR probes were installed approximately 0.5 m upslope from the downslope face of the soil columns and on the north side of the columns. The probes were placed at +0.05 m in the FF (where 0 cm is the FF-mineral soil interface), and at -0.1, -0.2, -0.3, -0.5, -0.75 m depth (Figure 3.2). Soil moisture measurements were recorded every 10 minutes during the 8 days of the irrigation experiments, and every 2 hours during the pre- and post-irrigation monitoring periods. All TDR probes were individually calibrated prior to the experiment. Soil moisture in the top 1 m of the mid-slope soil profile was measured weekly during the 2004 growing season. Measurements were taken using 0.2-m-long bifilar TDR probes installed horizontally at +0.05 m in the FF, and at -0.1, -0.2, -0.3, -0.5, and -1.0 m depth. Dielectric permittivity was determined by using a Tektronix 1502C cable tester (Tektronix Inc, Beaverton, OR). Soil moisture content was estimated using the Topp equation (Topp et al. 1980) for mineral soil and the Schaap et al. (1996) equation for FF.

Eight rainfall simulations were conducted over consecutive days from September 17 to 24, 2004 (DOY 261–268) (Table 3.2). During this period, tarps were suspended above the plots to minimize inputs of natural precipitation. Water was applied as evenly and rapidly as possible using a hand-held watering can; however, the uniformity of water application was not measured. Each plot was irrigated separately, and the RE plot was irrigated first each day (starting at ~0900 hrs). No water was applied to the soil surface within 0.05 m of the plot edges so that the potential for flow down the plastic sides of the plot or direct infiltration into the FF trough was minimized.

During the irrigation period, water balances for the top 1 m of soil (0.1 m FF and 0.9 m mineral soil) within each plot were calculated using the applied precipitation depth, lateral flow collected in the troughs, and change in soil moisture storage measured using TDR. Transpiration losses were assumed to be negligible since all tree and shrub uptake was removed by root exclusion and clipping of above-ground biomass. In addition, surface evaporation was probably negligible because the plots were shaded and air temperatures were cool during

the experiment. Consequently, the water balance equation was solved for drainage below the one metre depth:

$$D = P - \Delta S - R + e \qquad \text{[Equation 3.1]}$$

where D is drainage below one metre depth (mm), P is irrigation inputs (mm), ΔS is the change in soil moisture storage in the top 1 m (mm), R is the measured lateral flow (mm), and e is the measurement error (mm). Errors in water balance terms were estimated as 0.05 m^3 m^{-3} for volumetric water content (Campbell Scientific 2004), and 5% for measurements of runoff (Peters et al. 1995).

To examine infiltration depths, Cl^- and Br^- were added to irrigation water to act as tracers. The Cl^- tracer was added as KCl to the first irrigation event (30 L) at a concentration of 4100 mg L^{-1} ($[Cl^-]$ = 985 mg L^{-1}). The Cl^- acted as a drainage depth tracer for the percolating water because lateral flow was not expected from the first irrigation event. The Br^- tracer was added as LiBr to the seventh irrigation event (120 L) (Table 3.2) at a concentration of 2000 mg L^{-1} ($[Br^-]$ = 920 mg L^{-1}). Lateral flow was expected to occur after this event. The Br^- tracer was used to quantify the drainage depth associated with irrigation events 7 and 8.

Following the final (eighth) simulated rainfall event, the plots were covered (with tarps laid over the ground surface) and allowed to drain for two weeks, after which time the plots were excavated and soil samples were collected. The samples were used to characterize the spatial distribution of applied Cl^- and Br^- tracers, as well as soil properties within the plots. Samples were collected at the following depths along 18 vertical profiles within each plot: +0.05 (FF), -0.05, -0.15, -0.25, -0.35, -0.45, -0.55, -0.65, -0.75, -0.85, -0.95, -1.1, -1.3, and -1.5 m. From the surface to 0.95 m, samples were collected using a core sampler (0.06 m diameter, 0.05 m length). Below 0.95 m, samples were collected using a bucket auger. All soil samples were oven dried to determine moisture content and bulk density. To analyze Cl^- and Br^- concentrations, the samples were extracted using 1:5 (mineral soil) or 1:10 (FF) mixtures of dry soil and distilled deionized water

(DDW). Slurries were shaken for 1 hour and then filtered through Whatman No.42 filter paper and 0.2 μm Millipore syringe filters. Analysis of tracer concentrations (Br^-, Cl^-) for soil extracts was performed on a Dionex DX600 ICP (Dionex, Sunnyvale CA). Concerns over tracer recovery prompted a secondary experiment to examine the efficacy of using a second extraction to recover the applied tracers. A selection of 33 samples was extracted twice in DDW with different shaking times. Samples were chosen to represent the range of depths and soil textures encountered within the irrigation plots. Following the initial extraction, samples were re-dried, and the 33 subsamples were re-extracted (as above) and shaken for a further 16 hours (J. Robertson, University of Alberta, personal communication).

The first extraction using the standard method (extract in DDW and shaken for 1 hour) did not fully extract either Cl^- or Br^- from the soils. The combined recovery from the two extractions was 10–30% greater than from the initial extraction. For both Cl^- and Br^-, there was a strong positive relationship between the tracer concentration measured from the first extraction and the sum of tracer concentrations from the two extractions (Table 3.2). There were no strong relationships between recovery of the tracers and the depth of soil samples (Cl^- recovery: $r^2 = 0.31$, $P < 0.002$; Br^- recovery: $r^2 = 0.45$, $P<0.0001$) or the clay content of the soil samples (Cl^- recovery: $r^2 = 0.02$, $P < 0.03$; Br^- recovery: $r^2 = 0.19$, $P < 0.002$). The slope of the regression between the total tracer recovered (sum of concentrations for extractions 1 and 2) and the extraction 1 concentration for FF and mineral soils was used to estimate the total tracer recovery for samples that did not undergo a second extraction (Table 3.2).

The tracer mass balance (Cl^-, Br^-) was calculated using measured tracer concentrations in the lateral flow water and soil. The total mass of tracer in lateral flow water was calculated as the product of the concentration and the volume of water collected in a given time interval. Tracer mass stored in the soil after all the irrigation events was calculated two ways (using the corrected tracer concentrations): (1) the mean concentration of each depth interval, and (2) areally weighted concentration for each depth interval using the Thiessen Polygon

method. Background Cl^- and Br^- concentrations were determined from pre-irrigation samples collected during plot installation, and were supplemented with additional soil samples that were collected during the installation of nearby groundwater monitoring wells.

3.4 Results

3.4.1 Soil Properties

The soil properties of the two experimental plots were similar for most characteristics measured, with a predominance of silt (> 60%) and smaller amounts of clay and sand at each site (Figures 3.2 and 3.3). The RE plot had a higher mean clay content than the RU plot, but the differences were not statistically significant (Figure 3.3). K_s decreased with depth (Figure 3.3). The RE plot featured a BC horizon, which was absent in the RU plot.

3.4.2 Plot Water Balances

3.4.2.1 Pre-Irrigation Aspen Forest Soil Moisture Regime

Soil moisture storage dominated the water balance of the RE plot during the pre-irrigation period (Figure 3.4). Between DOY 204 and 261, the total precipitation, measured with a tipping bucket in an opening approximately 500 m from the plot, was 151 mm. On 29 of the 56 pre-irrigation days, precipitation was greater than 0.25 mm; on five days, rainfall exceeded 10 mm. The cumulative increase in soil moisture storage (126 mm) was similar to the cumulative rainfall during the same period (151 mm). The RE plot had an initial soil moisture storage of 411 mm (DOY 204) in the top metre of soil (0.1 m of FF and 0.9 m of mineral soil); final moisture storage was 537 mm (DOY 260, ΔS = +126 mm) over the period of isolation. Large increases in soil moisture were observed during the two large rain events in July and August. No lateral flow was observed during July and August even during the largest event in which 27.5 mm of rain fell with a maximum 30-minute intensity of 5 mm hr^{-1} (Figure 3.4).

In contrast to the large changes in soil moisture storage in the RE plot during July and August, there was little cumulative response of soil moisture to

summer rainfall at two other forested mid-slope sites adjacent to the RE plot. The increase in storage at these sites did not occur until large precipitation events (mixed rain and snow) occurred in late August and early September (Figure 3.4), when the canopy vegetation was no longer transpiring. Overall changes in soil moisture storage ranged from 247 to 389 mm (ΔS = +142 mm: "Mid-slope-1", 3 m north), and from 294 to 368 mm (ΔS = +74 mm: "Mid-slope-2", 50 m north).

3.4.2.2 Irrigation Period

Irrigation water was applied to simulate rainfall events of high intensity and relatively large volumes (Table 3.3). Over the eight days of applied irrigation events, the total simulated rainfall was 173.2 and 149.8 mm for the RE and RU plots, respectively (Table 3.2). The maximum total 8-day precipitation measured at Slave Lake, Alberta (1970–1997) was 177 mm (Environment Canada 2006b), which, in contrast to this study, occurred in summer when vegetation was actively using water. The intensities of the simulated precipitation ranged from 26 to 102 mm hr^{-1}, which corresponded to return periods of three years or more for smaller events and over 100 years for the largest events (Table 3.3) (Hogg and Carr 1985).

Soil moisture storage dominated the response of the RU plot to the simulated precipitation, whereas only a small increase in storage occurred on the RE plot. Soil moisture measurements (Table 3.3) indicate that the RU plot continued to have large increases in soil moisture storage through irrigation event 7. The increase in storage on the RE plot was small relative to irrigation inputs (10 mm out of 173 mm), and was within measurement error (Table 3.3). Over the course of the rainfall simulations, the increase in storage on the RU plot (167 ± 25 mm) was similar to the rainfall applied (150 mm), although within-plot sampling error indicates a slightly greater increase in storage than rainfall applied (Table 3.3). This discrepancy may be due to the spatial variability of the soils, non-uniformity of water application, and/or the placement of TDR probes near the downslope end of the plot. The effect of the addition of the Cl^- tracer on soil

electrical conductivity (EC) may also have influenced the readings of the CS616 probes (Campbell Scientific 2004).

Vertical drainage below 1 m dominated the hydrologic response of the RE plot but was minor on the RU plot. Drainage below 1 m was estimated (Equation 3.1) to be 123 ± 29 mm for the RE plot, and not different from zero (–26 ± 25 mm) for the RU plot (Table 3.3). The drainage estimate for the RU plot, which was solved as the residual of the water balance equation (Equation 3.1), was affected by the possible errors in the measured soil moisture storage discussed above.

Lateral flow collected in the troughs was a small proportion of the total water balance on the plots. For the RE plot, the total lateral flow for all events was 40 mm, which is a runoff coefficient of 24% for the eight events (Table 3.3). The RU plot produced a total of 8 mm of lateral flow, which is a runoff coefficient of 6% (Table 3.3).

Eighteen days following the final irrigation event, with no precipitation inputs or evaporation losses (plots were covered with tarps), the soil moisture storage in the top 1 m of the RE and RU plots had decreased from 547 to 520 mm (ΔS = -27 mm) and 495 to 448 mm (ΔS = -47 mm), respectively, due to drainage (Figure 3.4). No lateral flow was measured during this period. The differences in drainage suggest that variability in soil hydraulic properties are the likely cause of some of the observed differences in plot hydrologic response given that slopes and plot areas were similar.

3.4.3 Lateral Flow

Lateral runoff represented a small proportion of the plot water balances. Lateral flow response was related to antecedent soil moisture conditions, and rainfall amount and intensity. Significant lateral flow (> 1 mm) (e.g., Buttle et al. 2004) did not occur until the soil moisture content reached a relatively stable level between events (which is assumed to approach field capacity) to a depth of 0.75 m (Figure 3.5). The RE plot soils were wet to 0.75 m at the start of the experiment (Figure 3.5). The depth of the wetting front in the RU plot reached 0.50 m during

irrigation event 4 and 0.75 m during event 6 (Figure 3.6). However, no lateral flow was observed in either plot following any of the 10-mm events (Table 3.3). Significant lateral flow did not occur in the RE plot until event 4 (event P = 20.4 mm, cumulative P = 51 mm). Significant lateral flow did not occur in the RU plot until event 6 (P = 35.3 mm, cumulative P = 78 mm). These data indicate that threshold irrigation depths for lateral flow production on wet soils ranged from 20 mm for the RE plot to greater than 30 mm for the RU plot (Figure 3.6). These values correspond to precipitation events with return periods of 20 years or more (Figure 3.7).

No overland flow or flow through the FF was observed after any of the applied irrigation events. Lateral subsurface flow occurred mainly through the Bt horizon in both plots (Table 3.3). In both plots, lateral flow from the Ae horizon was associated with only the largest volume and highest intensity events, and outputs were very small (Table 3.3). In both plots, lateral flow collected from the C trough was a larger proportion of total lateral flow in later events (Table 3.3).

3.4.4 Tracer Studies

Vertical flow and soil moisture storage were much larger proportions of the water balance than lateral flow. Analysis of Cl^- tracer concentrations in soil samples collected pre- and post-irrigation indicates that the post-irrigation Cl^- concentrations in the soil were elevated above the pre-irrigation values to a depth of approximately 1.3 m in the RE plot and 1.0 m in the RU plot (Figure 3.8). Analysis of the same samples for Br^- tracer, added during irrigation event 7, indicate that the depth of infiltration for the final two events reached the deepest sampling depth (1.5 m) in both the RE and RU plots for a limited number of sample points (Figure 3.8). No Br^- was detected in the analysis of pre-irrigation samples, so all Br^- is assumed to have been added during event 7. The RU and RE plots had one and two (of 18) vertical profiles, respectively, with measureable Br^- concentrations to a depth of 1.5 m, indicating preferential flow at least to that depth within the C horizon.

Tracer loss in lateral flow water samples was lower for the RU plot (Cl^- = 0.6 g, Br^- = 9.0 g) than the RE plot (Cl^- = 3.0 g, Br^- = 27.0 g) (Table 3.4). The total recovery of Cl^- (calculation with means) was 82% and 98% for the RE and RU plots, respectively. Recovery of Br^- was 66% and 71% for the RE and RU plots, respectively. There were only small differences in recovery between the two methods of calculation (mean and Thiessen polygons) for the tracer mass balance (Table 3.4).

3.5 Discussion

3.5.1 Precipitation, Soil Moisture Storage Thresholds, and Vertical versus Lateral Flow

On the Boreal Plains, antecedent storage appears to be the most important control on subsurface flow because it determines how much precipitation is required to fill the available storage, before subsurface flow can begin. Previous studies from humid regions (reviewed by Weiler et al. 2005) indicated that the primary controls on subsurface flow generation are total event precipitation, and antecedent storage. However, these relationships pertain to systems with typically shallow soils that overlie a well-defined confining layer. The results of the rainfall simulations in this study indicate that little or no vertical drainage out of the plots or lateral subsurface flow occurred until the soil matrix above the C-horizon was wetted to near field capacity. For the RE plot, field capacity was assumed from the constant and high volumetric water content between events. Soils in the RU plot did not reach field capacity until after a total P accumulation of 132 mm was added; soil moisture storage dominated the overall hydrologic response during this time. Further, it appears that size of the precipitation event does not control the amount of lateral runoff, and potentially vertical recharge, prior to exceeding soil moisture storage. For example, no runoff from the RE plot was observed during the large July 2004 rain event of 27 mm. Further, a rain event of approximately 80 mm over 23 hours, with a maximum 30-minute intensity of 24 mm hr^{-1}, occurred during July 2005. It resulted in an increase in soil moisture storage of 65–80 mm at different monitoring locations (Redding and Devito,

unpublished data), but there was no evidence of hillslope contributions to receiving wetlands or ponds. Devito et al. (2005b) found that in a Boreal Plains catchment, there was no runoff response to three successive storms with a cumulative rainfall of greater than 60 mm, due to dry soil conditions. In this study, the changes in storage for the RE plot prior to the experiment (124 mm) were similar to the change in storage for the RU plot (167 mm) during the experiment, and provides an indication of the size of soil moisture storage thresholds in the region.

Once field capacity was reached in this study, precipitation amounts of at least 20 mm were required to generate more than 1 mm of lateral flow from soils (Figure 6). This threshold value is within the range of those recorded in other studies: 17–55 mm under wet antecedent conditions (Weiler et al. (2005), 4.5–53.6 mm (Buttle et al. (2004), and 55 mm (Tromp van Meerveld and McDonnell 2006).

Differences in lateral flow response between the RE and RU plots were observed when the soils on each plot had been wetted to field capacity. Although there was some variability in the amount and intensity of irrigation in both plots, differences in response may have been due to variability in moraine hillslope soils. This could include small differences in clay content (which was higher in the RE plot), soil structure, root distribution, or macropore characteristics, all of which influence water transmission and storage. There was evidence of greater vertical preferential flow below the 0.75 m depth in the RU plot (Figure 3.8), which may account for the reduced lateral flow response. In addition, the soils below 1 m in the RU plot may initially have been drier than those below the RE plot. This would have encouraged vertical flow below the depth of the lowest trough because there would have been a greater matric potential gradient across the shallower wetting front.

Precipitation intensity, not just total precipitation volume, is important in generating lateral flow in soils in the study area and in other subhumid or semi-arid regions (Rodriguez-Iturbe, 2000). The influence of precipitation intensity on lateral flow generation may be masked on sites with shallow soils and

impermeable bedrock-confining layers, such as the Boreal Shield. On these sites, strong relationships exist between lateral flow generation, soil depth, and the depth and connectivity of small depressions in the bedrock (Buttle et al. 2004, Weiler et al. 2005). In the study area, soil depth and a decrease in permeability (K_s) may result in a stronger relationship between P intensity, permeability of the soils, and the lateral flow generation process once the soils are close to saturation and preferential flow can be initiated. Irrigation events of similar size have been shown to produce less lateral flow at lower application intensities, likely due to vertical drainage into the confining layer (C-horizon) (Lehmann et al. 2007). An important finding of the irrigation experiment in this study was the dominance of vertical drainage below 1 m depth on the study plot water balance once soil moisture storage had been exceeded. It is significant that over 70% of the irrigation water in the RE plot moved vertically out of the plot, given the high intensities of simulated rainfall during the study. Previous research on fractured clay-rich glacial till in the Boreal Plains (Devito et al. 2005a) and Prairies (Hendry 1982, Hayashi et al. 1998) showed evidence of preferential flow to depth or to a confining layer. In this study, the detection of Br^- in isolated samples at 1.5 m depth provided evidence of deep preferential flow. In addition, tracer recoveries for both Cl^- and Br^- were greater for the RU plot, which indicated there was less drainage below the maximum sampling depth (Table 3.4, Figure 3.8).

Results from this study suggest that antecedent soil moisture and precipitation intensity are the first-order controls over hillslope response on the Boreal Plains, where soils are deep and can efficiently move water below the root zone. Topography is important primarily as it relates to depth to water table (closer to surface at toe slopes, and deeper farther upslope) since the water table does not follow surface topography (Figures 3.1 and 3.4). Preliminary modelling results for the study sites indicate that water table response to rainfall events is limited to toe slope locations and is not related to the hillslope topographic gradient (Smerdon and Redding, unpublished data).

3.5.1.1 Anion Tracer Extraction and Recovery

The results of this study indicate that the standard method for extraction of Cl^- and Br^- from soils (extraction in deionized distilled water and shaking for 1 hour) was insufficient for recovering all applied tracer from the soils in the study plots. This has important implications for tracer transport and mass balance determinations, as incomplete recovery from soils will be a large source of error in mass balance calculations and, therefore, in understanding flow paths. It is not clear what mechanism accounts for the retention of tracer in the soil. There may have been some adsorption by organic matter (Gerritse and George 1988) or by clays and minerals (Brooks et al. 1998). Tracer may also have been trapped within soil peds or physically complex organic structures, which would necessitate a longer shaking period to allow the tracer to diffuse out during the extraction process (J. Robertson, University of Alberta, personal communication). It will be necessary to perform further sequential extractions on a range of soil types to determine the total number of extractions or shaking time required to achieve near complete recovery of tracers. Given our findings, the results of previous studies that used Br^- tracer profiles to infer flow paths (Whitson et al. 2005) likely overestimated the amount of lateral flow in this region.

3.5.2 Lateral Flow and Recharge in Context of Long-Term Precipitation Records

Given that antecedent soil moisture and precipitation intensity are the first-order controls over vertical and lateral flow, respectively, the critical questions for predicting long-term potential hillslope runoff or recharge on the Boreal Plains are:

1. How frequently do soils wet up?
2. Are storms large and intense enough to generate lateral flow from hillslopes once soils are wet?

To produce significant lateral flow from the study hillslopes, rainfall intensity that exceeds the K_s of the C horizon in soils with high antecedent soil

moisture storage is required. Relating rainfall intensity-duration return periods for the URSA region to results from the irrigation studies indicate that rain events with return periods of about 20 years may produce modest hillsope runoff of around 10% (Figure 3.7). Large lateral runoff responses (> 25%) will occur infrequently, with return periods of 50 years or more. It is important to note that both the vertical and lateral flow produced in this experiment occurred under ideal conditions (wet antecedent conditions, no transpiration), which are rarely encountered under natural field conditions. The total volume of precipitation added to the experimental plots in this study represents a return period of approximately 100 years. In addition, large, long duration rain events are restricted to summer months, when canopy interception and plant transpiration offset precipitation inputs to soils. Thus, the return periods presented in this study are likely conservative estimates.

The timing of P relative to available storage capacity (as defined by depth to water table and antecedent moisture content) and evapotranspiration demand is the main factor determining hillslope hydrological response and runoff generation. Given the depth of the unsaturated zone at the study plots (Figures 3.1 and 3.4), it is not likely over the short term (years) that hillslope water tables will rise sufficiently to generate lateral subsurface flow by saturation from below. Therefore, subsurface flow will more likely be generated from seasonal or event-scale inputs and a percolation excess-type mechanism. Results from this study and from other catchments indicate that a soil moisture deficit of more than 100 mm must be satisfied to generate vertical flow and allow for lateral flow if high-intensity storms occur. Large precipitation events (> 20 mm day^{-1}) are rare in the study region and are even less common during periods of low transpiration demand (e.g., post-snowmelt in spring and post-senescence in fall). Snow accumulation and melt can exceed soil storage in some years. The potential for recharge below 1 m following snow melt is the topic of concurrent study (see also Devito et al. 2005b). Due to the small size of most rain events in the study region, accumulative P > ET of 100 mm, which is required to wet the soils to field

capacity and allow for vertical recharge during the growing season, is estimated to occur about every 10 to 20 years (Devito et al. 2005b).

3.5.3 Implications of Forest Harvesting on Hillslope Runoff and Recharge

There has been no conclusive evidence of the effects of harvesting aspen forests on runoff generation and streamflow on the Boreal Plains (Swanson and Rothwell 2001, Buttle et al. 2005, Devito et al. 2005a). As in this experiment, storage and vertical flow have been shown to dominate storm response on harvested hillslopes that were formerly forested with mature aspen stands (Elliott et al. 1998, Devito et al. 2005a, Whitson et al. 2005). The overall effects of aspen harvesting on hillslope runoff generation are expected to be small because of the rapid regeneration of aspen and subsequent soil moisture demand. In addition, there is a large variability in antecedent soil moisture storage, a low probability of filling soil moisture storage, and a low probability that rainfall intensity and magnitude will be sufficient to generate lateral flow.

Similar to the results from the RE plot in this study, reduced transpiration and interception following harvesting should allow soils to wet up to a greater depth during the growing season than would occur under a forest canopy (Hart and Lomas 1979, Elliott et al. 1998). Reducing the storage deficit increases the probability of vertical recharge and the potential for lateral flow during storms of sufficient size and intensity. However, the thick unsaturated zones typical of these uplands buffer recharge. Macrae et al. (2005) and Whitson et al. (2005) found no difference in surface (to 1 m) soil moisture content between harvested and unharvested portions of aspen stands in headwater catchments on the Boreal Plain. This was attributed to rapid regeneration of the clonal aspen and/or dry (drought) conditions that occurred during the measurement period. Because clonal aspen rapidly regenerates after harvesting, there is a limited time to fill available storage during periods of lower ET demand and interception losses (Devito et al. 2005a). Increased drainage below the rooting zone and potential for lateral flow generation is most likely if harvesting coincides with wet conditions, such as a

large snowpack and a wet summer during the first growing season after harvest, when aspen regeneration is at its minimum.

Mechanical disturbance of the surface forest floor and organic layers can reduce storage and infiltration capacity, especially in fine-textured soils (DeVries and Chow 1978, Whitson et al. 2003). Such disturbances reduce the rainfall intensity required to initiate preferential flow and increase the probability of lateral flow. However, the degree of disturbance and associated increased potential for lateral flow is influenced by the timing of disturbance and type of equipment used. Harvesting with tracked equipment on dry or frozen soils typically creates the least disturbance (Startsev and McNabb 2000). During the rainfall simulations in this study, overland flow was not observed despite the high intensity of rainfall applied and the presence of wet antecedent conditions. This suggests that the probability of Hortonian overland flow occurring broadly over harvested areas will be low. Furthermore, soil K_s for sites on the Boreal Plains that exhibited reduced surface infiltration capacity due to harvesting (Startsev and McNabb 2000) are greater than the typical precipitation intensities found in the region. Compacted road surfaces are likely to be the only areas where overland flow will be regularly observed.

Rising water tables and greater potential for lateral flow generation may be expected at toe slope locations following harvesting (e.g., Rex and Dube 2006). In these locations, soil storage potential is limited due to shallow water tables in adjacent wetlands or streams, or to contributions from upland recharge. However, the results from the experimental plots in this study indicate that even when soils wet up, there is only a low probability that the high-intensity storms required to cause recharge and lateral flow will occur (Figure 3.7). As with soil moisture regimes, increased water levels at toe slopes following aspen harvesting may be expected to be short lived as clones regenerate and increase water demand in riparian or toe slope areas. Further research on the timing and magnitude of the influence of aspen regeneration on the hillslope water balance is ongoing.

3.6 Conclusions and Summary

The results of the rainfall simulations in this study indicate that there is a large water storage capacity in till-derived Luvisolic soils on the Boreal Plains, and that once this threshold is exceeded, vertical drainage below 1 m depth is the dominant flow path. Generation of lateral flow from uplands depends on available soil moisture storage capacity, rainfall amount and intensity, and soil permeability. Results from the experimental plots indicate that soil storage thresholds of approximately 100 mm must be met for vertical drainage and lateral flow to occur in these, and probably similar, Luvisolic soils. Significant lateral flow (> 1 mm) did not occur for precipitation events with return periods of less than 20 years.

Understanding the return period or likelihood of occurrence of the large magnitude, high intensity precipitation events required to generate lateral flow and connect, or "turn on", Boreal Plains hillslopes with wetlands or surface waters is critical for predicting the export and transfer of water and solutes from a catchment (McDonnell 2003, Weiler et al. 2005). The irrigation experiment in this study provides further evidence that on the Boreal Plains, there is a low potential for lateral flow from the study site and similar hillslopes, and in most years, catchment runoff is typically dominated by water flowing from wetlands or ephemeral draws (Gibson et al. 2002, Devito et al. 2005b). However, although infrequent, both large scale regional runoff and hillslope soil recharge and lateral flow can occur during large precipitation events that follow extended wet periods, as was observed in 1997 (Table 3.1) (Devito et al. 2005a).

Results from the root exclusion plot indicate that forest harvesting of similar hillslopes in this region may result in increased recharge or lateral flow due to alteration of interception, transpiration demand, and soil storage and transmission properties. However, the probability of lateral flow generation is still low. Soil storage and vertical drainage will be the dominant response to rain events. Harvesting-related impacts will probably be short-lived due to the rapid regeneration of clonal aspen.

This study helps quantify hillslope runoff and recharge thresholds, which have not been tested previously under field conditions on the Boreal Plains. Further research is needed to clarify the role of soil spatial variability and hydrologic connectivity on hydrologic response at larger scales. To quantify the potential for lateral flow and drainage below the root zone on hillslopes in this region, it will be necessary to estimate the probability of both precipitation (depth-duration-frequency) and antecedent soil moisture storage (or soil water content) over the depth of interest. Given the remoteness of the study area and the lack of long-term monitoring of soil moisture for forested areas on the Boreal Plains, numerical models will need to be used to generate the probability distributions of soil moisture conditions.

Modelling of catchment hydrology in these low relief, wetland-dominated systems should be based on soil properties, surficial geology, and vegetation community rather on than topographic indices (e.g., TOPMODEL), because the soil properties and groundwater dynamics do not follow the assumptions of topographic index models (Devito et al. 2005a). In this region, which has flat or inverted water tables, topography is an indicator of depth to water table; therefore, it can be used to map and model processes such as storage potential and recharge rather than being used as an indicator of subsurface flow. Based on the precipitation return periods required to generate lateral flow from the study plots, it appears that forested hillslopes with fine-textured soils infrequently contribute lateral flow; therefore, they are typically decoupled from adjacent wetlands and ponds. This has important implications for the hydrology and biogeochemistry of wetland systems in this region, as well as the sustainability of wetland habitats under conditions of climate change or catchment disturbance.

Table 3.1. Annual precipitation (mm), runoff (mm), and runoff coefficients (%) for Red Earth Creek (619 km^2) and Lac La Biche 20 (0.5 km^2), Alberta. The Red Earth Creek gauging station is approximately 70 km north of the study site. The Lac La Biche 20 catchment is approximately 250 km southeast of the study site.

Year	Red Earth Creek		Lac La Biche 20[1]	
	P[2] (mm)	R[3] (mm)	P (mm)	R (mm)
1991	463	69 (15%)		
1992	403	58 (14%)		
1993	496	60 (12%)		
1994	465	63 (14%)		
1995	371	4 (1%)		
1996	629	171 (27%)		
1997	464	246 (53%)	426	251 (52%)
1998	242	14 (6%)	329	12 (4%)
1999	283	5 (2%)	318	2 (1%)
2000	388	27 (7%)	529	2 (0%)
2001	309	21 (7%)	444	0 (0%)

[1] Data are from Devito et al. (2005a).
[2] Precipitation data are from Slave Lake, Alberta, approximately 180 km south of Red Earth Creek (Environment Canada 2006b).
[3] Runoff data for Red Earth Creek are from Environment Canada (2006a).

Table 3.2. Correction factors for tracer recoveries using the double extraction. The relationship are linear, with an intercept of 0.

Tracer	Soil Type[1]	Correction Factor	R^2
Cl^-	FF	1.26	0.99
	Min	1.32	0.94
Br^-	FF	1.20	0.99
	Min	1.08	0.99

[1] FF: forest floor; Min: mineral soil

Table 3.3. Water balance components, by event, for the Root Exclusion (RE) and Root Uptake (RU) plots. Values in parentheses are the estimated error ranges (± mm). Return periods were calculated based on the intensity-duration-frequency relationships of Hogg and Carr (1985).

Plot	Event	P[1] (mm)	Intensity (mm hr^{-1})	Intensity-Duration Return Period (yr)	Ant S[2] (mm)	Lateral Flow (mm)						ΔS[3] (mm)	D[4] (mm)
						FF[5]	Ae	Trough B	Trough C	Σ All Troughs	RC[6] (%)		
RE	1	10.2	60	5	537 (27)	0	0	0	0	0	0	8	2 (27)
	2	10.2	60	5	545 (27)	0	0	0	0	0	0	-1	11 (27)
	3	10.2	60	5	544 (27)	0	0	0	0	0	0	-8	18 (27)
	4	20.4	62	50	536 (27)	0	0	2.5	0	2.5 (0.1)	12	-4	22 (27.1)
	5	20.4	62	50	533 (27)	0	0	4.1	0.4	4.5 (0.2)	22	4	12 (27.2)
	6	40.7	77	>100	537 (27)	0	0.2	12.1	2.6	14.9 (0.8)	37	3	23 (27.8)
	7	40.7	102	>100	539 (27)	0	0.4	11.2	4.0	15.5 (0.8)	38	5	20 (27.8)
	8	20.4	35	25	544 (27)	0	0	1.2	1.0	2.3 (0.1)	11	3	15 (27.1)
	Total	173.2	--	--	7 (27)	0	0.6	31.1	8.0	39.7 (2.0)	24	10	123 (29)
RU	1	8.8	52	3	329 (17)	0	0	0	0	0	0	11	-2 (17)
	2	8.8	52	3	339 (17)	0	0	0	0	0	0	8	1 (17)
	3	8.8	52	3	347 (17)	0	0	0	0	0	0	0	9 (17)
	4	17.6	53	20	347 (17)	0	0	0	0	0	0	44	-27 (17)
	5	17.6	53	20	391 (20)	0	0	0.2	0	0.2 (0)	1	38	-21 (20)
	6	35.3	78	>100	429 (21)	0	0.2	2.4	0.1	2.8 (0.1)	8	53	-20 (21.1)
	7	35.3	93	>100	482 (24)	0	0.8	3.0	0.9	4.7 (0.2)	13	10	21 (24.2)
	8	17.6	26	7.5	492 (25)	0	0	0.3	0	0.3 (0)	2	3	14 (25)
	Total	149.8	--	--	163 (25)	0	1.0	5.9	1.0	8.0 (0.4)	6	167	-26 (25)

[1] Precipitation depth
[2] Antecedent soil moisture storage in the top 1 m
[3] Change in soil moisture storage in the top 1 m
[4] Vertical drainage below 1 m
[5] FF: Forest floor
[6] Runoff coefficient

Table 3.4. Mass balance of Cl^- and Br^- tracers for top 1.5 m of the soil profile. The mass balance was calculated by summing the amount of tracer stored within each depth interval, using both the mean concentration for a depth interval and spatially distributed storage by applying the Thiessen polygon method. The residual is the difference between inputs and outputs. Positive residuals signify the mass of initial and applied tracer not accounted for by the lateral flow collection or post-experiment soil sampling.

Tracer	Plot[1]	Method	Input Mass		Output Mass		Residual (g)	Recovery (%)
			Soil Initial (g)	Applied (g)	Lateral Flow (g)	Soil Final (g)		
Cl^-	RE	Mean	32	34	3	51	12	82
		Thiessen	32	34	3	50	13	80
	RU	Mean	32	34	0.6	64	1	98
		Thiessen	32	34	0.6	63	2	97
Br^-	RE	Mean	0	121	27	53	41	66
		Thiessen	0	121	27	50	44	63
	RU	Mean	0	121	9	77	35	71
		Thiessen	0	121	9	75	37	69

[1] RE: root exclusion plot; RU: root uptake plot

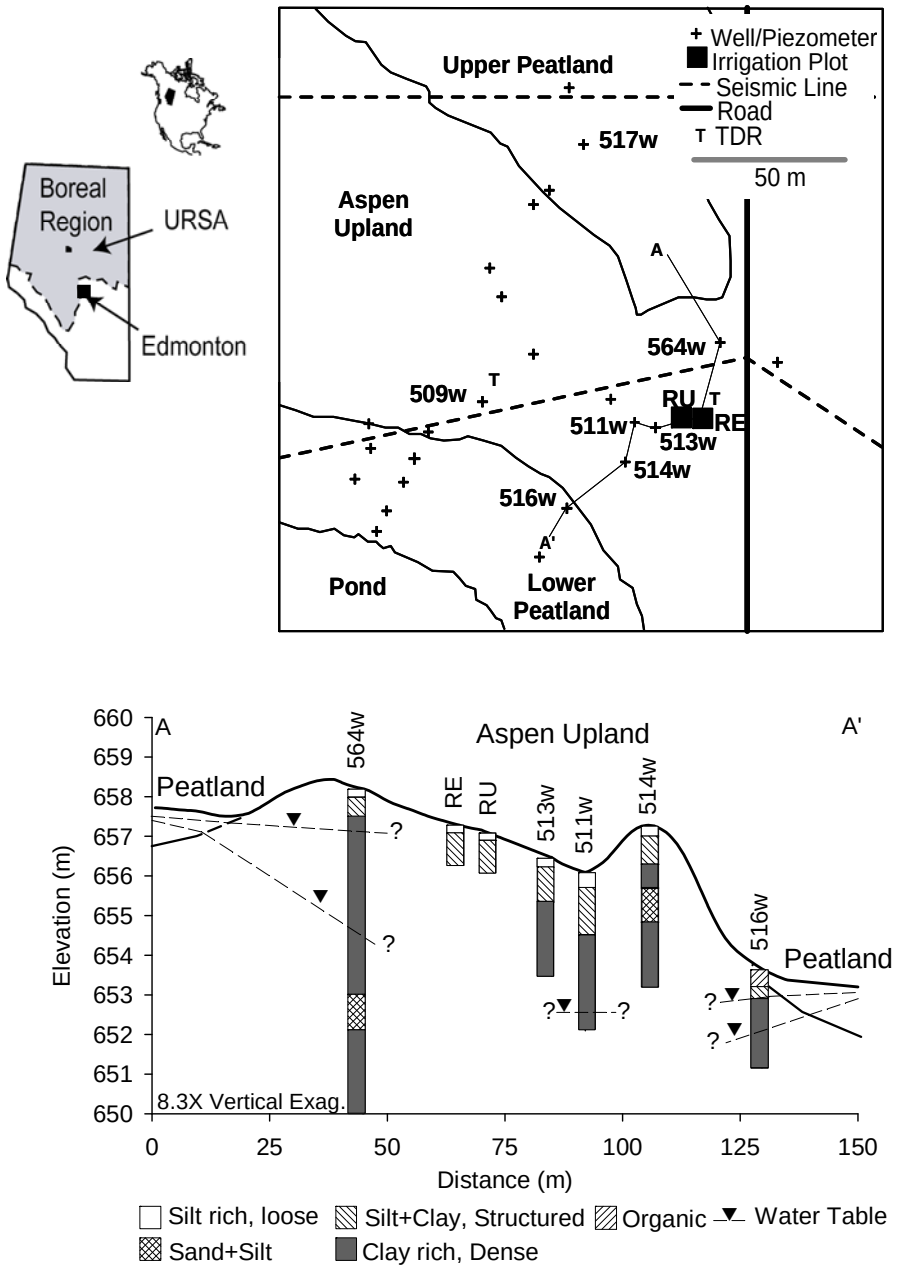

Figure 3.1. Location map, plan view map showing locations of irrigation plots and groundwater monitoring wells and cross-section showing stratigraphy along typical hillslope-wetland toposequence. Water table elevations are the maximum and minimum measured between April and October 2004. For well 511, the minimum water level was below the bottom of the well. Wells 513 and 514 were dry for the full period of monitoring during 2004.

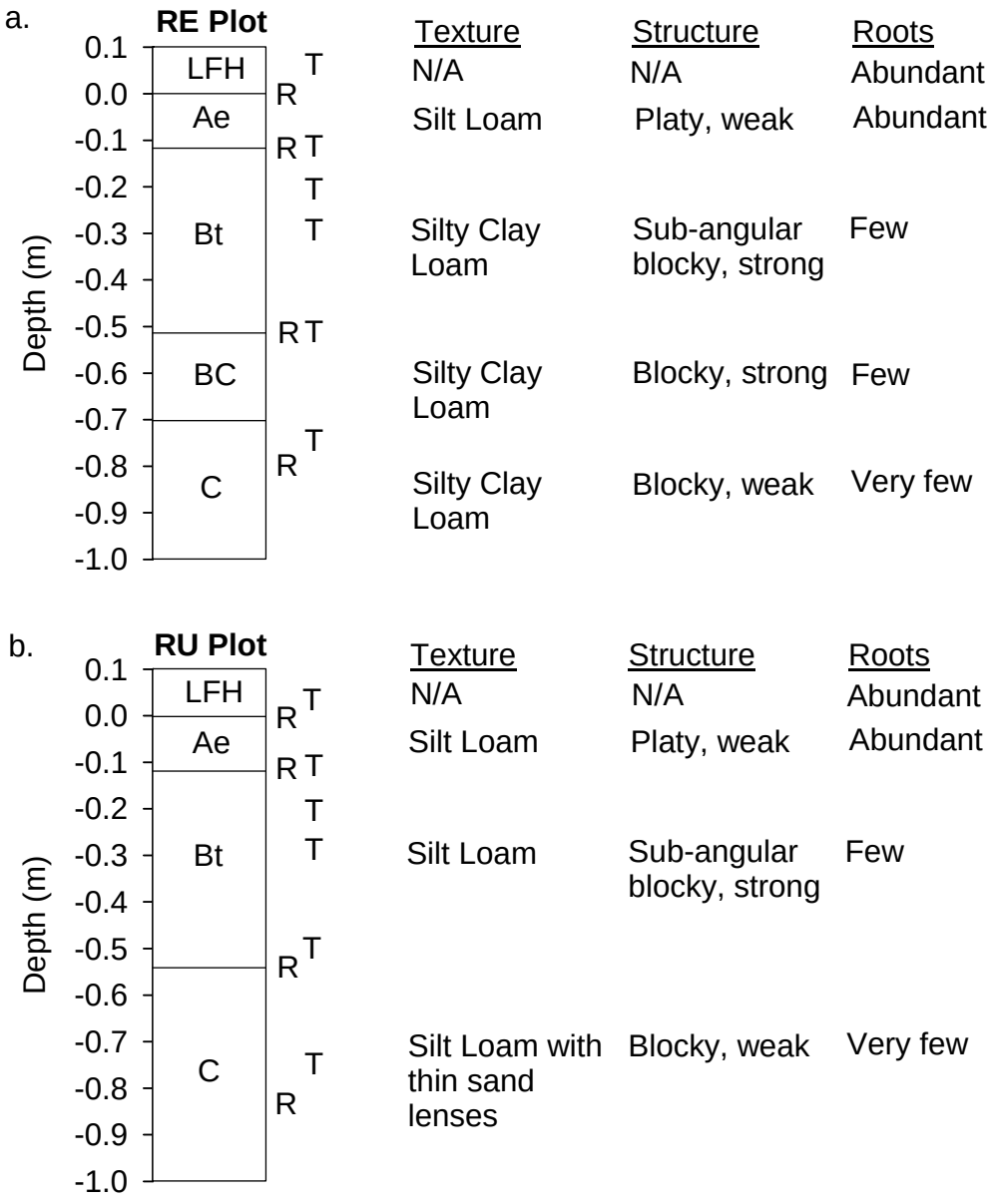

Figure 3.2. Schematic of soil profiles in the root exclusion (RE) (a) and root uptake (RU) (b) plots. Depths of runoff collection troughs are marked with R, locations of TDR probes are marked with T.

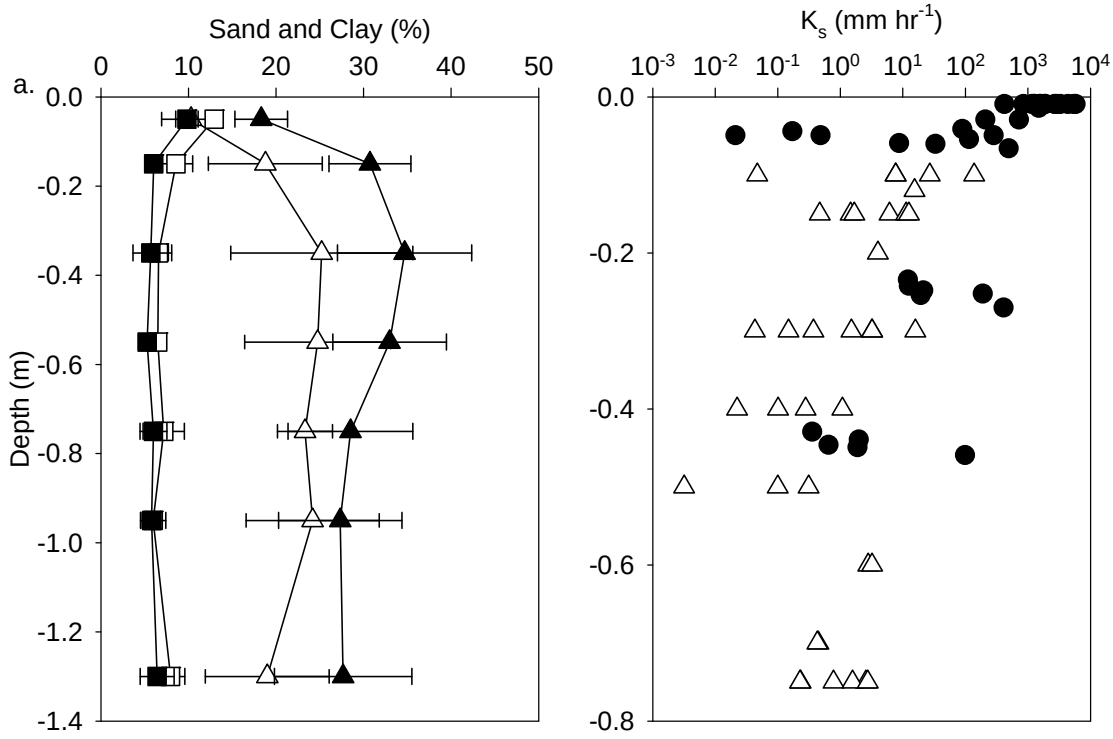

Figure 3.3. Depth profiles of particle size distribution (a) and saturated hydraulic conductivity (Ks) (b). In panel (a), triangles are clay content and squares are sand content, open symbols are the root uptake (RU) plot values, and the filled symbols are the root exclusion (RE) plot. Particle size values are mean and standard deviation (particle size n=9). In panel (b) Ks measurements were made using a single ring infiltrometer (filled circles) and with the Guelph Permeameter (open triangles).

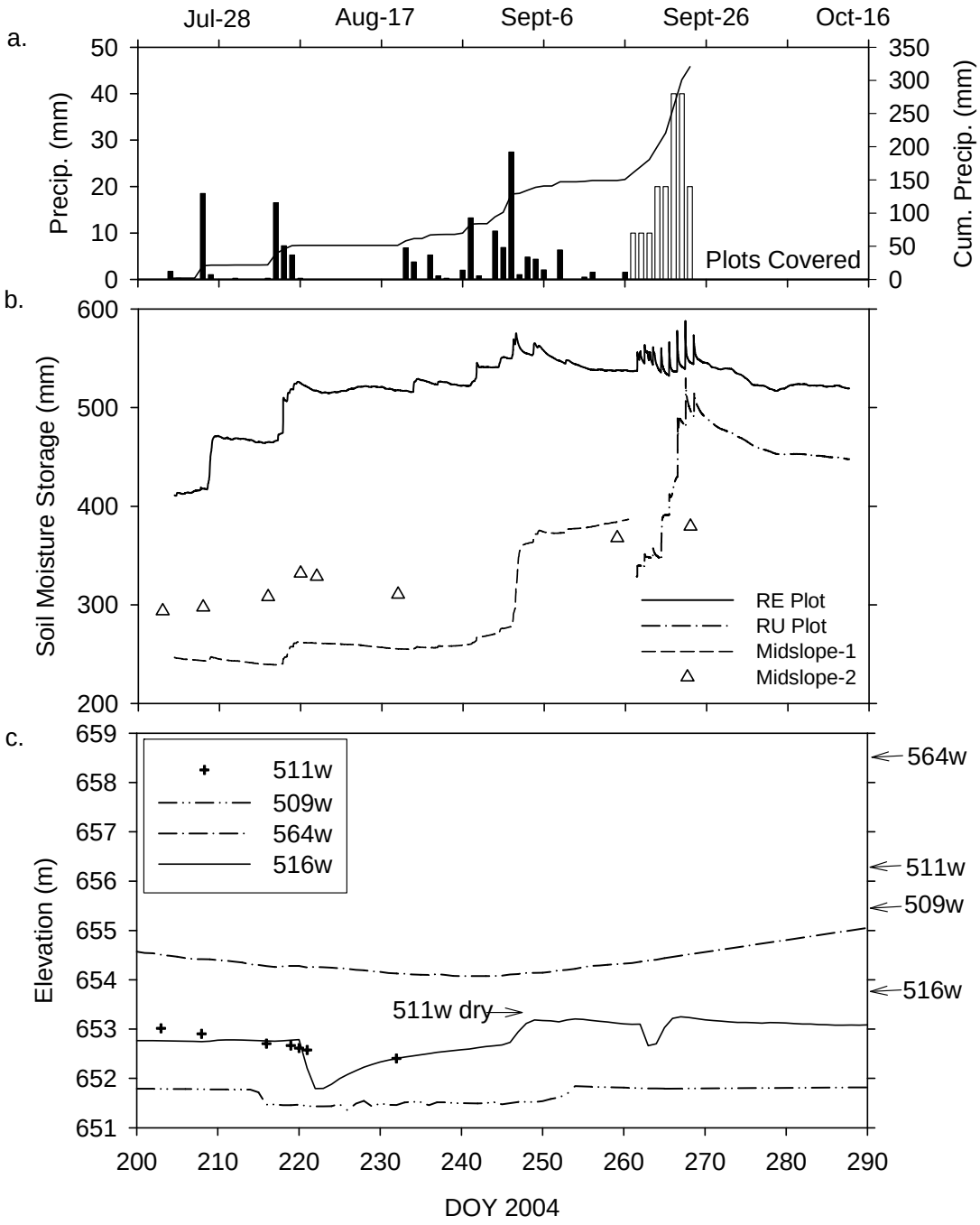

Figure 3.4. Time series of (a) daily and cumulative precipitation (simulated rainfall in open bars), (b) soil moisture storage for the root exclusion (RE) plot during the growing season and rainfall simulations, at sites adjacent to the RE plot during the growing season (Mid-slope-1), a second site (Mid-slope-2) during the growing season and rainfall simulation experiment, and for the root uptake (RU) plot during the rainfall, and (c) water table elevations relative to ground surface (arrows on right axis denote ground surface elevations for wells) during the growing season for wells across the study hillslope.

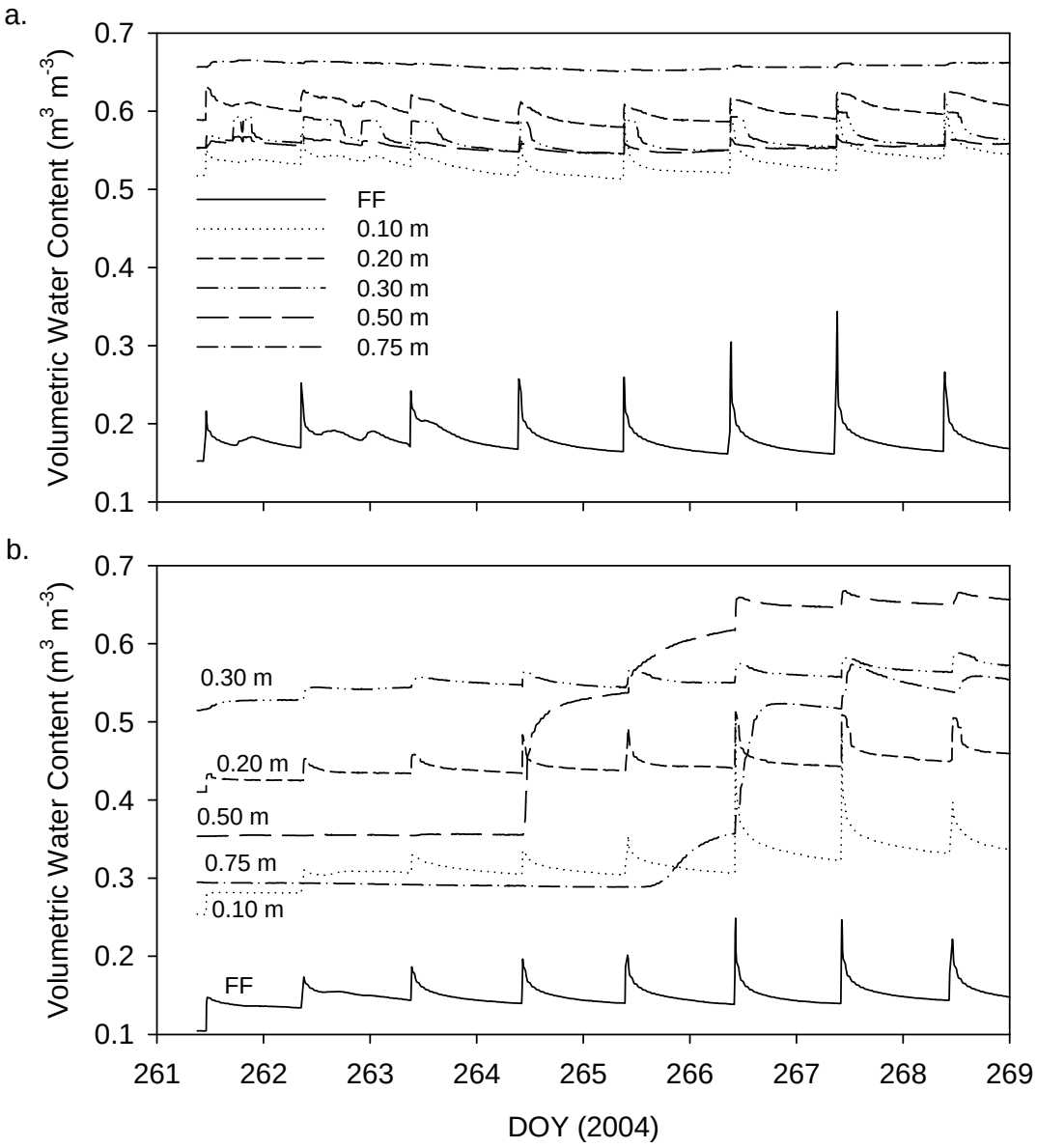

Figure 3.5. Time series of soil moisture content for the root exclusion (RE) (a) and root uptake (RU) (b) plots during the rainfall simulation experiment.

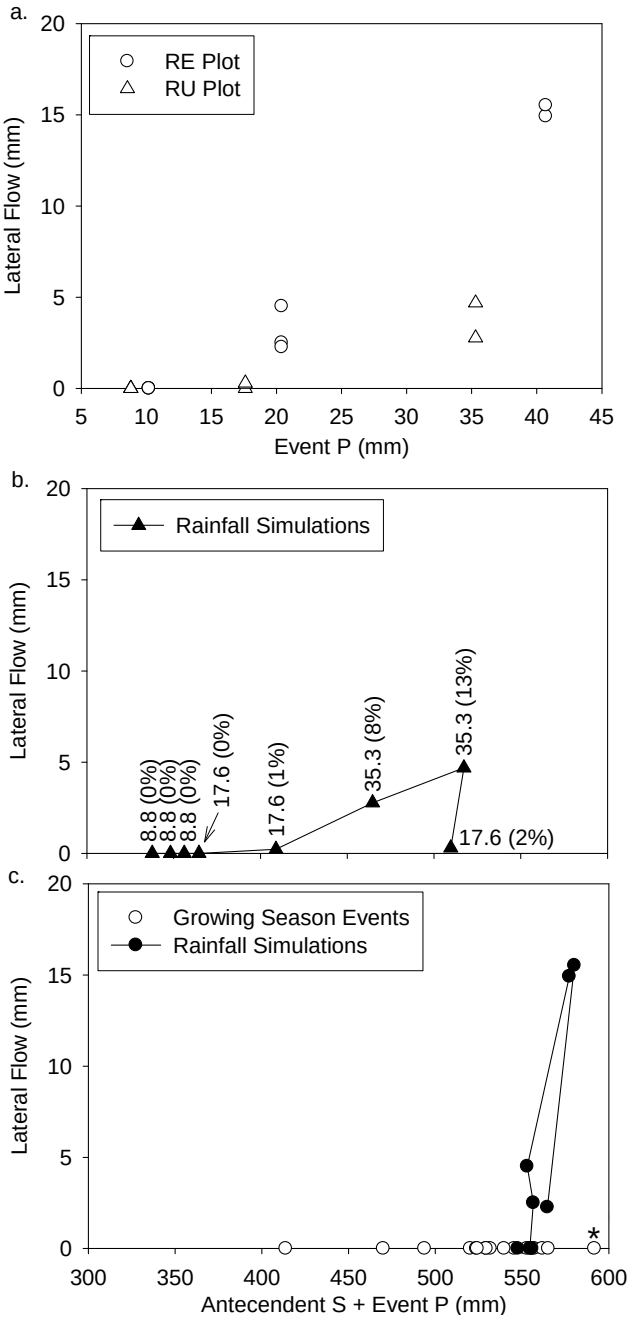

Figure 3.6. Precipitation (P) versus lateral flow for the root exclusion (RE) and root uptake (RU) plots (a), and antecedent soil storage (S) plus event precipitation versus lateral flow for the RU plot (b) and RE plot (c). For rainfall simulation events (closed symbols), the numbers written above the symbols are the event P depth (mm) and runoff coefficient (%). Plot (c) includes all rainfall events > 2 mm that occurred after plot installation and before the start of the rainfall simulations (open circles). Precipitation characteristics for the high P + S event on September 2, 2004 (DOY 246) (indicated with *) prior to irrigation study were P = 27.4 mm, duration = 16 hours, maximum 30-minute intensity = 5.1 mm hr^{-1}.

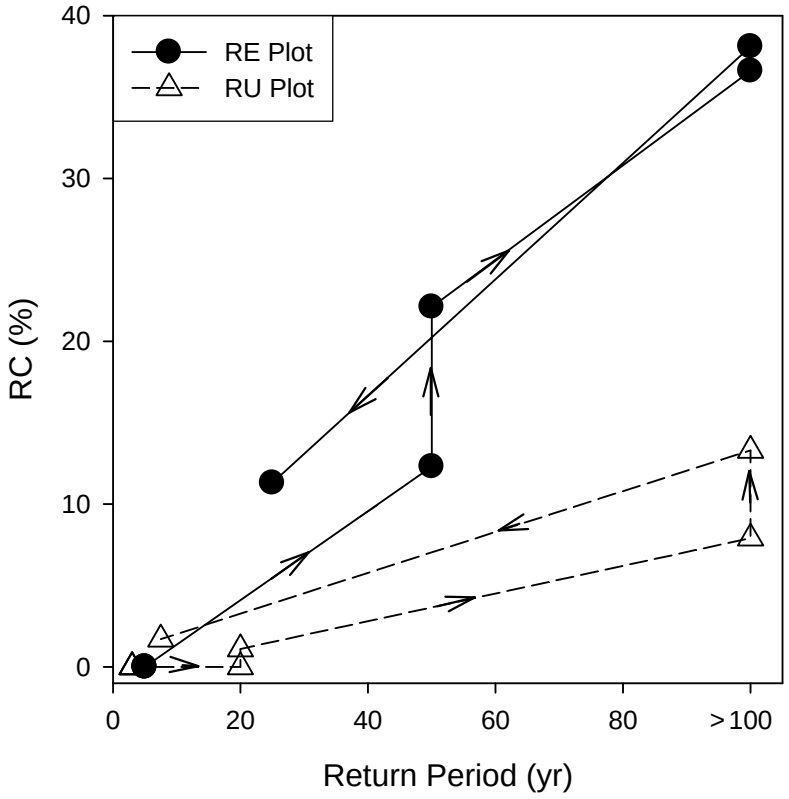

Figure 3.7. Plot of return periods for simulated rainfall event intensity-duration versus event runoff coefficients (RC), for all events. The lines and arrows indicate the order of events for each plot during the rainfall simulations. The return periods for the simulated rainfalls were calculated for the study area using the depth-duration-frequency relationships of Hogg and Carr (1986).

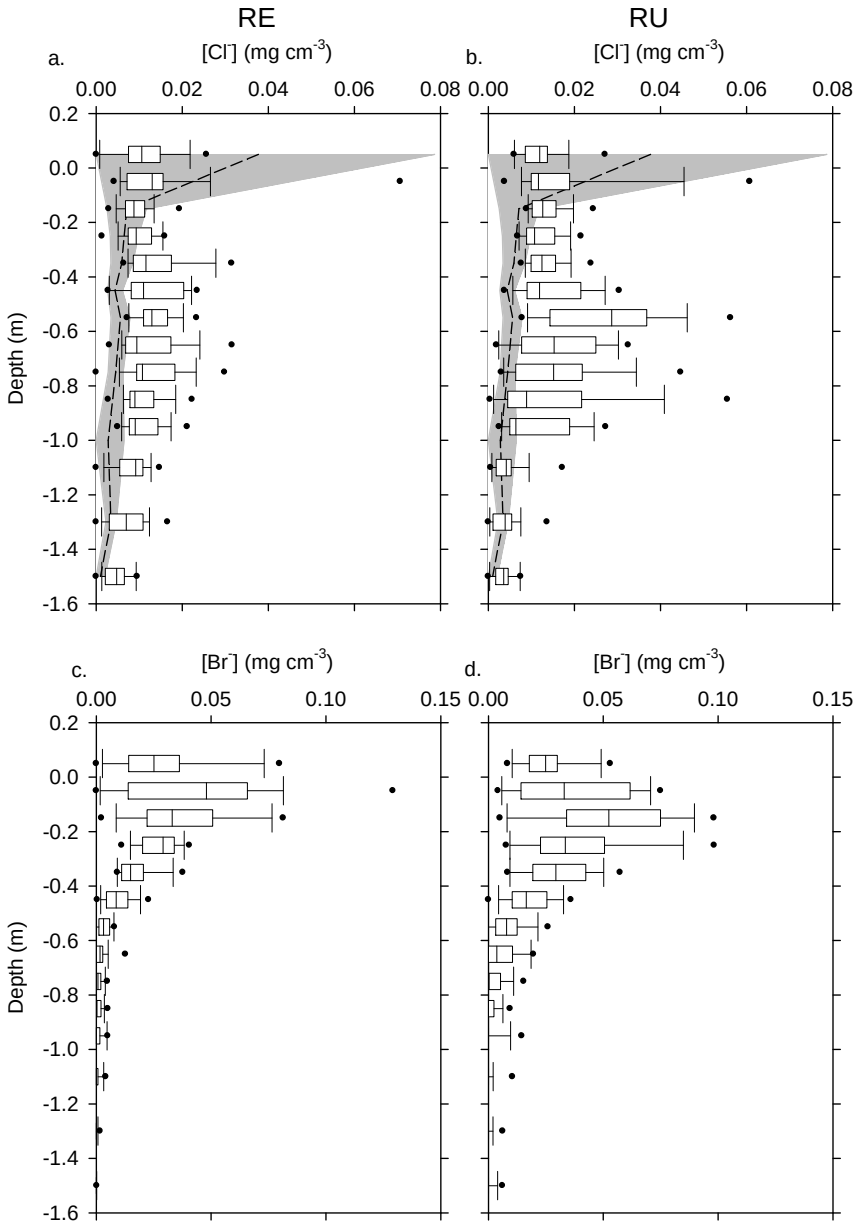

Figure 3.8. Soil Cl^- and Br^- concentrations for the root exclusion (RE) and root uptake (RU) plots: (a) RE plot Cl^-, (b) RU plot Cl^-, (c) RE plot Br^-, and (d) RU plot Br^-. For the Cl^- plots, the dashed line is the mean background Cl^- concentration, and the shaded area is the standard deviation. Boxplot features include the median, 25th and 75th percentiles (ends of rectangles), the 10th and 90th percentiles (whiskers), and outliers (circles). The amount of precipitation during the application of Cl^- through to the end of the experiment was 173 and 150 mm for the RE and RU plots, respectively. The amount of precipitation added from the application of Br^- through to the end of the experiment was 61 and 53 mm for the RE and RU plots, respectively. Prior to soil sampling, both plots were allowed to drain for 18 days after the final irrigation.

3.7 References

Brooks, S.C., Taylor, D.L. and Jardine, P.M. 1998. Thermodynamics of bromide exchange on ferrihydrite: Implications for bromide transport. Soil Science Society of America Journal 62: 1275-1279.

Buttle, J.M., Creed, I.F. and Moore, R.D. 2005. Advances in Canadian forest hydrology, 1999-2003. Hydrological Processes 19: 169-200.

Buttle, J.M., Dillon, P.J. and Eerkes, G.R. 2004. Hydrologic coupling of slopes, riparian zones and streams: an example from the Canadian Shield. Journal of Hydrology 287: 161-177.

Buttle, J.M. and McDonald, D.J. 2002. Coupled vertical and lateral preferential flow on a forested slope. Water Resources Research 38: DOI:10.1029/2001WR000773.

Campbell Scientific. 2004. Instruction Manual: CS616 and CS625 Water Content Reflectometers. Logan, Utah. Campbell Scientific, Inc. 50 p.

Devito, K., Creed, I., Gan, T., Mendoza, C., Petrone, R., Silins, U. and Smerdon, B. 2005a. A framework for broad-scale classification of hydrologic response units on the Boreal Plain: is topography the last thing to consider? Hydrological Processes 19: 1705-1714.

Devito, K.J., Creed, I.F. and Fraser C.J.D. 2005b. Controls on runoff from a partially harvested aspen-forested headwater catchment, Boreal Plain, Canada. Hydrological Processes 19: 3-25.

De Vries J. and Chow, T.L. 1978. Hydrologic behavior of a forested mountain soil in coastal British Columbia. Water Resources Research 14: 935-942.

Ecoregions Working Group. 1989. Ecoclimatic Regions of Canada, Ecological Land Classification Series No. 23.

Elliott, J.A., Toth, B.M., Granger, R.J. and Pomeroy, J.W. 1998. Soil moisture storage in mature and replanted sub-humid boreal forest stands. Canadian Journal of Soil Science 78: 17-27.

Environment Canada. 2006a. Archived Hydrometric Data, Red Earth Creek. http://www.wsc.ec.gc.ca/hydat/H2O/index_e.cfm?cname=main_e.cfm [Accessed March 23, 2009].

Environment Canada. 2006b. Climate Data Online, Slave Lake Alberta. http://www.climate.weatheroffice.ec.gc.ca/climateData/canada_e.html (Accessed March 23, 2009)

Fenton, M.M., Paulen, R.C. and Pawlowicz, J.G. 2003. Surficial geology of the Lubicon Lake area, Alberta (NTS 84B/SW). Alberta Geological Survey.

Gerritse, R.G. and George, R.J. 1988. The role of soil organic matter in the geochemical cycling of chloride and bromide. Journal of Hydrology 101: 83-95.

Gibson, J.J., Prepas, E.E. and McEachern, P. 2002. Quantitative comparison of lake throughflow, residency, and catchment runoff using stable isotopes: modelling and results from a regional survey of Boreal lakes. Journal of Hydrology 262: 128-144.

Hart, G.E. and Lomas, D.A. 1979. Effects of clearcutting on soil water depletion in an Engelmann spruce stand. Water Resources Research 15: 1598-1602.

Hayashi, M., van der Kamp, G. and Rudolph, D.L. 1998. Water and solute transfer between a prairie wetland and adjacent uplands, 1. Water balance. Journal of Hydrology 207: 42-55.

Hendry, M.J. 1982. Hydraulic conductivity of a glacial till in Alberta. Ground Water 20: 162-169.

Hogg, W.D. and Carr, D.A. 1985. Rainfall frequency atlas for Canada. Environment Canada. Ottawa

Kalra, Y.P. and Maynard, D.G. 1991. Methods Manual For Forest Soil And Plant Analysis. Edmonton, AB. Forestry Canada, Northern Forestry Centre. Information Report NOR-X-319.

Kirchner, J.W. 2006. Getting the right answers for the right reasons: Linking measurements, analyses, and models to advance the science of hydrology. Water Resources Research 42: DOI: 10.1029/2005WR004362.

Lehmann, P., Hinz, C., Tromp-van Meerveld, H.J. and McDonnell, J.J. 2007. Rainfall threshold for hillslope connectivity: an emergent property of flow pathway connectivity. Hydrology and Earth System Science 11: 1047-1063.

Macrae, M.L., Redding, T.E., Creed, I.F., Bell, W.R. and Devito, K.J. 2005. Soil, surface water and groundwater phosphorous relationships in a partially harvested Boreal Plain aspen catchment. Forest Ecology and Management 206: 315-329..

Marshall, I.B., Schut, P. and Ballard, M. (compilers). 1999. A National Ecological Framework for Canada: Attribute Data. Environmental Quality Branch, Ecosystems Science Directorate, Environment Canada and Research Branch, Agriculture and Agri-Food Canada, Ottawa/Hull. http://sis.agr.gc.ca/cansis/nsdb/ecostrat/data_files.html (Accessed March 23, 2009).

McDonnell, J.J. 2003. Where does the water go when it rains? Moving beyond the variable source area concept of rainfall-runoff response. Hydrological Processes 17: 1869-1875.

Peel, M.C., Finlayson, B.L. and McMahon, T.A. 2007. Updated world map of the Koppen-Geiger climate classification. Hydrology and Earth System Science 11: 1633-1644.

Peters, D.L., Buttle, J.M., Taylor, C.H. and LaZerte, B.D. 1995. Runoff production in a forested, shallow soil, Canadian Shield basin. Water Resources Research 31: 1291-1304.

Redding, T.E., Hannam, K.D., Quideau, S.A. and Devito, K.J. 2005. Particle density of aspen, spruce, and pine forest floors in Alberta, Canada. Soil Science Society of America Journal 69: 1503-1506.

Rex, J. and Dubé, S. 2006. Predicting the risk of wet ground areas in the Vanderhoof Forest District: Project description and progress report. BC Journal of Ecosystems and Management 7:57–71.

Reynolds, W.D. and Elrick, D.E. 2002. Constant Head Well Permeameter (Vadose Zone), Section 3.4.3.3. In Dane, J.H. and Topp, G.C. Methods of Soil Analysis, Part 4, Physical Methods. Madison, WI. Soil Science Society of America. P. 844-858.

Reynolds, W.D., Elrick, D.E. and Youngs, E.G. 2002. Ring or Cylinder Infiltrometer (Vadose Zone), Section 3.4.3.2a. In Dane, J.H. and Topp, G.C.

Methods of Soil Analysis, Part 4, Physical Methods. Madison, WI. Soil Science Society of America. P. 821-826.

Rodriguez-Iturbe, I. 2000. Ecohydrology: A hydrologic perspective of climate-soil-vegetation dynamics. Water Resources Research 36: 3-9.

Schaap, M.G., de Lange, L. and Heimovaara, T.J. 1996. TDR calibration of organic forest floor media. Soil Technology 11: 205-217.

Schoeneberger, P.J. and Wysocki, D.A. 2005. Hydrology of soils and deep regolith: A nexus between soil geography, ecosystems and land management. Geoderma 126: 117-128.

Soil Classification Working Group. 1998. The Canadian System of Soil Classification (Third Edition). Ottawa, ON. Agriculture and Agri-Food Canada.

Startsev, A.D. and McNabb, D.H.. 2000. Effects of skidding on forest soil infiltration in west-central Alberta. Canadian Journal of Soil Science 80: 617-624.

Swanson, R.H. and Rothwell, R.L. 2001. Hydrologic recovery of aspen clearcuts in northwestern Alberta. In USDA Forest Service Proceedings, RMRS-P-18. pp. 121-135.

Topp, G.C., Davis, J.L. and Annan, A.P. 1980. Electromagnetic determination of soil water content: measurements in coaxial transmission lines. Water Resources Research 16: 574–582.

Tromp van Meerveld, H.J. and McDonnell, J.J. 2006. Threshold relations in subsurface stormflow: 1. A 147-storm analysis of the Panola Hillslope. Water Resources Research 42: DOI :10.1029/2004WR003778

Vogwill, R. 1978. Hydrogeology of the Lesser Slave Lake area, Alberta. Edmonton, AB. Alberta Research Council. 30 pp.

Weiler, M., McDonnell, J., Tromp van Meerveld, I. and Uchida, T. 2005. Subsurface Stormflow. In: Vol. 3 of 5, Encyclopedia of Hydrologic Sciences, Anderson, M.G. and McDonnell, J.J. (eds). John Wiley and Sons: New York; 1719-1732.

Whitson, I.R., Chanasyk, D.S. and Prepas, E.E. 2003. Hydraulic properties of Orthic Gray Luvisolic soils and impact of winter logging. Journal of Environmental Engineering and Science 2: S1-S9.

Whitson, I.R., Chanasyk, D.S. and Prepas, E.E. 2005. Effect of forest harvest on soil temperature and water storage and movement patterns on Boreal Plain hillslopes. Journal of Environmental Engineering and Science 4: 429-439.

Chapter 4

Mechanisms and Pathways of Lateral Flow on Aspen-Forested, Luvisolic Soils, Western Boreal Plains, Alberta, Canada

4.1 Introduction

Subsurface flow from hillslopes is typically initiated when precipitation infiltrates the soil and moves vertically to an underlying flow restricting or impeding layer where it is redirected as lateral flow above the layer of restricted permeability (McDonnell 1990, Montgomery et al. 1997, Weiler et al. 2005). In many areas of the world where subsurface runoff mechanisms have been studied, lateral flow occurs at the soil-bedrock interface (e.g., McDonnell 1990, Peters et al. 1995, Tromp van Meerveld and McDonnell 2006). In areas without bedrock or another obvious restricting layer, such as many glacial landscapes, the mechanism of lateral flow generation may not be obvious (Lischeid 2008). It is often proposed that where soils feature a coarser-textured horizon over a finer-textured horizon, lateral flow will occur at that interface (Lin et al. 2005).

The Luvisolic soils found on aspen-forested uplands on the Boreal Plain region of Alberta feature a relatively coarse-textured Ae horizon (clays and organic matter eluviated) overlying a clay-enriched Bt horizon (Whitson et al. 2004). In other parts of the world where soils feature a coarse-texture A horizon overlying a finer-texture B horizon, lateral flow at the A/B interface has not been always been observed (Wilson et al. 1990, Newman et al. 1998, Lin et al. 2005, Lohse and Dietrich, 2005). Whitson (2003) and Whitson et al. (2004) studied lateral flow on aspen-forested hillslopes with Luvisolic soils on the Boreal Plains of Alberta. They found that lateral flow at the Ae/Bt interface was not significant (> 1 mm) during the snowmelt period or summer rainstorm events, but their measurements were made during years with below average precipitation. However, Whitson et al. (2005) speculated that lateral flow was occurring at the Ae/Bt horizon interface, based on their interpretation of vertical tracer profiles. A review of the literature on hillslope runoff on Luvisolic soils identified only a single instance where significant lateral flow was measured during snowmelt at

the Ae/Bt interface; this was in Minnesota (Timmons et al., 1977). However, it was unclear whether soil frost contributed to the development of transient perching which occurred during snowmelt. In addition, the contribution of lateral flow at the Ae/Bt interface to the annual water budget was only a small proportion (approximately 7%) of annual catchment outflow. Based on groundwater data for an aspen-forested Boreal Plains watershed during a large storm, Devito et al. (2005a) hypothesized that rapid vertical preferential flow to the clay-rich C horizon resulted in the development of a perched water table, and that lateral flow was generated via the transmissivity feedback mechanism (Rodhe 1987).

Redding and Devito (2008) used rainfall simulation experiments to examine lateral flow thresholds for an aspen-forested hillslope with Luvisolic soils, and noted that lateral flow occurred mainly as preferential flow through the Bt horizon rather than at the Ae/Bt interface. This chapter builds upon the results of Redding and Devito (2008) who found that on forested hillslopes with Luvisolic soils on the Boreal Plains, lateral flow generation is a function of P intensity relative to soil K_s and antecedent soil moisture storage. The conditions required for lateral flow generation are summarized graphically in Figure 4.1. This chapter presents detailed analysis of pore pressure, soil moisture, and tracer data from the rainfall simulation experiments, which is used to identify lateral flow generation mechanisms and flow pathways. The experimental design included two adjacent plots with subtle differences in soil properties and contrasting antecedent soil moisture conditions. The specific questions addressed are:

1. What is the mechanism of lateral flow generation and flowpaths?
2. What is the potential for lateral flow from these hillslopes under natural conditions?

The experimental approach allows for testing of specific hypotheses about lateral flow generation mechanisms and flowpaths, and it provides an indication of when lateral flow occurs on these and similar hillslopes (Kirchner 2006, Lischeid 2008). Understanding the mechanisms, flowpaths, and timing of lateral flow generation on forested hillslopes is critical for predicting the effects of

anthropogenic disturbances, such as forest harvesting and oil and gas development, on hydrological processes and biogeochemical exports to receiving wetlands and surface waters. For example, the research described herein may be used as an undisturbed analogue against which to evaluate mining reclamation practices in the Alberta oil sands region (e.g., Elshorbagy et al. 2005).

4.2 Study Site

The rainfall simulation experiments were carried out at the Utikuma Region Study Area (URSA) near Utikuma Lake (lat: 56^{o} N, long: 115^{o}30' W) in north-central Alberta (Devito et al. 2005b). The site is located within the Boreal Plains ecozone. Mean annual precipitation and potential evapotranspiration are 481 and 518 mm, respectively (Marshall et al. 1999). The climate at the study site is classified as subhumid in the Canadian Ecoregion system (Ecoregions Working Group 1989).

The rainfall simulation plots were established on a hillslope with Gray Luvisolic soils (Soil Classification Working Group 1998) that developed from the disintegration moraine deposits. These soils are typically silt-rich but spatially heterogeneous with zones of high clay or sand content (Fenton et al. 2003). The overstory canopy of the study hillslope is predominantly trembling aspen (*Populus tremuloides*) with minor amounts of balsam poplar (*Populus balsamifera*) in depressions and draws. The understory vegetation at the site includes prickly rose (*Rosa acicularis*) and high-bush cranberry (*Viburnum edule*) in the shrub layer, and twinflower (*Linnaea borealis*) in the herb layer. The forest floor surface is dominated by aspen litter with small amounts of moss and lichen. A more detailed description of the study site is available in Redding and Devito (2008).

4.3 Methods

Detailed descriptions of the methods used to establish the experimental plots, conduct the rainfall simulations, characterize soils, and measure lateral flow and soil moisture are provided in Redding and Devito (2008).

Within each plot, soil pore pressure was measured with tensiometers (Soil Measurement Systems, Tucson, Arizona) connected to data loggers (CR10X, Campbell Scientific Inc, Logan, Utah). The tensiometers were installed approximately 1.25 m upslope from the downslope face of the soil columns, and at depths of 0.3 and 0.5 m in the root exclusion (RE) plot and 0.1, 0.3, 0.5, and 0.75 m in the root uptake (RU) plot. The tensiometers were installed in vertical boreholes that were the same diameter as the tensiometer body. The porous cup was seated in a slurry of native soil from the appropriate depth and was sealed with bentonite at the soil surface. Above-ground sections of the tensiometers were covered with insulation to minimize temperature effects. Soil moisture and pore pressure measurements were recorded every 10 minutes during the 8 day irrigation experiment period, and every 2 hours during the pre- and post-irrigation monitoring periods. All TDR probes and pressure transducers were individually calibrated prior to the experiment. Unsaturated hydraulic conductivity was calculated from the field data using the TIDAP-6 software (Reynolds 1995). Macroporosity (%) was estimated following Buttle and McDonald (2000).

To quantify subsurface flowpaths, Cl^- and Br^- were added to irrigation water to act as tracers. The Cl^- tracer was added as KCl to the first irrigation event (30 L) at a concentration of 4100 mg L^{-1} ($[Cl^-]$ = 985 mg L^{-1}). The Br^- tracer was added as LiBr to the seventh irrigation event (120 L) at a concentration of 2000 mg L^{-1} ($[Br^-]$ = 920 mg L^{-1}). Lateral flow was expected to occur after this event. The Br^- tracer was used to quantify the pre-irrigation and irrigation water fractions in lateral flow. For each water sample collected, the proportion of water from the irrigation events was calculated based on the change from the initial concentration of Br^- in the irrigation water. More complex mixing models were not applicable as there was no background Br^- in the soil, and between-event concentrations of soil solution Cl^- were not measured. To calculate the overall event water proportion, the Br^- mass recovered in the lateral flow was compared with the total amount applied.

Subsurface flow velocities were estimated based on the time interval between the start of the irrigation application and the collection of the first lateral

flow sample for the shortest straight-line distance between the soil surface and the trough of interest (the vertical distance from the forest floor surface to the trough). The minimum vertical distance between the soil surface and the trough was used to calculate the velocity because it was not possible to determine the surface origin of the plot water that emerged at the pit face. Therefore, the calculated value is a conservative estimate of velocity because the shortest flowpath length was used and the emergence of preferential flow was noted visually on the pit face prior to collection of the first sample.

4.4 Results

4.4.1 Soil Properties

The soils of both plots were classified as Gray Luvisolic (Soil Classification Working Group, 1998); however, there were small differences in horizonation and texture (see Chapter 3, Figure 3.2). The plots were similar in sand content, but the RU plot had greater silt and lower clay content than the RE plot (Figure 4.2). The differences in texture corresponded to slightly higher bulk density and lower porosity in the RU plot (Figure 4.2).

There was a general decrease in saturated hydraulic conductivity (K_s) with depth on the study hillslopes (Figure 4.3). In the hillslope soils adjacent to the two runoff plots, K_s was highly spatially variable but variability decreased with depth (Figure 4.3). Higher rates of K_s were measured at the same depths with the single ring method than with the Guelph permeameter, indicating the contribution of macropores (e.g., Buttle and House 1997). Across the study hillslope, measured macroporosity was higher at the FF surface than at the underlying mineral soil surface. The calculated mean macroporosity from the tension infiltrometer measurements at the FF and mineral soil surfaces were 0.01% and 0.006%, respectively.

4.4.2 Soil Moisture Conditions Necessary for Subsurface Flow

To generate lateral flow, it was necessary to first satisfy the storage deficit required to bring the soils roughly to field capacity and then apply a threshold

amount of precipitation—in this case, 15–20 mm (Redding and Devito, 2008). Whereas the RE plot soils were wet prior to irrigation, available storage above the C horizon needed to be satisfied in the RU plot before lateral flow was generated (Figure 4.4 and 4.5). In the RE plot, where tree root uptake was eliminated, wetting occurred during the pre-irrigation period (Redding and Devito, 2008); however, no lateral flow was generated during this period. The RE plot generated lateral flow for all events ≥ 20 mm and 35 mm hr^{-1} in intensity (Figure 4.4). At the start of the irrigation experiments, the soil in the RU plot was wetted to field capacity to a depth of 0.3–0.5 m; however, lateral flow was not generated until soils were wetted to the C horizon (0.5–0.75 m) during irrigation event 5 (cumulative precipitation P = 62 mm) (Figure 4.5). The wetting front reached 0.5 m during event 4 and 0.75 m in event 6 (Figure 4.5).

4.4.3 Lateral Flow Mechanisms

Wetting of the soil profile occurred from the top down during all irrigation events. Event 7 produced the largest lateral flow response in both plots; therefore, it is used here as an example of the interactions of lateral flow, soil moisture, and pore pressure response. Subsurface flow in the RE plot occurred predominantly through the Bt horizon (B trough, 11.2 mm), with smaller contributions from the Ae horizon (A trough, 0.4 mm) and BC horizon (C trough, 4.0 mm) (Figure 4.6). Peak lateral flow rates occurred earlier for the A and B troughs than the C trough, in contrast to the RU plot where all three peaked simultaneously (Figure 4.7). For the RE plot, lateral flow into the B and C troughs persisted for almost 200 minutes from the time irrigation began. As with the RU plot, flow from the RE plot A trough occurred only during one measurement interval, while flow from the C horizon (C trough) ended at the same time as the B trough (Figure 4.6). Tensiometers responded first at 0.3 m, then at 0.5 m (Figure 4.6). The maximum pore pressure for the 0.3 m tensiometer (+75 cm H_2O) occurred prior to the peak in lateral flow rate and TDR response at any depth (Figure 4.6), possibly indicating a pressure wave-type response. Saturation at the 0.3 m depth persisted for approximately 160 minutes after the start of the irrigation application. At the

0.5 m depth, the soil moisture and pore pressure responses occurred at approximately 20 minutes after the start of irrigation (Figure 4.6). The response was muted because the soils were already very close to saturation. Approximately 50 minutes after the start of irrigation, the 0.5 m tensiometer showed an increase in pore pressure with no concurrent increase in soil moisture content. This pore pressure response is likely related to the increase in air temperature during the morning (e.g., Warrick et al. 1998).

In the RU plot during event 7, lateral flow occurred predominantly through the Bt horizon (B trough, 3.0 mm), with smaller contributions from the Ae horizon (A trough, 0.8 mm) and C horizon (C trough, 0.9 mm) (Figure 4.7). Lateral flow into the B trough persisted for almost 100 minutes from the time irrigation began. Flow from the A trough occurred only during one measurement interval, while flow from the C horizon (C trough) ended at the same time as the B trough (Figure 4.7). After the start of irrigation, tensiometers responded in the following depth order: 0.1, 0.3, 0.5, and 0.75 m (Figure 4.7). Tensiometer and TDR responses peaked at the 0.1 and 0.3 m depths at the same time as the peak lateral flow rate, whereas a slight lag occurred at 0.5 and 0.75 m. All depths became saturated (pore pressures > 0 cm H_2O). Saturation at the 0.10 and 0.30 m depths persisted for 120 to 150 minutes following the start of irrigation, whereas the response of the deeper tensiometers persisted for more than 250 minutes (Figure 4.7), indicating the presence of saturated conditions above and within the upper C horizon. While detailed results are presented only for event 7, the pattern of wetting from the surface downward was similar for all events (Figures 4.4 and 4.5).

In the RU plot during events 3 through 5, soil moisture content at 0.75 m depth, measured by TDR, was constant; however, there was a transient pressure response from the tensiometer at 0.75 m at the time of each irrigation application (Figure 4.5), although it was relatively short-lived. The magnitude of the pressure response increased between event 3 and 5 (from about +5 cm to +25 cm H_2O) as the wetting front moved deeper.

Flow from the pit face began rapidly during events in which lateral flow occurred. Lateral flow from the pit face was initiated as preferential (macropore) flow, primarily along root channels, and then the pit face appeared to wet-up outward from the macropore locations (T. Redding personal observation). Within the RE plot, nine preferential flow outlets were noted on the pit face; all were associated with tree roots (Figure 4.8), and the order of flow initiation and cessation (reverse of pattern of initiation) was consistent among events. Within the RU plot, six preferential flow outlets were noted, with none in the C horizon (Figure 4.8). Similar to the RE plot, the pattern of initiation and cessation was consistent among events. Although no preferential flow from the C horizon was noted in the RU plot, sand lenses, vertical cracks, and fine roots were visible in the pit face (T. Redding personal observation).

Event water dominated the subsurface flow response to event 7 in both the RE and RU plots (Table 4.1). In both the RE and RU plots, peak Br^- concentration corresponded with peak outflow rates (Figure 4.9). As the irrigation event progressed, the role of pre-event water became more pronounced, as indicated by a decrease in Br^-, which was added in event 7, and by an increase in Cl^-, which was present in the soil matrix. The maximum event water contributions were approximately 75% early in the event and decreased to about 25% at the cessation of subsurface flow (Figure 4.9). The total event water contribution for event 7 was 61% and 60% for the RE and RU plots, respectively, which corresponded to 9.5 mm and 2.8 mm of subsurface flow, respectively (Table 4.1). Event water outputs were higher for the A and B troughs than for the C trough (Table 4.1), possibly reflecting differences in preferential flow contributions to outflow. On the RU plot, the C trough event water contribution was 52% of the flow from this horizon (0.5 mm). On the RE plot, preferential flow emerged from the C horizon during events 6 and 7 by way of root channels. Flow from this horizon was 47% event water during event 7 (Table 4.1).

Subsurface flow velocities were much greater than the soil K_s, and ranged from less than 1000 mm h^{-1} for the A trough to a maximum of about 4000 mm hr^{-1} for the B and C troughs in the RE plot (Figure 4.10). Subsurface flow

velocities were positively related to irrigation intensity (Figure 4.10), and the relationship appears to be fairly linear over the range of applied precipitation intensities. There were no systematic differences in subsurface flow velocity between the RE and RU plots for the range of applied precipitation intensities (Figure 4.10).

4.5 Discussion

4.5.1 Lateral Flow Mechanisms and Flowpaths

In the two experimental plots in this study, lateral flow was not generated along the Ae/Bt interface as has been hypothesized for Luvisolic soils (Whitson et al. 2005, Lin et al. 2005, Wilson et al. 1990) or has been observed in Minnesota (Timmons et al. 1977). The soils in this study have no clear flow restricting layer, and lateral flow was generated primarily by macropore flow through root channels in the clay-enriched Bt horizon, similar to other Boreal Plains catchments (Devito et al. 2005a). The antecedent moisture conditions and precipitation intensities required to generate lateral flow in the experimental plots were much greater than those recorded by Whitson et al. (2004, 2005) during the lateral flow monitoring period on similar sites on the Boreal Plains. However, Whitson et al. (2004, 2005) measured very little lateral flow on their sites, similar to the results recorded in this study. Whitson et al. (2004, 2005) found no significant lateral flow (< 1 mm) at the Ae/Bt interface during snowmelt or summer rainstorms, but they did not measure the potential for lateral flow below the Ae/Bt horizon interface.

Similar flow pathways to those measured in this study have been noted in semi-arid forests in the southwestern U.S., during periods with high antecedent soil moisture conditions. In New Mexico, Newman et al. (1998) found that 80% of lateral flow occurred through the Bt horizon, and lateral subsurface flow was infrequent from the hillslopes in the region. Similar to this study, lateral flow was dominated by preferential flow through root channels, and wetting of the unsaturated profile occurred outward from macropore channels rather than from saturation from below (Newman et al. 2004). Peters et al. (1995) found that on the

Boreal Shield, lateral flow occurred mainly through the B horizon and at the soil-bedrock interface.

If preferential flow in this study was initiated in the forest floor or near the mineral soil surface, the lateral preferential flow component may be a function of the shape of the rooting profile of the aspen trees. Roots tend to follow an inverse parabolic shape (umbrella-like); thus, the pit face may have intersected the root channels where they were still trending laterally rather than deeper where they would have had a more vertical orientation deeper in the profile and not intersect the pit face. If this is the case, the plot measurements will overestimate lateral flow contributions. Root density decreases greatly with depth at the study site (see Chapter 3, Figure 3.2), so there are also fewer roots intersecting the pit face below the Bt horizon. There is tracer evidence of deep, vertical preferential flow into the C horizon on both the RE and RU plots, which is likely associated with root channels and or soil fractures (Hendry 1982, Redding and Devito 2008).

The large contribution of event water to lateral flow on both plots in this study differs from many other hillslope studies, which indicate that runoff response is dominated by water stored within the hillslope prior to a precipitation event (Buttle 1994, Lischeid 2008). The high event water contributions to lateral flow may be due to the initiation of preferential flow from near the surface early in the irrigation event, combined with low interaction between preferential flow water and the soil matrix early in the event (Kienzler and Naef 2008). The hypothesis about limited interaction between preferential flow pathways and the soil matrix (e.g., Weiler and Naef 2003, Scherrer et al. 2007) is supported in this study by the rapid transport of both water and tracers from irrigation inputs into lateral flow at the pit face. Wilson et al. (1990) noted that higher intensity precipitation produces a greater contribution of early event water contributions through preferential flow, and that the contribution of event water decreases through time. The increase in pre-event water during the progression of the event is likely due to the greater proportion of stored water contributing as the perched water table causes mixing. Kienzler and Naef (2008) reported similar findings of different event/pre-event water contributions for different flow pathways.

The subsurface flow velocities estimated in this study are within the range of those reviewed by Nimmo (2003) and measured by Tymchak and Torres (2007), Kienzler and Naef (2008), and Anderson (2008), but they are lower than those measured on forested New Zealand hillslopes with very large macropores (Mosley 1982). The high velocities recorded in this study may indicate a pressure wave (Torres 2002, Torres and Alexander 2002) or kinematic wave response (Beven 1982). Evidence of a transient pressure wave response was provided by the RU plot tensiometers where short-term pressure effects were noted at depth in unsaturated conditions; TDR probes at the same depth did not respond in kind (data not shown).

Preferential flow emerging from the Bt horizon in this study could have been caused by two different mechanisms, either working separately or in concert. The first mechanism is preferential flow initiation near the soil surface, followed by preferential flow both laterally and vertically through the soil profile. The second mechanism results from the development of a transient perched water table at the C horizon boundary due to conditions that result in percolation excess. The perched water table rises through the profile, causing the saturated zone to intersect with preferential flow pathways in the Bt horizon. This transmissivity feedback mechanism, which has been observed in many glacial till environments (e.g., Rodhe 1987, Buttle 1994, Kendall et al., 1999), likely accounts for the increasing proportions of pre-event water as the event progresses (Figure 4.9).

Determining the specific location of preferential flow initiation in the upper soil profile is important for deciphering the potential proportioning of lateral and vertical flow pathways. In this study, preferential flow may have been initiated at the forest floor-mineral soil interface, given the larger macroporosity at the forest floor surface than at the mineral soil surface, and the shingling effect of overlapping aspen litter, which may concentrate flow. In addition, the high-intensity irrigation may have initiated preferential flow in the forest floor or at the mineral soil surface, resulting in the high initial event water contributions to lateral flow. In steep, coastal soils, De Vries and Chow (1978) found that preferential flow was initiated in the forest floor. Wilson et al. (1990)

hypothesized that in soils with profiles with similar Ae/Bt horizons, preferential flow is initiated at the Ae/Bt boundary due to transient perching resulting from the permeability contrast. Future studies employing dye tracing methods may be able to clarify the location of preferential flow initiation (e.g., Weiler and Fluhler, 2004).

It is important to place the amount of lateral flow in the context of vertical flow and soil storage, which dominated the water movement in both plots in this study (Redding and Devito 2008). At other sites on the Boreal Plains, the hydrological response to precipitation is dominated by vertical flow and storage and loss to evapotranspiration, with little annual recharge below the root zone (Cuenca et al. 1997, Elliott et al.1998, Blanken et al. 2001, Devito et al. 2005a). Over two years of soil moisture monitoring, Elliott et al. (1998) measured greater rainfall infiltration depth on sandy soils but not on finer-texture Luvisolic soils with an aspen canopy, similar to those investigated here. Neither Elliott et al. (1998), Blanken et al. (2001), nor Cuenca et al. (1997) were able to account for vertical or lateral preferential flow in their measurements.

Limited sampling under natural conditions has not allowed for adequate testing of hypothesized flowpaths and mechanisms on the Boreal Plains. In contrast, this study highlights the power of manipulative experiments in directly testing flowpaths and mechanisms. Manipulative experiments are especially important for understanding the thresholds of hydrologic response in environments where they occur infrequently under natural conditions (Kirchner 2006).

4.5.2 The Role of Precipitation Intensity

The results of the current study are similar to other studies in which precipitation intensity was important for initiating preferential flow near the soil surface (Weiler and Naef 2003) and for partitioning lateral flow and deep percolation at the restricting-layer boundary (Lehman et al. 2007, Tromp van Meerveld et al. 2007, Jardine et al. 1990, Uchida et al. 2005). In this study, and in others on the Boreal Plains and Prairies (Hendry 1982, Hayashi et al. 1998,

Devito et al. 2005b), high forest floor and near-surface K_s exceeded both natural and simulated rainfall intensities, and together with large available soil storage, excluded lateral flow from the Ae/Bt horizon. Irrigation intensities during the latter events and observed subsurface flow velocities in the Ae and Bt horizons of the study plots were greater than the K_s of the C horizon. This allowed the C horizon to act as a restricting layer to downward infiltration, which lead to the accumulation of water in excess of deeper percolation, and the development of a transient perched water table. Water accumulating above the restricting layer could then back up within the profile and exit through the macropores, which were predominantly in the Bt horizon (Figure 4.8). Because the soil matrix was effectively saturated (Figures 4.6 and 4.7), preferential flow moved water laterally from the profile.

It is possible that the high irrigation rates in this study influenced the runoff generation mechanisms (e.g., preferential flow initiated at the soil surface) and consequently inflated the event water contributions to lateral flow (Pearce et al. 1986). Studies in New Zealand showed that artificial ponded infiltration (Mosley 1979) resulted in much higher event water contributions to lateral flow than occurred under natural rainfall conditions (Sklash et al. 1986). Therefore, in this study, the event water contributions to lateral flow may have been greater than what would normally occur under less extreme natural circumstances. It is also important to note that the average intensity of the irrigation applications was lower than the instantaneous application rates due to the small application area of the watering cans. These high instantaneous intensities may be important in determining where in the soil profile preferential flow is initiated and hence the event water contributions.

At the Panola study hillslope in Georgia, where the K_s of the bedrock is 5.8 mm hr^{-1}, lateral flow occurred when precipitation intensity was greater than 8 mm hr^{-1} (Tromp van Meerveld et al. 2007). Bedrock infiltration accounted for 20–70% of the rainfall of large storms (Tromp van Meerveld et al. 2007). Similarly, Kienzler and Naef (2008) found that bedrock infiltration was greater for lower intensity applications, and accounted for 30–50% of applied water. Lehmann et al.

(2007) conducted modelling experiments on Tromp van Meerveld et al.'s (2007) study site, which indicated there would be no lateral flow for events with a maximum precipitation intensity less than the K_s of the bedrock, and that total hillslope outflow increased linearly with maximum precipitation intensity. On the hillslope in this study, lateral flow will not occur during precipitation events that are less than 10 mm hr^{-1} in intensity. Even at these intensities when soils are wet to field capacity, flow will be predominantly vertical.

This study further illustrates the interaction between soil storage and rainfall intensity in generating lateral flow from Boreal Plains hillslopes. During this experiment, soils were wet to field capacity prior to event 8—the event with the lowest applied precipitation intensity, and consequently, only small amounts of lateral flow (Redding and Devito 2008). While this may be indicative of the importance of precipitation intensity, it is somewhat confounded by the fact that the rainfall depth of event 8 was approximately at the threshold necessary for lateral flow generation. This indicates that even at higher intensities, there may not have been enough surplus water beyond internal storage to generate significant lateral flow. Prior to the irrigation experiment, a rainfall event of 27.5 mm with a maximum 30-minute intensity of 5 mm hr^{-1} fell on the RE plot soils, which were at field capacity, and failed to produce lateral flow (Redding and Devito 2008). Further, during July 2005, a rain event of approximately 80 mm over 23 hours, with a maximum 30-minute intensity of 24 mm h^{-1}, resulted in an increase in soil moisture storage of 65–80 mm at different monitoring locations with no evidence of hillslope contributions to receiving wetlands or ponds (Figure 4.11). The overall event intensity of > 3 mm h^{-1} for 23 hours has a return period of approximately 100 years (Hogg and Carr 1985). This may also reflect the importance of roots or soil fractures in moving water vertically in the soil profile. This event, which was large for the research area, indicates the limited potential for lateral flow on these hillslopes with considerable soil storage capacity (Figure 4.11). To better understand the role of precipitation intensity on lateral flow generation on these hillslopes, it will be necessary to investigate the response of

large applications (well above threshold amounts) of precipitation at a range of intensities.

4.5.3 Spatial Variability of Soil Properties

The influence of spatial heterogeneity on variability in runoff threshold and amounts is critical in modelling and predicting hillslope responses. Although plots in this study were only 4 m apart, and similar flow mechanisms were observed once the soils were filled to field capacity, the lateral flow responses to the later irrigation events ranged from runoff coefficients of 0.15 to 0.35 in the RU and RE plots, respectively, even though similar irrigation volumes and intensities were applied. Runoff responses in this study were low compared to those on sites on the Boreal Shield that had soils with limited soil storage and relatively impervious bedrock. On those sites, runoff coefficients were 0.35–0.75 or greater (Hill et al. 1999, Buttle and McDonald 2002). Several factors could explain the difference in flow rate and magnitude between the two plots in this study during the later irrigation events. Once saturated, the differences in the surface slope of the plots (RE: surface slope = 0.15; RU: surface slope = 0.09) may have influenced the partitioning between vertical or lateral flow. In the RE plot, the higher clay content may have reduced the drainable porosity, thereby resulting in greater lateral flow due to reduced storage. After two weeks of post-irrigation drainage, changes in soil moisture storage in the top 1 m of the RU plot (-47 mm) were greater than those in the RE plot (-27 mm) (T. Redding, unpublished data). The longer period of wetting in the RE plot likely resulted in deeper wetting, thereby reducing the vertical water potential gradient that would have pulled water deeper. The RU plot had less wetting; therefore, the vertical water potential gradient would have more strongly influenced vertical flow and may have resulted in a reduced lateral flow response (Redding and Devito 2008). It is also possible that the rooting distribution or orientation was slightly different between the plots; therefore, fewer roots in the RU plot connected to the pit face and moved water laterally. This is supported by the fact that only six preferential flow outlets were observed in the RU plot pit face, whereas nine were observed in

the RE plot pit face. Due to differences in plot size, and similar total volumes and timing of water applications, rainfall depth and intensity were greater on the RE plot. There were no systematic differences between plots in the relationship between flow velocity and rainfall intensity (Figure 4.10); therefore, higher intensities in the RE plot could partially explain the greater lateral flow on that plot.

Soil heterogeneity may increase variability in lateral flow at depth and also influence the potential lateral connectivity along hillslopes. This will further complicate predictions of timing and magnitude of lateral flow from entire hillslopes or watersheds that have heterogeneous soils and surficial geology. Groundwater studies conducted adjacent to the experimental plots revealed the presence of large areas of dense clay, which may act as a restricting layer on hillslope segments that had increased lateral flow potential (K. Devito, unpublished data). However, lateral flow contributions to the hillslope base and adjacent wetlands or aquatic systems require that clay-rich areas be connected to each other or that they follow the slope. Given the heterogeneous stratigraphy of the hillslopes, with differences in depth to restricting layer (which controls available storage) and differences in particle size (which influences hydraulic properties), whole hillslope connectivity may be elusive because areas of deeper or more vertically conductive soils may act as barriers to spatially continuous lateral flow (McNamarra et al., 2005).

4.5.4 Potential for Lateral Flow Under Natural Conditions

On forested hillslopes with Luvisolic soils on the Boreal Plains, lateral flow generation is a function of available soil moisture storage to a given depth, K_s at the base of that depth, which forms the "effective" restricting layer, and precipitation depth and intensity. The minimum storage that must be satisfied (assuming soils are at field capacity ($S_{FC)}$) is determined by the precipitation intensity required to generate either preferential flow from the surface or lateral flow through percolation excess and transmissivity feedback. The conditions required for lateral flow generation can be summarized as follows (Figure 4.1):

1. Soil moisture storage must be filled to field capacity of the soil (S_{FC}) above the effective restricting layer.
2. Event P depth must be greater than internal storage (15–20 mm).
3. Event P intensity must be high enough for preferential flow initiation in the upper horizons, or greater than K_s at the depth of the effective restricting layer.

However, there is a low probability of satisfying each of these conditions (Figures 4.11 and 4.12).

Given the close relationship between precipitation and evapotranspiration on the Boreal Plains (Devito et al., 2005b), the probability of generating a moisture surplus sufficient to wet soils to field capacity is relatively low during the growing season. Plant water demand is lowest between snowmelt and leaf-out of the aspen canopy, and after senescence of the canopy and before the onset of winter. While soils are typically at their wettest immediately following snowmelt, the probability of rainfall events that satisfy criteria 2 and 3 above are very low (Figure 4.12). Precipitation data from Red Earth Creek indicates that in May, there is only a 1.5% probability that daily precipitation will be 20 mm or greater. In the fall, once the forest has senesced, soils are typically drier than they are post-snowmelt (Figure 4.11), and there is only a 1.1% probability that daily precipitation will be 20 mm or greater. Therefore, even if soils are at field capacity, which is uncommon, there is a low probability that daily precipitation will exceed the threshold required (Redding and Devito 2008). It is also clear from the data presented in Figure 4.11 that many locations do not reach the soil moisture storage thresholds over the spring, fall, or growing season. There is also considerable spatial variability between locations on the same or adjacent hillslopes with similar soils. During the 2005 growing season, some locations approached or exceeded the RU plot threshold, but only following snowmelt and after a rain event of approximately 80 mm (Figure 4.11).

To evaluate the threshold-based conceptual model, Figure 4.12 provides depth profiles of available soil moisture storage and K_s, and precipitation intensity-duration-frequency curves for the study region. Based on the model, lateral flow will occur only infrequently on moraine soils characteristic of the study region, along a continuum of precipitation intensity and soil moisture storage. The extremes of the continuum range from very high-intensity events that only need to saturate soils near the surface (shallow effective restricting layer) to low-intensity events on already wet soils (deeper effective restricting layer). In either case, the probability of exceeding the limiting factors (very high-intensity precipitation or filling soil storage to C horizon) is low. For example, to generate lateral flow from the Ae horizon, it is necessary to wet the profile to the C horizon and then have a precipitation event that provides adequate water to saturate the profile upwards from the restricting layer (C horizon) into the Ae horizon. The RU plot required 97 mm of applied precipitation before significant (> 1 mm) lateral flow was generated. This was additional to considerable wetting that had occurred between the end of the growing season and the beginning of the irrigation applications (Redding and Devito, 2008). Once soils are wetted to this depth, a rainfall event of 20 mm or greater is required to satisfy internal storage (Redding and Devito, 2008), and the intensity must be greater than the K_s of the C horizon (0.4-7 mm h^{-1}). The minimum return period observed is 2–5 years, which is for an event of 10 mm h^{-1} for 2 hours (Figure 4.12).

Alternatively, lateral flow may be generated from the Ae horizon if the required storage is filled (which is much less than filling storage to C horizon); however, the P intensity required to generate lateral flow by percolation excess must exceed the K_s of 10-400 mm hr^{-1}. The extreme rainfall intensities required under this scenario are highly unlikely. This also indicates that under unfrozen conditions that overland flow is extremely unlikely for these hillslopes during unfrozen conditions.

Both runoff generation extremes outlined above will be infrequent based on the precipitation depths required to fill storage to the C horizon or on the high precipitation intensities required to exceed K_s near the surface. Because K_s

decreases with depth, both lateral and vertical flow will be limited, and water will be stored and/or develop transient saturation. If transient saturation occurs, it will have to rise higher in the profile (transmissivity feedback) for lateral flow to occur through macropores. For most storms observed in the study region, the precipitation intensity is less than the K_s, and there is large available soil moisture storage in the unsaturated zone. Regional stream runoff responses indicate there is very little runoff (runoff coefficient less than 10%) in most years (Redding and Devito 2008). Significant lateral flow is produced only infrequently, usually by large and intense rainstorms that follow wet years, such as those experienced in 1997 (Devito et al. 2005b).

4.6 Summary and Conclusions

To predict when hillslope runoff and recharge may occur on the Boreal Plains, it is necessary to understand the thresholds for, and mechanisms of, lateral and vertical flow. Rainfall simulation experiments were used to elucidate the lateral flow mechanisms for Boreal Plains hillslopes with Luvisolic soils. Two complementary mechanisms produced lateral flow: the first was preferential flow generated from near the soil surface; the second involved the development of a perched water table above the C horizon and the generation of lateral flow by the transmissivity feedback mechanism. At the precipitation event scales tested, lateral subsurface flow paths were dominated by preferential flow through root channels in the B_t horizon rather than by flow at the Ae/Bt horizon boundary.

The controls on lateral flow generation are antecedent soil moisture storage, soil K_s, event P depth, and event P intensity. For areas without a well-defined restricting layer (e.g., impervious bedrock), which directs flow laterally, the layer upon which lateral flow develops is defined by the hydraulic conductivity of that layer relative to the rate of water input. In this study, hydraulic conductivity below approximately 0.5 m depth declined to a rate of < 10 mm hr^{-1}. Given the high intensity of applied rainfall, lateral flow occurred above this layer, through the Bt horizon.

Based on the climate and soil characteristics of the study site, there is a low potential for lateral flow from similar hillslopes in the Boreal Plains region. In wet years, the potential for lateral flow increases but remains low due to the high ET demand of the forest vegetation during the summer rainy season. To understand and predict the frequency of lateral flow and drainage from the soil profile, it will be necessary to combine an understanding of frequency distributions of precipitation and soil moisture storage. Long-term data on soil moisture conditions are not available for this area; therefore, models will have to be used to generate the probability distributions of soil moisture conditions.

Based on the precipitation return periods required to generate lateral flow from the study plots, it appears that forested hillslopes with fine-textured soils rarely contribute lateral flow and are, therefore, decoupled from adjacent wetlands and ponds. This has important implications for the hydrology and biogeochemistry of wetland systems in this region, and for the sustainability of wetland habitats under conditions of climate change or watershed disturbance.

Table 4.1. Event water contributions (%) for event 7 in the root exclusion (RE) and root uptake (RU) plots. Values are volume weighted event water % of lateral flow collected at each trough and total depth of event water in lateral flow (mm).

Trough	RE Plot	RU Plot
A	61 % (0.2 mm)	62 % (0.5 mm)
B	66 % (7.4 mm)	60 % (1.8 mm)
C	47 % (1.9 mm)	52 % (0.5 mm)
Total	61 % (9.5 mm)	60 % (2.8 mm)

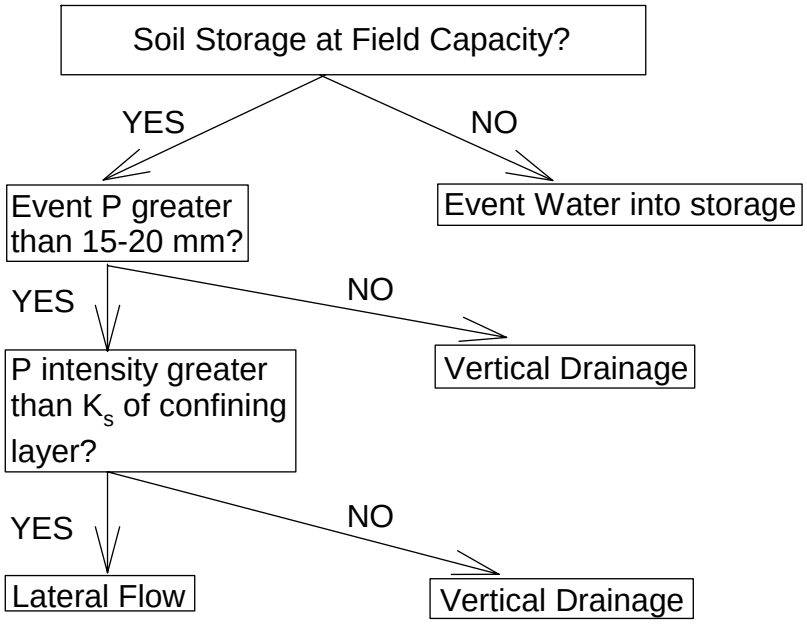

Figure 4.1. Threshold-based conceptual model of lateral flow generation.

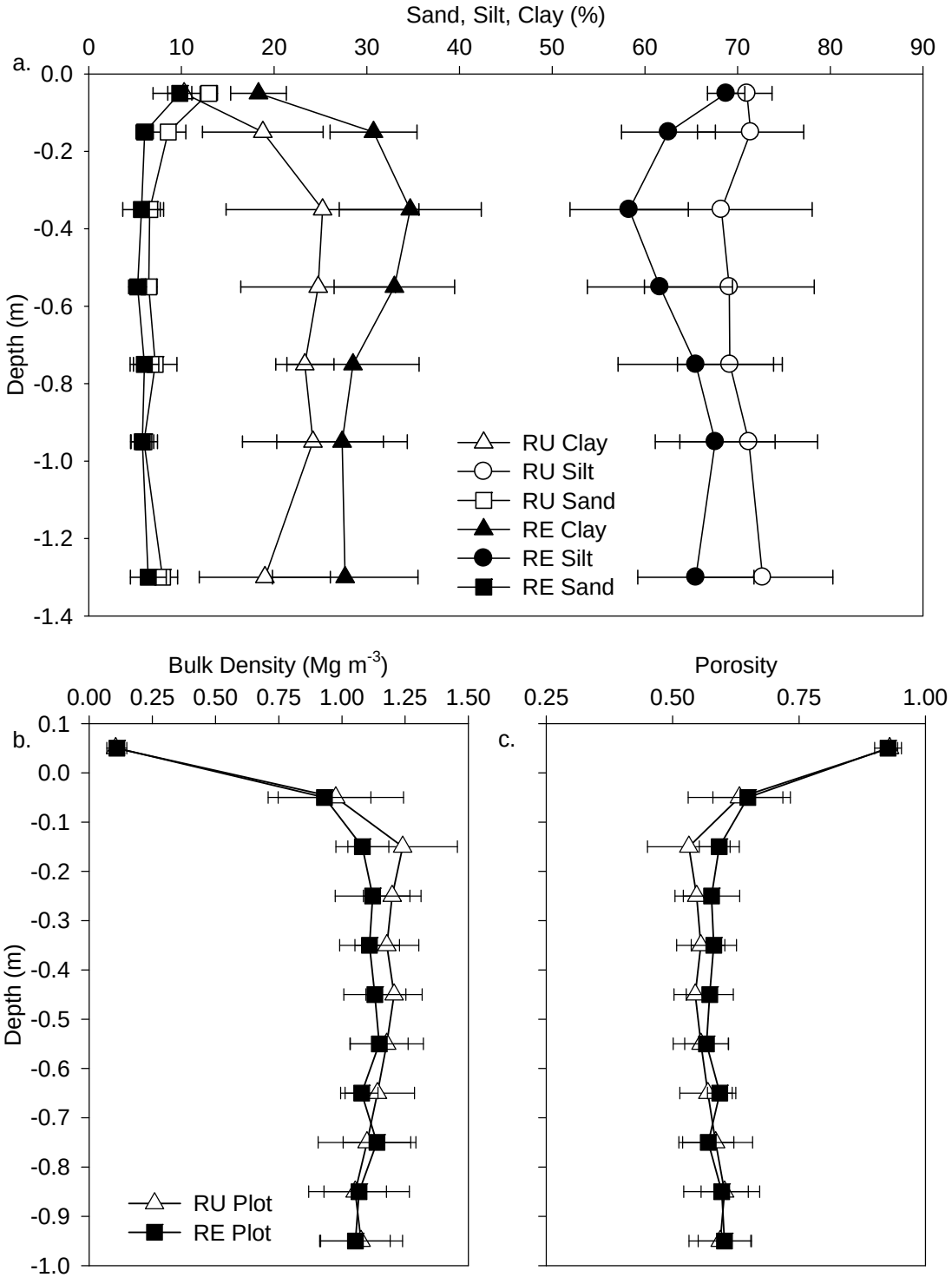

Figure 4.2. Depth profiles of (a) particle size distribution, (b) bulk density, and (c) porosity for the root exclusion (RE) and root uptake (RU) plots. Values are mean and standard deviation for particle size (n = 9), bulk density (n = 18), and porosity (n = 18).

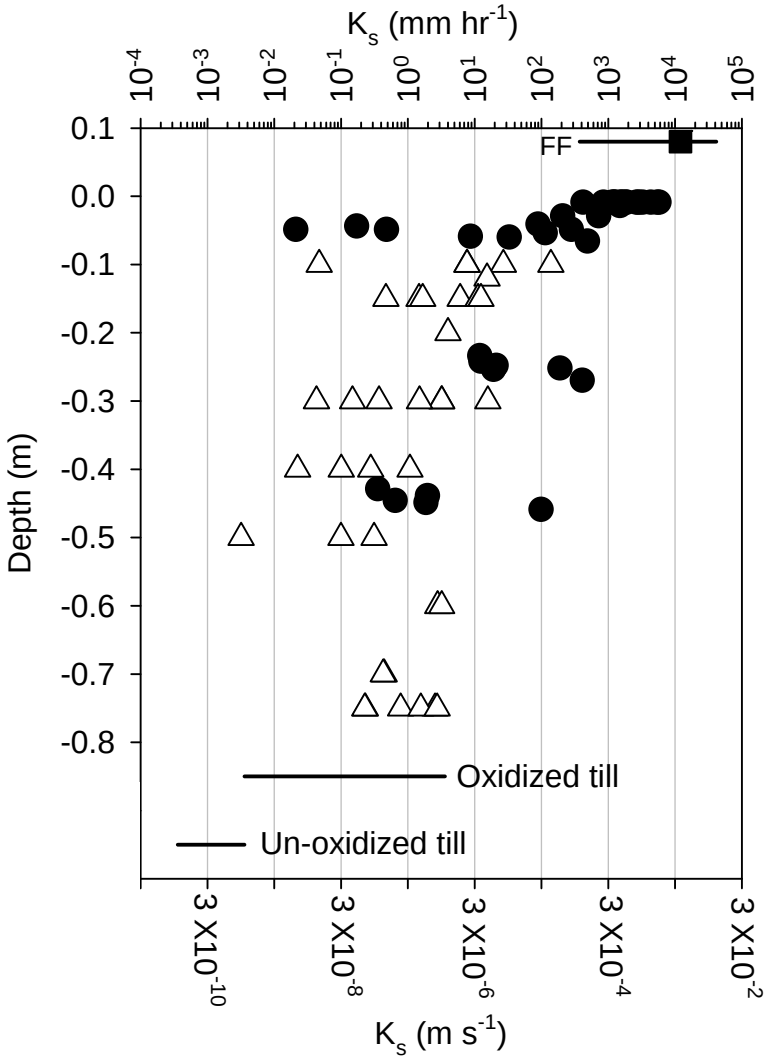

Figure 4.3. Field measured saturated hydraulic conductivity (K_s), determined in-situ using the single ring infiltrometer (filled circle) and Guelph permeameter (open triangle) methods. Values (mean and range) for forest floor (filled square) are taken from Lauren and Heiskanen (1997). The range in K_s for oxidized and unoxidized till materials is taken from Hendry (1982), Hayashi et al. (1998), and Ferone and Devito (2004), as measured at other Boreal Plains and Prairie locations with similar surficial geology.

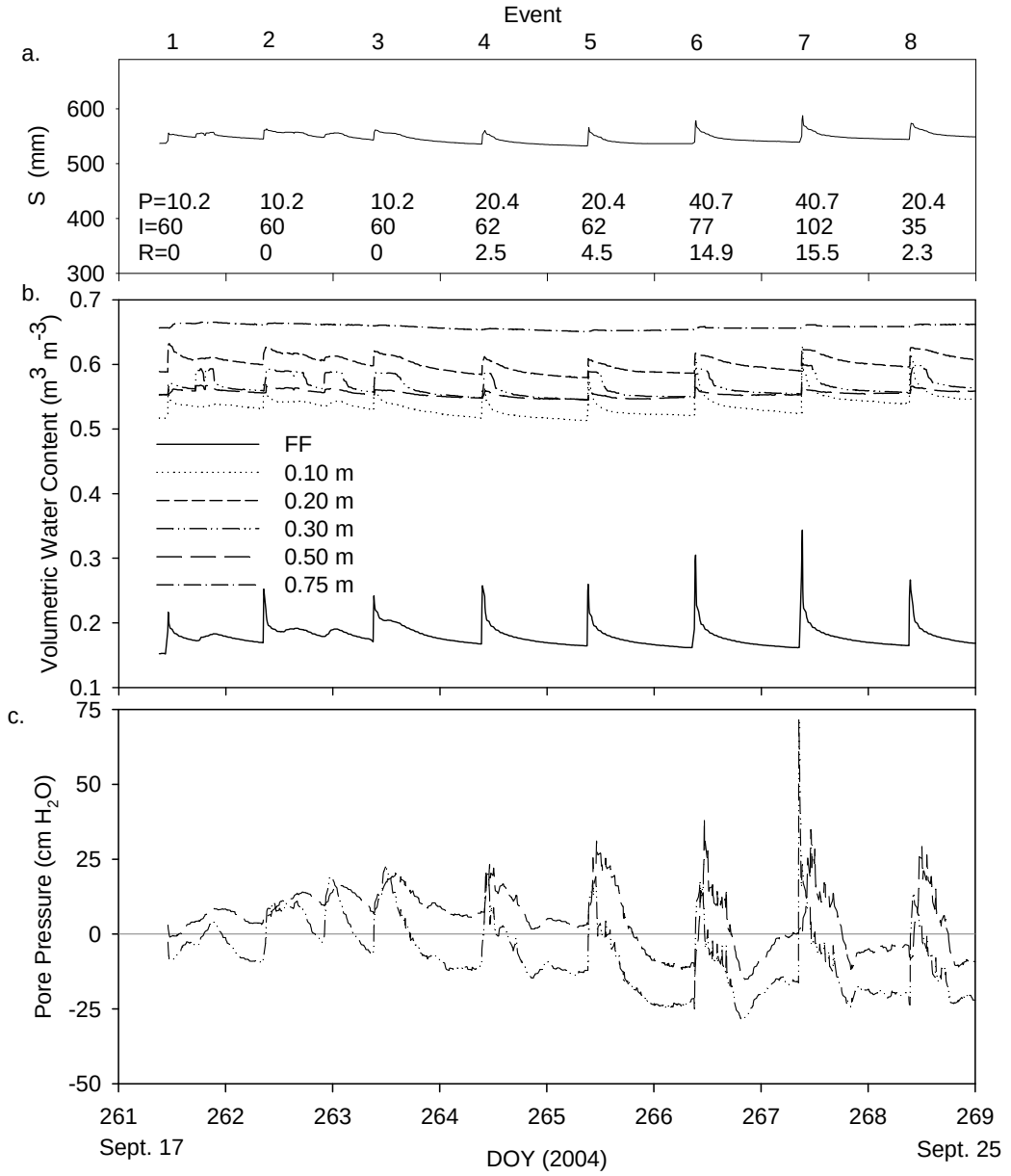

Figure 4.4. Root exclusion (RE) plot: (a) soil moisture storage (S), (b) volumetric water content, and (c) pore pressure over the duration of the experiment (DOY: day of year). Pore pressure data immediately prior to event 7 are missing due to the refilling of the tensiometers. Numbers along the top of (a) refer to event precipitation (P, mm), irrigation intensity (I, mm h^{-1}), and runoff (R, mm) for each event. In panel (b), FF refers to forest floor.

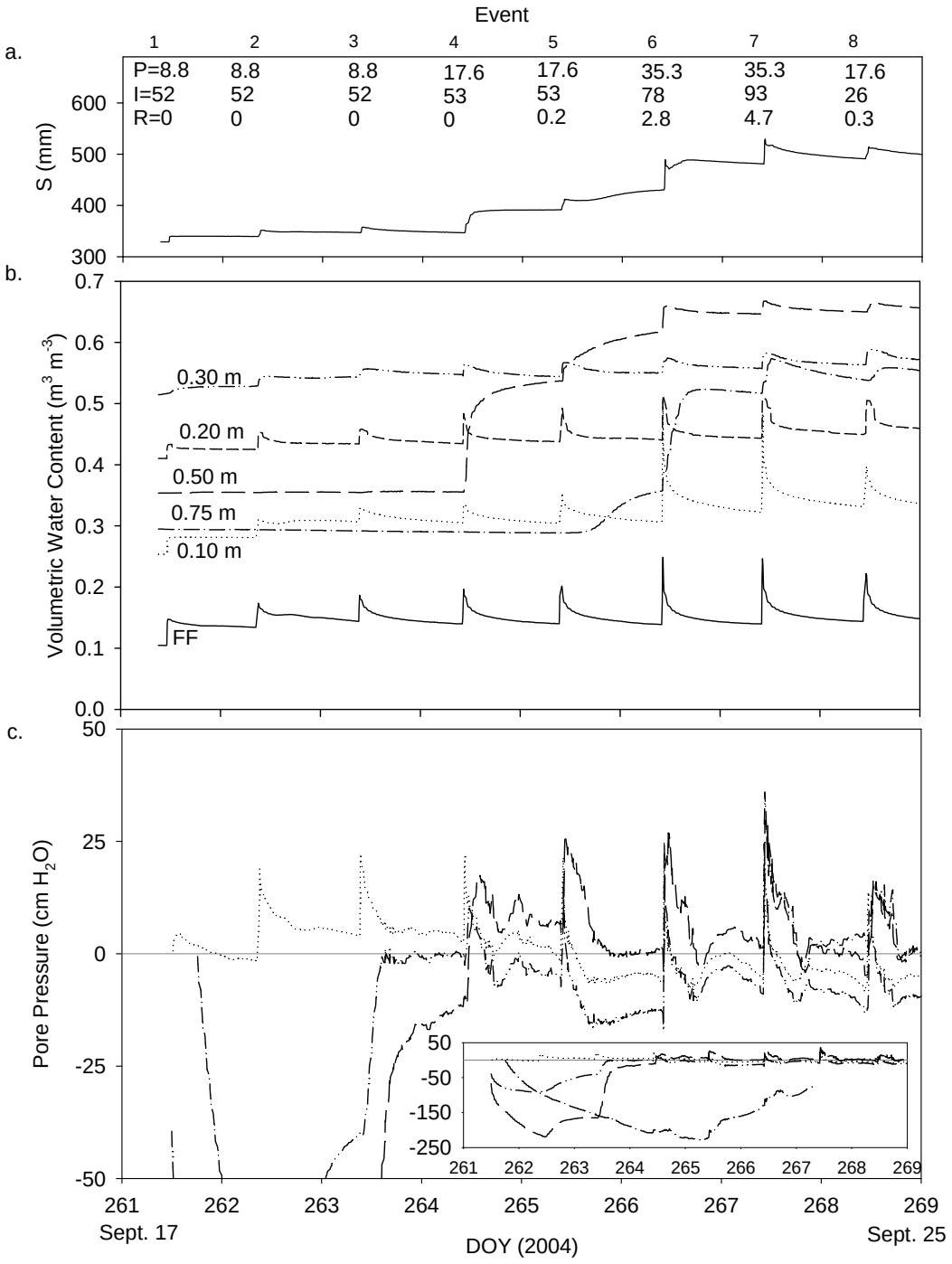

Figure 4.5 Root uptake (RU) plot: (a) soil moisture storage (S), (b) volumetric water content, and (c) pore pressure over the duration of the experiment (DOY: day of year). Pore pressure data prior to event 7 are missing due to the refilling of the tensiometers. Numbers along the top of (a) pertain to event precipitation (P, mm), irrigation intensity (I, mm h^{-1}), and runoff (R, mm) for each event. The line types for each measurement depth are consistent between panels (b) and (c). The inset in panel (c) shows the full range of pore pressures as the deeper tensiometers equilibrated. In panel (b), FF refers to forest floor.

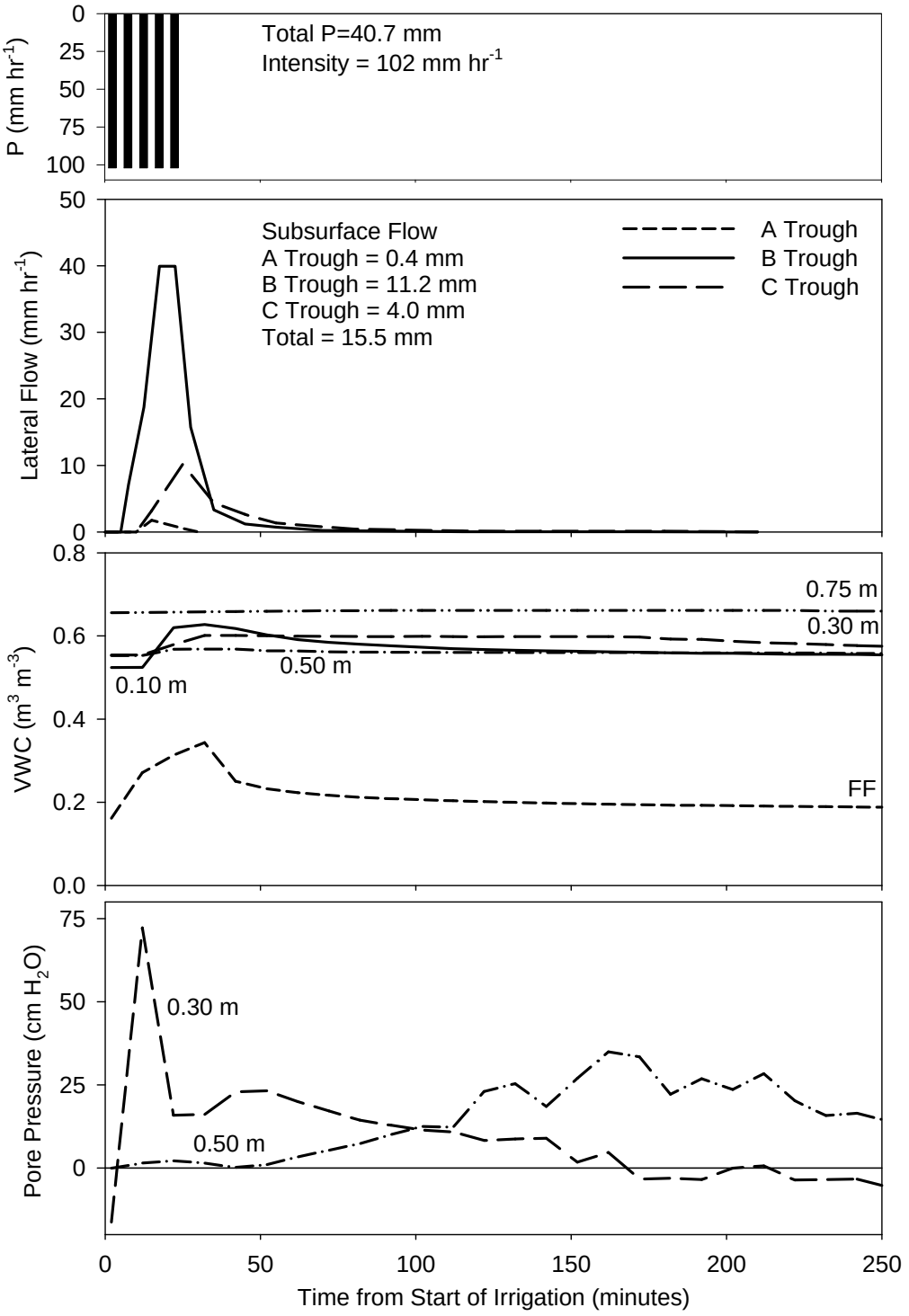

Figure 4.6. Root exclusion (RE) plot: Event 7 time-series for (a) precipitation intensity, (b) subsurface flow rates, (c) volumetric water content (VWC), and (d) pore pressure. The line types for each measurement depth are consistent between panels (b) and (c). For the sake of clarity, the volumetric water content data at 0.2 m depth are not shown.

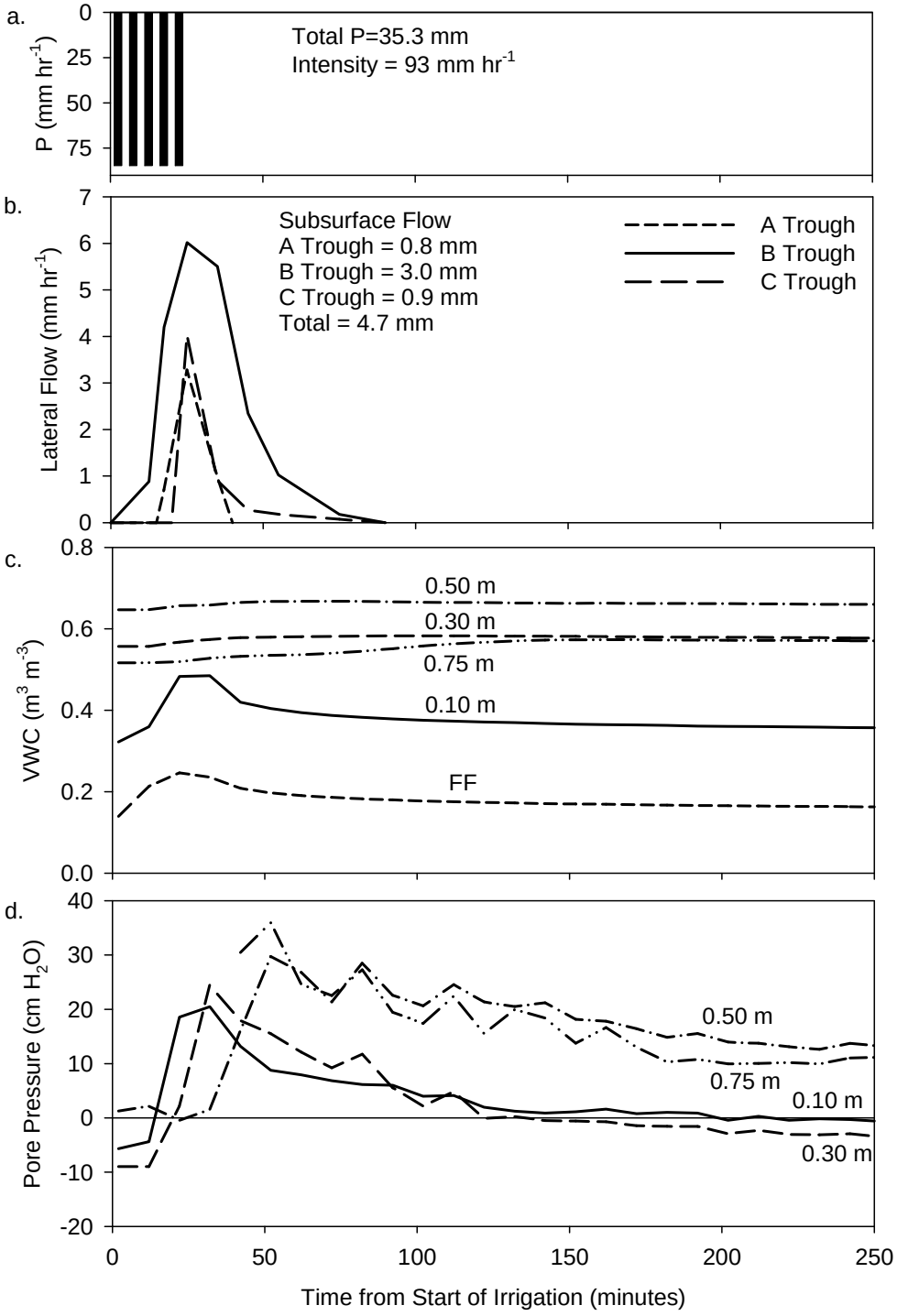

Figure 4.7. Root uptake (RU) plot: Event 7 time-series for (a) precipitation intensity, (b) subsurface flow rates, (c) volumetric water content (VWC), and (d) pore pressure. For the sake of clarity, the volumetric water content data at 0.2 m depth are not shown. Note the different scale of subsurface flow compared to Figure 4.6.

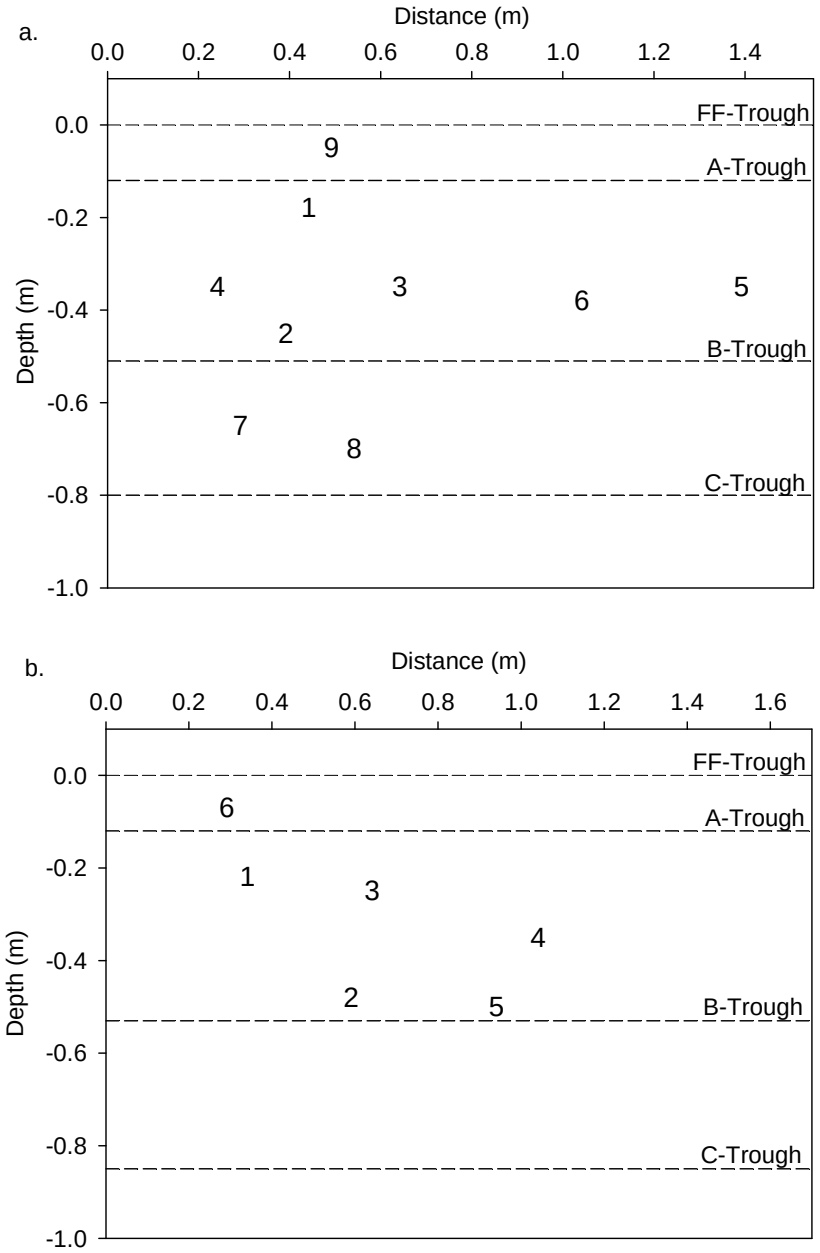

Figure 4.8. Locations of preferential flow outlets at the pit faces of the (a) root exclusion (RE) plot and (b) root uptake (RU) plot. Preferential flow outlets are labelled by the collection trough into which they drained, and are numbered in the order in which they began contributing flow. FF refers to forest floor.

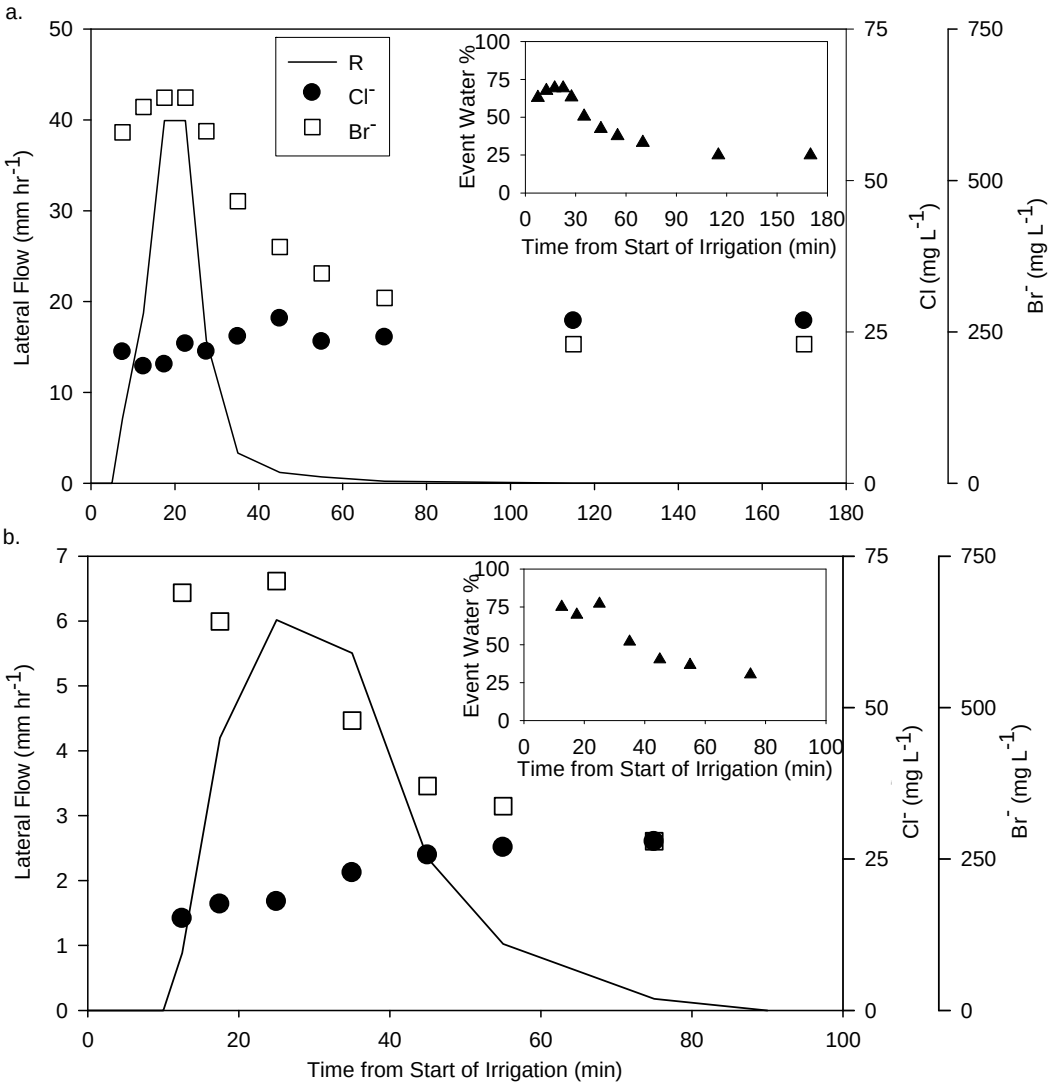

Figure 4.9. Event 7 (a) root exclusion (RE) plot B trough lateral flow rates and Cl^- and Br^- tracer concentrations, and (b) root uptake (RU) plot B trough lateral flow volumes and Cl^- and Br^- tracer concentrations. The inset plots show the time series of event water proportions (%) over the duration of flow. The Br^- tracer was applied during event 7 at a concentration of 920 mg L^{-1}.

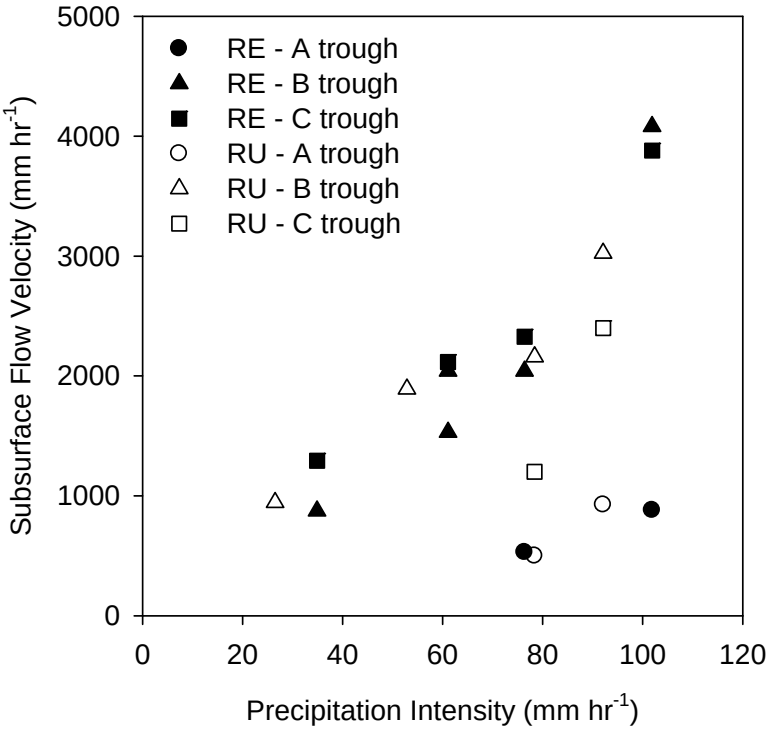

Figure 4.10. Calculated minimum subsurface flow velocities at each collection trough versus precipitation intensity for events with measured lateral flow. Filled symbols are for the root exclusion (RE) plot; open symbols are the root uptake (RU) plot. The A trough is denoted by circles, the B trough by triangles, and the C trough by squares.

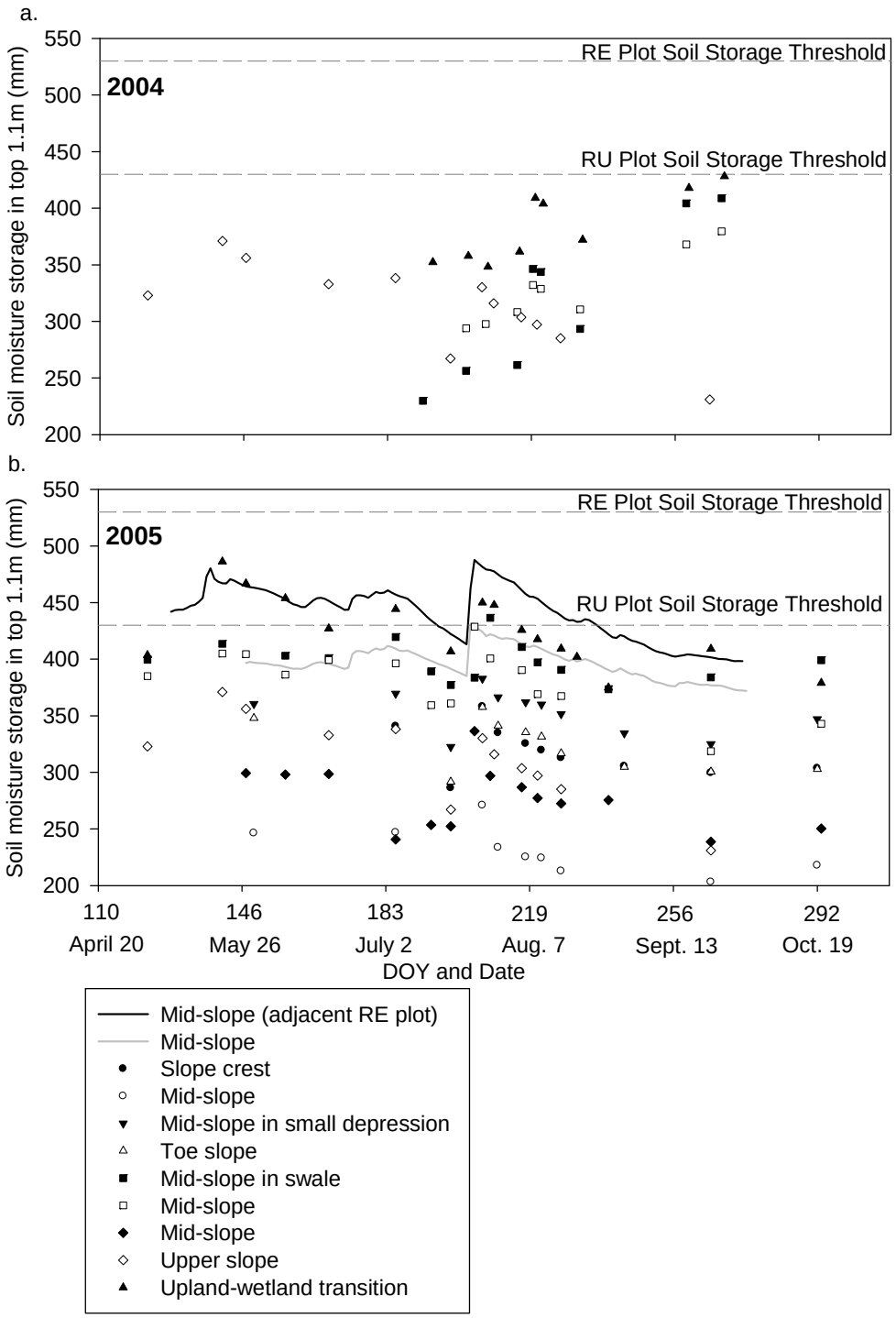

Figure 4.11. Measured soil moisture storage in top 1.1 m for the 2004 and 2005 growing seasons for the experimental hillslope and similar adjacent hillslopes. Individual symbols indicate sites with periodic manual TDR measurements. The black and gray lines are daily average soil moisture storage at sites with continuous measurement systems. Horizontal dashed lines indicate the storage thresholds required for lateral flow generation based on the results of Redding and Devito (2008).

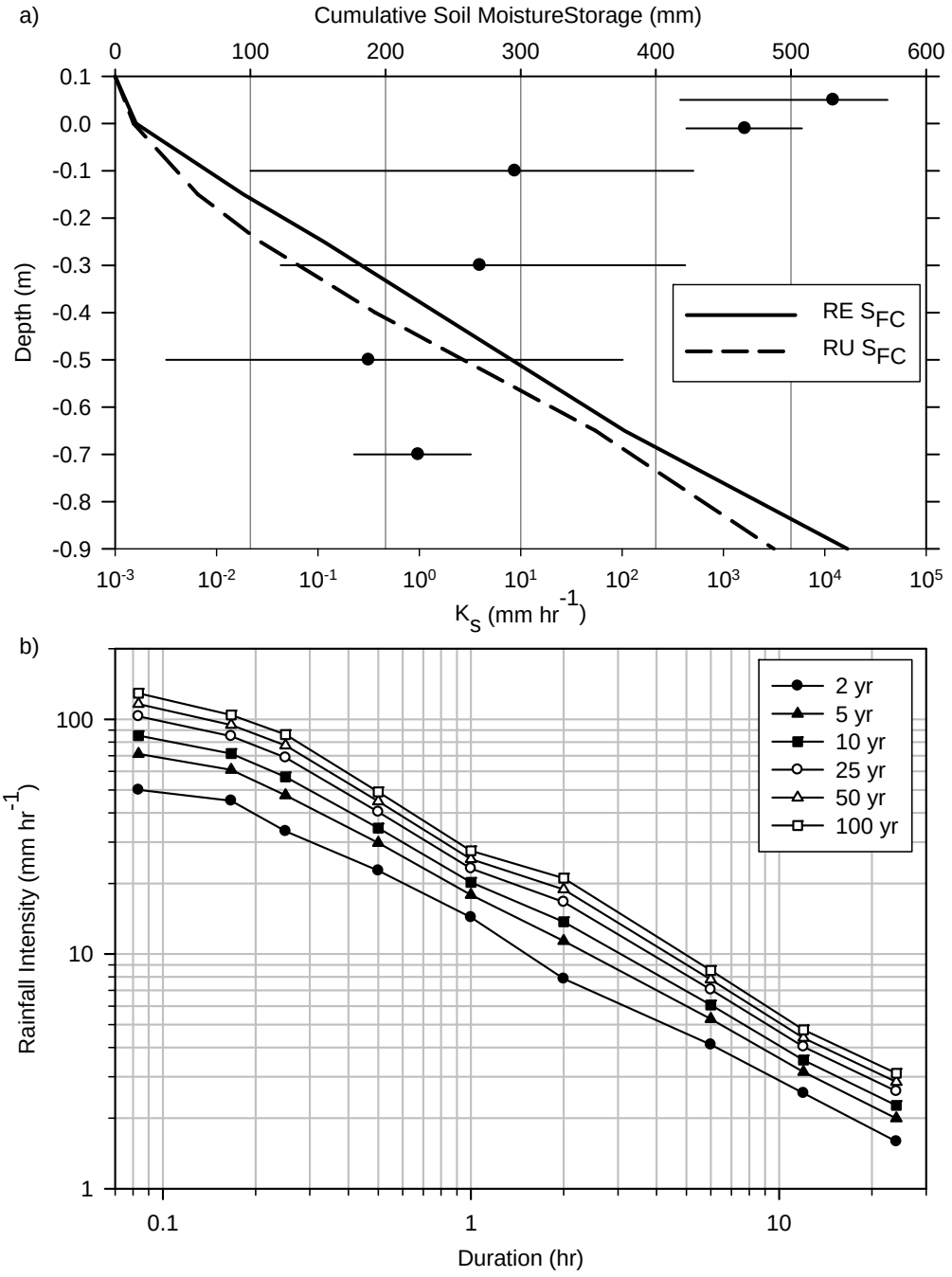

Figure 4.12. Plot showing cumulative available soil moisture storage at field capacity (S_{FC}) with depth for the root exclusion (RE) and root uptake (RU) plots. Estimates of S_{FC} are calculated from TDR data. Horizontal solid lines and filled circles are the range and geometric mean of measured saturated hydraulic conductivity (K_s) for given depth intervals. Plot (b) shows rainfall intensity-duration-frequency for the Utikuma Region Study Area region, taken from Hogg and Carr (1985). Each line is a separate return period (yr).

4.7 References

Anderson, A.E. 2008. Patterns of water table dynamics and runoff generation in a watershed with preferential flow networks. PhD. Thesis. University of British Columbia, Vancouver. , 130 pp.

Beven, K.J. 1982. On subsurface stormflow: Predictions with simple kinematic theory for saturated and unsaturated flows. Water Resources Research 18: 1627-1633.

Blanken, P.D., Black, T.A., Neumann, H.H., den Hartog, G., Yang, P.C., Nesic, Z. and Lee, X. 2001. The seasonal water and energy exchange above and within a boreal aspen forest. Journal of Hydrology 245: 118-136.

Buttle, J.M. 1994. Isotope hydrograph separations and rapid delivery of pre-event water from drainage basins. Progress in Physical Geography. 18: 16-41.

Buttle, J.M. and House, D.A. 1997. Spatial variability of saturated hydraulic conductivity in shallow macroporous soils in a forested basin. Journal of Hydrology 203: 127-142.

Buttle, J.M. and McDonald, D.J. 2000. Soil macroporosity and infiltration characteristics of a forest podzol. Hydrological Processes 14: 831-848.

Buttle, J.M. and McDonald, D.J. 2002. Coupled vertical and lateral preferential flow on a forested slope. Water Resources Research 38: doi:10.1029/2001WR000773.

Cuenca, R.H., Strangel, D.E. and Kelly, S.F. 1997. Soil water balance in a boreal forest. Journal of Geophysical Research 102(D24): 29355-29365.

Devito, K., Creed, I., Gan, T., Mendoza, C., Petrone, R., Silins, U. and Smerdon, B. 2005a. A framework for broad-scale classification of hydrologic response units on the Boreal Plain: is topography the last thing to consider? Hydrological Processes 19: 1705-1714.

Devito, K.J., Creed, I.F. and Fraser, C.J.D. 2005b. Controls on runoff from a partially harvested aspen-forested headwater catchment, Boreal Plain, Canada. Hydrological Processes 19: 3-25.

De Vries, J. and Chow, T.L. 1978. Hydrologic behavior of a forested mountain soil in coastal British Columbia. Water Resources Research 14: 935-942.

Ecoregions Working Group. 1989. Ecoclimatic Regions of Canada. Ecological Land Classification Series No. 23.

Elliott, J.A., Toth, B.M., Granger, R.J. and Pomeroy, J.W. 1998. Soil moisture storage in mature and replanted sub-humid boreal forest stands. Canadian Journal of Soil Science 78: 17-27.

Elshorbagy, A., Jutla, A., Barbour, L. and Kells, J. 2005. System dynamics approach to assess the sustainability of reclamation of disturbed watersheds. Canadian Journal of Civil Engineering 32: 144-158.

Fenton, M.M., Paulen, R.C. and Pawlowicz, J.G. 2003. Surficial geology of the Lubicon Lake area, Alberta (NTS 84B/SW). Alberta Geological Survey, Edmonton.

Ferone, J.M. and Devito, K.J. 2004. Shallow groundwater-surface water interactions in pond-peatland complexes along a Boreal Plains topographic gradient. Journal of Hydrology 292: 75-95.

Hayashi, M., van der Kamp, G. and Rudolph, D.L. 1998. Water and solute transfer between a prairie wetland and adjacent uplands, 1. Water balance. Journal of Hydrology 207: 42-55.

Hendry, M.J. 1982. Hydraulic conductivity of a glacial till in Alberta. Ground Water 20: 162-169.

Hill, A.R., Kemp, W.A., Buttle, J.M. and Goodyear, D. 1999. Nitrogen chemistry of subsurface storm runoff on forested Canadian Shield hillslopes. Water Resources Research 35: 811-821.

Hogg, W.D. and Carr, D.A. 1985. Rainfall frequency atlas for Canada. Environment Canada. Ottawa.

Jardine, P.M., Wilson, G.V. and Luxmoore, R.J. 1990. Unsaturated solute transport through a forest soil during rain storm events. Geoderma 46: 103-118.

Kendall, C.A., Shanley, J.B. and McDonnell, J.J. 1999. A hydrometric and geochemical approach to test the transmissivity feedback hypothesis during snowmelt. Journal of Hydrology 219: 188-205.

Kienzler, P.M. and Naef, F. 2008. Subsurface storm flow formation at different hillslopes and implications for the 'old water paradox'. Hydrological Processes 22: 104-116.

Kirchner, J.W. 2006. Getting the right answers for the right reasons: Linking measurements, analyses, and models to advance the science of hydrology. Water Resources Research 42: doi:10.1029/2005WR004362.

Lauren, A., and Heiskanen, J. 1997. Physical properties of the mor layer in a Scots pine stand I. Hydraulic conductivity. Canadian Journal of Soil Science 77: 627-634.

Lehmann, P., Hinz, C., Tromp-van Meerveld, H.J. and McDonnell, J.J. 2007. Rainfall threshold for hillslope connectivity: an emergent property of flow pathway connectivity. Hydrology and Earth System Science 11: 1047-1063.

Lin, H., Bouma, J., Wilding, L.P., Richardson, J.L., Kutilek, M. and Nielson, D.R. 2005. Advances in Hydropedology. Advances in Agronomy 85: 1-89.

Lischeid, G. 2008. Combining hydrometric and hydrogeochemical data sets for investigating runoff generation processes: Tautologies, inconsistencies and possible explanations. Geography Compass 2: 255-280.

Lohse, K.A. and Dietrich, W.E. 2005. Contrasting effects of soil development on hydrological properties and flow paths. Water Resources Research 41: doi:10.1029/2004WR003403.

Marshall I.B., Schut, P. and Ballard, M. 1999. A National Ecological Framework for Canada: Attribute Data. Environmental Quality Branch, Ecosystems Science Directorate, Environment Canada and Research Branch, Agriculture and Agri-Food Canada, Ottawa. http://sis.agr.gc.ca/cansis/nsdb/ecostrat/data_files.html (Accessed March 25, 2009).

McDonnell, J.J. 1990. A rationale for old water discharge through macropores in a steep, humid catchment. Water Resources Research 26: 2821-2832.

McNamara, J.P., Chandler, D., Seyfried, M. and Achet, S. 2005. Soil moisture states, lateral flow, and streamflow generation in a semi-arid, snowmelt driven catchment. Hydrological Processes 19: 4023-4038.

Montgomery, D.R., Dietrich, W.E., Torres, R., Anderson, S.P., Heffner, J.T. and League, K. 1997. Hydrologic response of a steep, unchanneled valley to natural and applied rainfall. Water Resources Research 33: 91-109.

Mosley, M.P. 1979. Streamflow generation in a forested watershed, New Zealand. Water Resources Research 15: 795-806.

Mosley, M.P. 1982. Subsurface flow velocities through selected forest soils, South Island, New Zealand. Journal of Hydrology 55: 65-92.

Newman, B.D., Campbell, A.R. and Wilcox, B.P. 1998. Lateral subsurface flow pathways in a semiarid ponderosa pine hillslope. Water Resources Research 34: 3485-3496.

Newman, B.D., Wilcox, B.P.. and Graham, R.C. 2004. Snowmelt driven macropore flow and soil saturation in a semiarid forest. Hydrological Processes 18: 1035-1042.

Nimmo, J.R. 2003. How fast does water flow in an unsaturated macropore?: Evidence from field and lab experiments. In Alvarez-Benedi, J., and Marinero, P., eds., Estudios de la Zona No Saturada del Suelo, v. VI: Valladolid, Spain, Instituto Tecnologico de Castilla y Leon, p. 1-8.

Pearce, A.J., Stewart, M.K., and Sklash, M.G. 1986. Storm runoff generation in humid headwater catchments 1. Where does the water come from? Water Resources Research 22: 1263-1272.

Peters, D.L., Buttle, J.M., Taylor, C.H. and LaZerte, B.D. 1995. Runoff production in a forested, shallow soil, Canadian Shield basin. Water Resources Research 31: 1291-1304.

Redding, T.E. and Devito, K.J. 2008. Lateral and vertical flow thresholds for aspen forested hillslopes on the Western Boreal Plain, Alberta, Canada. Hydrological Processes 23: 4287-4300.

Reynolds, W.D. 1995. TIDAP-6. Agriculture and AgriFood Canada. Ottawa.

Rodhe, A. 1987. The origin of streamwater traced by Oxygen-18. PhD Thesis. Uppsala University, Uppsala, 260 pp.

Scherrer, S., Naef, F., Faeh, A.O. and Cordery, I. 2007. Formation of runoff at the hillslope scale during intense precipitation. Hydrology and Earth System Science 11: 907-922.

Sklash, M.G., Stewart, M.K., and Pearce, A.J. 1986. Storm runoff generation in humid headwater catchments 2. A case study of hillslope and low-order stream response. Water Resources Research 22: 1273-1282.

Soil Classification Working Group. 1998. The Canadian System of Soil Classification (Third Edition), Agriculture and Agri-Food Canada, Ottawa. 187 pp.

Timmons, D.R., Verry, E.S., Burwell, R.E. and Holt, R.F. 1977. Nutrient transport in surface runoff and interflow from an aspen-birch forest. Journal of Environmental Quality 6: 188-192.

Torres, R. 2002. A threshold condition for soil-water transport. Hydrological Processes 16: 2703-2706.

Torres, R. and Alexander, L. 2002. Intensity-duration effects on drainage: Column experiments at near-zero pressure head. Water Resources Research 38: doi:10.1029/2001WR001048.

Tromp-van Meerveld, H.J. and McDonnell, J.J. 2006. Threshold relations in subsurface stormflow: 2. The fill and spill hypothesis. Water Resources Research 42: doi:10.1029/2004WR003800.

Tromp-van Meerveld, H.J., Peters, N.E. and McDonnell, J.J. 2007. Effect of bedrock permeability on subsurface stormflow and the water balance of a trenched hillslope at the Panola Mountain Research Watershed, Georgia, USA, Hydrological Processes 21: 750-769.

Tymchak, M.P. and Torres, R. 2007. Effects of variable rainfall intensity on the unsaturated zone response of a forested sandy hillslope. Water Resources Research 43: doi:10.1029/2005WR004584.

Uchida, T., Tromp-van Meerveld, H.J. and McDonnell, J.J. 2005. The role of lateral pipe flow in hillslope runoff response: an intercomparison of non-linear hillslope response. Journal of Hydrology 311: 117-133.

Warrick, A.W., Wierenga, P.J., Young, M.H.. and Musil, S.A. 1998. Diurnal fluctuations of tensiometric readings due to surface temperature changes. Water Resources Research 34: 2863-2869.

Weiler, M., and Fluhler, H. 2004. Inferring flow types from dye patterns in macroporous soils. Geoderma 120: 137-153.

Weiler, M. and Naef, F. 2003. An experimental tracer study of the role of macropores in infiltration in grassland soils. Hydrological Processes 17: 477-493.

Weiler, M., McDonnell, J., Tromp-van Meerveld, I., and Uchida, T. 2005. Subsurface Stormflow. In Encyclopedia of Hydrologic Sciences, Vol. 3 of 5, Anderson, M.G. and McDonnell, J.J. (eds.). John Wiley and Sons, New York. pp. 1719-1732,

Whitson, I.R. 2003. Phosphorous movement in a Boreal Plain soil (Gray Luvisolic) after forest harvest. PhD Thesis, University of Alberta, Edmonton, AB.

Whitson, I.R., Chanasyk, D.S. and Prepas, E.E. 2004. Patterns of water movement on a logged Gray Luvisolic hillslope during the snowmelt period. Canadian Journal of Soil Science 84: 71-82.

Whitson, I.R., Chanasyk, D.S. and Prepas, E.E. 2005. Effect of forest harvest on soil temperature and water storage and movement patterns on Boreal Plain hillslopes. Journal of Environmental Engineering and Science 4: 429-439.

Wilson, G.V, Jardine, P.M., Luxmoore, R.J. and Jones, J.R. 1990. Hydrology of a forested hillslope during storm events. Geoderma 46: 119-138.

Chapter 5
Vertical Water Movement on Forested Boreal Plains Hillslopes, Alberta

5.1. Introduction

Soil water movement and runoff generation on forested Boreal Plains hillslopes has been found to be predominantly vertical due to high infiltration rates and large available storage in the unsaturated zone (Elliott et al. 1998, Whitson et al. 2004, Whitson et al. 2005, Devito et al. 2005b, Redding and Devito 2008). However, it is unclear how much drainage below the root zone occurs and subsequently recharges the groundwater. Given the wide range of surficial materials and soil types that occur on the Boreal Plains, and that precipitation and potential evapotranspiration are of similar magnitude and timing in the region, studies of hillslope water movement are required to help clarify the role of forested uplands in the recharge of local, intermediate, and regional groundwater systems (Sophocleus 2002).

The results of research on root zone drainage and groundwater recharge on forested sites on the Boreal Plains indicate that rates of recharge are typically low and depend on soil texture. Greater drainage below the root zone occurs in sandy soils (0–30 mm yr^{-1}) (Kachanoski and DeJong 1982, Cuenca et al. 1997, Elliott et al. 1998) than in finer-textured soils, where often no drainage is detected below the root zone (Elliot et al. 1998, Blanken et al. 2001, Devito et al. 2005b). In fine-textured soils, enhanced recharge may occur through fractures or structural voids (Hendry 1983). Long-term recharge rates for semi-arid, fine-textured agricultural soils to the south of the Boreal Plains are typically less than 10 mm yr^{-1}, and recharge typically occurs during fallow periods and in small depressions that receive enhanced snowmelt inputs from runoff over frozen soils and/or accumulation of drifted snow (Keller et al. 1986, Hayashi et al. 1998, Dyck et al. 2003).

On the Boreal Plains, the snowmelt period appears to be the primary time of year when recharge of soil moisture storage and groundwater occurs on uplands with fine-textured soils (Devito et al. 2005b) or coarse-textured soils

(Smerdon et al. 2008). Modelling indicates that under sandy uplands forested with aspen, recharge is strongly controlled by water table depth, and it occurs mainly during the snowmelt period when plant uptake is minimized and relatively large inputs of water occur (Smerdon et al. 2008). On hillslopes with fine-textured parent materials and Luvisolic soils, little lateral flow is generated near the surface due to snowmelt (Whitson et al. 2004) or summer rain events (Whitson et al. 2005, Redding and Devito 2008). Determining the depth of infiltration and the residence time of water in the unsaturated zone is important for understanding the controls on plant water use and solute transport. Depth of infiltration from snowmelt or large rain events influences the movement of water below the rooting zone and potentially into groundwater recharge.

The objectives of this research are to use natural and applied tracers and hydrometric measurements to:

1. quantify the depth of infiltration of snowmelt inputs;
2. estimate groundwater recharge resulting from snowmelt and early spring rain;
3. estimate the depth of vertical water movement through the soil during the growing season and for a full year; and
4. estimate long-term rates of root zone drainage and recharge using the chloride mass balance technique across different landforms with a range of soil textures and vegetation cover.

It was hypothesized that both short- and long-term infiltration, root zone drainage, and groundwater recharge would be greater in coarser-textured soils that featured lower water holding capacity and higher saturated hydraulic conductivity than in finer-textured soils. Understanding soil water movement and groundwater recharge in this geologically heterogeneous landscape is critical for accurately predicting the potential impacts of land use change and natural disturbance on water cycling and surface water resources (Devito et al. 2005a).

5.2 Study Sites

The research was conducted at the Utikuma Region Study Area (URSA) near Utikuma Lake (lat: 56° N, long: 115°30' W) in north-central Alberta (Figure 5.1) (Devito et al. 2005a). The site is located within the Boreal Plains ecozone (EcoRegions Working Group 1989). Mean annual temperature is 1.2°C, and annual potential evapotranspiration is 518 mm (Marshall et al. 1999). Mean annual precipitation is 481 mm, of which 113 mm typically falls as snow (Marshall et al. 1999). The long-term (1987–2001) mean annual runoff for Red Earth Creek (619 km^2, 70 km north of URSA) is 67 mm yr^{-1}, and ranges between 4 and 246 mm (median 58 mm yr^{-1}), which corresponds to runoff coefficients of 1–53 % (median 14%) (Environment Canada 2006d).

In the study region, glacial till deposits are heterogeneous, and range from 20 to 240 m in thickness over Upper Cretaceous Smoky Group shale bedrock (Figure 5.1) (Vogwill 1978, Devito et al. 2005a). Three sites encompassing a range of surficial geology, soils, and forest cover were selected for this study, as described in Chapter 2. The sites are:

- SP: sand-jack pine, adjacent to lake 208 (56°6'51"N, 115°42'20'W);
- SA: sand-aspen, adjacent to lake 16 (56°6'8"N, 115°33'4"W); and
- LA: loam-aspen, adjacent to pond 40 (56°4'26'N, 115°28'35"W).

The SP site (Figure 5.1) is located in an area of glacial outwash (Fenton et al. 2003) with soils developed from sand and classified as Dystric Brunisols (Soil Classification Working Group 1998). The SA site (Figure 5.1) is also located in an area of glacial outwash (Fenton et al. 2003) as described in Smerdon et al. (2007); however, there are bands of finer-textured materials through the soil profile, and the soils are classified as Eutric Brunisols (Soil Classification Working Group 1998). The LA (Figure 5.1) site is located on a disintegration moraine (Fenton et al. 2003) that features heterogeneous soils with a predominantly loam texture in the A horizon and increased clay content in the B and C horizons. These soils are classified as Gray Luvisolic (Soil Classification Working Group 1998), as described in Redding and Devito (2008). The overstory at the SP site is comprised of jack pine (*Pinus banksiana*), while the overstory at

the SA and LA sites is dominated by trembling aspen (*Populus tremuloides*). There is very little shrubby understory vegetation at the SP site, but the ground is covered by a layer of feathermoss on north-facing slopes and by lichens on south-facing slopes. The SA site has a shrubby understory comprised largely of rose (*Rosa acicularis*), whereas the LA site has a thick understory of rose and high-bush cranberry (*Viburnum edule*).

5.3 Methods

At the three study sites, snowmelt runoff and infiltration was studied on north-facing (Nf) and south-facing (Sf) aspects. Four runoff frames, each with an area of 1 m^2, were constructed at each slope aspect. In total, eight runoff frames were constructed per site; 24 were established for the full study. Aluminum flashing was used around all sides of each frame and was inserted 0.05 m into the mineral soil (e.g., Harms and Chanasyk 1998). At the downslope end of the plot, a section of trough was inserted 0.06 m into the soil to collect flow from the top 0.05 m of mineral soil and the overlying forest floor. Water collected in the troughs was routed to a bucket in a pit downslope from the frame to measure runoff volumes. Within each frame, vegetation was clipped to a height of 0.05 m above the ground surface to eliminate differences in understory interception between plots.

To measure the amount of snowmelt water available for runoff or infiltration, a snowmelt lysimeter was installed at each plot. The lysimeters were located adjacent to runoff frames with similar aspect, slope and canopy cover. The lysimeters were constructed out of whitish, opaque plastic pans that had an area of 0.47 m^2 (0.52 x 0.9 m) and a depth of 0.11 m. The pans were installed so that all water would drain to one corner, where a hole was cut, and outflow was routed into a collection bucket buried downslope. Water volumes in the bucket were measured at the same time as runoff frame outflow. The lysimeters were monitored weekly or bi-weekly over the 2004 growing season. A climate monitoring station was located approximately 1.5 km from the SP site and featured a Belfort storage gauge.

The soils on all plots were described in the field, and samples were collected for laboratory analysis of texture, bulk density, and porosity. Soil bulk density was sampled using 6-cm diameter and 5-cm long cores. Mineral soil samples were dried at 105^{o}C for 24 hours; forest floor (FF) samples were dried at 70^{o}C for 48 hours. Particle size was analyzed using the hydrometer method with carbonate pre-treatment (Kalra and Maynard 1991). Porosity was calculated using the measured bulk density data and particle density values of 1.54 Mg m^{-3} for forest floor and 2.65 Mg m^{-3} for mineral soil (Redding et al. 2005).

To measure infiltration rates at each plot, four metal rings were inserted 0.05 m into the mineral soil, and the forest floor was left intact within the rings. Rings were installed on relatively flat ground at slope-crest locations. All infiltration measurements followed the procedure and calculation method of Reynolds et al. (2002). Depth profiles of saturated hydraulic conductivity (K_s) to 0.75 m depth were made at each site using a Guelph Permeameter and following the methods of Reynolds and Elrick (2002).

Soil moisture content and storage in the top 1 m of the soil was also monitored using the Profile Probe (PR-1, Delta-T Designs, UK). This instrument (like TDR) does not sense ice due to its low dielectric content; therefore, measurements were not made during the period when soils were frozen. The profile probe access tubes were installed, and initial measurements were made in October 2003 prior to soil freezing and then following soil thaw in late May 2004. A site-specific calibration equation was developed to improve measurement accuracy (Evett et al. 2006):

$$VWC = (0.00004 \times V^{1.4364}) \qquad \text{[Equation 5.1]}$$

where VWC is the volumetric water content (m^3 m^{-3}) and V is the voltage reading from the profile probe. The relationship has an $r^2 = 0.62$, and constrains the VWC estimates to realistic values at higher V, which is a problem with the factory calibration equation (Evett et al. 2006).

A combination of hydrometric water table analyses (e.g., Rosenberry and Winter 1997) and tracers were used to quantify seasonal and long-term infiltration depth and recharge. Isotopic concentrations ($\delta^{18}O$) were used to determine snowmelt infiltration depth from October 2003 to May 2004. Snowmelt infiltration depth and annual infiltration depth were measured using a bromide (Br^-) tracer. On October 21, 2003, 18.4 g of Br^- was added as LiBr to each frame. In 12 of the 24 plots, Br^- was added along with the equivalent of 40 mm of precipitation at 80 mm hr^{-1} intensity. In the other 12 plots, Br^- was added with the equivalent of 4 mm of precipitation. For the infiltration depth experiments, Br^- tracer data from the plots with 4 mm irrigation were used. To examine growing season water movement, on May 7, 2004 a chloride (Cl^-) tracer (23.8 g Cl^-) was added as KCl to the frames that were not scheduled to be destructively sampled in June 2004. The frames that had been irrigated with 40 mm of water were irrigated again with the equivalent of 20 mm of precipitation at an intensity of 40 mm hr^{-1}. The frames that had been irrigated with 4 mm of water were irrigated again with the equivalent of 2 mm of precipitation. The May 2004 irrigations were conducted on frozen soils; however, no surface runoff was recorded at that time or over the remainder of the measurement period to October 2004.

Groundwater monitoring wells were installed at the toe positions of the study hillslopes in the late summer or fall of 2003, with the exception of the SP-Sf plot, which was installed in the spring of 2004. A well was also installed at the crest of the SP site hillslope during the summer of 2003. At the SA site, a well was not installed at the Nf plot due to the presence of cobbles and stones, which did not allow for hand augering to the water table. Wells were constructed of slotted PVC (inside diameter = 0.038 m), which extended to depth from approximately 0.5 m below the ground surface, and solid PVC pipe, which was used in the upper soil and above-ground sections. The slotted segments were wrapped with commercial well sock to filter sediment inflow to the well.

Water level measurements were made using an electrical water level tape. All wells had recording pressure transducers (Model WL-14 or WL-15, Global Water Incorporated, Gold River, CA), except for the SP crest well.

To estimate recharge from changes in water table depth below ground surface (e.g., Healy and Cook 2002), specific yield (Sy) values were applied based on sediment texture from three sources: Loheide et al. (2005), Johnson (1967), and field determined values. Field determined Sy values for the SP site were derived from analysis of water table response to rainfall events at the SP-Nf well during 2004; methods followed Devito et al. (2005b). For the SA and LA sites, field determined Sy values were estimated as the difference between saturated soil moisture content and field capacity (following Loheide et al. 2005). The LA site Sy values determined through analysis of soil moisture measurements (Sy = 0.04–0.11) were similar to those determined by Devito et al. (2005b) (Sy = 0.06–0.08) using water table response to precipitation for a site on the Boreal Plains that had similar soils. Thickness of the capillary fringe was estimated based on soil texture, following the method of Dingman (2002).

Soil samples were collected in October 2003 and June 2004 to examine differences in the $\delta^{18}O$ isotopic signatures of soil moisture between fall and spring conditions as an indication of snowmelt infiltration depth. Samples were collected from the surface to 2 m depth prior to soil freezing (October 2003) and once soils had thawed (June 2004). At each depth, samples were collected using a 0.05-m internal diameter bucket auger and were stored in 250 mL sealed containers. Containers were packed as tightly as possible with soil to minimize air space, and samples were stored in cool, dark conditions prior to analysis. A second sample at each depth was collected for determination of soil moisture content. Isotopic analysis for $\delta^{18}O$ of the soil water was carried out at the Isotope Science Laboratory at the University of Calgary using the method of Koehler et al. (2000). Results were expressed as per mil difference (‰) relative to Vienna Standard Mean Oceanic Water (VSMOW).

To quantify infiltration depth using the applied Br^- and Cl^- tracers, soil samples were collected from the face of a soil pit. Samples were taken from the surface to 0.95 m using a core sampler (0.06 m diameter, 0.05 m length), and below 1 m were collected using a bucket auger. At all depths, four samples were collected, homogenized, and subsampled. All soil samples were oven dried to

measure moisture content and bulk density. All samples were extracted for analysis of Cl^- and Br^- concentrations using 1:5 (mineral soil) or 1:10 (FF) mixtures of dry soil and distilled deionized water. Slurries were shaken for 1 hour and then filtered through Whatman No.42 filter paper and 0.2 μm Millipore syringe filters. Analysis of tracer concentrations in soil extracts was performed on a Dionex DX600 ICP (Dionex, Sunnyvale CA). Results of analysis were corrected for incomplete extraction based on the double extraction process (Redding and Devito 2008) to reduce the potential for underestimating actual concentrations.

The tracer mass balance and recovery for Cl^- and Br^- was calculated using the measured tracer concentrations in the soil. Tracer mass stored in the soil was calculated using the corrected tracer concentrations as the mean concentration of each depth. Background Cl^- and Br^- concentrations were based on pre-irrigation sampling during plot installation.

Water samples collected for oxygen isotopic analysis ($\delta^{18}O$) were stored in 20 mL scintillation vials with a thin film of mineral oil on the surface to prevent evaporation. A PVC bailer was used to collect groundwater samples from monitoring wells one day after the wells were purged. Samples of snowmelt water were collected from the lysimeter outflow at each site. The water was collected in clean plastic bags and then transferred to scintillation vials for storage. Snow adjacent to study frames was periodically collected and melted in the laboratory (air temperature 20^oC). Samples of rain water were collected following rain events.

Stable isotope ratios for water samples (groundwater, rain, snow, and snowmelt water) were determined at the University of Calgary Isotope Science Laboratory. Oxygen isotopes were determined using the CO_2-H_2O and mass spectroscopy technique (measurement error 0.2 ‰). Results were expressed as per mil difference (‰) relative to Vienna Standard Mean Oceanic Water (VSMOW).

The chloride mass balance method (CMB) was use to estimate long-term rates of drainage below the root zone (Scanlon 2004) and groundwater recharge (Hayashi et al. 1998). This method uses soil pore-water chloride concentrations

(Cl_s) or groundwater chloride concentrations (Cl_g), precipitation inputs of chloride (Cl_p), and mean annual precipitation to estimate long-term rates of vertical drainage below the rooting zone or groundwater recharge (Scanlon 2004). This method has been widely applied in unglaciated arid and semi-arid areas of the world that have thick unsaturated zones; however, applications in subhumid and forested settings are limited. To calculate the drainage flux below the rooting zone the following equation was used:

$$D = P(Cl_p)/(Cl_s) \qquad \text{[Equation 5.2]}$$

where D is the annual residual drainage flux below the rooting zone (mm yr^{-1}), P is the mean annual precipitation (mm yr^{-1}), Cl_p is the mean annual chloride inputs in precipitation (mg L^{-1}), and Cl_s is the soil pore-water chloride concentrations in the unsaturated zone below the rooting zone (mg L^{-1}).

Long-term aerially averaged recharge to the groundwater table can be estimated using measured groundwater Cl^- concentrations (Cl_g) substituted for the soil pore-water chloride concentrations from the unsaturated zone (Cl_s) in equation 5.2 (Wood 1999, Joshi and Maule 2000).

Chloride inputs in precipitation (Cl_p) are difficult to determine for the study region due to a lack of local long-term monitoring and uncertainty in dry deposition inputs. Mean chloride concentration calculated from the short-term data set (1999–2006) of precipitation chemistry collected at URSA was 0.26 mg L^{-1} in rainfall and 0.25 mg L^{-1} in snow (measured in the open and under leafless aspen) (K. Devito, unpublished data). The URSA values are similar to long-term mean annual chloride inputs in precipitation (wet deposition) of 0.23 mg L^{-1} from Beaverlodge, Alberta, approximately 300 km west of the study site (Environment Canada 2006c). There are no available data for chloride dry deposition in northern Alberta; however, it is expected that dry deposition would constitute half of the total annual chloride deposition at the ground surface (M. Shaw, Environment Canada, personal communication). For this reason, in CMB calculations three Cl_p scenarios were applied. Scenarios 1 and 2 used the wet deposition concentrations

from URSA, as well as a doubling of those in an attempt to account for the contribution of dry deposition. A further source of uncertainty in the Cl_p values results from the fact that samples were collected in the open, as per standard procedures, rather than under a forest canopy. The solute concentrations of throughfall and stemflow beneath a forest canopy are generally higher than those measured in the open (Levia and Frost 2006). A limited data set of throughfall chemistry is available from the URSA study (K. Devito, unpublished data). It was used in a third scenario for Cl_p. The mean throughfall Cl_p value from this data set is 0.91 mg L^{-1}, which was also assumed to account for dry deposition (scenario 3).

Soil pore-water chloride concentrations in the unsaturated zone were determined for five profiles across the study area. At the SP site, a 5.5-m deep profile was sampled in the sandy soils under the jack pine canopy during June 2004. At the LA site, which has silt and clay-dominated soils, four profiles were sampled during the installation of groundwater monitoring wells. Three profiles on the LA-Sf hillslope were sampled using a hand auger during May 2004. Groundwater monitoring well LA-511w, located at the base of a small depression, was sampled to a depth of 4 m. Groundwater monitoring well LA-513w, located approximately 5 m east of LA-511w at the edge of the depression, was sampled to a depth of 3.25 m. Groundwater monitoring well LA-514w, located on the slope crest above LA-511w and LA-513w, was sampled to a depth of 4 m. The deepest profile, groundwater monitoring well LA-565w, located below an aspen canopy at the slope crest above the LA-Nf study plot, was sampled to 12 m using a track-mounted drill rig during August 2003.

Soil samples were collected from the profiles and were used to represent major textural and stratigraphic units of the subsurface materials. Samples were dried and extracted as described previously. The pore-water chloride concentration was determined by using the following equation (Gee et al. 2005):

$$Cl_s = ([Cl_{ext}]/w)n \qquad \text{[Equation 5.3]}$$

where Cl_s is the pore-water chloride concentration (mg L^{-1}), Cl_{ext} is the concentration of Cl^- in the extract, w is the gravimetric water content (w, g H_20 g^{-1} oven-dry soil), and n is the solution/soil ratio (mass water added/mass oven dried soil [n is 0.2 for mineral soil and 0.1 for forest floor]).

The CMB recharge estimate was calculated based on the mean Cl_s concentration below the rooting zone. For the study sites, it was assumed that the bottom of the root zone was equal to the maximum rooting depth of canopy species on similar soils, as measured by Strong and LaRoi (1983): 1.5 m for aspen and 2.0 m for jack pine. These values agree with observations made during the installation of wells in this study (T. Redding, personal observations). However, deep profiles indicated that there was little change in [Cl^-] with depth below 0.5–1m. Thus, background [Cl^-] from 1 to 2m depth at all six plots was used.

The CMB method was also used to estimate groundwater recharge based on groundwater chloride concentration (Cl_g) (Wood 1999) at select groundwater monitoring wells on the LA site. Groundwater samples for Cl^- analysis were collected during the growing seasons of 2004 and 2005 using either a WATTERRA (LA565w) or PVC bailer (LA509w, LA510w). Wells were purged one day prior to sampling, except for LA565w, which could not be pre-purged due to slow recovery. All groundwater samples were filtered through 0.2 μm Millipore syringe filters and were analyzed on a Dionex DX600 ICP (Dionex, Sunnyvale CA).

5.4 Results

5.4.1 Site Characteristics

Study site characteristics varied in terms of canopy tree species, canopy cover, slope, surface soil texture, and forest floor thickness (Table 5.1). The SA and LA sites had an aspen overstory; therefore, canopy cover was greater during the growing season than in winter. The SP site had an overstory of jack pine and a coniferous canopy that persisted through the winter period. Canopy cover at the SP-Sf plot was much lower than at the Nf plot. Slope gradients ranged from 14 to 23% across all study plots. Surface soil textures ranged from sands on the SP site

to loamy sands on the SA site to loams on the LA site. The LA site had the thickest forest floor, which was composed of aspen leaf litter. The SA site also had a forest floor comprised of aspen leaf litter. At the SP-Nf plot, the forest floor was dominated by red-stemmed feathermoss (*Pleurozium schreberi*).The SP-Sf plot had the thinnest forest floor, which was composed of lichens and pine needles (Table 5.1).

The soil profiles of the three sites showed a range of soil textures from sand at the SP site to fine-textured at the LA site (Figure 5.2). At the SP site, the soils were greater than 90% sand to depth, whereas the soils on the SA site had slightly greater amounts of silt and clay. Soils on the LA-Sf plot site were more variable and coarser-textured than on the LA-Nf plot (Figure 5.2).

The differences in soil properties among sites resulted in differences in saturated hydraulic conductivity (K_s) (Figure 5.2). The surface soils at all sites had similar K_s values in the range of 1×10^{-4} to 1×10^{-3} m s^{-1}; however, the soils differ greatly with depth. The K_s of the SP site soils was approximately 1×10^{-4} m s^{-1}. At the SA site, there was greater variability with depth, with K_s ranging from 1×10^{-6} to 1×10^{-4} m s^{-1}. The LA site, with the finest and most variable soil textures, had the greatest range in K_s from 1×10^{-9} to 1×10^{-4} m s^{-1}.

5.4.2 Precipitation Inputs for the Study Period

Over the 12-month study period, there were small differences in precipitation inputs among the study sites (Table 5.2). For the period November 1, 2003 to October 17, 2004, the estimate of precipitation in the open (SP Belfort) was 359 mm. This was within 5% of the 374 mm measured at Red Earth Creek and was much lower than the 525 mm measured at Slave Lake, which are both Environment Canada monitoring stations located approximately 55 km to the northeast and 105 km south of the study, respectively. Annual precipitation estimates from the lysimeters at each plot ranged from 325 to 390 mm, which is within 10% of the estimates from the open (SP Belfort). Annual precipitation on south-facing slopes (Sf) was greater at each of the three sites.

The greatest difference in precipitation inputs among sites was observed during the winter period and spring snowmelt (November 1, 2003 to April 30, 2004). The estimate from the open (SP Belfort) of 85 mm was within the range of lysimeter estimates, which ranged from 72-163 mm (Table 5.2). Winter precipitation depths were greater on Sf plots than on Nf plots.

Precipitation during the snow-free period (May 1, 2004 to October 17, 2004) was 2–4 times greater than winter precipitation. The estimate of precipitation in the open (SP Belfort) was 274 mm, which was similar to 288 mm measured at Red Earth Creek (Table 5.2). Snow-free precipitation estimates from lysimeters ranged from 227 to 274 mm, and were within 15% of the open measures. There was no clear relationship between snow-free precipitation and aspect among sites (Table 5.2). July and August 2004 was the wettest two-month period during the monitoring period. Fall 2003 (September to October) and early summer 2004 (May to June) was drier than the long-term average for Slave Lake. Fall 2004 was about twice as wet as fall 2003 and was greater than the long-term Slave Lake average (Table 5.2).

5.4.3 Snowmelt Infiltration and Drainage

In all the frames and plots, snowmelt infiltration was greater than runoff (Table 5.3). Significant runoff occurred consistently only among frames on the SA site and the SP-Sf plot. No runoff occurred after May 1, 2004. Runoff was also not influenced by changes in fall soil moisture related to the 40 mm irrigation in October 2003or the 20 mm of irrigation applied May 2004. Total depth of infiltrated water was influenced by snowmelt inputs, and ranged from 74 to 260 mm. The greatest infiltration amounts occurred at the LA site due to larger snowmelt inputs. Infiltration exceeded 95% of water inputs on the LA site and on the SP-Nf and SA-Nf plots. Infiltration on the SP-Sf and SA-Sf plots ranged from 55 to 96% of melt inputs due to greater lateral flow (Chapter 2).

Although there was significant infiltration, there were no large increases in soil moisture storage at the SP and SA sites between October 2003 and June 2004 according to profile probe measurements (Table 5.3). Therefore, almost all

snowmelt inputs at these sites drained below the 1 m measurement depth of the profile probes, and drainage coefficients were influenced by runoff and infiltration coefficients. The SP and SA-Nf frames had drainage coefficients greater than 95%. Drainage coefficients for SA-Sf frames were slightly less at 85–90% due to greater runoff. In contrast, at the LA site, changes in soil moisture storage ranged from 13 to 63 mm, and although there was no significant runoff, this soil moisture storage resulted in lower drainage coefficients of 36–82 %. The total amount of snowmelt and spring rain drainage from the LA frames ranged from 72 to184 mm, and was the highest among all study frames due to the larger snowmelt inputs (Table 5.3). Between June and October 2004, there were only small changes in soil moisture storage in the top 1m (-28 - +12 mm) at all sites even though September and October had more precipitation than normal (Table 5.3).

5.4.4 Depth of Snowmelt Infiltration

Depth of snowmelt infiltration was greatest at the SP site and least at the LA site as indicated by the shift from a more enriched $\delta^{18}O$ snowmelt signature in fall 2003 to a less enriched signature in spring 2004 (Figures 5.3-5.5). The presence of the applied Br^-, which is not naturally found in the soils, combined with and an increase in moisture content between fall and spring show similar trends to the $\delta^{18}O$ tracer (Figures 5.3–5.5). At all sites, $\delta^{18}O$ of snow was generally less enriched (< 20 ‰) than that of rain. Snowmelt water was more enriched than snow. The $\delta^{18}O$ of groundwater samples was intermediate between snow and rain. The $\delta^{18}O$ signature at the base of the soil profiles was similar to $\delta^{18}O$ of groundwater at each plot.

Infiltration depths at both the SP-Sf and Nf plots were greater than 2 m based on $\delta^{18}O$ and Br^- profiles (Figure 5.3). The $\delta^{18}O$ signature of unsaturated soils at the bottom of the sampled profiles approached the $\delta^{18}O$ signature of groundwater. Soil moisture content showed little change between fall 2003 and spring 2004 measurements, which agrees with the soil moisture measurements (Table 5.3). At the SA-Sf plot, the infiltration depth appeared to be 0.8–1 m

(Figure 5.4). Despite a restricted sampling depth due to large cobbles, the infiltration depth at SA-Nf plot appeared to be near 0.75 m (Figure 5.4). The LA-Nf plot had infiltration depths of approximately 1 m based on all three tracer methods (Figure 5.5). At the LA-Sf site, the $\delta^{18}O$ profiles indicated infiltration depth was approximately 0.5 m; the Br^- profile indicated it was 0.8 m (Figure 5.5). At the LA-Sf site, there was a small increase in soil moisture to a depth of 0.5 m (Figure 5.5). It is important to note that the $\delta^{18}O$ profiles at each plot were for a single sampling location; therefore, some of the differences between the fall and spring profiles and soil moisture were likely due to spatial variability among sampling locations (typically within 5 m of each other).

The recovery of Br^- in spring 2004 was highly variable among frames (Table 5.4); the median recoveries for the four frames at each site were 13, 32 and 30% at the SP, SA and LA sites respectively. Recovery of Br^- tended to follow a flushing pattern, as shown in Figures 5.3–5.5. However, at the SP and SA sites, recovery rates were highly skewed. Two frames on the SP site had the lowest recovery (range 0–100%), and two frames on the SA site had the next two lowest recoveries, indicating high rates of vertical or lateral flushing in isolated locations of the sandy soil. Recovery was consistent among frames at the LA site. In addition, there was no clear influence of fall 2003 irrigation on Br^- recovery.

5.4.5 Snowmelt Season Groundwater Recharge and Growing Season Groundwater Dynamics

Water table dynamics showed strong seasonal trends at all sites, but with differences in snowmelt response and recession timing among the sites (Figure 5.6). At the SP-Sf plot, the primary snowmelt period started at day of year (DOY) 90, and the water table elevation peaked at DOY 130. The 0.11 m change in water table (WT) elevation from DOY 70 to 130 represents 29–48 mm of recharge due to the high specific yield (Table 5.5). This is considerably less than the estimated drainage below 1 m (108–138 mm) on the SP-Sf study plot. While the summer period had highest precipitation, there was a consistent decline in WT elevation from DOY 130 through DOY 240, indicating plant water uptake. The decline in

WT elevation of 0.15 m to DOY 240 represents a loss of 39–66 mm of water over a 110 day period, or a recession rate of 0.4–0.6 mm d^{-1}. The groundwater record at this location was very noisy, likely due to the shallow water table, highly conductive sediments, and proximity to the pond edge.

The SP-Nf well was installed too late to capture the full WT increase during and following snowmelt (Figure 5.6). There was an initial peak at DOY 115, perhaps in response to early snowmelt, and a second peak at DOY 150 (early June). The peak WT elevation occurred later (DOY 150) than at the Sf location, and at a similar time as the crest location. The recession from about DOY 150–180 was approximately 30–50 mm of water, a rate of 1–2 mm d^{-1}.

At the crest of the SP site hillslope, water levels were monitored manually over the snowmelt and summer periods (Figure 5.6). Similar to the Sf toe slope, water table depth dropped over the winter. Recharge estimates based on water table rise at this well ranged between 78 and 132 mm (Table 5.5), which was similar to the estimated drainage below 1 m from the SP-Sf and SP-Nf plot non-irrigated frames (103–138 mm) (Table 5.3). During summer, the recession of water from the date of peak WT elevation (approximately DOY 150) through DOY 210 was roughly 0.25 m or 65–110 mm. This translates to a recession rate of approximately 1–2 mm d^{-1}. Isolated instances of growing season recharge were apparent for the Sf and Nf wells in response to precipitation; however, the rise in water table was small (typically less than 0.05 m) and was followed by a rapid recession. During the early fall of 2004, water table levels increased at all three SP site wells (Figure 5.6), corresponding to recharge of 42–70, 44-75 and 65-100 mm at the Sf, Nf and crest wells respectively.

Water table levels were influenced by lateral groundwater flow between the upland and adjacent pond. At the SP-Sf site, there were small water table gradients from the upland crest to the upland toe to the pond during most of the measurement period (Figure 5.7). In the immediate post-snowmelt period, the gradients indicated flow occurred from the toe-slope position (SP-Sf, Figure 5.6) toward both the pond and into the upland. Once peak water levels occurred, the gradients were from the crest to the pond. Water table gradients were small (less

than 0.05 m difference in elevation between crest and pond); however, the conductivity of the sediments is high, indicating the potential for a large flux and interaction with a larger-scale flow system.

At the SA site, the only well was located at the Sf toe slope, and was dry in the late fall 2003 and early spring 2004. Initial peak response was delayed relative to the SP site; it occurred at DOY 125 and extended to DOY 155 (early June) (Figure 5.6). This represents a change in WT elevation of 0.43 m and an estimated recharge of 108–138 mm (Table 5.5). However, this is an underestimate because the true initial WT elevation was not measured. The recharge estimates are greater than the estimated drainage below 1 m from the SA-Sf plot, possibly due to lateral inflow from the adjacent wetland. Similar to the SP plots, from DOY 155, the WT dropped steadily through the late spring and summer, representing a loss of about 125 mm over 25 days (5 mm d^{-1}). There was no evidence of growing season recharge as the water table was below the bottom of the monitoring well (Figure 5.6). The water table rose in fall 2004 (Figure 5.6) in response to precipitation inputs and the absence of vegetation uptake. The water table rise indicates recharge of at least 75-96 mm. Over the full period of monitoring, water table gradients indicated flow occurred from the peatland to the upland (Figure 5.7).

The LA-Sf and Nf plots showed a delayed response to spring recharge compared to the SP and SA sites. This was possibly related to the greater depth to water table, available unsaturated zone storage, and lower conductivity fine-textured sediments on the LA plots. The change in WT was also much larger on the LA than the SP and SA sites, which was a reflection of the lower specific yield of the fine grained sediments (Table 5.5).

At the LA-Sf plot, early spring 2004 water levels were higher than those the previous fall (Figure 5.6). The WT showed rapid response about DOY 125, followed by a steady increase to DOY 155 (early June). The WT rise of 0.7 m represents an estimated recharge of 28–77 mm (Table 5.5). This was much less than the estimated drainage below 1 m (Table 5.3), and likely indicates storage of water in the unsaturated zone. Following DOY 155, the WT dropped consistently

through the summer season. The total recession was approximately 0.75 m over an 80-day period, representing 30–83 mm of water at a rate of 0.4–1.0 mm d^{-1}. On the LA-Nf plot, the water level pre-snowmelt was similar to that of the previous fall. Response to snowmelt started after DOY 100 and peaked at DOY 172 (mid-June) (Figure 5.6). The increase in WT elevation of 0.93 m represents recharge of 37–102 mm (Table 5.5), which was similar to the estimated drainage below 1 m (Table 5.3). The recession at LA-Nf started DOY 175 and continued to DOY 225. Recession was 1.0 m, representing 40–120 mm of water at a rate of 0.8–2.4 mm d^{-1}. Neither the Sf nor Nf wells showed recharge during the summer growing season or in fall 2004 (Figure 5.6).

Water table gradients at the LA hillslopes indicate the direction of flow was from the riparian zone into the upland (Figure 5.7). The gradient was relatively large but the conductivity was very low, so the flux was likely small. The gradient was at the minimum in June at the time of maximum water levels in the upland. In early fall, there was a recovery in water level in the riparian zone but not in the upland. Similar to LA-Sf, the water table gradient for LA-Nf (Figure 5.7) indicates the direction of flow was from the riparian zone into the upland; however, flux was small due to the low conductivity of the sediments. The gradient was at a minimum in June when the water level in the riparian zone began to drop before the upland water level. As with the LA-Sf plot, the riparian water levels recovered earlier in fall 2004 and more in the riparian zone than in the upland.

It should be noted that the wells used for the recharge estimates were all (with the exception of the SP-crest well) located at toe slopes, while the study plots where snowmelt and rainfall inputs were measured were located at mid- and upper-slope positions which ranged from roughly 2-8 m higher in elevation. As a result, the water table elevations are influenced by the gradients of flow to or from adjacent wetlands and can therefore result in over or underestimates of recharge. At the toe slope locations, which have shallower water tables, there is also an increased potential for the capillary fringe to approach the surface and influence water table dynamics and recharge estimates (Rosenberry and Winter 1997).

Estimates of capillary fringe thickness were 0.01–0.03 m at the SP and SA sites, and 0.4–1.3 m at the LA site. Differences in recharge estimates calculated using the Sy values of Loheide et al. (2005), Johnson (1967), and field estimated values were generally small (Table 5.5).

Use of $\delta^{18}O$ signature of the groundwater to estimate timing of recharge appears to be limited as there was little change in $\delta^{18}O$ during the recharge period (Figure 5.6). The $\delta^{18}O$ signature of the groundwater at all wells remained intermediate between the snowmelt and rain inputs, and was similar to values observed at the base of soil profiles (Figures 5.3–5.5). Given the relatively small amounts of recharge, it is possible that the isotopic signature of the groundwater did not change due to the small amount of inputs relative to the volume of stored water.

5.4.6 Growing Season and Annual Infiltration Depth

During the growing season, there was no runoff measured from any of the frames, or in response to the 20 mm application of water in May 2004. At the LA site, no lateral flow was measured deeper in the soil profile over the period of July to September 2004 (Redding and Devito 2008). There were some differences between vertical profiles of soil Br^- sampled in October 2004 and those sampled in June 2004 (Figures 5.3–5.5). This is assumed to be due to vertical water fluxes over the growing season. The SP-Sf profile in October 2004 showed no Br^- below the FF, possibly indicating that all added Br^- had been flushed from the profile over the growing season (Figure 5.3). The SP-Nf profile showed detectable Br^- to a depth of 1 m in October 2004. At the SA site, both the Sf and Nf profiles appear to be either vertically or laterally flushed below the FF and surface mineral soils, which are have the highest organic matter content (Figure 5.4). The LA site fall 2004 profiles were similar to those sampled in the spring (Figure 5.5).

Recovery of Br^- was generally greater in the spring than in the fall at all sites except for the LA-Nf plot (Table 5.4). Recoveries in four frames at both the SP and SA sites dropped from 32% in spring 2004 to 3 % and 6 % in fall 2004, which suggests vertical or lateral flushing occurred, as indicated in the depth

profiles (Figure 5.3–5.5). The decline in average Br^- recovery in fall 2004 in four frames at the LA site was much less than that on the SP and SA sites, dropping from 32 to 16%, which indicates limited redistribution of Br^- in the LA-Sf and LA-Nf plots. There was no apparent trend in Br^- recovery associated with aspect.

The Cl^- recoveries were similar to changes in Br^-. There were no consistent differences in the effects of irrigation history (40/20 or 4/2 mm) on the Cl^- profiles (Figure 5.8). Soil samples collected in October 2004 at SP and SA sites showed little difference between the background variation in Cl^- and the profiles with applied Cl^- (Figure 5.8). Mean recovery of the Cl^- that was added May 7, 2004 was 3% and -15% for the SP and SA sites, respectively, which indicates soil flushing occurred through the summer (Table 5.4). There appeared to be much less flushing at the LA site. Cl^- concentrations peaked at 0.3 m in the LA-Sf and Nf plots, followed by a secondary peak in the LA-Nf profiles, which indicated infiltration to 0.8–1 m depth (Figure 5.8). Average recovery of the Cl^- that was added May 7, 2004 in four frames at the LA site was 31%, which was much greater than recovery at the SP and SA sites (Table 5.4).

5.4.7 Long-Term Root Zone Drainage and Groundwater Recharge

The long-term root zone drainage rates estimated using the CMB unsaturated zone method were lower for the sites with sandy soils than finer-textured soils (Table 5.6). In addition, the trends in soil texture and recharge amount estimated by CMB are opposite to those estimated by using snowmelt recharge (Table 5.5). Estimates using CMB show that the sandier SP site had a long-term annual recharge rate that was an order of magnitude lower than the fine-grained LA site (Table 5.6). Estimated rates of root zone drainage for the three Cl_p scenarios ranged from 1 to 3 mm yr^{-1} at the SP site and 1 to 15 mm yr^{-1} at the LA site (Table 5.6).

Long-term groundwater recharge estimates made using groundwater Cl^- (Cl_g) concentrations at the LA site were an order of magnitude higher than those made using the unsaturated zone Cl^- (Cl_s) concentrations (Table 5.6). For the three wells sampled at the LA site, estimated recharge ranged from 45 to 503 mm yr^{-1},

depending on the Cl_p scenario (Table 5.6). Water table depths for the groundwater Cl^- sampling periods were approximately 11 m below ground at LA565w, and 3–4 m below ground at LA509w and LA510w.

5.5 Discussion

5.5.1 Snowmelt Infiltration Depth

Vertical infiltration dominated over lateral flow in all substrate textures, similar to the results of other studies that have been conducted in areas with subhumid climates and deep unsaturated zones (Elliott et al. 1998, Devito et al. 2005b, Redding and Devito 2008). Infiltration depth increased with substrate permeability. The agreement between estimates of snowmelt infiltration depths made using the two tracers ($\delta^{18}O$, Br^-) and soil moisture content increases confidence in the results of this study. Similar to the findings at the LA site, a study on fine-textured till in boreal Alberta, which used Br^- as an infiltration tracer, showed that snowmelt water infiltration was limited to a depth of 0.8–1.0 m for a winter with a maximum measured SWE of approximately 80 mm (Whitson et al. 2005). Devito et al. (2005a) found that on fine-grained till-derived soils, soil moisture content increased from fall to spring to at least 0.6 m depth over 3 years of measurement. On fine-grained soils on the Canadian Prairies, Hendry (1982) found deeper than expected vertical flow as a result of preferential flow through fractures in the soil and underlying till. At the SA site in this study, depth of infiltration may be partially controlled by the presence of fine-textured layers (Hunt and Zahner 1980). This could result in reduced recharge due to barriers to vertical flow and greater storage within the unsaturated zone.

Significant drainage below 1 m depth occurred at all sites, based on tracer profiles from the applied Br^- and changes in soil moisture storage. A considerable amount of the applied Br^- tracer was unaccounted for between the October 2003 application and the June 2004 sampling. The results indicate that as drainage below 1 m increases, recovery of Br^- and Cl^- tracers decreases. The calculated tracer recoveries for the June 2004 sampling period showed less spatial variability than expected. Recovery was similar for all sites, with the LA site (median 30%,

range 16-49%) with fine-textured soils being similar to the outwash sites, with the SA site (median 32%, range 9-54%) and SP site (median 13%, range 0-105%). The wide range in recovery at the SP site may be due to drainage through preferential flow pathways. Soil pits excavated at the SP site during frozen soil conditions showed vertical columns of frozen saturated soil (indicating preferential flow pathways), which may be related to the patchiness of the concrete frost (Chapter 2).

In this study, it is likely that vertical recharge dominated in coarse-textured material with deeper infiltration depths; however, the incomplete recoveries of Br^- in the fine-textured soils, and recharge depths of 1 m or less, is problematic. An average Br^- recovery of 35% has been reported for fine-textured Luvisolic soils on the Boreal Plains (Whitson et al. 2005). The missing Br^- may have been due to a number of factors functioning individually or in concert, including: loss of Br^- in snowmelt runoff water (not measured), incomplete extraction (Redding and Devito 2008), vertical preferential flow (below sampling depth or preferential flow pathways not sampled), flow out of the sampling volume either vertically or laterally, or diffusion of Br^- tracer outside of the sampling volume.

While melt rates were typically very low (Chapter 2), if spatially discontinuous concrete frost was present near the soil surface, vertical preferential flow could be initiated by flow concentration and infiltration in the frost-free spaces. The patchy nature of the concrete frost across the SP and SA hillslopes (data not shown) indicates that even if there are relatively high amounts of runoff from some areas, that water is likely to infiltrate at some point downslope (Price and Hendrie 1983), resulting in recharge of the soil moisture storage or possibly groundwater. This may lead to an uneven spatial distribution of Br^- within the area sampled, or preferential flow in the frozen soil to below the deepest depth of sampling (Stahli et al. 2004).

The Br^- concentration in runoff water was not measured from the frames; therefore, it was not possible to quantify the extent of Br^- losses due to near-surface runoff during the snowmelt period. However, near-surface runoff ranged

from 1 to 60 mm, and was greatest from sites with a south-facing aspect. It does not appear that Br^- recoveries were any lower for plots with a south-facing than north-facing aspect, which indicates that near-surface runoff was not a large source of error. Whitson et al. (2005) attributed low Br^- recovery primarily to lateral flow losses, however, the data for this site do not agree with this pathway (Redding and Devito 2008). Redding and Devito (2008) discussed the inadequacy of the standard 1-hour extraction for Br^- and Cl^- in the fine-textured soils of the LA site. Even with the application of a correction factor for incomplete extraction, there may have been unrecovered Br^- in the soil.

Diffusion of Br^- from within the 1-m^2 area of application is likely as there is no measurable Br^- resident within the soil and the experiment occurred during the snowmelt period when soils are typically the wettest of the year.

Sampling snowmelt water, as opposed to snow, results in more enriched values of $\delta^{18}O$. This demonstrates the importance of sampling snowmelt water rather than just snow to determine water sources (Buttle and Sami 1990, Unnikrishna et al. 2002, Laudon et al. 2007). The $\delta^{18}O$ measurements of snow and snowmelt water agree with previous research that showed that $\delta^{18}O$ became more enriched as the melt period progressed (Unnikrishna et al. 2002, Murray and Buttle 2005, Laudon et al. 2007). This signature of snowmelt water allows snowmelt infiltration depth to be clearly identified. The soil moisture $\delta^{18}O$ profiles show a similar offset between fall and spring profiles to that measured in till-derived soils in Sweden (Laudon et al. 2007).

5.5.2 Seasonal Groundwater Dynamics

The groundwater response following snowmelt was the largest response of the 2003/2004 measurement period and represents the highest annual water table elevations (minimum depth to water table) for the study wells. The water table response following the snowmelt season is typically the largest annual groundwater recharge event on the Boreal Plains (Devito et al. 2005a, Smerdon et al. 2008). This response is a combination of the relatively large amount of water entering the soil over a short period and the low water demand by vegetation

(Devito et al. 2005a, Smerdon et al. 2008). At all sites, water levels decreased following the spring peak, and did not recover until fall at the SP and SA sites, while no fall recovery was noted at the LA site.

It was expected that coarse-textured sediments would have greater recharge rates than finer-textured materials because they are highly conductive and have higher specific yield (Sy) (Smerdon et al. 2008). However, the range in estimated recharge at the SP and SA sites was similar to that at the LA site. The differences in water table-based recharge values compared to estimated drainage below 1 m depth were related to the thickness and storage properties of the unsaturated zone. While there was some difference between these two estimates, the error inherent in both measurement systems (Sy uncertainty and measurement error with the profile probes) indicates that the results are likely within the correct general range.

5.5.2.1 Coarse-Textured Outwash Sites

The amount of recharge at the coarse-texture outwash sites depended on the unsaturated zone storage capacity. The sandy soils at the SA and SP sites were both close to field capacity and had little water storage capacity in fall 2003 and there was generally no water taken into storage over the snowmelt and soil thaw period. At the SP site, the snowmelt and rainfall inputs between November 1, 2003 and June 30, 2004 were 105–149 mm, which was similar to the estimated drainage from the top 1 m of soil of 103–138 mm and groundwater recharge of 78–132 mm at the crest of the upland. The sandy soils at this site have low total storage capacity (approximately 60 mm water per meter of soil; Saxton et al. [1986]), indicating that most of the snowmelt and spring rain can pass through the soil profile without being taken into storage. For a water table depth of approximately 8 m at the SP-crest site, the estimated recharge of 78–96 mm is similar to the model based estimates of long-term net annual average recharge flux of 50–75 mm yr^{-1} (Smerdon et al. 2008). At the SA site, the greater estimated recharge compared to soil moisture storage estimates of drainage below 1 m was likely a result of lateral inflow of water from the adjacent peatland, which had

standing water following the melt of frozen peat. There was a consistent and large groundwater gradient indicating flow from the peatland to the upland throughout the measurement period. This gradient may be related to larger scale flow systems in this area or the storage properties of the adjacent peat (Smerdon et al. 2007).

The primary mechanism of recharge at the SP sites appears to be piston flow due to the similarity of the drainage and recharge estimates. Buttle and Sami (1990) and Saxena (1984) both noted that snowmelt water moved vertically as piston flow through sandy glacial sediments, and displaced stored water as the wetting front moved downwards. This displaced water will propagate through the soil profile, and recharge soil moisture storage or groundwater as indicated by the homogeneous groundwater $\delta^{18}O$.

The apparent underestimation of recharge at the SP toe slope well (SP-Sf) relative to the crest location may be due to several reasons. The first possible explanation is that the recharge estimate of 35–48 mm at the toe slope well means there would have to be at least 45–55 mm or as much as 85 mm (total input) of water stored in the approximately 1 m of sand above the water table. This seems unlikely, as the maximum available water holding capacity for these sand soils is 60–70 mm per 1 m of soil thickness (Saxton et al. 1986). Water use by vegetation in the riparian area may have reduced antecedent moisture content. A second possible explanation is that snowmelt from the toe slope location infiltrated and moved laterally to the adjacent pond (SP-Sf) or peatland (SP-Nf), while groundwater mounded under the crest of the upland increasing the water table gradient (SP-crest), as modelled by Winter (1983) for coarse-grained deposits in Minnesota. Water table gradients indicated flow from the toe slope to the adjacent pond, with low gradients and high conductivity. Given the outwash location, the groundwater dynamics at this site may also reflect large-scale (regional) groundwater flow systems such as have been identified at the SA site (Smerdon et al. 2007). This emphasizes the challenges of using toe slope wells in environments with coarse-grained soils; however depth to water table limits well installation at higher elevation locations on the uplands.

At the SA site, snowmelt and spring rain inputs were 123–138 mm, which was similar to the estimated drainage of 71–114 mm and estimated recharge of 108–138 mm. Drainage on the Nf plot was greater than on the Sf plot, and was a function of lower runoff losses that resulted from less concrete frost. Due to the shallow water table at the SA site, most of the inputs drain to groundwater. At the SA site, the greater estimated recharge compared to soil moisture balance estimates of drainage below 1 m may be a result of lateral inflow of water from the adjacent wetland, which had standing water near the upland boundary when the snow had melted but the peat was still frozen, or from a groundwater flow system above the site (Smerdon et al. 2005). This highlights the potential of focussed recharge through wetlands on the forested Boreal Plains, similar to prairie environments (e.g., Hayashi et al. 1998). Finally, some water may have been stored above or within layers of fine-textured material and then taken up by plants prior to when measurements were made in June 2004. Devito et al. (2005b) report up to 30–40 mm of soil moisture loss by this time at a sand/silt site. At URSA in 2004, soil moisture measurements indicated little soil water depletion during May and early June. Plant water uptake was likely limited in spring by soil frost and cool soil temperatures (Mellander et al. 2004).

The senecense of forest vegetation in late August and early September 2004 combined with relatively large precipitation events resulted in significant fall recharge for all wells at the outwash sites. The increases in water tables at the SP site were similar to those measured following snowmelt. As a consequence, the water levels in the SP-Sf and crest wells were greater in October 2004 than October 2003. The juxtaposition of the drier than normal fall 2003 and slightly wetter than normal fall 2004 highlights the importance of fall precipitation, when plant water uptake is low, in priming the hillslopes to provide recharge in the subsequent spring.

5.5.2.2 Fine-Textured Moraine Sites

Vertical flow and storage dominated the subsurface hydrological response to snowmelt and spring rain. At the LA site, snowmelt and spring rain inputs were

148–210 mm, while estimated drainage below 1 m ranged from 93 to 173 mm and estimated recharge to the WT was 49–112 mm. The difference between drainage and recharge values likely indicates that the fine-textured soils had considerable available storage capacity at the start of snowmelt, and water went into storage and was potentially available for plant uptake, rather than recharge. The storage deficit is likely a function of the dry fall in 2003. Within the top 1 m of soil, there was 20–46 mm of stored water. This is reasonable for the soil textures at this site, which have an estimated available water holding capacity of approximately 180 mm m^{-1} of soil (Saxton et al. 1986). Devito et al. (2005) showed that as much as 150 mm of water can be stored within the top 0.6 m for a site with similar soils as this study. Manual sampling of soil moisture content in June 2004 indicated that increases in soil moisture storage occurred below 1 m depth at the LA site (Figure 5.4). It is likely that storage was the primary fate of water as snowmelt rates were too low to create lateral flow at depth (Redding and Devito 2008). Similarly, as the unsaturated zone thickness increased (moving upslope), the amount of available storage increased. It is important to note that the wells associated with the study plots were located at toe slope positions so they could be installed with a hand auger to a sufficient depth to intersect the water table.

Plant uptake of water has the potential to influence water table dynamics over the growing season at the LA site. Soil moisture measurements made during spring 2004 indicated that there was little plant uptake by June 13; thus, plant uptake did not reduce soil moisture storage or create upward fluxes of water from the water table at this time. In fine-grained sediments with a large capillary fringe, small amounts of water reaching the water table can cause a large increase in WT elevation (e.g., Rosenberry and Winter 1997). At the LA site, recharge may be overestimated due to incorrect estimation of specific yield in the presence of the capillary fringe (Loheide et al. 2005). An estimate of capillary fringe thickness based on soil texture indicated that thickness ranged from 0.4 to1.3 m at the LA site. This means that at the LA-Nf upland well, at the maximum water level and maximum capillary fringe thickness, there would still be more than 1 m between the ground surface and top of the capillary fringe. At the LA-Sf site, the

maximum capillary fringe height would have been at least 2 m below the ground surface at the time of maximum water level, which would limit the type of rapid hydrological response observed by Rosenberry and Winter (1997). At the maximum estimated capillary fringe thickness and water level, plant uptake may draw water from the capillary fringe zone, which would influence the growing season water table recession.

There was no fall recharge recorded for the moraine sites in contrast to the outwash. While the fall 2004 water level at the LA-Sf well was greater than fall 2003, the LA-Nf well had essentially the same water level. The water added during the fall rains was taken up in unsaturated zone storage. This is evident from the lack of large differences between soil moisture storage in the top 1 m from early in the growing season (June)through the fall (October).

5.5.2.3 Influence of Precipitation Timing on Groundwater Dynamics

Snow accumulation for the winter of 2003–2004 was slightly lower than the long-term average at Slave Lake, which suggests that there might be slightly more recharge in average years. Due to lower than average winter precipitation, which was preceded by a dry fall, lower than average recharge to groundwater may have occurred at all sites during the study period. Dry antecedent conditions have a relatively larger impact on snowmelt recharge in years of low to average winter precipitation. This is especially important for landforms with finer-textured soils, which have a greater unsaturated zone storage capacity. Model simulations by Smerdon et al. (2008) showed that for outwash sites adjacent to the SA site, the time period that influences antecedent soil moisture conditions becomes longer for deeper unsaturated zones.

Precipitation during the snow-free period from May 1, 2004 to October 17, 2004 comprised approximately 75% of the annual precipitation during the period of monitoring (Table 5.2). While there was considerable precipitation during this period, there was little groundwater recharge as the water table elevations dropped following their peaks in late May and early June through the growing season into late August. The period of declining water tables coincides

with the main period of vegetation growth and hence plant water demand in this region (Blanken et al. 2001). Devito et al. (2005b) also noted declining water tables over the summer growing season on the Boreal Plains. Water table recession rate estimates ranged from 0.4 to 5 mm d^{-1} across the three sites. These recession rates are generally similar to measured growing season evapotranspiration rates on the Boreal Plains of 1.1–3.5 mm d^{-1} for jack pine stands on sandy soils (e.g., Baldocchi et al. 1997, Moore et al. 2000, Amiro et al. 2006) and 2.0–3.0 mm d^{-1} for aspen stands on fine-textured soils (e.g., Blanken et al. 2001, Swanson and Rothwell 2001, Amiro et al. 2006). The high recession rate at the SP site may also be a result of interactions of recharge with large-scale flow systems. The groundwater recession rates indicate that either direct uptake or upflux through the unsaturated zone at least partially sustains plant transpiration over the growing season (e.g., Rosenberry and Winter 1997, Smerdon et al. 2008).

Changes in soil moisture storage between June 13 and October 17, 2004 were small (-28 to +12 mm), and any increases likely occurred during the fall once the forest vegetation had senesced. The September/October 2004 period was slightly wetter than the long-term average at Slave Lake, and twice as wet as the same period in 2003. Precipitation is either being stored in the forest floor and upper soil horizons and then used by plants, or if it drains past the rooting zone, it may be stored within the deeper unsaturated sediments at the LA site or recharging groundwater at the SP and SA sites. It is also possible that upward fluxes from shallow water tables are occurring in response to plant demand (Smerdon et al. 2008). It is unlikely that significant lateral flow is occurring due to the large available soil moisture storage and precipitation intensity that must be exceeded to generate subsurface flow on these Luvisolic soils (Redding and Devito 2008). In addition, no lateral flow was measured at the LA site over July and August 2004, the wettest months of the study period. The results of soil moisture and groundwater monitoring indicate that most recharge of unsaturated zone storage and groundwater occurs in response to snowmelt and spring rains. Once the forest vegetation begins to transpire, stored water is consumed and the

rate of downward percolation decreases due to drying soils, and hence recharge does not occur readily until the vegetation has senesced.

5.5.3 Growing Season and Annual Infiltration Depth

Some movement of water during the growing season was evident from decreased Br^- recovery and concentration with depth below the organic-rich forest floor and Ahe horizons. Greater growing season and annual infiltration and drainage was noted at the SP and SA sites which had coarse-textured and highly conductive soils with low water holding capacity as compared with the LA site. At the SP and SA sites, with the exception of the SP-Nf plot, Br^- was flushed out of the soil profile except in the forest floor and upper mineral soil horizons, which had high organic matter content. Similarly, at the SP and SA sites, Cl^- concentrations were rarely above the background levels, which suggested that the applied Cl^- had been flushed out of the measured depth. In the fine-textured soils at the LA site, the Br^- front had moved to a depth of 1.0–1.2 m, which was 0.3–0.4 m deeper than the Br^- profiles measured in June 2004. Whitson et al. (2005) recorded similar annual infiltration depths in fine-textured Luvisolic soils on the Boreal Plains; infiltration depth at 14 months after application was 0.8–1.0 m. The greater retention of Br^- in the top 2 m of the soil at the LA site is reflected in the greater recovery of the tracer after 12 months compared to sites with sandy soils.

At the LA site, water is held in storage in the rooting zone and then may be used by the vegetation, which results in little water movement below the rooting zone during the growing season (e.g., Elliot et al. 1998, Blanken et al. 2001, Devito et al. 2005b). At the sandy sites, the water holding capacity of the mineral soil is low; therefore, water readily drains below the rooting zone (e.g., Cuenca et al. 1997). The estimates of infiltration depth may be slightly elevated due to the clipping of understory vegetation on the plots, which will have reduced interception and transpiration losses. However, the effects of clipping are expected to be minor given that the understory vegetation was generally sparse, especially at the SP and SA sites.

Previous research conducted by Whitson et al. (2005) on the Boreal Plains showed no difference in depth profiles of Br^- between June and October sampling dates, which indicated that there had been no further drainage deeper into the soil. The researchers attributed this to the removal of the Br^- tracer from the sampling zone by subsurface lateral flow. However, no lateral flow was reported during summer rainstorms (Whitson 2003). The lack of change in depth of Br^- recovery combined with a lower total Br^- recovery could be the result of preferential flow and diffusion losses. The lack of an increase in depth of the tracer profile suggests that precipitation that infiltrated the soil was held in storage near the surface and then used by plants during the growing season. Similarly, upland hillslopes at the LLB20 catchment on the Boreal Plains showed an annual pattern of deep infiltration and soil moisture recharge during the snowmelt period, followed by a gradual drying during the growing season (Devito et al. 2005b). Late summer and fall rains resulted in recharge to the groundwater at the outwash sites, but not at the LA site, where the water inputs were likely stored in the unsaturated zone.

It appears that the concentration of applied Cl^- was too low to provide a clear interpretation of growing season water movement due to the similar background concentrations of the tracer. Alternatively, some of the Br^- and Cl^- could have moved out of the frames due to lateral flow or diffusion into the soils surrounding the plots. Rainfall simulation experiments conducted on the LA slope showed no lateral flow over the summer of 2004 (Redding and Devito 2008). For lateral subsurface flow to occur at the LA site, wet antecedent conditions, low plant demand, and large high intensity precipitation events are required. However, these conditions did not occur over the 2004 growing season, and are likely rare in most years (Redding and Devito 2008).

5.5.4 Long-Term Root Zone Drainage and Groundwater Recharge

The CMB method produced a wide range of estimates for drainage below the root zone and for groundwater recharge. The estimates of root zone drainage in the fine-textured unsaturated zone on the LA site ranged from 1 to 15 mm yr^{-1} and varied by location and Cl_p scenario. These estimates are similar to those for

semi-arid, fine-textured agricultural soils on the Canadian prairies, which are typically less than 10 mm y^{-1} (Keller et al. 1986, Hayashi et al. 1998, Joshi and Maule 2000, Dyck et al. 2003). The range of results for the LA site appears to be reasonable given the results from other studies.

The recharge estimates based on the Cl_g measurements and Cl_p scenario 1 at the LA site are similar to the water table response estimates. The recharge estimates based on Cl_g and Scenarios 2 and 3 are much higher than the 2004 water table estimates or other studies conducted on the Boreal Plains and the Canadian Prairies (Hayashi et al. 1998, Joshi and Maule 2000). Given the results of these studies and our understanding of the hydrology of aspen-forested hillslopes with fine-textured soils (Devito et al. 2005b, Redding and Devito 2008), it seems likely that the CMB estimates of groundwater recharge in this study are overestimates. Studies that used the CMB method on the Canadian Prairies reported groundwater Cl^- concentrations that were similar to pore water Cl^- in the unsaturated zone (Hayashi et al. 1998, Joshi and Maule 2000). The Cl_g concentrations measured in this study (0.9–2.8 mg L^{-1}) are much lower than those measured at sites with fine textured soils and sediments on the Canadian Prairies (22–55 mg L^{-1}) (Hayashi et al. 1998, Joshi and Maule 2000), but the Cl_s concentrations are similar (LA site: range 18-226 mg L^{-1}, median 37 mg L^{-1}; prairies: 10–70 mg L^{-1}) (Figure 5.9) (Hayashi et al. 1998, Joshi et al. 2000).

For the SP site, estimates of root zone drainage (1–7 mm yr^{-1}) based on the unsaturated zone Cl_s profiles are at the low end of estimates from other studies conducted in the Boreal Plains. Recharge on sandy soils ranges from 0 to 30 mm yr^{-1} (Kachanoski and DeJong 1982, Cuenca et al. 1997, Elliott et al. 1998). However, these long-term estimates are much lower than the snowmelt recharge estimates that are based on the water table method (10–96 mm) and soil moisture storage budget for drainage below 1 m (103–146 mm). The chloride mass balance results are also much lower than the model estimates of Smerdon et al. (2008), which showed 50–75 mm yr^{-1} of net average annual recharge to the water table on the SA site, with a 6–9-m deep unsaturated zone. For shallow water tables (2–3 m), net average annual recharge to the water table was 15 mm yr^{-1} (Smerdon et al.

2008). Based on the CMB results measured in this study, there appears to be problems with the CMB estimates of root zone drainage for the sandy soils on the SP site and the groundwater recharge estimates for the LA site.

The 2003–2004 snowmelt recharge appears to be average based on precipitation inputs. The average winter precipitation across the study sites was 104 mm compared to the long-term average at Slave Lake of 114 mm. Fall 2003 precipitation was roughly 50% of the long-term average fall precipitation at Slave Lake. Consequently, soils in the study area, especially the finer-textured soils, may have started with a storage deficit in the spring, which would have reduced recharge. The available water holding capacity of sandy soils (SP and SA) and till soils (LA) is estimated at 60–70 mm m^{-1} and 180 mm m^{-1}, respectively (Saxton et al. 1986). Therefore, if fall conditions are dry, it is likely that recharge will be reduced. To determine the relative roles of climate variability, soil properties, and depth to water table on recharge, it will be necessary to conduct scenario experiments that use numerical models (e.g., Smerdon et al. 2008).

5.5.5 Potential Errors in Applying the Chloride Mass Balance Method on the Boreal Plains

It was expected that the estimated long-term root zone drainage would be greater at the sites with coarser-textured soils (SP, SA) than fine-textured soils (LA site). While this was the case for one-year estimates of snowmelt recharge, the long-term rates did not follow the expected pattern. This discrepancy appears to be a function of the CMB method in which soils with higher water contents (w) have a lower Cl_s value and hence a reduced estimate of root zone drainage (Equation 5.2). There appears to be a relationship between sand content and the measured Cl_s values (Figure 5.9). The reason for the higher Cl_s and low estimated drainage rates at the SP site relative to the LA site may be due to a number of factors. The first is that Cl_s is elevated relative to the LA site due to lower soil moisture content. Based on Equation 5.3, for a given extract concentration, lower soil moisture content results in higher pore water concentrations. It is clear that moisture content is lower in the sandy soils on the SP site than in the fine-textured

soils on LA site. There is greater total Cl^- stored per unit depth in the soils on the LA site than on the SP site (data not shown). However, due to the interaction of moisture content, the pore water chloride concentrations are elevated at the SP site, which lowers the estimated drainage rates. No literature was found that compares CMB drainage estimates from profiles on nearby sites with contrasting soil textures (fine and coarse), so it remains unclear as to whether this is a site-specific result, or is more widely applicable.

Discrepancies in results between methods and sites are likely related to violations of the assumptions of the CMB method. The following are key assumptions of the CMB method for root zone drainage in the unsaturated zone: (1) there is a steady input of water and Cl^-; (2) there is a steady-state vertical flux of Cl^- below the root zone; (3) there are no soil sources or sinks of Cl^-; and (4) piston flow of Cl^- is such that point measurements of Cl^- are spatially representative (Gee et al. 2005). For the unsaturated zone drainage estimates, the first assumption of steady input of water over the long term may be violated due to long-term changes in post-glacial climate in the Boreal Plains region (Vance 1986). Long-term changes in climate have been noted in tracer studies conducted in the southwestern U.S. (Scanlon et al. 2003). It is possible that the unsaturated zone Cl_s profiles in this study are not in equilibrium, as it would be expected that at some depth below the root zone there will be a bulge where upward and downward water fluxes are balanced (Wood 1999). This feature is not present in the profiles from URSA. That may be a function of the site's relatively young geological age (as compared to studies in the desert areas of the U.S.—e.g., Scanlon et al. [2003]) and low Cl_p inputs, which would result in a profile that is still developing. It is possible that models could be used to examine the development of the Cl^- profile over longer time periods (> 10,000 years) and under different climate, geological, and soil conditions. It is not clear if there are sources or sinks of Cl^- in the soil profile. Given that Cl_s is considerably higher than Cl_g, the system may not be in equilibrium, possibly due to an unsaturated zone that is functioning as a Cl^- sink, or to the relatively young age of the glacial sediments. The assumption about piston flow of water and Cl^- may not be

applicable at this site. Rainfall simulation studies at the LA site showed considerable preferential flow occurred within the upper 1.5 m of the soil profile (Redding and Devito 2008).

As with the unsaturated zone application of the CMB method, the groundwater-based recharge estimates may violate some assumptions. The following are key assumptions of the CMB method using Cl_g values: (1) the chloride in the groundwater originates only from precipitation directly on the aquifer; (2) Cl^- is conservative in the system; (3) Cl^- mass flux has not changed over time; and (4) there is no recycling or concentration of Cl^- within the aquifer (Wood 1999). The groundwater-based CMB method estimates an aerially averaged groundwater recharge flux for a given aquifer. Therefore, this approach may not be in agreement with local-scale measurements made with unsaturated zone Cl_s data (Wood 1999). At the LA site, the low Cl_g values relative to the Cl_s values at the LA site may indicate that little water is infiltrating to the water table, although this does not agree with the snowmelt recharge measured by the changes in water table depth. In addition, the Cl_g values may reflect the Cl^- concentrations in the adjacent peatland and pond at the LA site which, given the typical water table gradients for this area (Ferone and Devito 2004), may be moving laterally to the wells sampled in this study. The non-extraction of a relatively large proportion of the Cl^- held within the soil at the LA site may be evidence that Cl^- is non-conservative in these soils and sediments (Redding and Devito 2008). As the disturbance history of this site is unknown, it is not possible to say if the Cl^- mass flux has varied over time or if the system is at steady state. In addition, natural disturbances, such as fire, will change both the hydrological and biogeochemical dynamics of the site.

5.5.6 Conceptual Model of Upland Water Movement

Conceptual models of water movement on the coarse-textured soils (SP) and fine-textured soils (LA) in the study area are presented in Figure 5.10. At upper slope and crest positions on the uplands with coarse-textured soils, the combination of low storage capacity and high conductivity soil allows water to

move below the rooting zone and eventually recharge groundwater, especially during early spring and fall when plant water uptake is at a minimum. At these slope positions, the amount of upflux from the water table is minimized due to the thick unsaturated zone (Smerdon et al. 2008). At lower slope and toe slope positions, the depth to water table is reduced; however, the potential for upflux during the growing season is increased. It is difficult to separate the influences of site-specific factors on outwash landscapes from the role of larger-scale flow systems. In addition, the results from the SA site indicate that there were consistent gradients between the peatland and upland that are likely a function of both larger-scale flow system influences and different water retention properties of the peat compared with the outwash sand. The results for the SP and SA site are representative of the flow-through systems found on outwash landscapes in this region (Smerdon et al. 2005).

At the upper slope and crest positions on the uplands with fine-textured soils, direct recharge of infiltrating water is unlikely due to the large storage capacity of the unsaturated sediments and unsaturated zone thickness. In addition, the potential for lateral flow is low due to the high threshold soil moisture storage and rainfall intensity necessary (Redding and Devito 2008). Water infiltrating at upper slope positions is likely to be returned to the atmosphere by plant transpiration. The lower slope and toe slope positions are more likely to have direct recharge due to the presence of a thinner unsaturated zone and the potential for the capillary fringe to rise to relatively near the surface. However, the potential for upflux from the water table is increased at these locations. There is a consistent gradient indicating that flow from peatlands and riparian zones to adjacent uplands occurs at this site and others in this area (Ferone and Devito 2004). However, given the low conductivity of the fine-textured sediments, the flux of water to the upland is likely small. In addition, these fine-textured forested moraine hillslopes appear to be disconnected from larger-scale groundwater flow systems.

5.6 Summary and Conclusions

A multiple methods approach was used to estimate seasonal, annual, and long-term rates of vertical water movement and groundwater recharge on forested hillslopes on the Boreal Plains. Snowmelt infiltration was greater than runoff on all plots. Natural and applied tracers showed that the depth of infiltration of snowmelt water was greater on sites with sandy soils than fine-textured soils. On the hillslopes with coarse-textured soils, very little snowmelt water went into soil moisture storage in the top 1 m of soil, while on the hillslopes with fine-textured soils, 20–40% of the infiltrated snowmelt water remained in storage in the top 1 m of soil. Given that infiltration depths of less than 1 m were recorded, yet water table elevation increased, it appears that water is displaced in the unsaturated zone by piston flow (Saxena 1984, Buttle and Sami 1990). If the capillary fringe is relatively close to the ground surface and large water table responses to small precipitation inputs are possible, then depth to the water table at different hillslope positions controls recharge (Rosenberry and Winter 1997). Therefore, greater recharge should be expected at toe slope positions, such as those in this study. However, the corollary is that shallower water tables are more susceptible to upflux driven by plant uptake (Rosenberry and Winter 1997, Smerdon et al. 2008) and recharge to a declining water table is not easy to interpret from hydrometric data alone. Over the growing season, there was limited tracer evidence of deeper infiltration beyond the snowmelt infiltration front. Over the growing season, there was a drop in water table elevations during July and August, a period of relatively high precipitation inputs concurrent with maximum annual plant uptake, which indicates there was very little potential for recharge.

Recharge and groundwater dynamics were strongly controlled by soil texture. Groundwater recharge from snowmelt peaked in June, about a month after the end of the melt period, and was greatest at the sites with coarse-textured soils. At the SP-crest well, the recharge estimated from water table change was similar to the drainage from the top 1 m. At the toe slope wells on the SP site, water table increases were less than drainage, indicating flow occurred from the upland to the adjacent pond and wetlands. At the SA site, estimated water table

recharge was similar to water budget estimates of drainage below 1 m, indicating that little water went into storage. At the LA site, more water drained below 1 m than was reflected in the water table rise, indicating substantial storage in the unsaturated zone. If this water was stored in the upper 1–3 m of the unsaturated zone, it could be available to vegetation over the growing season due to upward flow gradients driven by plant uptake.

Conceptual models of water movement were developed for coarse-textured outwash and fine-textured moraine upland hillslopes. The models outline the major controls on water movement and the direction and fate of water movement. These conceptual models can be used to generalize these results to other outwash and moraine landscapes on the Boreal Plain, and they can function as hypotheses to test with future field-based and modelling research.

Use of the CMB method to estimate long-term root zone drainage and recharge estimates had mixed results. Recharge estimates using unsaturated zone chloride profiles indicated relatively low recharge. At the sandy SP site, the results showed anomalously low drainage compared with measured drainage below 1 m and water table responses following snowmelt. On the sites with fine-textured soils, the estimated recharge was similar to the groundwater response measured after spring snowmelt. Recharge estimated through examination of groundwater chloride at the fine-textured soil site was much greater than would be reasonably expected. This is possibly related to water table gradients between wetlands and adjacent hillslopes that resulted in lateral recharge from the wetlands to the uplands, and possibly reflects recharge from more dilute surface water. Future research is needed to determine if lateral recharge from wetlands to adjacent uplands is the cause of rising water tables during spring.

The application of the CMB method to subhumid, forested uplands on the Boreal Plains needs to be examined in greater detail to resolve the issue of lower estimated recharge rates on coarse-textured than on fine-texture upland soils. This would provide a powerful yet inexpensive and simple tool for estimating recharge rates in remote locations such as the Boreal Plains. The field-based results presented herein should be verified and extended with numerical modelling, such

as presented by Smerdon et al. (2008). To supplement the CMB estimates, long-term numerical modelling could be used to examine the development of unsaturated zone and groundwater geochemistry and recharge dynamics, which could clarify some of the questions raised herein.

Table 5.1. Site characteristics for study plots.

Site[1]	Canopy Spp.[2]	Plot	Orientation (degrees)	Slope (%)	Canopy Cover (%)[3]	Surface Mineral Soil Texture[4]	Forest Floor Thickness (m)
SP	JP	Nf	35	14	35	S	0.1
	JP	Sf	200	16	<10	S	0.04
SA	At	Nf	70	20	5 (30)	LS	0.06
	At	Sf	206	23	5 (30)	LS	0.06
LA	At	Nf	350	20	15 (60)	L	0.13
	At	Sf	160	18	10 (50)	L	0.1

[1] SP: sand-pine; SA: sand-aspen; LA: loam-aspen
[2] JP: jack pine; At: trembling aspen
[3] Canopy cover in leafless and full-leaf (in parentheses) conditions
[4] S: sand; LS: loamy sand; L: loam

Table 5.2. Precipitation on each site during the study period. The lysimeter values (Lys) are the amount of precipitation received at the ground surface for rain, and the equivalent depth of snowmelt water. These values include the effects of canopy interception and sublimation, and as such, are an estimate of the amount of water available to infiltrate the soil surface. "Belfort" refers to Belfort Gauges connected to data loggers. The SP-Sf lysimeter was damaged by a falling tree on September 15, 2004; therefore, data for the remaining period were filled using data from the SP-Nf lysimeter. Sf: south facing; Nf: north facing.

Site	Msmt. Method	Aspect	Sept 1-03 to Oct 31-03	Nov 1-03 to Apr30-04	May 1-04 to June 30-04	July 1-04 to Aug 31-04	Sept 1-04 to Oct 17-04	Nov1-03 to Oct17-04
SP	Lys	Sf	--	116	33	104	116	369
		Nf[1]	--	72	33	113	112	330
	Belfort[2]		42	85[2]	49	120	105	359
SA	Lys	Sf	--	94	44	122	101	361
		Nf[1]	--	87	36	108	94	325
LA	Lys	Sf[1]	--	163	47	96	84	390
		Nf[1]	--	104	44	109	83	340
Red Earth Creek 2003–04[2,3]			56	85	55	127	106	374
Slave Lake 2003–04[2,3]			40	104	57	206	158	525
Slave Lake Normals[2,4]			78	125	132	171	78[5]	506[5]

[1] Indicates lysimeters located under the canopy
[2] Snowfall only; does not account for sublimation or redistribution
3 Source: Environment Canada (2006b)
[4] Climate normals for 1971–2000 (Environment Canada 2006a)
[5] To October 31

Table 5.3. Frame water balances for October 21, 2003 to June 13, 2004 (DOY 165). The study sites are SP (sand-pine), SA (sand-aspen), and LA (loam-aspen). Irrigation applications were conducted on October 21, 2003 prior to soil freezing, and May 7, 2004 following snowmelt but prior to soil thaw. Precipitation inputs include lysimeter measurements of snowmelt and rainfall at each plot and the fall 2003 and spring 2004 irrigation additions for each frame. Change in soil moisture storage is denoted by ΔS. Blank cells in the ΔS June 13 to Oct 17 2004 column indicate locations where the profile probes were removed in June 2004 following frame excavation and sampling.

Site	Plot	Frame	Oct. 2003 Irrig Depth	May 2004 2004 Irrig. Depth	Snowmelt + Rain Inputs Oct 21 2003 to June 13 2004 (DOY 165)	Runoff to June 13, 2004 (DOY 165)	Infiltration to June 13, 2004 (DOY 165)	Infiltration Coefficient to June 13 2004 (DOY 165)	ΔS Oct 21, 2003 to June 13, 2004 (DOY 165)	Drainage below 1 m to June 13 2004 (DOY 165)	Drainage Coefficient to June 13, 2004 (DOY 165)	ΔS June 13 to Oct 17, 2004
			(mm)	(mm)	(mm)	(mm)	(mm)	(%)	(mm)	(mm)	(%)	(mm)
SP	Sf	4	40	20	213	8	205	96	-1	206	97	4
		3	40	--	193	14	179	93	-3	182	94	
		2	4	2	159	14	145	91	2	143	90	5
		1	4	--	157	45	112	71	0	112	71	
	Nf	4	40	20	165	4	161	98	-4	165	100	10
		3	40	--	145	5	140	97	-4	144	99	
		2	4	2	111	2	109	98	0	109	98	8
		1	4	--	109	3	106	97	-2	108	99	
SA	Sf	3	40	20	188	38	150	80	-1	151	80	8
		1	40	--	168	33	135	80	-1	136	81	
		4	4	2	134	60	74	55	1	73	54	10
		2	4	--	132	33	99	75	14	85	64	
	Nf	2	40	20	176	5	171	97	-2	173	98	12
		1	40	--	156	4	152	97	0	152	97	
		3	4	2	122	2	120	98	0	120	98	No data
		4	4	--	120	22	98	82	-2	100	83	
LA	Sf	4	40	20	265	5	260	98	17	243	92	9
		1	40	--	245	12	233	95	13	220	90	
		3	4	2	211	9	202	96	23	179	85	10
		2	4	--	209	9	200	96	39	161	77	
	Nf	3	40	20	200	5	195	98	63	132	66	-28
		4	40	--	180	7	173	96	48	125	69	
		1	4	2	146	3	143	98	20	123	84	11
		2	4	--	144	1	143	99	46	97	67	

Table 5.4. Recoveries of applied tracers. Each frame had 18.4 g of Br^- applied on October 21, 2003, and 23.8 g of Cl^- was applied to half of the frames on May 7, 2004. Background concentrations of Br^- were below instrumental detection limits; therefore, all measured Br^- was assumed to have been applied in October 2003. Soil samples for Br^- analysis were collected to a depth of 2 m. Negative values for Cl^- recovery indicate where post-experiment sampling measured less Cl^- than was found in the pre-experiment background values.

					Br^- Recovery		Cl^- Recovery		
Site and Frame		Fall 2003 Irrig. Depth (mm)	Spring 2004 Irrig. Depth (mm)	Tracer Sample Date	Mass Br^- (g)	Br^- Recovery (%)	Background Cl^- (g)	Mass Applied Cl^- Recovered (g)	Recovery Applied Cl^- (%)
SP-Sf	3	40		June-04	0	0			
	1	4		June-04	4.3	23			
SP-Nf	3	40		June-04	0.8	4			
	1	4		June-04	19.4	105			
SA-Sf	1	40		June-04	10	54			
	2	4		June-04	9	49			
SA-Nf	1	40		June-04	2.6	14			
	4	4		June-04	1.7	9			
LA-Sf	1	40		June-04	3	16			
	2	4		June-04	9	49			
LA-Nf	4	40		June-04	7	38			
	2	4		June-04	4	22			
SP-Sf	4	40	20	Oct-04	0.1	0.5	23.5	3.1	13
	2	4	2	Oct-04	0.2	1	23.5	2.3	10
SP-Nf	4	40	20	Oct-04	0.2	1	33.1	1.5	6
	2	4	2	Oct-04	1.3	7	33.1	-4.2	-18
SA-Sf	3	40	20	Oct-04	4	22	33.4	-0.6	-2
	4	4	2	Oct-04	0.2	1	33.4	-6.5	-27
SA-Nf	2	40	20	Oct-04	0.1	0.5	29.7	9.8	41
	3	4	2	Oct-04	0.04	0.2	29.7	-16.8	-71
LA-Sf	4	40	20	Oct-04	0.1	0.5	30.1	4.9	21
	3	4	2	Oct-04	3	16	30.1	-5.2	-22
LA-Nf	3	40	20	Oct-04	4	22	25.7	11	46
	1	4	2	Oct-04	5	27	25.7	9.7	41

Table 5.5. Snowmelt recharge estimated from changes in water table (WT) depth. WT depth is the depth below the ground surface and the values in parentheses are the DOY of the minimum or maximum measurement. Texture is the percentages (by mass) of sand and clay. The specific yield (Sy) is estimated using the mean (and standard deviation) values presented in Loheide et al. (2005), Johnson (1967) and field-estimated values from the study sites. Recharge is calculated using the three different Sy estimates and including the standard deviation for the Johnson estimates.

Site	Aspect	WT Depth			Texture		Sy			Recharge		
		Min (DOY) (m)	Max (DOY) (m)	ΔWT (m)	Sand %	Clay %	Loheide	Johnson	Field	Loheide (mm)	Johnson (mm)	Field (mm)
SP	Sf	0.9 (70)	0.79 (130)	0.11	96	0	0.32	0.26 (0.05)	0.44	35	29 (6)	48
	Crest	8.26 (73)	7.96 (150)	0.3	96	0	0.32	0.26 (0.05)	0.44	96	78 (15)	132
SA	Sf	1.51 (109)	1.08 (153)	0.43	92	1	0.32	0.26 (0.05)	0.25	138	112 (22)	108
LA	Sf	4.35 (88)	3.65 (160)	0.7	50	21	0.08	0.07 (0.03)	0.04-0.11	56	49 (21)	28-77
	Nf	3.35 (90)	2.42 (172)	0.93	17	29	0.12	0.07 (0.02)	0.04-0.11	112	65 (19)	37-102

Table 5.6. Long-term drainage estimates obtained using the chloride mass balance method for the SP and LA sites. The estimates were made using the mean soil pore-water chloride (Cl_s) measured below the rooting zone and three scenarios of atmospheric Cl^- inputs (Cl_p). The atmospheric input scenarios used were: (1) the URSA wet deposition value (0.26 mg L^{-1}); (2) a value of twice the wet deposition value (0.52 mg L^{-1}) based on the assumption that dry deposition is 50% of total annual deposition (Mike Shaw, Environment Canada, personal communication); and (3) a precipitation weighted wet deposition value that substitutes throughfall data for rainfall and the snow data from leafless aspen stands (0.91 mg L^{-1}). Annual precipitation was assumed to be 481 mm, with 75% occurring as rain (Marshall et al. 1999).

Site	Location		Scenario 1 $[Cl_p]$ 0.26 mg L^{-1}	Scenario 2 $[Cl_p]$ 0.52 mg L^{-1}	Scenario 3 $[Cl_p]$ 0.91 mg L^{-1}
Unsaturated Zone	Method	$[Cl_s]$ (mg L^{-1})	D (mm yr^{-1})	D (mm yr^{-1})	D (mm yr^{-1})
SP	Sf	238	1	1	2
	Nf	400	0	1	1
	Crest	128	1	2	3
SA	Sf	172	1	2	3
	Nf	92	1	3	5
LA	Sf	175	1	1	3
	Nf	94	1	3	5
	565w	37	3	7	12
	511w	31	4	8	14
	513w	30	4	8	15
	514w	81	2	3	5
Groundwater Method		$[Cl_g]$ (mg L^{-1})	R (mm yr^{-1})	R (mm yr^{-1})	R (mm yr^{-1})
LA	565w	2.8	45	89	156
	509w	1.3	96	192	337
	510w	0.9	144	287	503

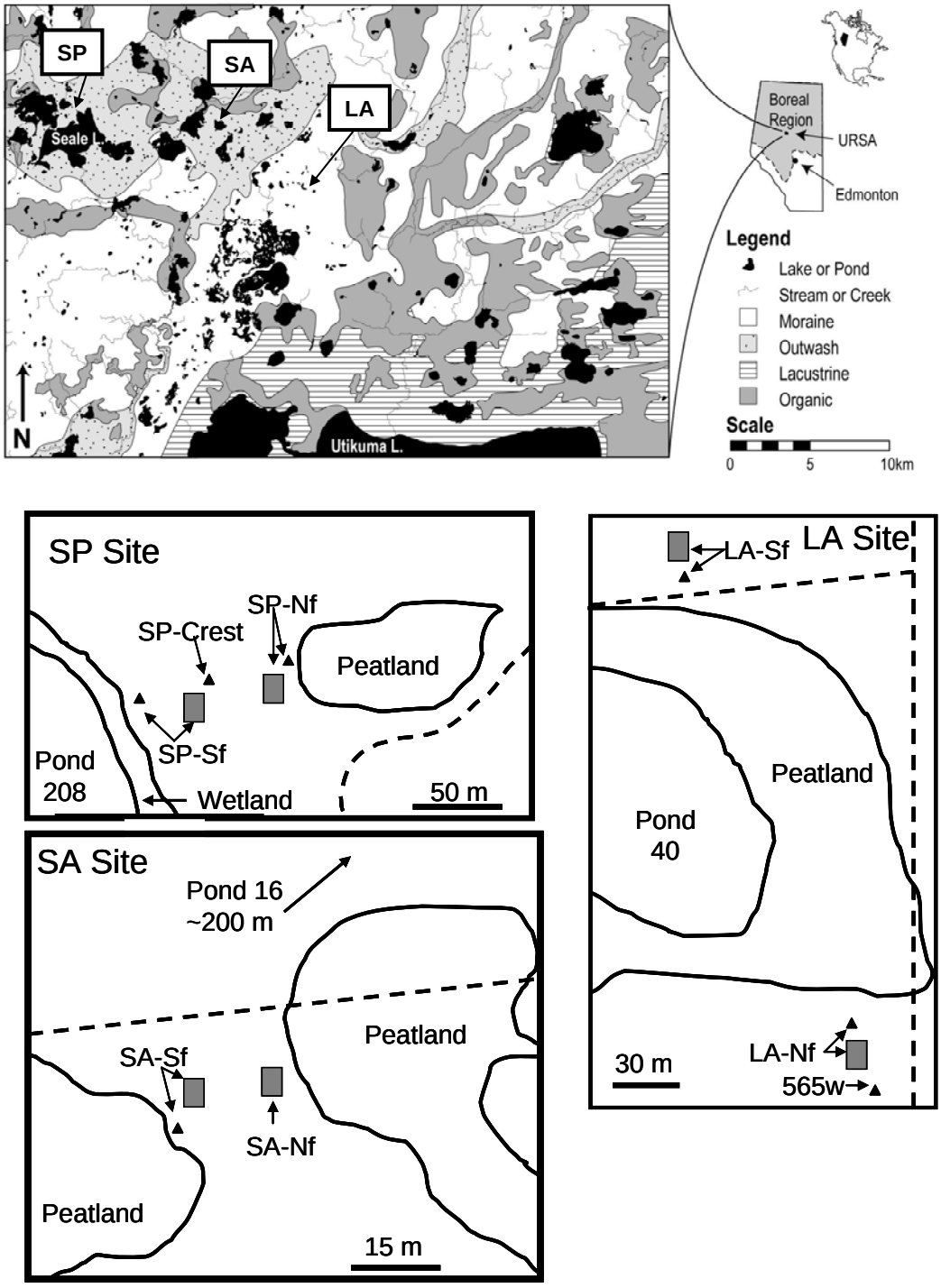

Figure 5.1. Study site locations, surficial geology, and study site layouts. Gray rectangles indicate the location of study plots, triangles indicate the location of groundwater monitoring wells, and dashed lines indicate roads or seismic lines. SP: sand-pine; SA: sand-aspen; LA: loam-aspen; Sf: south-facing; Nf: north-facing.

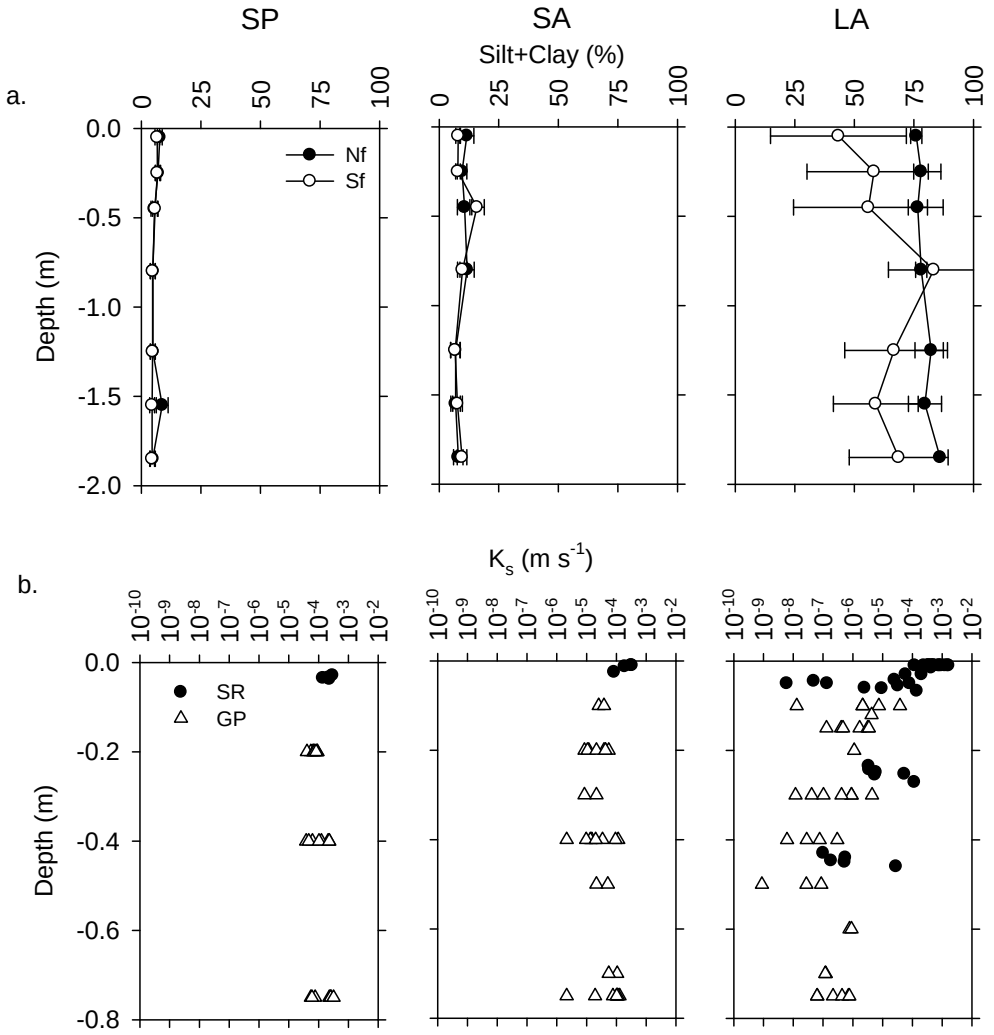

Figure 5.2. Soil texture (a) and K_s (b) for study sites. Open circles are values for the south-facing (Sf) plot samples; filled circles are for the north-facing (Nf) plot samples. Error bars around soil texture are one standard deviation. The K_s values are for individual measurements. Filled circles represent measurements using the single ring infiltration method; open triangles are Guelph permeameter measurements. SP: sand-pine; SA: sand-aspen; LA: loam-aspen.

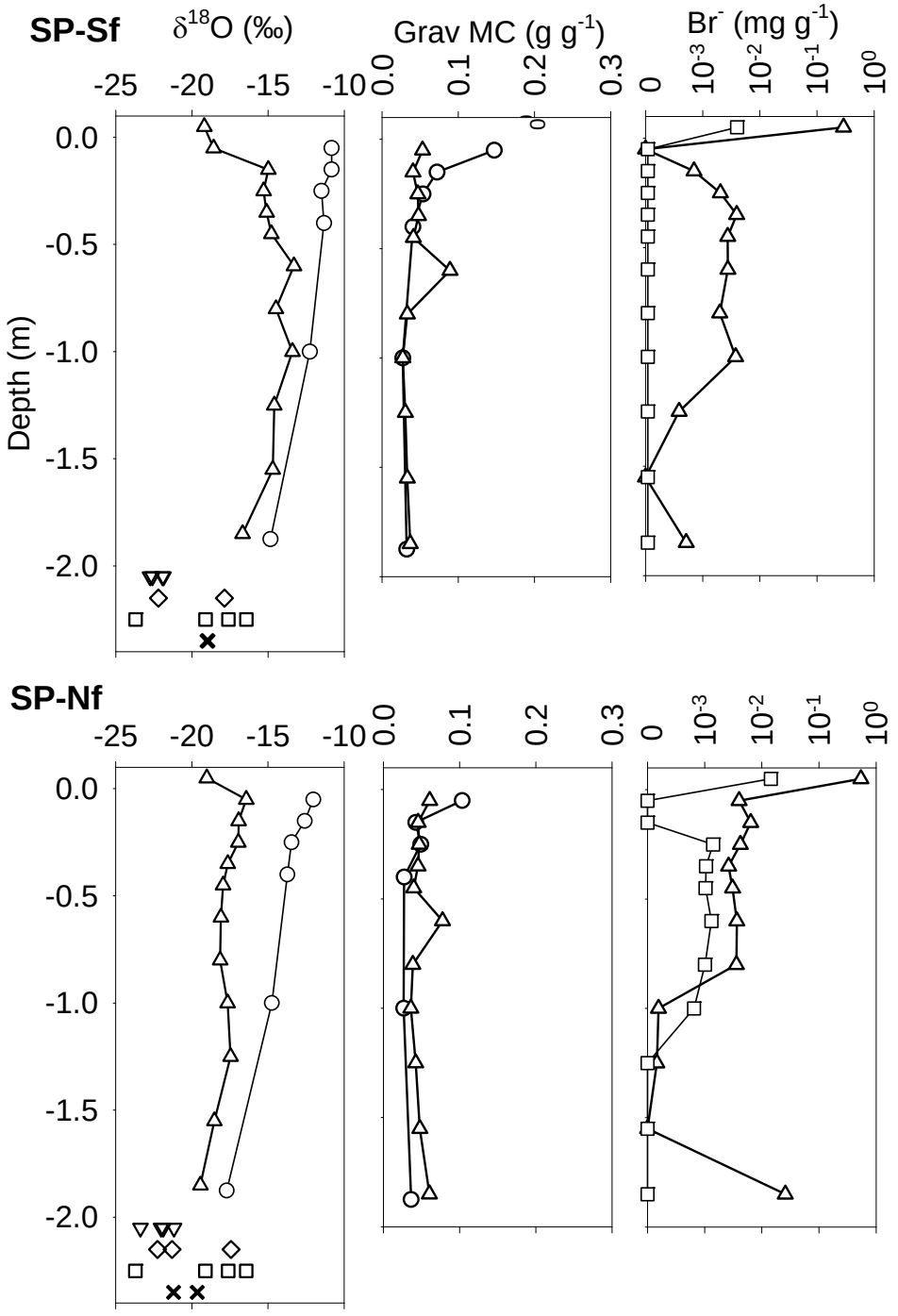

Figure 5.3. Depth profiles of $\delta^{18}O$, Br^-, and gravimetric moisture content profiles for the SP (sand-pine) site made on October 21, 2003 (DOY 294, open circles), June 13, 2004 (DOY 165, open triangles), and October 16, 2004 (DOY 290, open squares). At the base of the panels showing $\delta^{18}O$ profiles are symbols showing the range of measured $\delta^{18}O$ of precipitation inputs (snow = triangle, snowmelt = diamond, rain = square, groundwater = X). Sf: south-facing; Nf: north-facing.

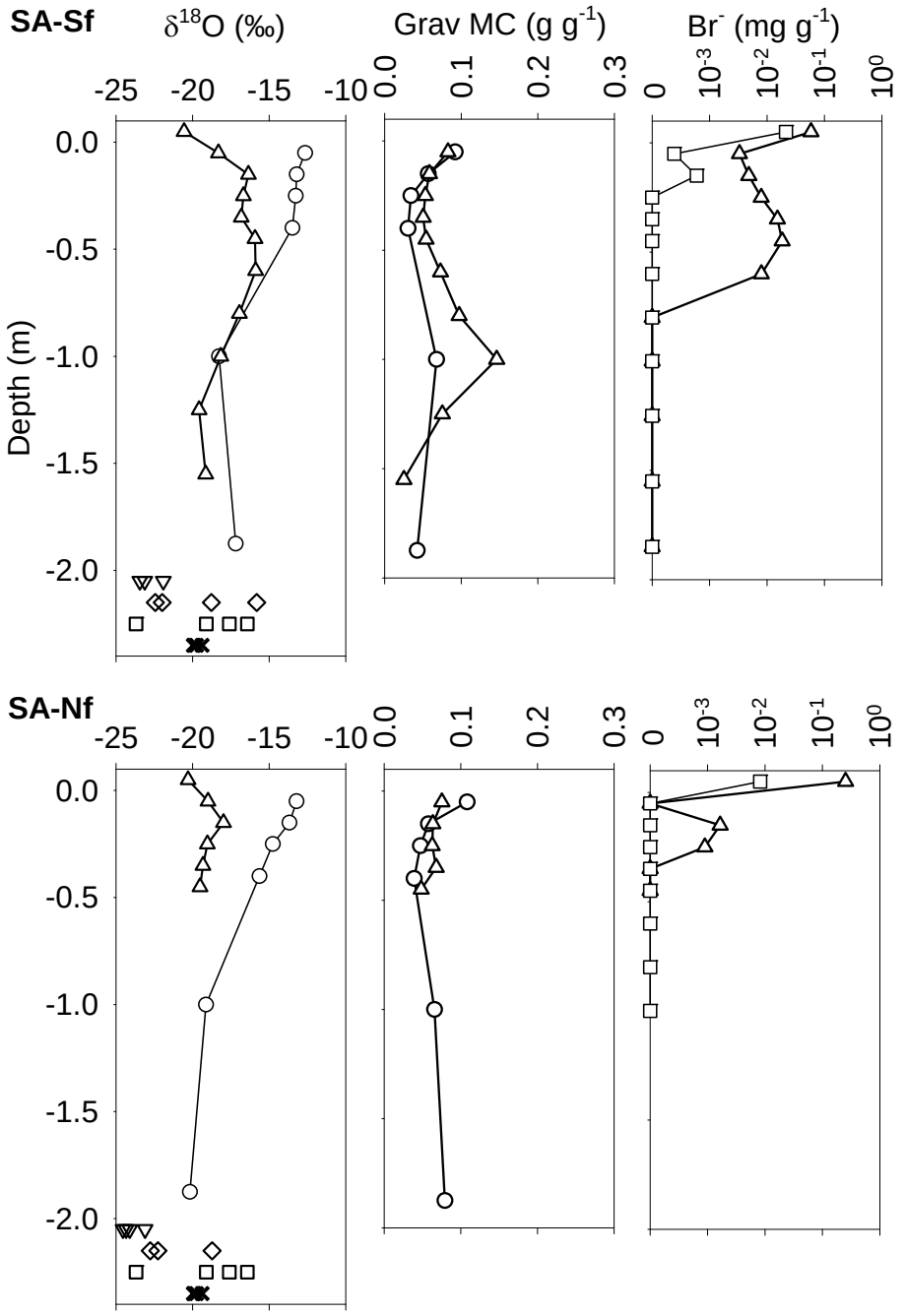

Figure 5.4. Depth profiles of $\delta^{18}O$, Br^-, and gravimetric moisture content profiles for the SA (sand-aspen) site made on October 21, 2003 (DOY 294, open circles), June 11, 2004 (DOY 163, open triangles), and October 15, 2004 (DOY 289, open squares). At the base of the panels showing $\delta^{18}O$ profiles are symbols showing the range of measured $\delta^{18}O$ of precipitation inputs (snow = triangle, snowmelt = diamond, rain = square, groundwater = X). Sf: south-facing; Nf: north-facing.

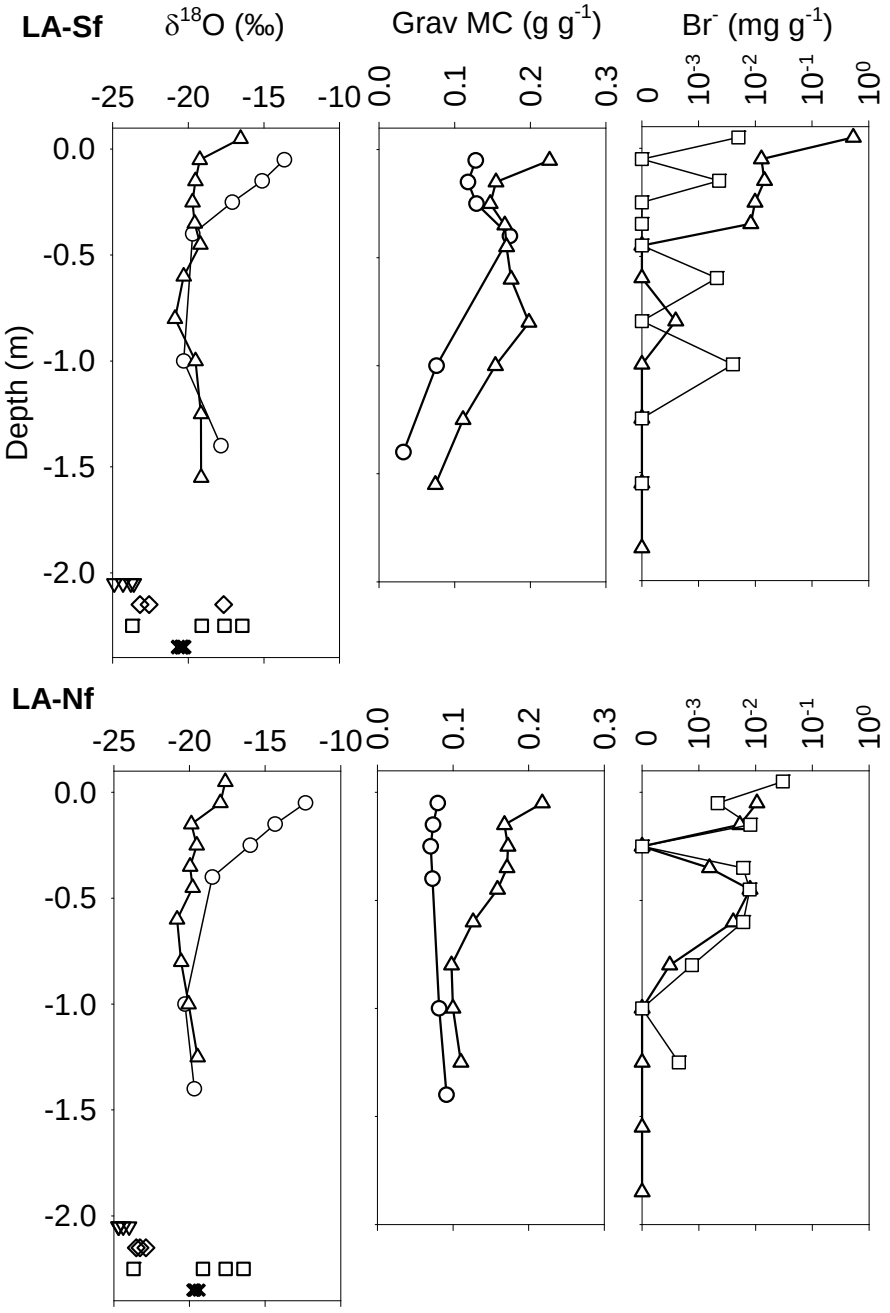

Figure 5.5. Depth profiles of $\delta^{18}O$, Br^-, and gravimetric moisture content profiles for the LA (loam-aspen) site made on October 21, 2003 (DOY 294, open circles), June 12, 2004 (DOY 164, open triangles), and October 13, 2004 (DOY 287, open squares). At the base of the panels showing $\delta^{18}O$ profiles are symbols showing the range of measured $\delta^{18}O$ of precipitation inputs (snow = triangle, snowmelt = diamond, rain = square, groundwater = X). Sf: south-facing; Nf: north-facing.

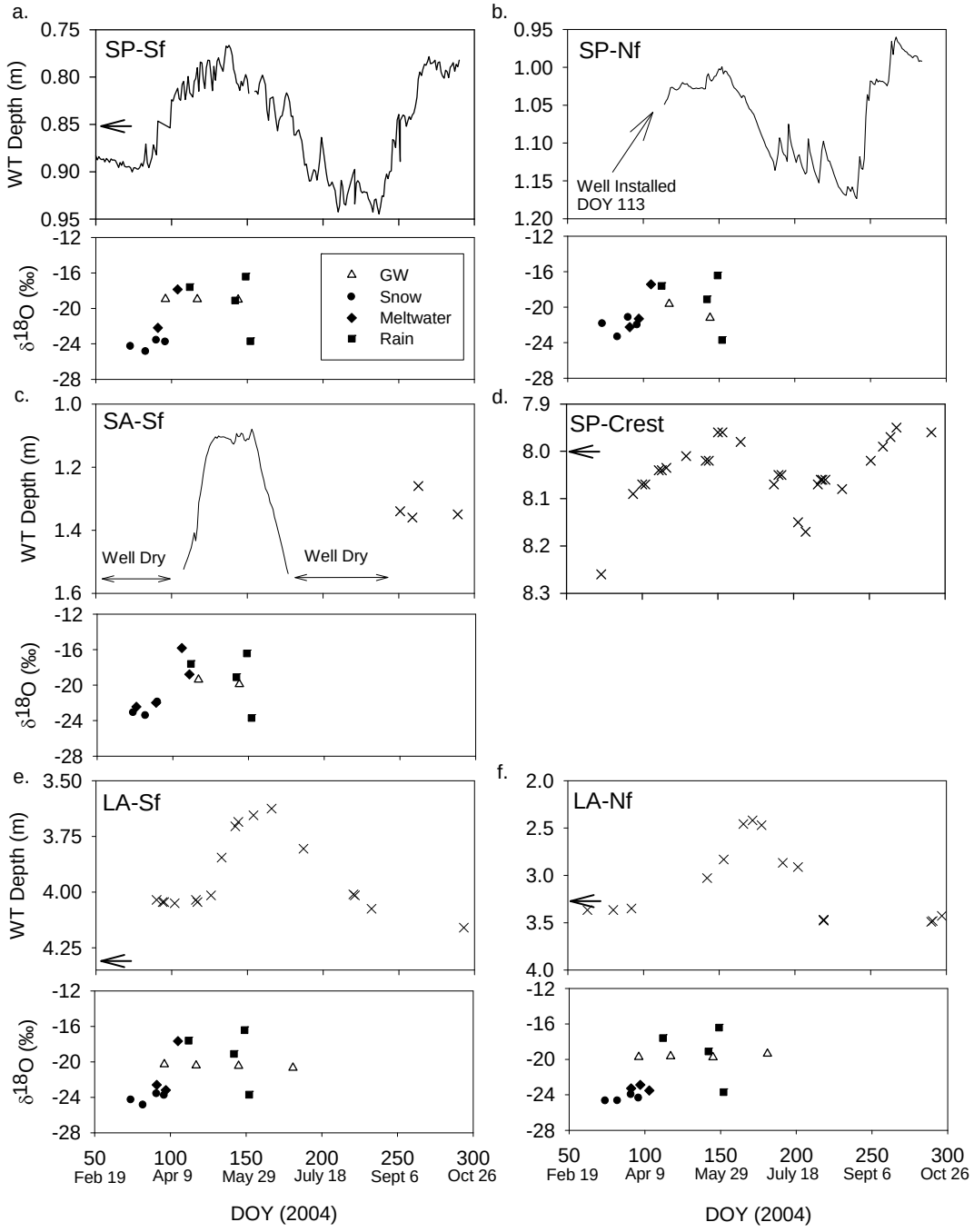

Figure 5.6. Groundwater levels and $\delta^{18}O$ composition of groundwater and precipitation sources for study wells at a) SP-Sf, b) SP-Nf, c) SA-Sf, d) SP-Crest, e) LA-Sf and f) LA-Nf. Symbols for $\delta^{18}O$ panels are:groundwater: open triangle, snow: filled circle, snowmelt water: filled diamond, rain: filled square. Arrows next to the Y-axis indicate the water levels in late October 2003. Note that SA-Sf well was dry, and SP-Nf well had not been installed. WT: water table; SP: sand-pine; SA: sand-aspen; LA: loam-aspen; Sf: south-facing; Nf: north-facing.

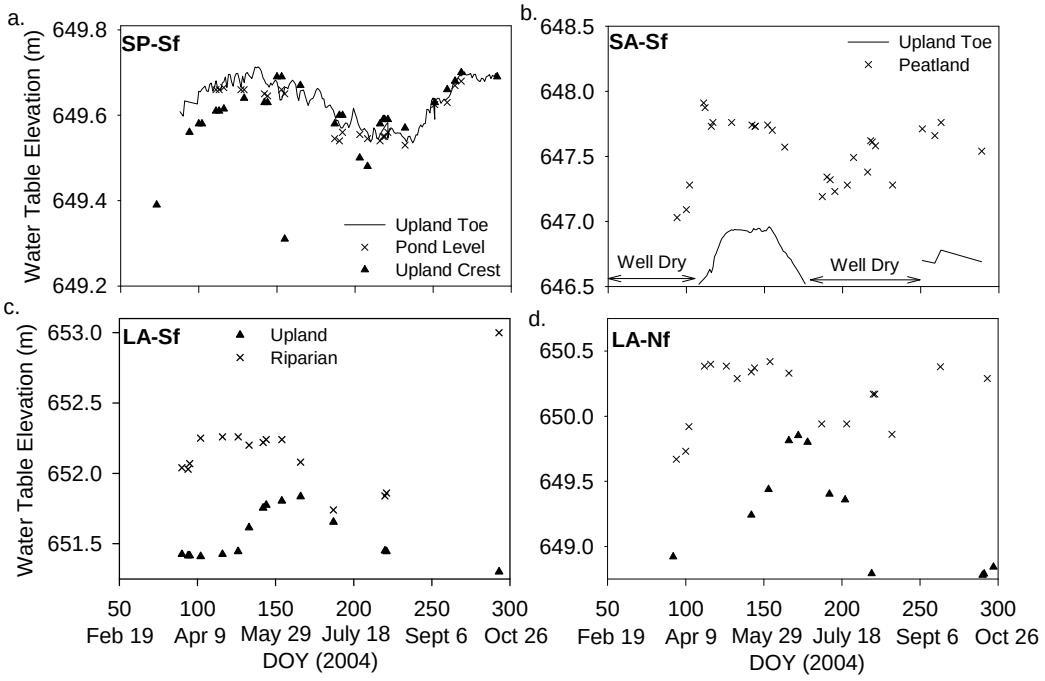

Figure 5.7. Groundwater elevations for upland wells and adjacent wetland wells or ponds to indicate directions of lateral groundwater flow at (a) SP-Sf, (b) SA-Sf, (c) LA-Sf, and (d) LA-Nf. SP: sand-pine; SA: sand-aspen; LA: loam-aspen; Sf: south-facing; Nf: north-facing.

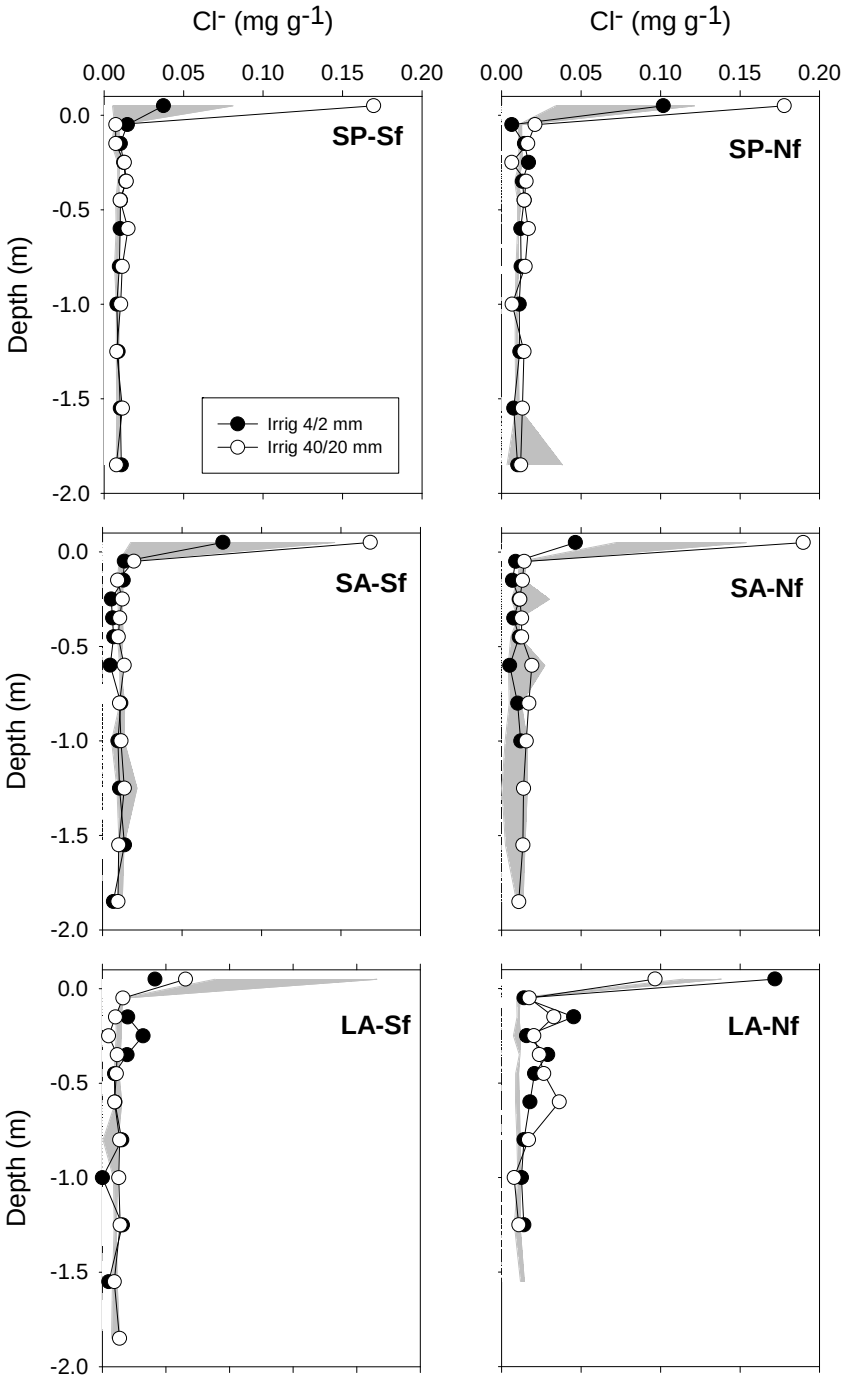

Figure 5.8. Background soil Cl^- profiles (mean ± 1 standard deviation in gray) and those measured in October 2004, six months after Cl^- application. Frames with tracers applied with 4 and 2 mm of irrigation in fall 2003 and spring 2004, respectively, are shown with filled circles. Frames with tracers applied with 40 and 20 mm of irrigation in fall 2003 and spring 2004, respectively, are shown with open circles. SP: sand-pine; SA: sand-aspen; LA: loam-aspen; Sf: south-facing; Nf: north-facing.

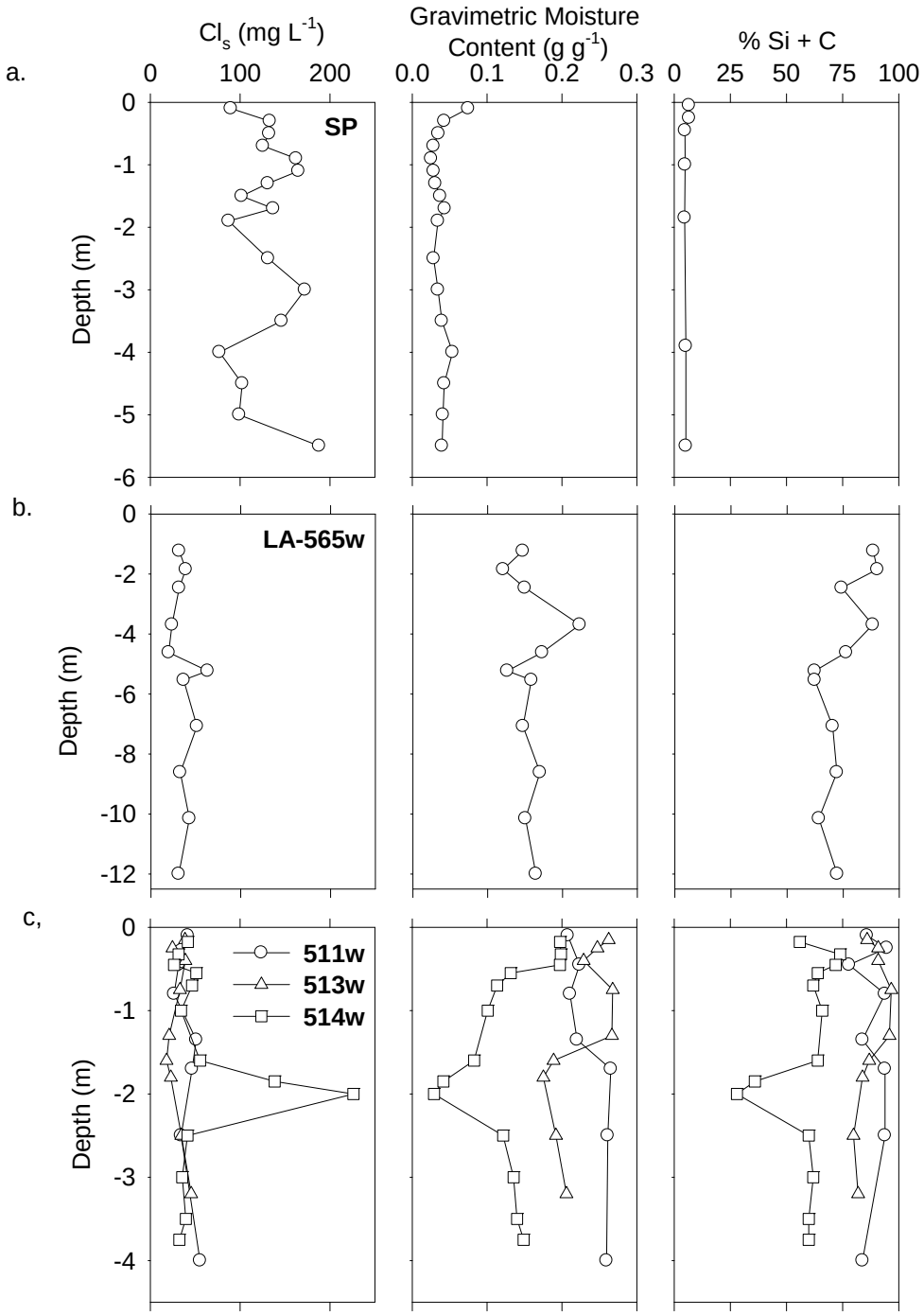

Figure 5.9. Depth profiles of pore-water chloride concentration (Cl_s), gravimetric moisture content, and particle size for (a) SP (sampled May 2004), (b) LA-565 (sampled August 2003), and (c) LA-511w, LA-513w, and LA-514w (sampled May 2004). Soil texture is shown as the fine fraction (e.g., the percentage of silt and clay, % Si + C). SP: sand-pine; SA: sand-aspen; LA: loam-aspen; Sf: south-facing; Nf: north-facing.

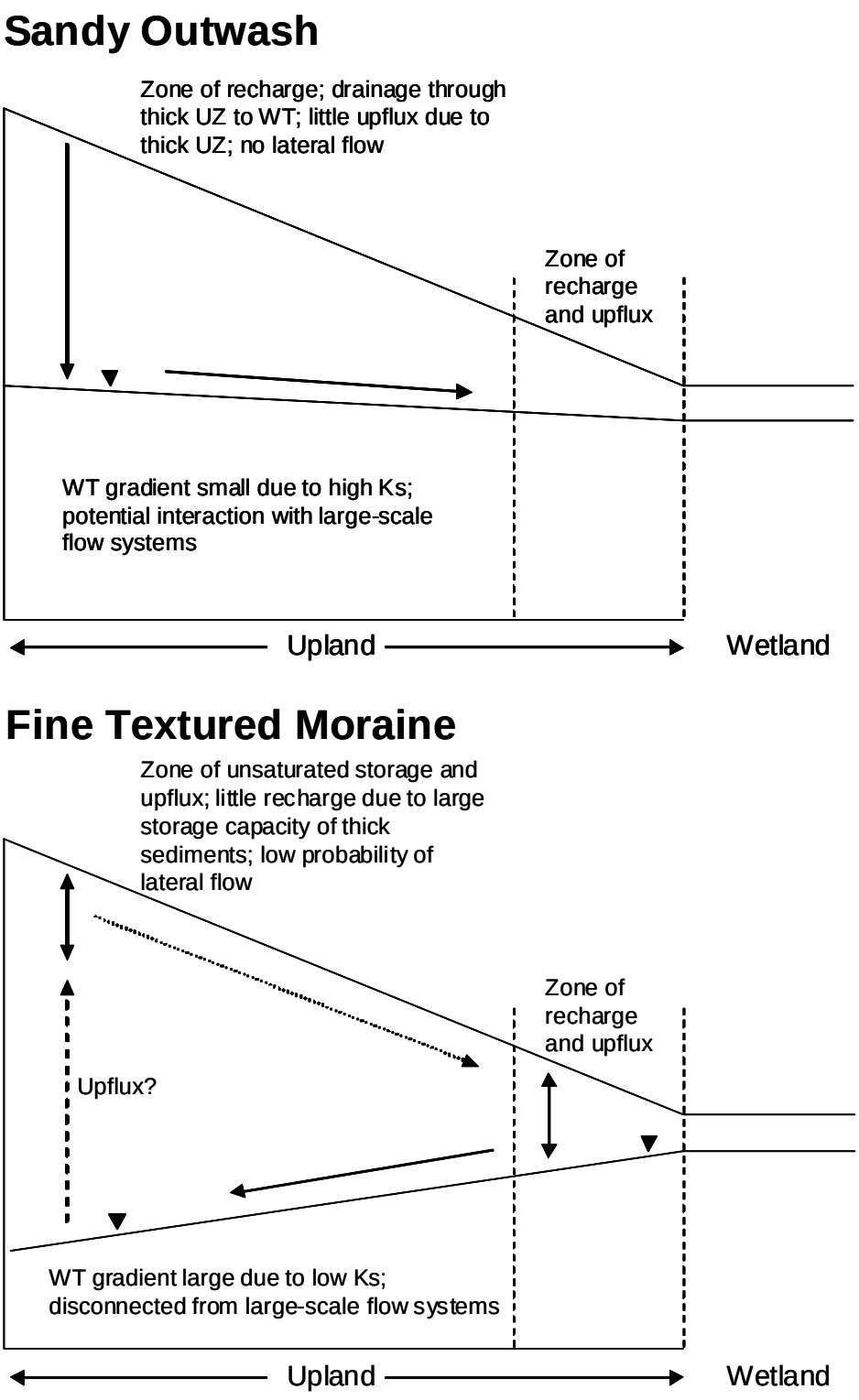

Figure 5.10. Conceptual model of water movement for sandy and fine-textured (silt-clay) uplands. Arrows indicate the direction of flow. WT: water table; UZ: unsaturated zone.

5.7 References

Amiro, B.D., Barr, A.G., Black, T.A., Iwashita, H., Kljun, N., McCaughey, J.H., Morgenstern, K., Murayama, S., Nesic, Z., Orchansky, A.L. and Saigusa, N. 2006. Carbon, energy and water fluxes at mature and disturbed forest sites, Saskatchewan, Canada. Agricultural and Forest Meteorology 136: 237-251.

Baldocchi, D.D., Vogel, C.A. and Hall, B. 1997. Seasonal variation of energy and water vapour exchange above and below a boreal jack pine forest canopy. Journal of Geophysical Research 102(D24): 28939-28951.

Blanken, P.D., Black, T.A., Neumann, H.H., den Hartog, G., Yang, P.C., Nesic, Z. and Lee, X. 2001. The seasonal water and energy exchange above and within a boreal aspen forest. Journal of Hydrology 245: 118-136.

Buttle, J.M. and Sami, K. 1990. Recharge processes during snowmelt: An isotopic and hydrometric investigation. Hydrological Processes 4: 343-360.

Cuenca, R.H., Strangel, D.E. and Kelly, S.F. 1997. Soil water balance in a boreal forest. Journal of Geophysical Research 102: 29355-29365.

Devito, K., Creed, I., Gan, T., Mendoza, C., Petrone, R., Silins, U. and Smerdon, B. 2005a. A framework for broad-scale classification of hydrologic response units on the Boreal Plains: is topography the last thing to consider? Hydrological Processes 19: 1705-1714.

Devito, K.J., Creed, I.F. and Fraser, C.J.D. 2005b. Controls on runoff from a partially harvested aspen-forested headwater catchment, Boreal Plains, Canada. Hydrological Processes 19: 3-25.

Dingman, S.L. 2002. Physical Hydrology. Prentice-Hall Inc., Upper Saddle River, NJ.

Dyck, M.F., Kachanoski, R.G. and deJong E. 2003. Long-term movement of a chloride tracer under transient, semi-arid conditions. Soil Science Society of America Journal 67: 471-477.

Ecoregions Working Group. 1989. Ecoclimatic regions of Canada. Ecological Land Classification Series No. 23.

Elliot, J.A., Toth, B.M., Granger, R.J. and Pomeroy, J.W. 1998. Soil moisture storage in mature and replanted sub-humid boreal forest stands. Canadian Journal of Soil Science 78: 17-27.

Environment Canda. 2006a. Canadian Climate Normals 1971-2000, Slave Lake Alberta. Environment Canada, Ottawa, ON. http://climate.weatheroffice.ec.gc.ca/climate_normals/index_e.html [Accessed February 8, 2009].

Environment Canada. 2006b. Canadian Climate Data Online. http://www.climate.weatheroffice.ec.gc.ca/climateData/canada_e.html [Accessed March 27, 2009].

Environment Canada. 2006c. Canadian National Atmospheric Chemistry Precipitation Database: Beaverlodge, AB. Environment Canada, Meteorological Service of Canada. URL. http://www.msc.ec.gc.ca/natchem/precip/index_e.html [Accessed March 27, 2009].

Environment Canada. 2006d, Archived Hydrometric Data, Red Earth Creek. http://www.wsc.ec.gc.ca/hydat/H2O/index_e.cfm?cname=main_e.cfm [Accessed March 27, 2009].

Evett, S.R., Tolk, J.A. and Howell, T.A. 2006. Sensors for soil profile moisture measurement: Accuracy, axial response, calibration, precision and temperature dependence. Vadose Zone Journal 5: 894-907.

Fenton M.M., Paulen, R.C., and Pawlowicz, J.G. 2003. Surficial geology of the Lubicon Lake area, Alberta (NTS 84B/SW). Alberta Geological Survey.

Ferone, J.M. and Devito, K.J. 2004. Shallow groundwater-surface water interactions in pond-peatland complexes along a Boreal Plains topographic gradient. Journal of Hydrology 292: 75-95.

Gee, G.W., Zhang, Z.F., Tyler, S.W., Albright, W.H. and Singleton, M.J. 2005. Chloride mass balance: Cautions in predicting increased recharge rates. Vadose Zone Journal 4: 72-78.

Harms, T.E. and Chanasyk, D.S. 1998. Variability of snowmelt runoff and soil moisture recharge. Nordic Hydrology 29: 179-198.

Hayashi, M.,van der Kamp, G. and Rudolph, D.L. 1998. Water and solute transfer between a prairie wetland and adjacent uplands, 2. Chloride cycle. Journal of Hydrology 207: 56-67.

Healy, R.W. and Cook, P.G. 2002. Using groundwater levels to estimate recharge. Hydrogeology Journal 10: 91-109.

Hendry, M..J. 1982. Hydraulic conductivity of a glacial till in Alberta. Ground Water 20: 162-169.

Hunt, P.R. and Zahner, R. 1970. Nonpedogenic texture bands in outwash sands of Michigan: their origin, and influence on tree growth. Soil Science Society of America Proceedings 34: 134-136.

Johnson, A.I. 1967. Specific Yield – compilation of specific yields for various materials. US Geological Survey Water Supply Paper 1662-D, 74 pp.

Joshi, B., and Maule, C. 2000. Simple analytical models for interpretation of environmental tracer profiles in the vadose zone. Hydrological Processes 14: 1503-1521.

Kachanoski, R. and DeJong, E. 1982. Comparison of soil water cycle in clear-cut and forested sites. Journal of Environmental Quality 11: 545-549.

Kalra, Y.P. and Maynard, D.G. 1991. Methods Manual for Forest Soil and Plant Analysis. Edmonton, AB. Forestry Canada, Northern Forestry Centre. Information Report NOR-X-319.

Keller, C.K., van der Kamp, G. and Cherry, J.A. 1986. Fracture permeability and groundwater flow in clayey till near Saskatoon, Saskatchewan. Canadian Geotechnical Journal 23: 229-240.

Koehler, G., Wassenaar, L.I. and Hendry, M.J. 2000. An automated technique for measuring δD and $\delta^{18}O$ values of porewater by direct CO_2 and H_2 equilibration. Analytical Chemistry 72: 5649-5664.

Laudon, H., Sjoblom, V., Buffam, I., Siebert, J. and Morth, M. 2007. The role of catchment scale and landscape characteristics for runoff generation of boreal streams. Journal of Hydrology 344: 198-209.

Levia, D.F. and Frost, E.E. 2006. Variability of throughfall volume and solute inputs in wooded ecosystems. Progress in Physical Geography 30: 605-632.

Loheide II, S.P., Butler Jr, J.J., and Gorelick, S.M. 2005. Estimation of groundwater consumption by phreatophytes using diurnal water table fluctuations: A staturated-unsaturated flow assessment. Water Resources Research 41, W07030, DOI: 10.1029/2005WR003942.

Marshall I.B., Schut P., Ballard M. (compilers). 1999. A National Ecological Framework for Canada: Attribute Data. Environmental Quality Branch, Ecosystems Science Directorate, Environment Canada and Research Branch, Agriculture and Agri-Food Canada, Ottawa/Hull. http://sis.agr.gc.ca/cansis/nsdb/ecostrat/data_files.html [Accessed March 27, 2009].

Mellander, P.-E., Bishop, K. and Lundmark, T. 2004. The influence of soil temperature on transpiration: plot scale manipulation in a young Scots pine stand. Forest Ecology and Management 195: 15-28.

Moore, K.E., Fitzjarrald, D.R., Sakai, R.K. and Freedman, J.M. 2000. Growing season water balance at a boreal jack pine forest. Water Resources Research 36: 483-493.

Murray, C.D. and Buttle, J.M. 2005. Infiltration and soil water mixing on forested and harvested slopes during spring snowmelt, Turkey Lakes Watershed, central Ontario. Journal of Hydrology 306: 1-20.

Price, A.G. and Hendrie, L.K. 1983. Water motion in a deciduous forest during snowmelt. Journal of Hydrology 64: 339-356.

Redding, T.E. and Devito, K.J. 2008. Lateral and vertical flow thresholds for aspen forested hillslopes on the Western Boreal Plains, Alberta, Canada, Hydrological Processes 23: 4287-4300.

Redding, T.E., Hannam, K.D., Quideau, S.A. and Devito, K.J. 2005. Particle density of aspen, spruce, and pine forest floors in Alberta, Canada. Soil Science Society of America Journal 69: 1503-1506.

Redding, T.E., Smerdon, B.D., Kaufman, S.C. and van Harlem, J.R. 2006. Evapotranspiration from boreal forests: A summary of methods and flux rates. Western Boreal Forest Hydrology Research Group, Unpublished Report. 17 p.

Reynolds, W.D. and Elrick, D.E. 2002. Sing-ring and double-or concentric-ring infiltrometers. In: Dane, J.H. and Topp, G.C. Methods of Soil Analysis: Part 4, Physical Methods. Madison, WI. Soil Science Society of America. P.821-826.

Reynolds, W.D., Elrick, D.E. and Youngs, E.G. 2002. Constant head well permeameter (vadose zone). In: Dane, J.H. and Topp, G.C. Methods of Soil Analysis: Part 4, Physical Methods. Madison, WI. Soil Science Society of America. P.844-858.

Rosenberry, D.O. and Winter, T.C. 1997. Dynamics of water-table fluctuations in an upland between two prairie-pothole wetlands in North Dakota. Journal of Hydrology 191: 266-289.

Saxena, R.K. 1984. Seasonal variations of Oxygen-18 in soil moisture and estimation of recharge in esker and moraine formations. Nordic Hydrology 15: 235-242.

Saxton, K.E., Rawls, W.J., Romberger, J.S. and Papendick, R.I. 1986. Estimating generalized soil-water characteristics from texture. Soil Science Society of America Journal 50:1031-1036.

Scanlon, B.R. 2004. Evaluation of methods of estimating recharge in semiarid and arid regions of the Southwestern U.S. In: Hogan, J.F., Phillips, F.M. and Scanlon, B.R. eds. Groundwater Recharge in a Desert Environment: The Southwestern United States. Washington, DC, American Geophysical Union, Water Science and Application 9. p 235-254.

Scanlon, B.R., Keese, K. and Reedy, R.C. 2003. Variations in flow and transport in thick desert vadose zones in response to paleoclimatic forcing (0-90 kyr): Field measurements, modelling and uncertainties. Water Resources Research 39: doi:10.1029/2002WR001604.

Smerdon, B.D., Devito, K.J. and Mendoza, C.A. 2005. Interaction of groundwater and shallow lakes on outwash sediments in the sub-humid Boreal Plains of Canada. Journal of Hydrology 314: 246-262.

Smerdon, B.D., Mendoza, C.A. and Devito, K. J. 2007. Simulations of fully coupled lake-groundwater exchange in a subhumid climate with an integrated hydrologic model. Water Resources Research 43: doi:10.1029/2006WR005137.

Smerdon, B.D., Mendoza, C.A. and Devito, K.J. 2008, Influence of sub-humid climate and water table depth on groundwater recharge in shallow outwash aquifers. Water Resources. Research. 44: doi:10.1029/2007WR005950.

Soil Classification Working Group. 1998. The Canadian System of Soil Classification (Third Edition). Ottawa, ON. Agriculture and Agri-Food Canada.

Sophocleous, M. 2002. Interactions between groundwater and surface water: the state of the science. Hydrogeology Journal 10: 52-67.

Stahli, M, Bayard, D., Wydler, H., and Fluhler, H. 2004. Snowmelt infiltration into alpine soils visualized by dye tracer technique. Arctic, Antarctic and Alpine Research 36: 128-135.

Strong, W.L. and LaRoi, G.H. 1983. Root-system morphology of common boreal forest trees of Alberta, Canada. Candian Journal of Forest Research 13: 1164-1173.

Swanson, R.H. and Rothwell, R.L. 2001. Hydrologic recovery of aspen clearcuts in northwestern Alberta. In: USDA Forest Service Proceedings RMRS-P-18. p. 121-135.

Unnikrishna, P.V., McDonnell, J.J. and Kendall, C. 2002. Isotope variations in a Sierra Nevada snowpack and their relation to meltwater. Journal of Hydrology 260: 38-57.

Vance, R.E. 1986. Aspects of postglacial climate of Alberta: Calibration of the pollen record. Geographie physique et Quaternaire 40: 153-160.

Vogwill R. 1978. Hydrogeology of the Lesser Slave Lake area, Alberta. Edmonton, AB. Alberta Research Council. 30.

Whitson, I.R. 2003. Phosphorous movement in a Boreal Plains soil (Gray Luvisolic) after forest harvest. PhD Thesis, University of Alberta, Edmonton, AB.

Whitson, I.R., Chanasyk, D.S. and Prepas, E.E. 2004. Patterns of water movement on a logged Gray Luvisolic hillslope during the snowmelt period. Canadian Journal of Soil Science 84: 71-82.

Whitson, I.R., Chanasyk, D.S. and Prepas, E.E. 2005. Effect of forest harvest on soil temperature and water storage and movement patterns on Boreal Plains hillslopes. Journal of Environmental Engineering and Science 4: 429-439.

Winter, T.C. 1983. The interaction of lakes with variably saturated porous media. Water Resources Research 19: 1203-1218.

Wood, W.W. 1999. Use and misuse of the chloride-mass balance method in estimating groundwater recharge. Ground Water 37: 2-3.

Chapter 6
Summary and Conclusions

6.1 Hydrology of Forested Uplands on the Boreal Plains

The preceding chapters provide data and interpretation to increase knowledge of temporal and spatial hydrologic response to precipitation of Boreal Plain uplands. The research examined hydrological processes at plot and hillslope scales for moraine and outwash landforms. The research also considered rainfall and snowmelt conditions at event, seasonal, annual and long-term time scales.

Previous research at the Utikuma Region Study Area (URSA) has clearly shown that both the amount and timing of precipitation is important for driving hydrological response (Ferone and Devito 2004, Devito et al. 2005b, Smerdon et al. 2005, Smerdon et al. 2008, Riddell 2008). Precipitation timing is important due to the interplay between the evaporative demand and subsurface water storage, both of which are large relative to the average precipitation. The growing season (May to August) accounts for roughly half of the annual precipitation (Table 6.1), but is also the period of the year with the highest evaporative demand.

Snowmelt represents approximately 25% of average annual precipitation, and occurs during a time of year when evaporative demand is at a minimum. Water movement during and following snowmelt period was dominated by infiltration at most sites. Near-surface runoff during snowmelt was a small portion of the water balance at most hillslope locations. Where snowmelt runoff was significant, it occurred on south-facing outwash hillslopes with coarse-textured soils and a large proportion of the area of the runoff frames underlain by concrete frost. It appears that the runoff from south-facing outwash hillslopes is related to lower canopy cover resulting in greater solar radiation reaching the ground surface, increasing snowmelt rates, and the potential for the development of concrete frost. These results differ from results from the Boreal Cordillera, where runoff was noted from north-facing slopes underlain by an ice layer, as compared to south-facing slopes underlain by frozen, but permeable, soils (Carey and Woo

1999). Analysis of longer-term air temperature data indicates that the weather conditions necessary to generate concrete frost occur at least once in most years. Warmer temperatures and earlier spring melt resulting from climate change (Barnett et al. 2005) could increase the frequency of concrete frost development.

Water inputs from snowmelt and spring rainfall were the primary source of groundwater recharge during the 2004 study period. Similar results have been observed for fine-textured moraine uplands by Devito et al. (2005b) and using numerical models for outwash (Smerdon et al. 2008). During the study period, water table elevations peaked following snowmelt and then declined until the fall when all outwash sites showed a rise in water table due to large precipitation inputs and senescence of overstory trees. At the moraine site, the direction of groundwater flow was into the upland from the adjacent wetland, while at the outwash sites the flow direction was variable.

The results of the rainfall simulations indicate that lateral flow is generated through the transmissivity feedback mechanism, similar to speculated by Devito et al. (2005b). For lateral flow to occur antecedent soil moisture content must be close to field capacity above the C-horizon, which acts as an effective confining layer. Lateral and vertical flow both indicated the presence of preferential flow, similar to observations from the Boreal Plain (Devito et al. 2005b) and Prairies (Hendry 1982). The potential for lateral flow is low given the large threshold amounts of antecedent moisture content and precipitation magnitude and intensity. The probability of daily rainfall greater than 20 mm threshold is low, ranging from 1.1 to 2.8 % (Table 6.1).

The importance of antecedent conditions for vertical and lateral flow varies by landform. For the outwash, the low water holding capacity and high conductivity of the soils and sediments means that wet antecedent conditions do not occur within the unsaturated zone. Lateral flow is highly unlikely for the outwash due to the lack of a confining layer. High water tables as a result of wet conditions will affect recharge and upflux by reducing the depth to water table.

Antecedent soil moisture conditions on the moraine are more important than on the outwash for the generation of vertical and lateral flow. This is a

function of the large storage capacity of the fine-textured soils and sediments, and decreasing hydraulic conductivity with depth (Devito et al. 2005b, Redding and Devito 2008). Soil moisture storage within the rooting zone or within a depth that is accessible to plants through upflux will lead to a seasonal antecedent soil moisture storage deficit. Higher water tables will bring the capillary fringe closer to the surface, increasing the potential for upflux and rapid groundwater response to precipitation (e.g., Rosenberry and Winter 1997).

The timing of wet conditions is of the essence given the limited time periods of soils with adequate antecedent conditions to generate significant vertical or lateral flow. For flow on moraine uplands, there needs to be a temporal convergence of high antecedent moisture content and precipitation events with large magnitude and high intensity. To have high antecedent conditions in the late spring or early summer, two primary pathways may be followed. The first is a wet fall followed by a large snowpack and cool spring which suppresses plant water demand. It is then possible that the system will be primed for rainfall induced lateral flow or recharge in June and July when the potential for large rainstorms is at the annual maximum. The second pathway is a wet period (precipitation exceeds evapotranspiration over a given period of time) during the growing season. The month of year with the greatest potential for a 40 mm rain event is June (daily probability of exceedence of 0.5%) (Table 6.1).

The results of this and other research at URSA (e.g., Ferone and Devito 2004, Redding and Devito 2008, Riddell 2008) indicate that the potential for significant recharge or lateral flow from upland hillslopes is a function of the amount of precipitation, antecedent conditions and the slope position and landform. Table 6.2 provides a summary of the potential for water movement at the toe slope/lower slope and mid-slope/upper slope positions on the outwash and moraine for various time periods. On the outwash landforms with highly conductive soils with low storage capacity, lateral flow is unlikely while recharge is common (Table 6.2). However, recharge on the outwash is also influenced by interactions with regional groundwater flow systems (Devito et al. 2005a, Smerdon et al. 2005). While the fine-textured uplands on the moraine have soils

that are more conducive to the generation of lateral flow, the high storage capacity, small rainfall event magnitudes and intensities, and vegetation demand, result in a low potential for lateral flow (Redding and Devito 2008) (Table 6.2). Recharge on the moraine is limited at upper slope locations due to the large available storage in the unsaturated zone, and potential for water stored to be pulled upward by vegetation. Toe slope locations on moraine uplands likely have the greatest potential for recharge. For significant recharge or lateral flow to occur on this landscape, requires extended wet periods that exceed the available storage capacity of the unsaturated soils.

This research has clearly shown that vertical flow and unsaturated zone storage are the dominant flow pathways for Boreal Plain uplands. The role of topography is related to the depth to the water table, rather than as an indication of lateral flow. To successfully model the hydrology of forested uplands on the Boreal Plain, an explicit consideration of the characteristics of the soils and surficial geology is required.

6.2 Implications for Forest Harvesting

There are two primary pathways for which forest harvesting can influence the hydrology of forested uplands on the Boreal Plain: loss of forest cover and alteration of the surface soil properties. These effects will be similar to those of disturbance due to traditional oil and gas development. A loss of forest cover typically results in a decrease in canopy interception and transpiration, leading to more water being available to satisfy storage deficits in the soil and potentially to be available for groundwater recharge or generate runoff. Wetter soils have been observed following clearcut harvesting (e.g., Hart and Lomas 1979, Elliott et al. 1998). Given the importance of antecedent conditions for vertical and lateral flow from moraine hillslopes, this is likely to be the primary hydrologic effect of harvesting. However, even under conditions of high antecedent storage, there was a high threshold of event precipitation magnitude and intensity required to generate lateral flow. So, while harvesting may increase the potential for lateral flow generation, the probability will still be controlled by the probability of

precipitation events of sufficient magnitude and intensity to exceed thresholds, and these events to have a frequency of roughly 1 in 20 years (Hogg and Carr 1985).

For aspen forested hillslopes, the potential window for harvesting related increases in soil moisture storage, and hence vertical and lateral flow potential, may be quite small. This is a result of the rapid regeneration of clonal aspen that can return to leaf area and water use capacities similar to that of a mature stand within a few years of harvest (Devito et al. 2005b). The young stands are able to grow at a high rate by exploiting water and nutrients through the pre-existing root network.

For uplands on coarse-textured outwash sediments, vertical flow will dominate regardless of harvesting. An increase in recharge is likely following the loss of canopy interception and transpiration. The effects of harvesting are likely to persist longer for coniferous stands than aspen forested uplands due to slower regeneration. However, the immediate post-harvest hydrological effect of jack pine harvesting may be lower than for aspen due the lower reported evapotranspiration rates from jack pine stands on sandy soils similar to the SP site (e.g., Baldocchi et al. 1997, Moore et al. 2000, Amiro et al. 2006) than aspen stands on fine-textured soils more similar to the LA site (e.g., Blanken et al. 2001, Swanson and Rothwell 2001, Amiro et al. 2006). The net change in recharge following harvest on the outwash is likely greater on the outwash than the moraine due to the lower storage capacity of the soils which allow for greater drainage below the rooting zone.

A further impact of canopy removal on water movement is the potential for increased near surface snowmelt runoff. With the loss of the overstory canopy, greater snow accumulation is expected. Increased snowmelt rates are also likely due to the greater incoming solar radiation, as is a potential increase in concrete frost development.

Alteration of the ground surface occurs primarily as compaction and disturbance of the soil surface (e.g. rutting) both on-block and associated with roads. Compaction can result in decreased infiltrability of the soil surface,

potentially leading to overland flow (Startsev and McNabb 2000). In addition, compaction changes the pore structure of the surface soils, potentially altering the initiation of preferential flow pathways that move water both laterally and vertically at high velocities. At the URSA, the only visually observed occurrence of overland flow was on roads on the Moraine landscape, during the period of maximum snowmelt in 2004 and during a large rain event (approximately 80 mm over 24 hours) during the 2005 growing season (T. Redding, personal observation). A further hydrological effect of compaction on fine-textured soils is that aspen regeneration is slower and less successful where soils have been compacted (Kabzems and Haeussler 2005). The potential soil surface disturbance effects of logging can be minimized through careful practices (e.g. avoiding known wet areas), proper timing (e.g. harvesting on frozen soils and thick snowpack) and minimizing the extent of roads.

6.3 Recommendations for Future Research

While the results of the research discussed within this dissertation shed light on a number of questions regarding the hydrology of forested uplands, there remain many unanswered questions. Future research needs to combine field based measurement with the development and application of numerical models to help predict the effects of climate variability, climate change and landscape disturbance on the hydrology of forested uplands, and the hydrologic interactions between uplands and wetlands. Specific topics and potential approaches for future research are presented below:

1. Climatic controls on soil moisture dynamics and recharge: To understand the climatic controls on soil moisture dynamics and recharge across a range of time scales, long-term modelling should be employed (e.g., Smerdon et al. 2008). This type of modelling would help to clarify climate-landform-vegetation controls on soil moisture storage, lateral flow thresholds, vertical water movement and groundwater recharge. This would also provide a check on tracer-based estimates of long-term

recharge. In the absence of adequate long-term climate data, a probabilistic approach (e.g., Rodriguez-Iturbe 2000) could be applied that would allow alternate scenarios that may account for climate change effects. As a first step, the monthly precipitation and recharge data generated by Smerdon et al. (2008) could be examined to clarify the time scales of precipitation that drive recharge for the coarse textured SP site and fine textured LA site.

2. Tracer based estimates of long-term recharge: The inconsistencies encountered using the CMB method need to be investigated to determine if there are relatively straight-forward ways this method could be applied to the Boreal Plain landscape. Given the low-cost of sample collection and analysis for Cl^-, this method, if workable, could be widely applied to estimate recharge and root-zone drainage on a regional basis. To test both CMB and model-based estimates of long-term recharge, analysis of other tracer methods (e.g. tritium) to estimate long-term recharge rates should be applied. This could be especially useful in areas such as the transition between moraine and outwash where extremely deep unsaturated zones are present (e.g. Riddell 2008).
3. Simplified models of upland-wetland-pond systems: Can simple models be developed (e.g. bucket models) to allow for greater generalizability than the previously applied, highly-parameterized physically based models (e.g., Smerdon et al. 2008, Riddell 2008). Given the threshold dependence for vertical and lateral flow on these hillslopes, these detailed models may not be required, and simpler models could be applied where only basic data (e.g. vegetation type, soil type) are available.
4. Unsaturated flow connections between uplands and wetlands: It is unclear as to the role of unsaturated lateral flow from uplands to wetlands (or wetlands to uplands). Detailed measurement of soil water potential and physically based modelling could be combined to quantify the magnitude and direction of unsaturated fluxes.

5. Snowmelt driven subsurface flow: A gap in this research is the lack of measurement of lateral subsurface flow during snowmelt. This would likely involve the assessment of interactions of snowmelt rates and the presence of frozen soils. While there may be a possibility of lateral unsaturated flow following snowmelt, this will be difficult to measure during this time of low plant demand, due to low air and soil temperatures.
6. Preferential flow at the plot and hillslope scales: Given the dominance of both vertical and lateral preferential flow noted during the rainfall simulation experiments, a greater understanding of the dynamics of preferential flow across the range of landforms would be helpful to understand the potential movement of water and solutes. An improved understanding of preferential flow initiation and the lengths and connectivity of flowpaths at the plot and hillslope scales during both rainfall and snowmelt conditions could be addressed through the use of dye tracing for both rainfall (Weiler and Naef 2003) and snowmelt (Stahli et al. 2004) conditions.

Table 6.1. Monthly rainfall exceedence probabilities during the growing season for Red Earth Creek.

		April	May	June	July	Aug	Sept	Oct	May-Sept
Record Length (yrs)		32	47	47	47	47	40	20	
Mean Monthly Rainfall (mm)		10.2	44	79.6	84.8	63.5	48.9	12.9	320.8
Daily	>0.2 mm	12	30	42.5	46	41	34.9	19	39.4
Rainfall	1 mm	9.7	23.7	34.5	36.5	32	27.4	13.3	31
Exceedence	5 mm	2.3	8.2	15.2	16.5	12	9.7	2.0	12.5
Probability	10 mm	0.4	3.8	8.0	8.2	5.3	3.5	0.2	5.9
(%)	20 mm	0	1.2	2.8	2.8	1.7	1.1	0	2.0
	30 mm	0	0.5	1.2	1.0	0.8	0.7	0	0.8
	40 mm	0	0.07	0.5	0.3	0.3	0.3	0	0.3

Table 6.2. The potential for water movement by landform and slope position over various time periods. Water fluxes considered are drainage below the root zone (RZ Drain.), groundwater recharge (GW Recharge) and lateral flow (Lat. Flow). Potential for various fluxes is: H: high, M: moderate, L: low, VL: very low.

	Landform	Outwash		Moraine	
	Slope Position	Mid-Upper	Lower-Toe	Mid-Upper	Lower-Toe
Time Period	Water Flux				
Snowmelt	RZ Drain.	H	H	L-M	L-M
	GW Recharge	H	H	L	M-H
	Lat. Flow	M[1]	M[1]	L[1]	L[1]
Growing Season	RZ Drain.	M	M	L	L
	GW Recharge	L	L-M	VL	L
	Lat. Flow	VL	VL	VL	VL
Fall	RZ Drain.	M	H	L	L
	GW Recharge	M	H	L	M
	Lat. Flow	VL	VL	VL-L	VL-L
Large Magnitude – High Intensity Rain Event	RZ Drain.	H	H	L	L
	GW Recharge	M	H	VL	L
	Lat. Flow	VL	VL	VL	L

[1] near surface lateral flow dependent on presence of concrete frost

6.4 References

Amiro, B.D., Barr, A.G., Black, T.A., Iwashita, H., Kljun, N., McCaughey, J.H., Morgenstern, K., Murayama, S., Nesic, Z., Orchansky, A.L. and Saigusa, N. 2006. Carbon, energy and water fluxes at mature and disturbed forest sites, Saskatchewan, Canada. Agricultural and Forest Meteorology 136: 237-251.

Baldocchi, D.D., Vogel, C.A. and Hall, B. 1997. Seasonal variation of energy and water vapour exchange above and below a boreal jack pine forest canopy. Journal of Geophysical Research 102(D24): 28939-28951.

Barnett, T.P., Adam, J.C. and Lettenmaier, D.P. 2005. Potential impacts of a warming climate on water availability in snow-dominated regions. Nature 438: 303-309.

Blanken, P.D., Black, T.A., Neumann, H.H., den Hartog, G., Yang, P.C., Nesic, Z. and Lee, X. 2001. The seasonal water and energy exchange above and within a boreal aspen forest. Journal of Hydrology 245: 118-136.

Carey, S.K. and Woo, M.K. 1999. Hydrology of two slopes in subarctic Yukon, Canada. Hydrological Processes 13: 2549-2562.

Devito, K., Creed, I., Gan, T., Mendoza, C., Petrone, R., Silins, U. and Smerdon, B. 2005a. A framework for broad-scale classification of hydrologic response units on the Boreal Plain: is topography the last thing to consider? Hydrological Processes 19: 1705-1714.

Devito, K.J., Creed, I.F. and Fraser, C.J.D. 2005b. Controls on runoff from a partially harvested aspen-forested headwater catchment, Boreal Plain, Canada. Hydrological Processes 19: 3-25.

Elliot, J.A., Toth, B.M., Granger, R.J. and Pomeroy, J.W. 1998. Soil moisture storage in mature and replanted sub-humid boreal forest stands. Canadian Journal of Soil Science 78: 17-27.

Ferone, J.M. and Devito, K.J. 2004. Shallow groundwater-surface water interactions in pond-peatland complexes along a Boreal Plains topographic gradient. Journal of Hydrology 292: 75-95.

Hart, G.E., and Lomas, D.A. 1979. Effects of clearcutting on soil water depletion in an Engelmann spruce stand. Water Resources Research 15: 1598-1602.

Hendry, M.J. 1982. Hydraulic conductivity of a glacial till in Alberta. Ground Water 20: 162-169.

Hogg, W.D. and Carr, D.A. 1985. Rainfall frequency atlas for Canada. Environment Canada. Ottawa.

Kabzems, R., and Haeussler, S. 2005. Soil properties, aspen and white spruce responses for five years after organic matter removal and compaction treatments. Canadian Journal of Forest Research 35: 2045-2055.

Moore, K.E., Fitzjarrald, D.R., Sakai, R.K. and Freedman, J.M. 2000. Growing season water balance at a boreal jack pine forest. Water Resources Research 36: 483-493.

Redding, T.E. and Devito, K.J. 2008. Lateral and vertical flow thresholds for aspen forested hillslopes on the Western Boreal Plain, Alberta, Canada. Hydrological Processes 23: 4287-4300.

Riddell, J.T.F. 2008. Assessment of surface water-groundwater interaction at perched boreal wetlands, north-central Alberta. Unpublished M.Sc. Thesis, University of Alberta, Edmonton, AB. 106 p.

Rodhe, A. 1987. The origin of streamwater traced by Oxygen-18. PhD Thesis. Uppsala University, Uppsala, 260 pp.

Rodriguez-Iturbe, I. 2000. Ecohydrology: A hydrologic perspective on climate-soil-vegetation dynamics. Water Resources Research 36: 3-9.

Rosenberry, D.O. and Winter, T.C. 1997. Dynamics of water-table fluctuations in an upland between two prairie-pothole wetlands in North Dakota. Journal of Hydrology 191: 266-289.

Smerdon, B.D., Devito, K.J. and Mendoza, CA. 2005. Interaction of groundwater and shallow lakes on outwash sediments in the sub-humid Boreal Plains of Canada. Journal of Hydrology 314: 246-262.

Smerdon, B.D., Mendoza, C.A. and Devito, K.J. 2008, Influence of sub-humid climate and water table depth on groundwater recharge in shallow outwash

aquifers. Water Resourources. Research. 44: doi:10.1029/2007WR005950.

Stahli, M., Bayard, D., Wydler, H. and Fluhler, H. 2004. Snowmelt infiltration into alpine soils visualized by dye tracer technique. Arctic, Antarctic and Alpine Research 36: 128-135.

Startsev, A.D. and McNabb, D.H. 2000. Effects of skidding on forest soil infiltration in west-central Alberta. Canadian Journal of Soil Science 80: 617-624.

Swanson, R.H. and Rothwell, R.L. 2001. Hydrologic recovery of aspen clearcuts in northwestern Alberta. In: USDA Forest Service Proceedings RMRS-P-18. p. 121-135.

Weiler, M. and Naef, F. 2003. An experimental tracer study of the role of macropores in infiltration in grassland soils. Hydrological Processes 17: 477-493.